



# University of HUDDERSFIELD

## University of Huddersfield Repository

Kozlowski, Aleksandra

Study of Hydrolytic Degradation of Heparin in Acidic and Alkaline Environments

### Original Citation

Kozlowski, Aleksandra (2021) Study of Hydrolytic Degradation of Heparin in Acidic and Alkaline Environments. Doctoral thesis, University of Huddersfield.

This version is available at <http://eprints.hud.ac.uk/id/eprint/35518/>

The University Repository is a digital collection of the research output of the University, available on Open Access. Copyright and Moral Rights for the items on this site are retained by the individual author and/or other copyright owners. Users may access full items free of charge; copies of full text items generally can be reproduced, displayed or performed and given to third parties in any format or medium for personal research or study, educational or not-for-profit purposes without prior permission or charge, provided:

- The authors, title and full bibliographic details is credited in any copy;
- A hyperlink and/or URL is included for the original metadata page; and
- The content is not changed in any way.

For more information, including our policy and submission procedure, please contact the Repository Team at: [E.mailbox@hud.ac.uk](mailto:E.mailbox@hud.ac.uk).

<http://eprints.hud.ac.uk/>

STUDY OF HYDROLYTIC DEGRADATION OF HEPARIN IN ACIDIC AND  
ALKALINE ENVIRONMENTS

Aleksandra Maria Kozlowski

Thesis submitted to the University of Huddersfield in partial fulfilment of the  
requirements for the degree of Doctor of Philosophy.

*University of*  
**HUDDERSFIELD**

April 2021

The author of this thesis (including any appendices and/or schedules to this thesis) owns any copyright in it (the “Copyright”) and s/he has given The University of Huddersfield the right to use such Copyright for any administrative, promotional, educational and/or teaching purposes.

Copies of this thesis, either in full or in extracts, may be made only in accordance with the regulations of the University Library. Details of these regulations may be obtained from the Librarian. This page must form part of any such copies made.

The ownership of any patents, designs, trademarks and any and all other intellectual property rights except for the Copyright (the “Intellectual Property Rights”) and any reproductions of copyright works, for example graphs and tables (“Reproductions”), which may be described in this thesis, may not be owned by the author and may be owned by third parties. Such Intellectual Property Rights and Reproductions cannot and must not be made available for use without permission of the owner(s) of the relevant Intellectual Property Rights and/or Reproductions.

*Sapiens nihil affirmat quod non probet... Quod gratis asseritur gratis negatur.*

The wise man affirms nothing which he does not prove... What costs nothing to affirm, costs nothing to deny.



Diderot, *Diderot et L'abbé Barthélemy, Dialogue Philosophique Inédit*

## ABSTRACT

The pharmaceutical heparin is a complex polysaccharide of the glycosaminoglycan family, usually derived from porcine mucosa, and is a mainstay of anticoagulant therapy worldwide. Its activity can be modified, most notably, through depolymerisation. Yet, owing largely to the chain complexity, the progressive effects of environmental conditions on the heparin structure have not been fully described. A systematic study of the progressive effects of acidic and alkaline hydrolysis on heparin chain length and sulfate substitution has therefore been conducted.

The initial analysis concerned the changes of weight-average molecular weight of heparin, induced by applied conditions. In acidic environments, the relation between the molecular weight loss and pH was inversely correlated, whilst the rate of degradation increased with temperature. In alkaline environments, the molecular weight loss was proportional to pH and temperature, although less effective.

Under milder acidic conditions, desulfation was the major factor affecting the molecular weight of the polysaccharide, whilst in alkaline conditions, the hydrolytic sulfate scission was not as prominent. Glycosidic scission was observed only after the prolonged hydrolytic processing at pH 1, at 80 °C. Stability studies confirmed the chain stability between pH 2 and pH 12.

To understand desulfation order and further investigate possible rearrangements, selected acid and alkaline hydrolysates were monitored *via* 2D (HSQC) NMR. This study revealed that in acidic environments all sulfate groups of heparin were altered. It was observed that the sulfate groups were hydrolytically removed in the following order: N-sulfate (NS-), then 2-O-sulfate (2OS-), and finally 6-O-sulfate (6OS-), although the selectivity of last two was strongly dependent upon applied conditions. On the other hand, the NMR analysis of alkali treated heparin demonstrated that applied environments catalysed only iduronate desulfation (2OS-), followed by its exclusive rearrangements to a galacturonic residue.

The research discussed in this thesis investigated the behaviour of heparin in aqueous systems altered by temperature and pH over time. The selected stressing factors closely resembled conditions applied over the industrial and/or pharmacological processing. Therefore, the contribution of presented findings reaches beyond theoretical knowledge and extends to possible practical applications, *i.e.*, optimisation of manufacturing, storage and administration of pharmacologically active heparin products.

## ACKNOWLEDGEMENTS

The work described in this thesis was generously funded by LEO Pharma A/S (Ballerup, Denmark).

Firstly, I would like to thank my academic supervisors, Professor Gordon Morris, and Professor Alan Smith, for their advice, support, and patience through the course of the project. I am grateful to my industrial supervisors, Dr Johannes Roubroeks and Dr Kristoffer Tømmerraas, for creating this great research opportunity, and for their help and advice in our collaboration.

I would also like to thank:

Dr Edwin Yates (University of Liverpool), for his support, encouragement and both personal and professional mentoring. Dr Duncan Gill, for interesting discussions and his advice regarding the degradative mechanism of heparin.

Dr Richard Hughes and Dr Neil McLay and the other technical staff for their technical assistance. Dr Mohammad Alyassin for his kind assistance with ion chromatography. The Innovative Physical Organic Solutions (IPOS) team for their help with size exclusion chromatography. The practitioners of The Royal Liverpool University Hospital and analytical scientists of Global MSAT Department (LEO Pharma, Ballerup, Denmark), for their help with the activity studies.

My friends and colleagues (past and present), especially Izabela Lepiarz-Raba, Mirek Raba, Inmaculada Barragán Vázquez and Gabriele Pesimena, for sharing ideas and moral support in times of despair.

Adam, without whom nothing would have happen.

Finally, to my sister Agnieszka and my parents, for their love and support.

## TABLE OF CONTENTS

<b>TABLE OF CONTENTS</b> .....	<b>V</b>
<b>LIST OF TABLES</b> .....	<b>XIX</b>
<b>LIST OF ABBREVIATIONS</b> .....	<b>XX</b>
<i>Chapter 1- INTRODUCTION</i> .....	<i>1</i>
1.1 BACKGROUND .....	1
1.2 INTRODUCTION TO HEPARIN .....	2
1.2.1 Significance of heparin .....	2
1.2.2 Biosynthesis and structure of heparin .....	5
1.2.3 Physicochemical characteristics.....	8
1.2.3.1 <i>Molecular weight</i> .....	8
1.2.3.2 <i>Polyelectrolyte properties</i> .....	10
1.2.3.3 <i>Conformation</i> .....	11
1.3 DIFFERENT ANGLES OF HEPARIN RESEARCH – THE VALUE OF STABILITY STUDIES .....	12
1.4 GENERAL APPROACH TO HYDROLYTIC STABILITY STUDY OF PHARMACEUTICALLY ACTIVE SUBSTANCES .....	15
1.4.1 Introduction.....	15
1.4.2 General reaction of hydrolysis .....	15
1.4.3 Mechanisms of hydrolytic reaction.....	16
1.4.4 Kinetics concept of hydrolytic degradation .....	17
1.4.4.1 <i>Apparent kinetic order of hydrolytic reaction</i> .....	17
1.4.4.2 <i>Hydrolytic catalysts and catalysis rate</i> .....	19
1.4.4.2.1 Specific acid-base catalysis.....	19
1.4.4.2.2 Solvent catalysis.....	21
1.4.4.2.3 General acid-base catalysis .....	23
1.4.4.3 <i>Concentration- activity relation of hydrolytic reaction</i> .....	24
1.4.4.4 <i>Effect of temperature</i> .....	27
1.4.5 Practical approach to hydrolytic degradation study of pharmacologically active substances .....	28

1.5	RESEARCH SCOPE .....	29
1.5.1	Research motivation.....	29
1.5.2	Research aim .....	30
1.5.3	Outline of presented work.....	31
1.5.4	Research ambitions .....	31
1.5.5	Summary of research accomplishments.....	32
1.5.5.1	<i>Publications</i> .....	32
1.5.5.2	<i>Conferences</i> .....	32
<b>Chapter 2- EXPERIMENTAL.....</b>		<b>33</b>
2.1	INTRODUCTION .....	33
2.2	HEPARIN HYDROLYSIS.....	35
2.2.1	Introduction.....	35
2.2.2	Aim of hydrolysis .....	35
2.2.3	Materials .....	35
2.2.3.1	<i>Heparin sodium</i> .....	35
2.2.3.2	<i>Reagents</i> .....	36
2.2.3.3	<i>Stock solutions</i> .....	36
2.2.3.4	<i>Buffering systems</i> .....	36
2.2.4	Hydrolysis protocols .....	37
2.2.4.1	<i>Acidic environments</i> .....	37
2.2.4.2	<i>Alkaline environments</i> .....	38
2.2.4.3	<i>TFA degradation</i> .....	38
2.2.4.3.1	Thin Layer Chromatography for the control of TFA hydrolysis of heparin.....	39
2.3	ANALYSIS OF THE MOLECULAR WEIGHT OF HEPARIN HYDROLYSATES IN HYDROLYTIC ENVIRONMENTS.....	40
2.3.1	Introduction.....	40
2.3.2	General aim of analytical method .....	40
2.3.3	Materials .....	41
2.3.3.1	<i>Reagents</i> .....	41
2.3.3.2	<i>Standard solutions</i> .....	41
2.3.3.3	<i>Sample preparation</i> .....	42
2.3.3.4	<i>Mobile phase</i> .....	42
2.3.4	Instrumental details .....	43

2.3.5	Chromatographic protocol .....	43
2.3.5.1	<i>System normalization</i> .....	44
2.3.5.2	<i>Analysis</i> .....	44
2.3.6	Data processing .....	45
2.4	CONFIRMATION OF HEPARIN CHAIN DEGRADATION - GEL ELECTROPHORESIS AS THE REDUCING ENDS ASSAY .....	45
2.4.1	Introduction.....	45
2.4.2	General aim of analytical method .....	45
2.4.3	Materials .....	46
2.4.3.1	<i>Reagents</i> .....	46
2.4.3.2	<i>Standard preparation</i> .....	47
2.4.3.3	<i>Sample preparation</i> .....	47
2.4.3.4	<i>Preparation of electrophoretic buffers and gel intermediates</i> .....	48
2.4.3.5	<i>Degradation indicators</i> .....	49
2.4.4	Electrophoresis protocol .....	49
2.4.4.1	<i>Fluorescent labelling</i> .....	49
2.4.4.2	<i>Acrylamide gel casting</i> .....	51
2.4.4.3	<i>Electrophoresis</i> .....	51
2.4.4.4	<i>Azure A staining</i> .....	52
2.4.5	Data processing .....	53
2.5	UV-VIS SPECTROPHOTOMETRY FOR THE DETECTION OF COLOUR CHANGE OF HYDROLYSED SAMPLES .....	53
2.5.1	Introduction.....	53
2.5.2	General aim of analytical method .....	54
2.5.3	Materials .....	54
2.5.3.1	<i>Samples preparation</i> .....	54
2.5.4	Measurements .....	55
2.5.5	Data processing .....	55
2.6	THE COMPLETE SACCHARIDE ANALYSIS OF POST-HYDROLYTIC SAMPLES OF HEPARIN .....	55
2.6.1	Introduction.....	55
2.6.2	General aim of analytical method .....	55
2.6.3	Materials .....	56
2.6.3.1	<i>Reagents</i> .....	56

2.6.3.2	<i>Standards preparation</i> .....	57
2.6.3.3	<i>Samples preparation</i> .....	57
2.6.3.4	<i>Mobile phases</i> .....	57
2.6.4	Instrumental details.....	58
2.6.5	Chromatographic protocol.....	58
2.6.5.1	<i>Analysis of standards</i> .....	58
2.6.5.2	<i>Analysis of heparin samples</i> .....	59
2.6.6	Data processing.....	59
2.7	THE QUANTITATIVE ANALYSIS OF ANIONS IN POST-HYDROLYTIC SAMPLES OF HEPARIN.....	60
2.7.1	Introduction.....	60
2.7.2	General aim of analytical method.....	60
2.7.3	Materials.....	60
2.7.3.1	<i>Reagents</i> .....	61
2.7.3.2	<i>Standards preparation</i> .....	61
2.7.3.3	<i>Samples preparation</i> .....	61
2.7.3.4	<i>Mobile phase</i> .....	61
2.7.4	Instrumental details.....	62
2.7.5	Chromatographic protocol.....	62
2.7.5.1	<i>Analysis of standards</i> .....	62
2.7.5.2	<i>Analysis of heparin hydrolysates</i> .....	63
2.7.6	Data processing.....	63
2.8	AN INSIDE LOOK INTO STRUCTURAL CHANGES OF HEPARIN WITHIN THE CONTEXT OF HYDROLYTIC CONDITIONS.....	63
2.8.1	Introduction.....	63
2.8.2	General aim of analytical method.....	64
2.8.3	Materials.....	65
2.8.3.1	<i>Reagents</i> .....	65
2.8.3.2	<i>Heparin standard preparation</i> .....	65
2.8.3.3	<i>Hydrolysed samples preparation</i> .....	66
2.8.4	NMR system details.....	66
2.8.4.1	<i>Instrumental details</i> .....	66
2.8.4.2	<i>Acquisition details</i> .....	66
2.8.5	Analytical protocols.....	67

2.8.6	Data processing .....	67
<b>Chapter 3- STABILITY OF HEPARIN IN ACIDIC ENVIRONMENTS .....</b>		<b>68</b>
3.1	INTRODUCTION .....	68
3.2	SUMMARY OF APPLIED ANALYTICAL METHODS .....	69
3.3	RESULTS AND DISCUSSION .....	71
3.3.1	The effect of acidic environments on molecular weight of heparin as a function of time and temperature .....	71
3.3.1.1	<i>The results of average weight molecular weight analysis</i> .....	71
3.3.1.2	<i>Concluding remarks</i> .....	74
3.3.2	The influence of applied conditions on glycosidic bonds of heparin - verification of chain fragmentation .....	75
3.3.2.1	<i>PAGE-based reducing-ends assay</i> .....	75
3.3.2.1.1	Summary of method optimisation .....	75
3.3.2.1.2	Fluorescent analysis of acid hydrolysates of heparin .....	76
3.3.2.1.3	Cationic dye staining of acid hydrolysates of heparin .....	78
3.3.2.1.4	PAGE electrophoresis concluding remarks .....	79
3.3.2.2	<i>UV-Vis spectrophotometry</i> .....	80
3.3.2.3	<i>The complete saccharide analysis</i> .....	81
3.3.2.3.1	Summary of method optimisation .....	82
3.3.2.3.2	Hydrolysates analysis .....	85
3.3.2.3.3	The complete monosaccharides analysis concluding remarks .....	88
3.3.3	The effect of degradative environments on heparin sulfate groups .....	88
3.3.3.1	<i>Quantitative analysis of inorganic sulfate in post-hydrolytic samples</i> ..	89
3.3.3.1.1	Summary of method optimisation .....	89
3.3.3.1.2	Analysis of hydrolysates .....	91
3.3.3.2	<i>The influence of desulfation on molecular weight of heparin</i> .....	93
3.3.3.3	<i>The effect of sulfate loss on anticoagulant activity of heparin</i> .....	97
3.3.3.4	<i>Concluding remarks</i> .....	98
3.3.4	Inside look at acid-catalysed, hydrolytic desulfation of heparin, its selectivity, and a follow up to molecule chain fragmentation .....	99
3.3.4.1	<i>Standard spectra acquirement and analysis</i> .....	100
3.3.4.2	<i>NMR- based model of heparin desulfation order and selectivity</i> .....	104
3.3.4.2.1	NMR confirmed lability of N-linked sulfate of heparin .....	105
3.3.4.2.2	Unexpected order of reactivity of O-linked sulfates of heparin .....	107

3.3.4.2.3	Inside look at continuous desulfation and degradation of heparin.	111
3.3.4.2.4	NMR model of hydrolytic desulfation of heparin - concluding remarks .....	115
3.3.4.3	<i>A second (NMR) glance at pharmacological activity of hydrolysed heparin.....</i>	<i>117</i>
3.4	THE KINETIC APPROXIMATION OF HYDROLYTIC DEGRADATION OF HEPARIN IN ACIDIC ENVIRONMENTS .....	118
3.4.1	Introduction.....	118
3.4.2	Proposed kinetic model of hydrolytic degradation of heparin in acidic environments .....	119
3.4.3	The choice of kinetic plots in a proof-of-concept verification of presented kinetic approximation of acid hydrolysed heparin.....	125
3.4.4	Concluding remarks .....	128
3.5	CHAPTER CONCLUSIONS .....	129
	<b>Chapter 4- STABILITY OF HEPARIN IN ALKALINE ENVIRONMENTS .....</b>	<b>130</b>
4.1	INTRODUCTION .....	130
4.2	SUMMARY OF APPLIED ANALYTICAL METHODS .....	132
4.3	RESULTS AND DISCUSSION.....	133
4.3.1	The effect of alkaline environments on molecular weight of heparin as a function of time and temperature .....	133
4.3.1.1	<i>Results of average weight molecular weight analysis.....</i>	<i>133</i>
4.3.1.2	<i>Concluding remarks .....</i>	<i>135</i>
4.3.2	The influence of applied alkaline conditions on glycosidic bonds of heparin- verification of chain fragmentation.....	137
4.3.2.1	<i>PAGE-based reducing-ends assay.....</i>	<i>137</i>
4.3.2.1.1	Fluorescent analysis of alkaline hydrolysates of heparin.....	137
4.3.2.1.2	Cationic dye staining of alkaline hydrolysates of heparin .....	139
4.3.2.1.3	PAGE electrophoresis concluding remarks .....	139
4.3.2.2	<i>UV-Vis spectrophotometry .....</i>	<i>140</i>
4.3.2.3	<i>The complete saccharide analysis .....</i>	<i>142</i>
4.3.2.3.1	Summary of method optimisation.....	142
4.3.2.3.2	Hydrolysates analysis.....	142
4.3.2.3.3	The complete monosaccharides analysis concluding remarks.....	144
4.3.3	The effect of degradative environments on heparin sulfate groups.....	144
4.3.3.1	<i>Quantitative analysis of inorganic sulfate in post-hydrolytic samples</i>	<i>144</i>

4.3.3.1.1	Summary of method optimisation.....	144
4.3.3.1.2	Hydrolysates analysis.....	145
4.3.3.2	<i>The influence of desulfation on molecular weight of heparin</i> .....	147
4.3.3.3	<i>Concluding remarks</i> .....	148
4.3.4	Inside look at alkaline-catalysed, hydrolytic degradation of heparin; final confirmation of iduronate modifications and desulfation.....	150
4.3.4.1	<i>Standard spectra acquirement and analysis</i> .....	150
4.3.4.2	<i>NMR- illustrated 2-O-desulfation of iduronate as initial step of alkali-catalysed degradation of heparin</i> .....	150
4.3.4.3	<i>NMR illustrated modifications of iduronate residue of heparin at alkali-catalysed hydrolysis</i> .....	154
4.3.4.4	<i>NMR analysis of heparin samples treated with milder alkaline conditions</i> .....	160
4.3.4.5	<i>NMR analysis of alkali hydrolysed samples - concluding remarks</i> .....	161
4.4	THE KINETICS APPROXIMATION OF HYDROLYTIC DEGRADATION OF HEPARIN IN ALKALINE ENVIRONMENTS.....	163
4.4.1	Introduction.....	163
4.4.2	Proposed kinetic model of hydrolytic degradation of heparin in alkaline environments.....	163
4.4.3	The choice of kinetic plots in a proof-of-concept verification of presented kinetics approximation.....	165
4.4.4	Concluding remarks.....	166
4.5	CHAPTER CONCLUSIONS.....	167
<b>Chapter 5- CONCLUSIONS.....</b>		<b>169</b>
5.1	CONCLUDING REMARKS.....	169
5.2	FUTURE WORK.....	171
<b>APPENDICES.....</b>		<b>172</b>
APPENDIX A	SEC-MALS-RI OUTPUT OF PROLONGED ACID HYDROLYSIS OF HEPARIN.....	172
APPENDIX B	ACTIVITY TEST OF HYDROLYSED SAMPLES OF HEPARIN.....	173
<b>REFERENCES.....</b>		<b>175</b>

## LIST OF FIGURES

- Figure 1.1** Graphical summary of the most important biological processes controlled by action of heparin-activated proteins.....3
- Figure 1.2** Model of the anticoagulation mechanism of **a)** unfractionated heparin **b)** low-molecular weight heparin and **c)** synthetic pentasaccharide. **a)** Heparin binds and activates AT *via* characteristic pentasaccharide linker. The AT/heparin complex inactivates the coagulation cascade of factor Xa and IIa (antithrombin). The characteristic ‘bridge’ is created during the interaction with thrombin. **b-c)** Shorter heparin chains containing the pentasaccharide sequence have a capacity to stimulate the antithrombin conformational changes and inhibit factor Xa. Picture adapted from (Jaffer & Weitz, 2014). .....4
- Figure 1.3** The sequence of heparin’s pentasaccharidic antithrombin-binding region (ATBR). The 3-O-sulfated glucosamine (3<sup>rd</sup> monosaccharide from left), followed by a non-sulfated glucuronic acid (4<sup>th</sup> mono-unit from left) are the typical residues of ATBR.....5
- Figure 1.4** Biosynthetic pathway of heparin. The tetrasaccharide linker of Xyl-Gal-Gal-GlcA is initially connected to serine, localized on the core protein chain. The linker is a foundation for saccharide chain elongation promoted by GlcA and GlcNAc transferases. Through the following modification of polysaccharide chains, stimulated by NDST, C5 epi and 6-/3-OST enzymes, the mature structures reach of low and highly sulfated domains (NA and NS respectively) and antithrombin binding sites are formed. Diagram based on (Sufliita et al., 2015). .....6
- Figure 1.5 a)** Monosaccharides of heparin and their possible modifications. The elemental blocks may be arranged in various disaccharide sequences. The major and minor repeating disaccharide unit are distinguished in **b)**, respectively. The saccharide structures and arrangements were created as described previously (Rabenstein 2002).....8
- Figure 1.6** The cause-and-effect diagram assessing the flexibility of heparin chain. Based on: <sup>a</sup> (Rubinson et al., 2016) <sup>b</sup>(Skidmore et al., 2008) <sup>c</sup> (Hricovíni, 2015) <sup>d</sup> (Mulloy & Forster, 2000) <sup>e</sup> (Hsieh et al., 2016) <sup>f</sup> (Mulloy et al., 2012) <sup>g</sup> (Pomin, 2014a) <sup>h</sup> (Casu et al., 2015) <sup>i</sup> (Rabenstein, 2002) <sup>j</sup> (Khan et al., 2013) <sup>k</sup> (Gray et al., 2008) <sup>l</sup> (Sufliita et al., 2015)..... 12
- Figure 1.7** Graphical summary of the scientific branches concerning heparin. The diagram presents the most considered issues crucial for development, application, regulatory and pharmacopeia revision of pharmacologically active heparins. The chart is based on literature reviewed for the purpose of this section discussed further in text. .... 13
- Figure 1.8** Simplified diagram showing the major stages of the heparin manufacturing process..... 14

<b>Figure 1.9</b> An example of Arrhenius plot applied for experimental data to determine activation energy ( $E_a$ ) and to extrapolate the reaction rates at studied temperatures. ....	28
<b>Figure 1.10</b> Graphical abstract of research aim presented at mini-symposium organised by study sponsor LEO Pharma A/S in Copenhagen/ Ballerup, Denmark, May 2019.....	30
<b>Figure 2.1</b> SEC-MALS-RI system for molecular weight analysis includes HPLC instruments (Agilent Technologies), MALS and RI detectors (Wyatt Technology) and ASTRA® software loaded to computer receiver. Diagram adapted from Wyatt Technology (Wyatt Technology, n.d.).....	43
<b>Figure 2.2</b> Simplified mechanism of heparin saccharides labelling with ANDSA fluorophore. See for example, (Drummond et al., 2001; Vuong et al., 2017; Yan et al., 2015). ....	50
<b>Figure 2.3</b> Graphical summary of the PAGE electrophoresis protocol, applied as the reducing ends assay to confirm the scission of heparin chain, at studied hydrolytic conditions.....	52
<b>Figure 2.4</b> Schematic representation of Azure A dye heparin staining (Ehrlich & Stivala, 1973; Mulloy, 2012; Warttinger et al., 2017). ....	53
<b>Figure 3.1</b> Graphical illustration of heparin hydrolysis process in acidic environments..	70
<b>Figure 3.2</b> Elution profiles of heparins hydrolysed at <b>a)</b> pH 1/ 40 °C after 24 h, <b>b)</b> pH 3/ 60 °C after 24 h, and <b>c)</b> pH 6/ 80 °C after 24 h. Samples were analysed <i>via</i> size exclusion chromatography with multi-angle-light-scattering detector and refractive index detector. Presented chromatograms are results of normalized refractive index detector signal.....	71
<b>Figure 3.3</b> Average weight molecular weight of heparin hydrolysed at <b>a)</b> 40 °C, <b>b)</b> 60 °C, and <b>c-d)</b> 80 °C, plotted as function of time at pH 1 - 6. The extrapolated $M_w$ (120, 144 & 168 h) in <b>d</b> are marked by ◦ data point. The averaged uncertainty defines the 95% confidence interval. ● pH 1, ● pH 2, ● pH 3, ● pH 4, ● pH 5, ● pH 6 .....	72
<b>Figure 3.4</b> Results of load optimisation for the reducing-ends assay. Pictures <b>a/a')</b> present acrylamide gels of electrophoretic-separated, ANDSA tagged dp oligosaccharides, used as ladder of standards during the PAGE analysis of acid hydrolysed heparin, while at <b>b)</b> bands of TFA hydrolysed heparin unit are visualised (sample positive); H <sub>2</sub> O- blank load.....	76
<b>Figure 3.5</b> Fluorescent images of acrylamide gels of acid degraded heparins. Comparison of samples aliquoted at various time-points at pH 3, pH 2 and pH 1 degradation, at 40, 60 and 80 °C. Weak, newly formed bands observed at 24 h and 48 h time-point on pH 1/ 80 °C gel are highlighted in yellow; Std- standard dp ladder, H <sub>2</sub> O- blank load.....	77
<b>Figure 3.6</b> Fluorescent image of acrylamide gel, showed in inverted colours, of extended acid hydrolysis of heparin (chosen time- points), carried out at pH 1 and 80 °C.....	78
<b>Figure 3.7</b> Images of acrylamide gels of heparin hydrolysed at pH 1 at <b>a)</b> 40 °C, <b>b)</b> 60 °C and <b>c-d)</b> 80 °C (chosen aliquots), stained with Azure A dye; Hep- unhydrolysed heparin reference standard. ....	79

**Figure 3.8** The absorbance spectra of sample hydrolysed at pH 1/ 80 °C over the 168 h. Each line represents hydrolytic time-point, plotted in ascending manner, *i.e.*: **a) 0.25** (the lowest), 1, 3, 6, 9, 12, 24, **b) 48**, 72, **c) 96**, 144, **c) 168** h (the highest). .....81

**Figure 3.9** The illustrative elution profile of monosaccharide standards at concentration of 100 ppm, chosen for the complete saccharide analysis of acid hydrolysed heparin. ....82

**Figure 3.10** The representative calibration curves of **a) Fuc**, **b) Gal**, **c) GlcNS**, **d) GlcNAc**, **e) GalA**, **f) GlcNS(3S)**, **g) GlcA**, **h) IdoA** and **i) GlcNS(6S)** plotted as a function of concentration (ppm), against the peak area (nC\*min). The vertical error bars (where visible) represent standard error of regression, calculated for each analytical range. ....83

**Figure 3.11** The illustrative chromatogram of final TFA hydrolysate of heparin used to mirror its degradation profile. The presence of GlcN, GlcA and IdoA peaks was based on the assignment of standards shown in **Figure 3.9**. The unidentified peaks most probably represent the post-hydrolytic heparin oligosaccharides. The narrow peak at ~ 20 min marks system peak, characteristic for gradient elution. ....85

**Figure 3.12** The illustrative elution profiles of heparin hydrolysed at pH 1/ 80 °C over **a) 24h**, **b) 48 h**, **c) 96 h**, **d) 120 h**, **e) 144 h** and **f) 168 h**. The GlcN/GlcNS and (most probably) IdoA peaks were assigned according to elution of calibration standards, shown in **Figure 3.9**. The position missing peak of GlcN/GlcNS in **f)** is marked by \*. The narrow peak at ~ 27 min marks system peak, characteristic for gradient elution. The elevation of chromatographic baseline before the system peak is a result of chromatogram magnification, common in analysis of saccharides at low concentration *via* gradient elution (see for example (Hardy & Reid Townsend, 1994). Fuc- internal standard. ....87

**Figure 3.13** Chromatograms of **a) acetate** standard and **b) multi-anion** standard applied in anion analysis of acid hydrolysed heparin, collected at concentration of 5 ppm. ....89

**Figure 3.14** The representative calibration curves of **a) acetate**, **b) chloride** and **c) sulfate** anions plotted as a function of concentration (ppm), against peak area ( $\mu\text{S}^*\text{min}$ ). The vertical error bars (too small to see) represent standard deviation from the mean of plotted peak area (triplicated run). ....90

**Figure 3.15** The illustrative chromatograms of sulfate anion, detected in heparin samples hydrolysed at **a) pH 1/ 80 °C**, with peaks corresponding to chosen time points (6, 12, 24, 48 and 168 h) and **b) pH 5/ 80 °C**. The large chloride peak in **a)** corresponds to buffering salt (KCl + HCl), while in **b)** it represents free anion detected in initial sample. Sample concentration equal to 10 ppm. ....92

**Figure 3.16** Measured concentration of sulfate anions of thermally stressed heparin at **a) 40 °C**, **b) 60 °C** and **c-d) 80 °C** plotted as a function of time at pH 1 - 6. The vertical error bars (not visible) represent standard deviation from concentrations, calculated from peak area *via* calibration curve method. ● pH 1, ● pH 2, ● pH 3, ● pH 4, ● pH 5, ● pH 6. ....93

**Figure 3.17** The results of **a**) Activated Partial Thromboplastin Time (aPTT) and **b**) Partial Thromboplastin Time (PTT) tests of heparin acid hydrolysates, showing the change in clotting time (s) (delay of clotting time) due to addition of GAG (mg/ml). The blue line marks the normal clotting time that for **a**) aPTT test is ~ 35 s, and **b**) PTT test is ~ 15 s. Plot markers, *i.e.*: ●- heparin standard; ■- pH 2/ 40 °C/ 48 h; ▲- pH 3/ 60 °C/ 12 h; ▼- pH 4/ 80 °C/ 6 h; ◆- pH 5/ 40 °C/ 24 h; ○- pH 6/ 60 °C/ 48 h are overlapping due to negligible differences between the anticoagulation times of tested samples. Courtesy of The Royal Liverpool University Hospital. .... 98

**Figure 3.18** One dimensional **a**) proton (<sup>1</sup>H) and **b**) carbon (<sup>13</sup>C) NMR spectra of heparin standard in D<sub>2</sub>O acquired according to protocol described in section 2.8.4. The details of labelled peaks are given in Table 3.7. The standard spectra were treated as a reference for following desulfation study (based on chemical shift differences between chosen peaks). .... 101

**Figure 3.19** Two-dimensional HSQC spectra of heparin standard, also used as reference for the following desulfation study. Picture **a**) and **b**) represents anomeric and aliphatic regions of polysaccharide, respectively. .... 102

**Figure 3.20** The NMR spectra (HSQC) of heparin hydrolysed at pH 1/ 80 °C/ 48 h (**yellow**) over the standard sample (**black**). The green arrows and grey region mark the shift of peaks in **a**) anomeric and **b**) aliphatic regions, which reflects (the beginning of) N-desulfation of the molecule under applied conditions. .... 106

**Figure 3.21** The NMR spectra (HSQC) of heparin hydrolysed at pH 1/ 60 °C/ 24 h (orange) over the N-desulfated standard (blue), showing the resemblance of spectra in **a**) anomeric and **b**) aliphatic regions. .... 107

**Figure 3.22** The NMR spectra (HSQC) of heparin hydrolysed at pH 1/ 60 °C/ 48 h (**orange**) over the standard sample (black). The green arrows and grey region mark the shift of peaks in **a**) anomeric and **b**) aliphatic regions. The shift of A-1 and A-2 marks completed N-desulfation, while changes of I-I reflect 2-O-desulfation. .... 109

**Figure 3.23** The NMR spectra (HSQC) of heparin hydrolysed at pH 1/ 80 °C/ 48 h (**red**) over the standard sample (**black**). The green arrows and grey region mark the shift of peaks in **a**) anomeric and **b**) aliphatic regions. The shift of A-6 marks the beginning of 6-O-desulfation, while I-I reflect continuous 2-O-desulfation. The new peak signed and circled in **a**) probably reflects C-1 of severed glucosamine unit. .... 110

**Figure 3.24** The NMR spectra (HSQC) of heparin hydrolysed at pH 1/ 80 °C/ 96 h (red) over the standard sample (black). The green arrows mark the continuous 2-O-desulfation in **a**) anomeric and 6-O-desulfation in **b**) aliphatic regions. In **a**) the new, unidentified peaks are highlighted in yellow square, while signed and green-circled probably reflects C-1 of hydrolytically liberated GlcN unit. .... 113

**Figure 3.25** The NMR spectra (HSQC) of heparin hydrolysed at pH 1/ 80 °C/ 168 h (red) over the standard sample (black). The green arrows mark the continuous 2-O-desulfation in **a**) anomeric and 6-O-desulfation in **b**) aliphatic regions. In **a**) the new, unidentified peaks are highlighted in yellow square, while signed and green-circled probably reflects C-1 of hydrolytically liberated GlcN unit. .... 114

**Figure 3.26** Proposed mechanism of hydrolytic degradation of heparin in acidic environments based on the conclusions drawn from the experimental study presented in Chapter 3. The individual sulfate groups, liberated at each characteristic stage of the mechanism, were highlighted in yellow. The last stage of the mechanism assumes two pathways: one targeting the GlcN/GlcNS-(1→ bond and resulting in GlcN monomer and heparin oligomers (left) and one that assumes the additional scission of IdoA and further degradation of monomeric-units (right). The bracket left after the final arrow indicates the (probable) subsequent degradation of the polymer chain. R= H or SO<sub>3</sub><sup>-</sup> (conditional upon applied factors)..... 116

**Figure 3.27** Proton NMR spectrum of pH 6/ 60 °C/ 48 h sample, which showed low(er) anticoagulant activity in aPTT and PTT study with zoomed in doublet of doublets typical of citric acid. .... 118

**Figure 3.28** The natural logarithm of molecular weight of heparin, measured after hydrolysis **a**) pH 1/ 80 °C over 168 h, plotted as a function of time according to first-order kinetics equation. Figure **b**) shows the magnification of the first 48 h in **a**). .... 127

**Figure 3.29** The fraction of molecular weight of heparin, measured after hydrolysis at pH **a**)1/ 80 °C/ 168 h, plotted as a function of time according to second-order kinetics equation. Figure **b**) shows the magnification of the first 48 h in **a**) ..... 128

**Figure 4.1** Reaction scheme summarising the structural changes of the 2-O-sulfated iduronate and N,3,6-sulfated glucosamine units of heparin chain, catalysed by various alkaline conditions. Figure based upon the literature discussed in text above, *i.e.*, (Casu & Lindahl, 2001; Jaseja et al., 1989; Rej & Perlin, 1990; Santini et al., 1997)..... 131

**Figure 4.2** Graphical illustration of heparin hydrolysis process in alkaline environments. .... 133

**Figure 4.3** Elution profiles of heparins hydrolysed at **a**) pH 7/ 80 °C after 24 h, **b**) pH 9/ 60 °C after 24 h, and **c**) pH 12/ 40 °C after 24 h. The sample buffer in **b**) (boric acid buffer for pH 9) was eluted with mobile phase, thus buffer peak is not visible. Samples were analysed *via* size exclusion chromatography with multi-angle-light-scattering detector and refractive index detector. Presented chromatograms are results of normalized (against the highest value) refractive index assessment. .... 134

**Figure 4.4** Average weight molecular weight of heparin hydrolysed at **a**) 40 °C, **b**) 60 °C, and **c-d**) 80 °C, plotted as function of time at pH 7 - 12. The averaged uncertainty defines the 95% confidence interval. ● pH 7, ● pH 8, ● pH 9, ● pH 10, ● pH 11, ● pH 12 ..... 134

**Figure 4.5** Fluorescent images of acrylamide gels of alkaline degraded heparins. Comparison of samples aliquoted at various time-points at pH 10, pH 11 and pH 12 degradation, at 40, 60 and 80 °C. Std- standard dp ladder..... 138

**Figure 4.6** Fluorescent image of acrylamide gel, showed in inverted colours, of extended alkaline hydrolysis of heparin (chosen time- points), carried in pH 12 at 80 °C. Std- standard dp ladder..... 138

**Figure 4.7** Images of acrylamide gels of heparin hydrolysed at pH 12 at **a)** 40 °C, **b)** 60 °C and **c-d)** 80 °C (chosen aliquots), stained with Azure A dye; Hep- unhydrolysed heparin reference standard. Std- standard dp ladder..... 140

**Figure 4.8** The absorbance spectra of sample hydrolysed at pH 12/ 80 °C over the 168 h. Each line represents hydrolytic time-point, plotted in ascending manner, *i.e.*: **a)** 0.25 (the lowest), 1, 3, 6, 9, 12, 24, **b)** 48, 72, **c)** 96, 144, **c)** 168 h (the highest). The differences between the plotted absorbance spectra are result of systematic error and magnification, not a result of increasing absorbance. .... 141

**Figure 4.9** The illustrative elution profiles of heparin hydrolysed at pH 12/ 80 °C over **a)** 24h, **b)** 48 h, **c)** 96 h, and **d)** 168 h. The small, unidentified peak is marked by \* in **d)**. The narrow peak at ~ 27 min marks system peak, characteristic for gradient elution. Fuc-internal standard..... 143

**Figure 4.10** Illustrative chromatograms of sulfate anion, detected in heparin samples hydrolysed at **a)** pH 12/ 80 °C, with peaks corresponding to chosen time points (6, 12, 24, 48 and 168 h), and **b)** pH 9/ 80 °C. The chloride and phosphate peaks correspond to neutralisation agentS and buffering salts ( HCl and NaH<sub>2</sub>PO<sub>4</sub> + NaOH, respectively). Sample concentration equal to 10 ppm..... 145

**Figure 4.11** Measured concentration of sulfate anions of thermally stressed heparin at **a)** 60 °C and **b)** 80 °C plotted for as a function of time at pH 7 - 12. The vertical error bars represent standard deviation from concentrations, calculated from peak area *via* calibration curve method. Triplicated runs. ● pH 7, ● pH 8 ● pH 9, ● pH 10, ● pH 11, ● pH 12..... 146

**Figure 4.12** The NMR spectra (HSQC with <sup>13</sup>C projection) of heparin hydrolysed at pH 12/ 40 °C/ 24 h (pink) over the standard sample (black). The glucosamine and iduronate regions, with most important peaks are circled in both **a)** anomeric and **b)** aliphatic regions. The stretched signal under I-1 of hydrolysate marks the continuous desulfation of IdoA(2S). .... 152

**Figure 4.13** The NMR spectra (HSQC with <sup>13</sup>C projection) of heparin hydrolysed at pH 12/ 60 °C/ 24 h (purple) over the standard sample (black). The glucosamine and iduronate regions, with most important peaks are circled in both **a)** anomeric and **b)** aliphatic regions. The stretched signal under I-1 of hydrolysate marks the continuous desulfation of IdoA(2S). .... 153

**Figure 4.14** The NMR spectra (HSQC with <sup>1</sup>H/ <sup>13</sup>C projection) of heparin hydrolysed at pH 12/ 80 °C/ 24 h (purple) over the standard sample (black). The glucosamine, iduronate and new, galacturonate peaks are circled in both **a)** anomeric and **b)** aliphatic regions. 155

**Figure 4.15** The NMR spectra (HSQC with  $^1\text{H}/^{13}\text{C}$  projection) of heparin hydrolysed at pH 12/ 80 °C/ 96 h (violet) over the standard sample (black). The glucosamine, iduronate and new, galacturonate peaks are circled in both **a)** anomeric and **b)** aliphatic regions. 158

**Figure 4.16** The NMR spectra (HSQC with  $^1\text{H}/^{13}\text{C}$  projection) of heparin hydrolysed at pH 12/ 80 °C/ 168 h (violet) over the standard sample (black). The glucosamine, iduronate and new, galacturonate peaks are circled in both **a)** anomeric and **b)** aliphatic regions. 159

**Figure 4.17** The anomeric regions of **a)** • pH 10/ 60 °C; • pH 11/ 60 °C hydrolysates and **b)** • pH 10/ 80 °C; • pH 11/ 80 °C hydrolysates over the heparin standard in HSQC NMR spectra. **c)** The complete NMR spectra of • pH 10/ 60 °C, • pH 11/ 60 °C hydrolysates and heparin standard in proton multi-display. .... 161

**Figure 4.18** Reaction scheme showing the intramolecular changes of major disaccharide unit of heparin, observed in this study, after hydrolysis in pH 12 at 80 °C. .... 162

**Figure 4.19** The natural logarithm of molecular weight of heparin, measured after hydrolysis at pH 12/ 80 °C/ 168 h, plotted as a function of time according to first-order kinetics equation. .... 166

**Figure 4.20** The fraction of molecular weight of heparin, measured after hydrolysis at pH 12/ 80 °C/ 168 h, plotted as a function of time according to second-order kinetic-equation. .... 166

## LIST OF TABLES

<b>Table 1.1</b> Summary of major characteristics of heparins extracted from various sources. .....	10
<b>Table 2.1</b> Summary of analytical methods used during presented research study.....	34
<b>Table 2.2</b> Details of buffering systems applied in heparin hydrolysis protocol.....	37
<b>Table 3.1</b> Summary of the analytical methods applied in acid hydrolysis study of heparin. .....	70
<b>Table 3.2</b> Summary of approximate average weight molecular weight decrease (%) of acid hydrolysed heparins (chosen time-points) in respect to the initial heparin standard. ....	73
<b>Table 3.3</b> The summary of statistical data of monosaccharide standards. ....	84
<b>Table 3.4</b> The summary of statistical data of anion standards. ....	91
<b>Table 3.5</b> Hydrolysed sulfate data of chosen acid-treated heparin samples.....	94
<b>Table 3.6</b> Summary of calculated and measured $M_w$ of selected heparin hydrolysates. ...	96
<b>Table 3.7</b> Details of NMR signals of heparin standard, shown in <b>Figure 3.18 - Figure 3.19</b> . .....	103
<b>Table 3.8</b> $^{13}\text{C}$ and $^1\text{H}$ chemical shifts of heparin standards and pH 1 hydrolysates. ....	104
<b>Table 4.1</b> Summary of approximate average weight molecular weight decrease (%) of alkaline hydrolysed heparins (chosen time-points) in respect to the initial heparin standard. .....	136
<b>Table 4.2</b> Hydrolysed sulfate data of chosen alkali-treated heparin samples. ....	147
<b>Table 4.3</b> Summary of calculated and measured $M_w$ of selected heparin hydrolysates. .	149
<b>Table 4.4</b> $^{13}\text{C}$ and $^1\text{H}$ chemical shifts of heparin standards and pH 12 hydrolysates. ....	156

## LIST OF ABBREVIATIONS

ANSDA	7-amino-1,3-naphthalenedisulfonic acid monopotassium monohydrate
API	Active Pharmacological Ingredient
aPTT	Activated Partial Thromboplastin Time
dp	Degree of polymerisation
Fuc	D-fucose
GAG(s)	Glycosaminoglycan(s)
GalA	D-galacturonic acid
GalN	D-galactosamine
GlcA	D-glucuronic acid
GlcN	D-glucosamine
GlcNAc	N-acetyl-D-glucosamine
GlcNS	N-sulfated-glucosamine
GlcNS(3S)	D-glucosamine-2-N-3-O-disulfate
GlcNS(6S)	D-glucosamine-2-N-6-O-disulfate
HPAEC-CD/PAD	High-Performance Anion-Exchange Chromatography with Conductivity Detector/ Pulsed Amperometric Detector
HSQC NMR	Heteronuclear Single Quantum Coherence Nuclear Magnetic Resonance
IdoA	L-iduronic acid
LMWH	Low Molecular Weight Heparin
LOD	Limit of Detection
LOQ	Limit of Quantification
$M_w$	Weight-average molecular weight (g/mol)
MALS	Multi-Angle Light Scattering (previously called Multi-Angle Laser Light Scattering (MALLS))
PAGE	Polyacrylamide Gel Electrophoresis
PTT	Partial Thromboplastin Time
SEC-MALS-RI	Size Exclusion Chromatography - Multi-Angle Light Scattering- Refractive Index
UV-Vis	Ultraviolet-visible light spectroscopy

# 1

## INTRODUCTION

---

### 1.1 BACKGROUND

Heparin is a linear polyanionic polysaccharide found on the cell surface of higher animals, the pharmacological activity of which has been recognised for over a century. It is one of the oldest drugs of natural origin that has been applied in the regulation of a wide range of biological processes (Lima et al., 2017; Linhardt, 2003; Mulloy, 2012; Mulloy et al., 2015; Oduah et al., 2016). It therefore comes as no surprise that the subjects of heparin structure, activity or purity have gained a lot of attention, and been under investigation ever since its discovery. Yet, next to the extensively studied pharmacological and biological properties, the chemical stability of heparin has been explored to a lesser degree. This research imbalance has caused a gap in the fundamental understanding of the principal features of the macromolecule and its behaviour in various systems. Considering the dependency of commercially available heparin from the animal sources and highlighting the number of factors that are being applied during the purification and modification of compound (Linhardt, 1992; Van Der Meer et al., 2017; Xie et al., 2018), there is a necessity to dispel as many scientific unknowns, concerning one of the most important drugs in the world, as possible. Manufacturing processes of heparin therapeutics are for the most part carried out in the aqueous environments. Furthermore, heparin-based pharmaceuticals are reconstituted in aqueous medium. Previous studies demonstrated that water molecules themselves affect the chemical stability of pharmacologically active substances (Bauer et al., 2012; Loftsson, 2013; Zhou et al., 2016). Therefore, there is a high possibility that applied manufacturing and storage conditions influence heparin stability. Consequently, the hydrolytic stability and degradation mechanisms of aqueous solutions of heparin

subjected to combinations of external factors (pH and temperature) over time, are the main subjects of this thesis.

## 1.2 INTRODUCTION TO HEPARIN

### 1.2.1 Significance of heparin

When in 1916 Jay McLean accidentally copurified the fraction of heparin during his study of tissue's procoagulant extracts (McLean, 1959), he certainly could not predict that his unintended discovery would lead to the development of one of the most effectively and widely used drugs of 20<sup>th</sup> century (Linhardt, 2003; Mulloy, 2012; Mulloy et al., 2015; Oduah et al., 2016). The form of heparin that we recognise today is associated with a compound of exceptional pharmacological activity, with a great application potential for numerous medical treatments (for an extensive summary see Mulloy et al., 2015). The wide spectrum of therapeutic applications follows from the structural heterogeneity of heparin. More specifically, the activity of heparin is a result of the direct interaction (electrostatic or hydrogen bonding) between the negatively charged sulfo- and carboxyl groups, densely populated over the polymer chain and basic amino acid residues on heparin-binding proteins (Linhardt, 2003; Meneghetti et al., 2015; Mulloy et al., 2015; Skidmore et al., 2008). The high selectivity of the binding is further adapted to control many biological processes, of which the most important ones are summarised in **Figure 1.1**. Among many important features, the ability of heparin to control the coagulation of blood, *i.e.*, anticoagulation activity, deserves special attention. It is the main characteristic of heparin, which over 100 years ago confused McLean during his study, and that ensures heparin of its place on the World Health Organisation List of Essential Medicines (*WHO / WHO Model Lists of Essential Medicines*, n.d.).

The anticoagulation activity of heparin follows from its unique ability to potentiate the inhibitory action of an actual anti-coagulation factor: antithrombin (AT). The covalently bound heparin/AT complex inactivates the coagulation proteins, particularly factors Xa and IIa (thrombin) (Jaffer & Weitz, 2014). The response of these two factors to the anticoagulant action of the heparin/AT complex is conditional upon its sequence.

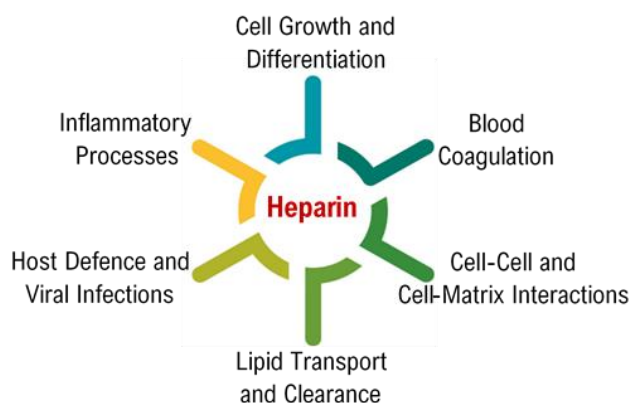


**Figure 1.1** Graphical summary of the most important biological processes controlled by action of heparin-activated proteins.

To trigger the IIa inhibition, heparin must simultaneously connect both thrombin (IIa) and antithrombin (AT), as presented in **Figure 1.2a**. This requires at least 18 saccharide units ( $M_w \approx 5.4 \times 10^3$  g/mol), 5 of which must be specifically arranged to target the stable heparin/AT connection (Onishi et al., 2016). This unique pentasaccharide linker, the structure of which is presented in **Figure 1.3**, is on average present in  $\frac{1}{3}$  of chains in commercially available, unfractionated heparin ( $M_w \approx 15 - 20 \times 10^3$  g/mol). Thus unfractionated heparin is an ideal compound to stabilise the IIa-AT connection (Mulloy et al., 2014).

In contrast to factor IIa, factor Xa does not require ‘heparin bridging’. Its activity is restrained throughout the immediate interaction with tailored reactive centre loop of antithrombin, as shown in **Figure 1.2b-c**. The conformational changes of AT, conditional upon factor Xa reactivation, are induced *via* heparin’s pentasaccharide linker (Jaffer & Weitz, 2014; Mulloy et al., 2015). The low-molecular weight heparin (LMWH,  $M_w \approx 3 - 5 \times 10^3$  g/mol) and synthetic heparin pentasaccharide (*e.g.*, Arixtran,  $M_w \approx 1.5 \times 10^3$  g/mol) are usually applied to sustain AT-Xa connection (Lima et al., 2011; Turnbull, 2011). The application of LMWHs have been considered advantageous to unfractionated heparin since it significantly reduces the interaction of drug with platelet factor IV (Stringer et al., 1999) and minimises the chances of heparin-induced thrombocytopenia (HIT), a serious side-effect observed in a few percent of recipients of unfractionated heparin, particularly in the long-term therapy cases.

The structural manipulations have clear consequences in the pharmacological activity of heparin. This, in turn, has created an opportunity to diversify the therapeutic profile of heparin. It has also underlined the necessity to cautiously examine heparin preparations to avoid undesired pharmacological effects. The natural heterogeneity of heparin chains, being the result of the complex biosynthetic pathway, certainly does not make this task any easier.

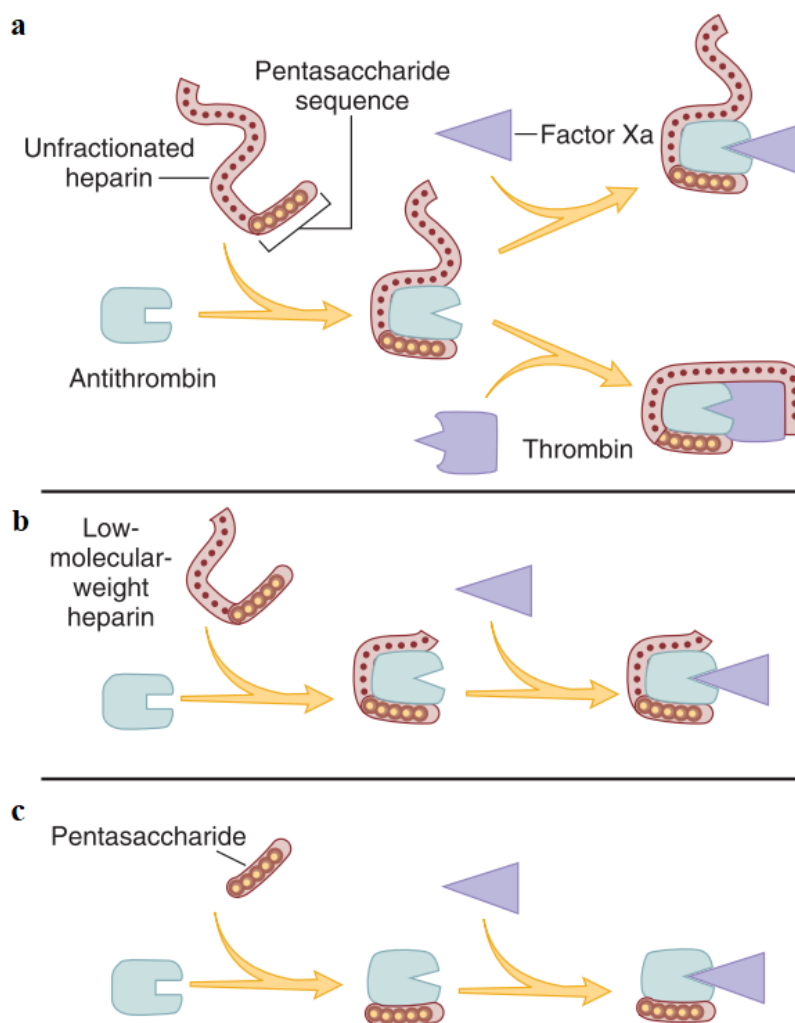


**Figure 1.2** Model of the anticoagulation mechanism of **a)** unfractionated heparin **b)** low-molecular weight heparin and **c)** synthetic pentasaccharide. **a)** Heparin binds and activates AT *via* characteristic pentasaccharide linker. The AT/heparin complex inactivates the coagulation cascade of factor Xa and IIa (antithrombin). The characteristic ‘bridge’ is created during the interaction with thrombin. **b-c)** Shorter heparin chains containing the pentasaccharide sequence have a capacity to stimulate the antithrombin conformational changes and inhibit factor Xa. Picture adapted from (Jaffer & Weitz, 2014).

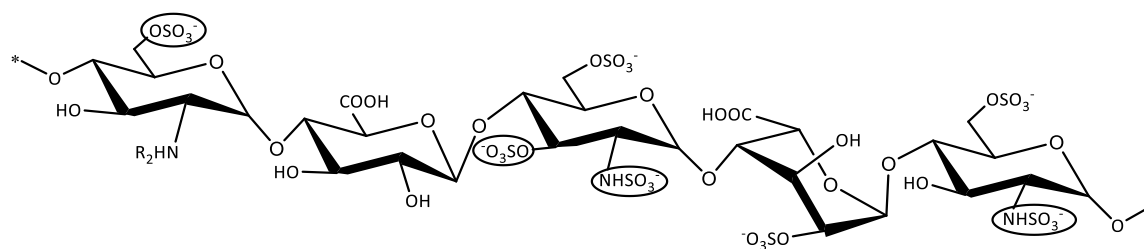


**Figure 1.3** The sequence of heparin’s pentasaccharidic antithrombin-binding region (ATBR). The 3-O-sulfated glucosamine (3<sup>rd</sup> monosaccharide from left), followed by a non-sulfated glucuronic acid (4<sup>th</sup> mono-unit from left) are the typical residues of ATBR.

### 1.2.2 Biosynthesis and structure of heparin

Unlike other biopolymers (*e.g.*, proteins or nucleic acids) biosynthesis of glycosaminoglycans (GAGs) cannot be described by means of an organised pattern. Consequently, an exact process involved in formation of heparin as well as the complete arrangement of the primary sequence of polysaccharide remain topics of ongoing discussion. Nevertheless, in the light of numerous conformational and bioengineering studies, the general pathway of heparin biosynthesis has been established (see for example Bhaskar et al., 2012; Fu et al., 2016; Puvirajesinghe & Turnbull, 2012; Rudd et al., 2010; Suflita et al., 2015). It has been agreed that heparin is exclusively biosynthesised in the mast cells of various animal species (Mulloy et al., 2017). As shown in **Figure 1.4** the biosynthetic process is initiated *via* the formation of a specific tetrasaccharide linker of xylose (Xyl), two galactose (Gal) and a glucuronic acid (GlcA) attached to serine residue of the core protein (“chain initiation” in **Figure 1.4**) (Rabenstein, 2002). The crucial step that specifically targets heparin rather than other GAGs relies on a repeated addition of 1→4 linked disaccharide unit of D-glucuronic acid (GlcA) and N-acetyl-D-glucosamine (GlcNAc) to the linkage region of the tetrasaccharide (“polymerisation” in **Figure 1.4**) (Linhardt, 2003; Rabenstein, 2002). The [GlcA-(1,4)-GlcNAc]<sub>n</sub> polymer is successively modified by 12 different biosynthetic enzymes. Among these the actions of N-deacetylase/N-sulfotransferase (NDST), C-5 epimerase (C5 epi) and O-sulfotransferases (OSTs) result in production of highly sulfated, uronic acid rich heparin chains (“polymer modification” in **Figure 1.4**) (Rabenstein, 2002; Suflita et al., 2015). Lastly, during the mast cell degranulation, protease enzymes separate the mature polysaccharide chains from the serglycin and the free peptidoglycan of heparin in process (by β-endoglucuronidase) into the glycosaminoglycan form (Linhardt, 2003).

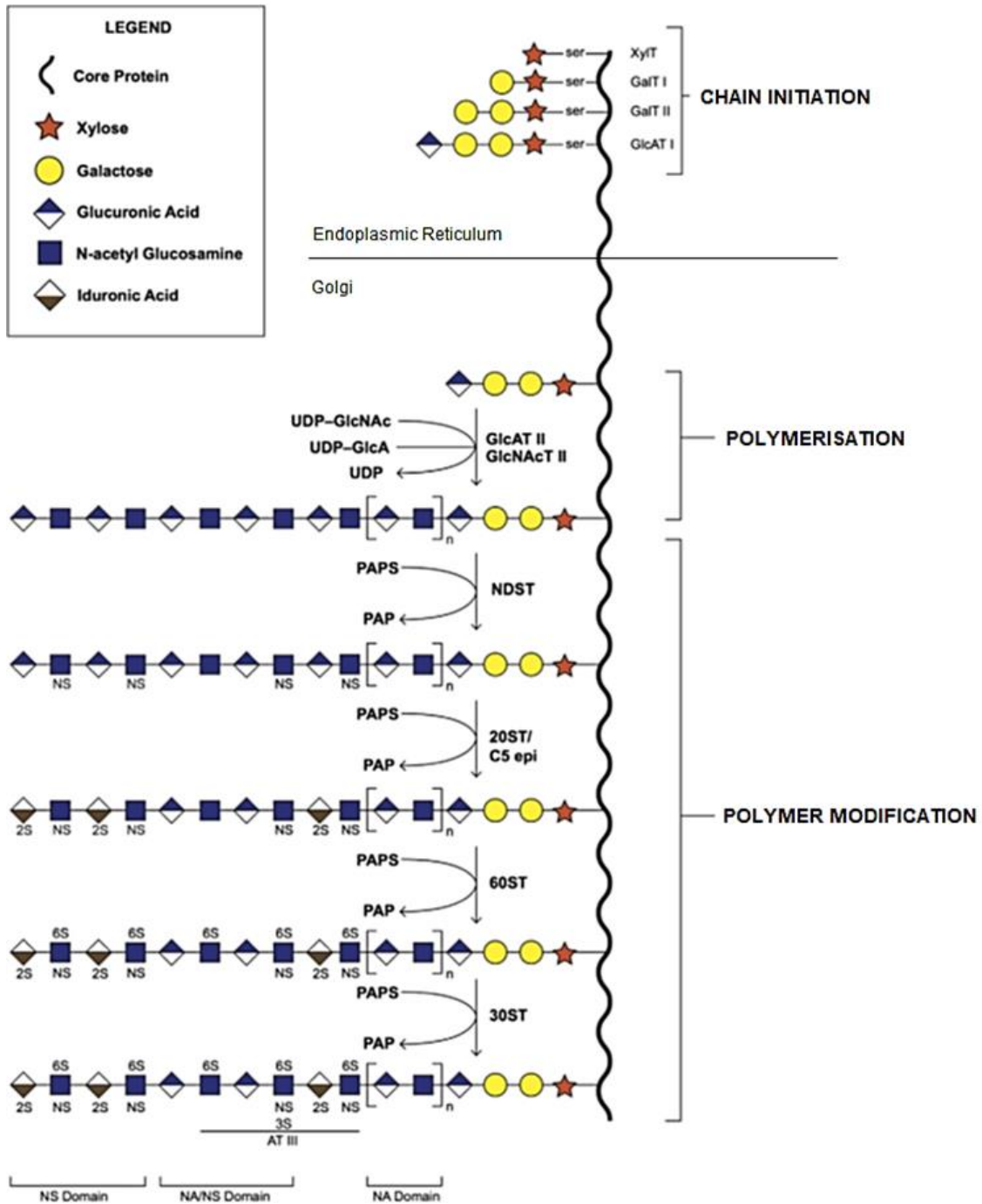


**Figure 1.4** Biosynthetic pathway of heparin. The tetrasaccharide linker of Xyl-Gal-Gal-GlcA is initially connected to serine, localized on the core protein chain. The linker is a foundation for saccharide chain elongation promoted by GlcA and GlcNAc transferases. Through the following modification of polysaccharide chains, stimulated by NDST, C5 epi and 6-/3-OST enzymes, the mature structures reach of low and highly sulfated domains (NA and NS respectively) and antithrombin binding sites are formed. Diagram based on (Suflita et al., 2015).

The non-template driven biosynthesis leads to an astonishing compositional variation occurring at the elementary level of heparin between distinct animal or tissue sources (*e.g.*, porcine intestinal mucosa vs bovine lung) and within samples of the same origin. As explained in the paragraph above, the polysaccharide chains of heparin are based predominantly on 1,4 linked, alternating residues of glucosamine and uronic acid. The acidic unit of the major disaccharide may be arranged as either  $\alpha$ -L-iduronate (IdoA) or less commonly, as  $\beta$ -D-glucuronate (GlcA). Both units can be sulfated at position 2 (C-2), as highlighted in **Figure 1.5a**. On the other hand, the  $\alpha$ -D-glucosamine (GlcN) may exist in each of two forms: N-sulfated (GlcNS) or N-acetylated (GlcNAc). As marked in **Figure 1.5a**, both glucosamine units may carry additional sulfo groups; those at position 6- being the most prevalent, whereas sulfation at position 3-, although found more rarely, plays a significant role in the anticoagulant activity of the molecule (as explained in **1.2.1**). Not all rearrangements are targeted with the same efficiency. Amongst the 32 ( $2^5$ ) possible structural modifications (at each disaccharide building block) IdoA(2S)(1 $\rightarrow$ 4) GlcNS(6S) shown in **Figure 1.5b** constitutes from 60 to 90% of heparin structure, while disaccharide repeat units arranged differently make up the remainder (Rabenstein, 2002; Rubinson et al., 2016).

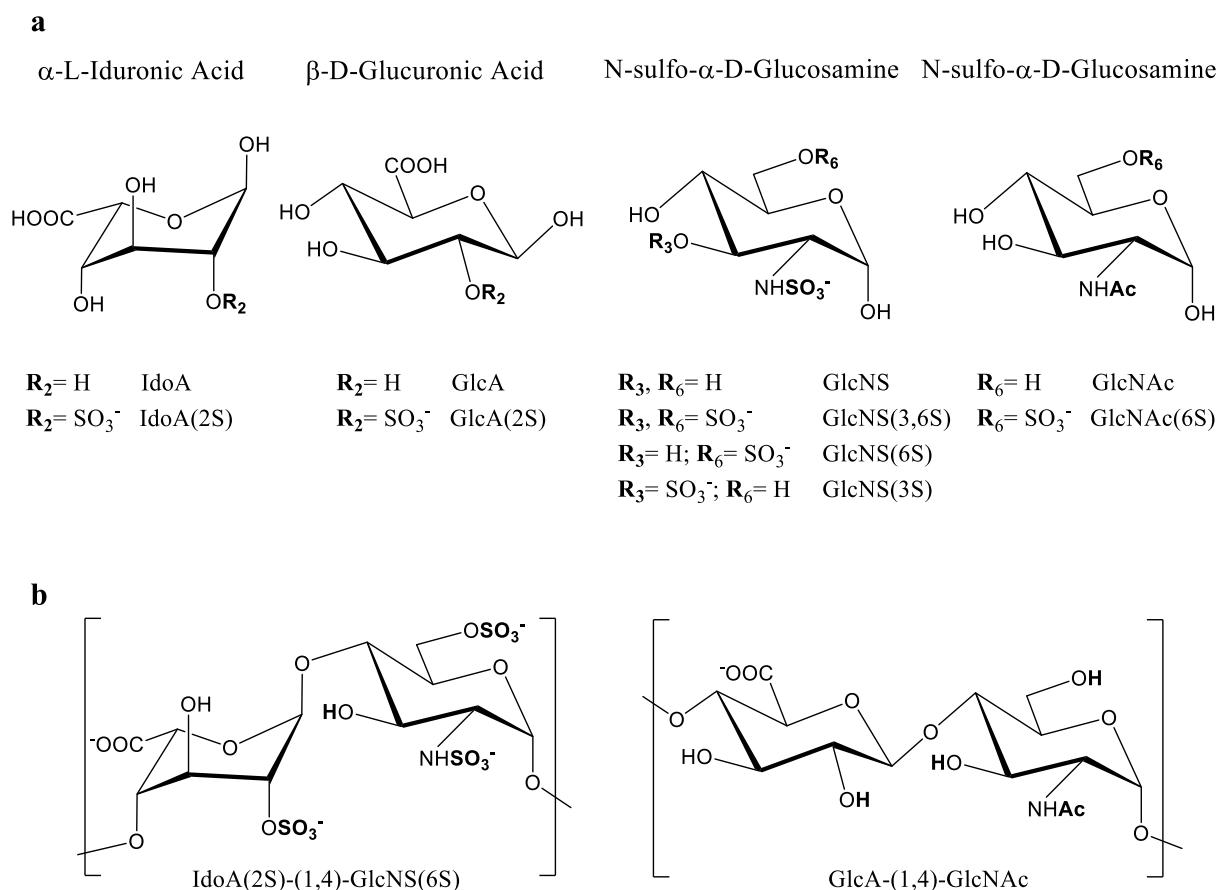


**Figure 1.5 a)** Monosaccharides of heparin and their possible modifications. The elemental blocks may be arranged in various disaccharide sequences. The major and minor repeating disaccharide unit are distinguished in **b)**, respectively. The saccharide structures and arrangements were created as described previously (Rabenstein 2002).

### 1.2.3 Physicochemical characteristics

#### 1.2.3.1 Molecular weight

Polysaccharide behaviour is driven by various physicochemical properties, amongst which molecular weight has been recognized as being crucial to underpinning of the functionality of biopolymers (Harding et al., 1991, 2017). Heparin is a polydisperse mixture of many chains that differ in molecular weight, similarly to other polysaccharides of a natural origin. Therefore, it is convenient to express its molecular weight (MW) as distribution, commonly described by a means of weight-average molecular weight ( $M_w$ ) and/or number-average molecular weight ( $M_n$ ), which are defined as:

$$M_w = \frac{\sum_{i=1}^{\infty} M_i^2 n_i}{\sum_{i=1}^{\infty} M_i n_i} = \frac{\sum_{i=1}^{\infty} M_i c_i}{\sum_{i=1}^{\infty} c_i} \quad 1.1$$

$$M_n = \frac{\sum_{i=1}^{\infty} M_i n_i}{\sum_{i=1}^{\infty} n_i} = \frac{\sum_{i=1}^{\infty} c_i}{\sum_{i=1}^{\infty} c_i / M_i} \quad 1.2$$

where  $n_i$  is number of the molecules or  $c_i$  the concentration of the sample characterised by the molecular weight  $M_i$ . The ratio of  $M_w/M_n$  is known as the (poly)dispersity index, which refers to the spread of molecular weights in a biopolymer sample.

The scientific sources mostly agree on the polydispersity of the heparin API (active pharmaceutical ingredient). The value generally ranges between 1.1 and 1.6 (Gray et al., 2008; Linhardt, 2003; Liu et al., 2009), which indicates uniformity (in terms of molecular weight) of heparin chains in pharmaceutical samples. On the other hand, the molecular weight of heparin therapeutics is strictly associated with its activity (as discussed in **1.2.1**). Therefore, heparin pharmaceuticals of different molecular weights are distinguished. The molecular weight of very short 3<sup>rd</sup> generation heparin products, like Aritrax, is around  $1.5 \times 10^3$  g/mol (Turnbull, 2011). The molecular weight of 2<sup>nd</sup> generation low molecular weight heparins typically lies between  $3.5$  and  $6.5 \times 10^3$  g/mol (Gray et al., 2008; Turnbull, 2011), whilst the 1<sup>st</sup> generation unfractionated heparins reach up to  $20.0 \times 10^3$  g/mol (Bertini et al., 2017; Gray et al., 2008). Furthermore, the upper limit of  $M_w$  of unfractionated heparin, which has pharmacological potential varies with regards to geographical location and source material, as summarised in **Table 1.1**. Therefore, the molecular weight of heparin needs to be carefully assessed and always presented within the context of investigated factors.

**Table 1.1** Summary of major characteristics of heparins extracted from various sources.

Source	Average $M_w$ $\times 10^3$ (g/mol)	aXa Activity (IU/mg) <sup>c</sup>	aPPT Activity	References
Porcine <sup>a</sup>	15.0 – 20.0	148 – 219	168 – 277	Gray et al., 2008 Mulloy et al., 2014 Bertini et al., 2017 Fu et al., 2013
Bovine <sup>a</sup>	15.0 – 16.2	123 – 156	103 – 181	Gray et al., 2008 St Ange et al., 2016 Bertini et al., 2017
Ovine	20.0	182	n.d.	Fu et al., 2013
Camel	24.0	50 – 60	n.d.	Warda et al., 2003
Salmon	< 8.0 <sup>b</sup>	110 – 137	n.d.	Flengsrud et al., 2010
Shrimp	8.5	95 – 100	n.d.	Dietrich et al., 1999
Clam	14.9	347	317	Cesaretti et al., 2004

<sup>a</sup> Intestinal mucosa; <sup>b</sup> 96% of extracted material; n.d.- not determined; <sup>c</sup> anticoagulation activity units per milligram of heparin; potency of heparin is determined *via* biological assay using a USP reference; 1 unit of heparin is understood as the amount of heparin required to keep 1 ml of cat's blood fluid for 24 hours at 0°C; it is equivalent approximately to 0.002 mg of pure heparin (Kuizenga et al., 1943; Pharmacopeial Forum, 2009).

### 1.2.3.2 Polyelectrolyte properties

Together with molecular weight the polyelectrolyte properties can be thought of as a kind of heparin fingerprint. In heparins, particularly in the commercial ones, the sulfated domains significantly predominate the amount of the acetylated domains (Mulloy et al., 2012). As a result, the average degree of sulfation of heparin characterised by  $M_w = 10 \times 10^3$  g/mol equals  $\sim 2.7$  per disaccharide unit (for sulfation centres see **Figure 1.3** or **Figure 1.5**). This calculates to almost 40 sulfo groups per polymer chain. The overall negative charge density is additionally increased by carboxyl groups of uronic acids. In consequence to the sulfo–carboxyl combination heparin is one of the most negatively charged biological macromolecules currently recognised by science (Linhardt, 2003; Pomin, 2014a). A major

contribution to the biological activity of heparin results from electrostatic interactions between these negatively charged (especially sulfo) groups with basic amino acid residues (arginine, lysine and, at appropriate pH values, also histidine) of heparin-binding proteins (see **1.2.1** for more details) (Bhaskar et al., 2012; Skidmore et al., 2008; Yates et al., 2019). Thus, it is crucial to recognise environments that may influence the degree of sulfation of the heparin molecule.

### 1.2.3.3 Conformation

As with other mammalian glycosaminoglycans, heparin has a linear sequence without any additional branches. The major sources of flexibility of linear polysaccharides like this are the torsion angles of the glycosidic bonds,  $\Phi$  and  $\Psi$ , located between the monosaccharide residues (Cui, 2005; Finch, 1999; Sun, 2004). However, since the early work on heparin conformation, the aqueous form of the macromolecule was matched with a more extended, helical model (Casu et al., 2015; Mulloy et al., 1993). The following studies on the heparin structure in solution clarified that the unique flexibility of the chain is a gross effect of the factors summarised in diagram in **Figure 1.6**. Furthermore, it has been recently suggested that the pharmacological activity of heparin is not only a result of an effective interaction between the polysaccharidic sulfate groups and heparin-binding proteins, but is perhaps conditional upon the chain conformation (Hricovíni, 2015; Meneghetti et al., 2015; Mulloy et al., 2012). The chain conformation itself seems to be strongly dependent upon the dynamics of IdoA that, to quote Mulloy, “*has potential consequences for the overall conformation of the polysaccharide as well as for “induced fit” models of interactions with proteins*” (Mulloy et al., 2012, p. 66).

The review of physicochemical characteristics of heparin elucidates a clear connection between these and pharmaceutical activities of the molecule. The molecular weight as well as degree of sulfation and chain flexibility can be equally affected by a physical and/or chemical stressor. To maintain the medical functionality of heparin it is essential to recognise the conditions that may alter both of these features.

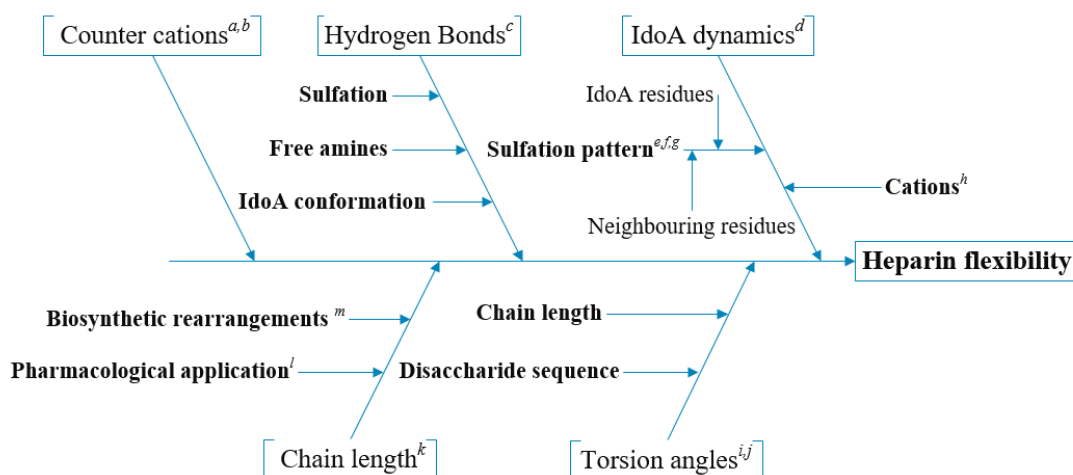


**Figure 1.6** The cause-and-effect diagram assessing the flexibility of heparin chain. Based on: <sup>a</sup> (Rubinson et al., 2016) <sup>b</sup> (Skidmore et al., 2008) <sup>c</sup> (Hricovíni, 2015) <sup>d</sup> (Mulloy & Forster, 2000) <sup>e</sup> (Hsieh et al., 2016) <sup>f</sup> (Mulloy et al., 2012) <sup>g</sup> (Pomin, 2014a) <sup>h</sup> (Casu et al., 2015) <sup>i</sup> (Rabenstein, 2002) <sup>j</sup> (Khan et al., 2013) <sup>k</sup> (Gray et al., 2008) <sup>l</sup> (Sufliita et al., 2015).

### 1.3 DIFFERENT ANGLES OF HEPARIN RESEARCH – THE VALUE OF STABILITY STUDIES

The wide range of clinical applications (see **1.2.1**) along with the structural and physicochemical complexity (see **1.2.2** and **1.2.3**, respectively) expanded the visibility of heparin to various scientific branches. As summarised in **Figure 1.7**, the molecule has been studied from a variety of different angles that contribute to increasing knowledge about its complex nature.

Since its discovery by McLean in 1916, numerous studies have been undertaken to understand the pharmacological **activity** and interactions between heparin and various molecules. Due to the extensive research targeting this subject differences between the binding specificity of heparin/AT complex to factors Xa and IIa have been recognised (Jaffer & Weitz, 2014; Mulloy, 2012; Onishi et al., 2016) and low molecular weight heparins (LMWHs) of improved anti-factor Xa activity have been produced (Gray et al., 2008; Lima et al., 2011). Moreover, the non-anticoagulant properties of heparin therapeutics have been explored (for examples see Lima et al., 2017; Meneghetti et al., 2015; Oduah et al., 2016). Among these the activity of the molecule against virus receptor proteins (including SARS-associated coronavirus) has recently been of particular importance (Mycroft-West, Su, Elli, et al., 2020; Mycroft-West, Su, Pagani, et al., 2020).

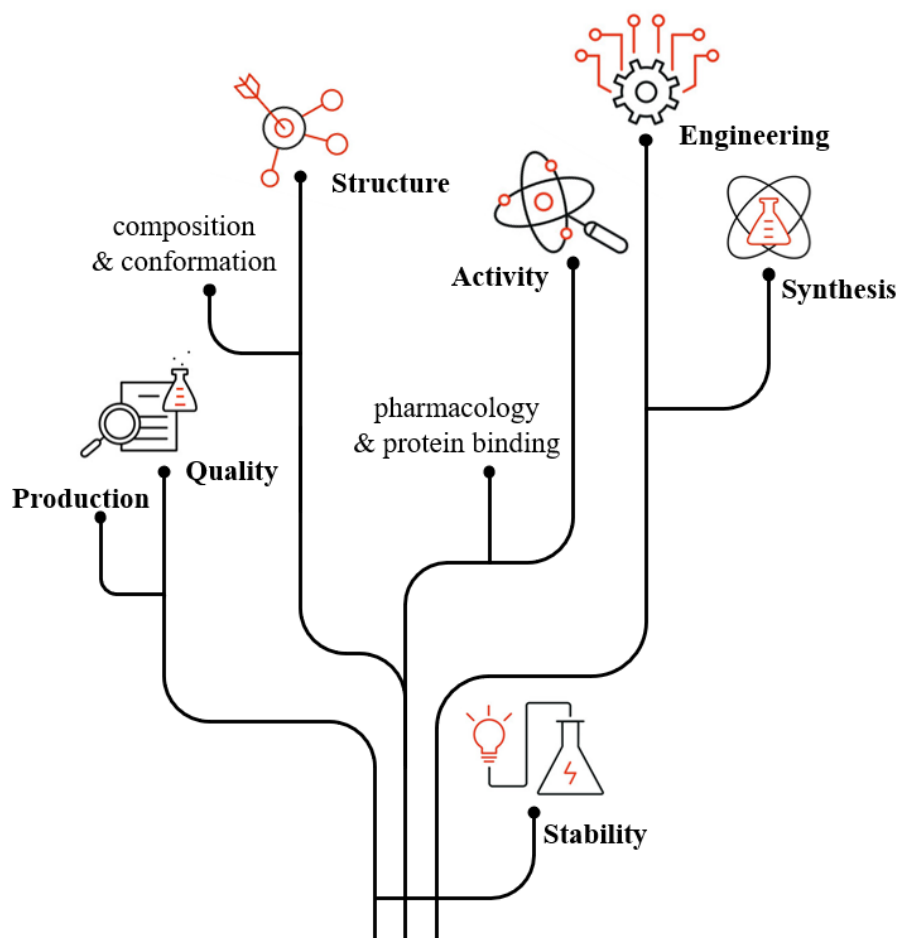


**Figure 1.7** Graphical summary of the scientific branches concerning heparin. The diagram presents the most considered issues crucial for development, application, regulatory and pharmacopeia revision of pharmacologically active heparins. The chart is based on literature reviewed for the purpose of this section discussed further in text.

The intensive conformational and compositional studies have demonstrated the relation between the heparin functionality and its **structure** (for more details see **1.2.2** and **1.2.3.3**) (Mulloy & Forster, 2000; Rabenstein, 2002; Rudd et al., 2010). These studies have also addressed the fundamentals for chemoenzymatic **synthesis** and **bioengineering** of new heparin derivatives (Bhaskar et al., 2012; Suflita et al., 2015; Turnbull, 2011). Interest in both subjects has increased exponentially in recent years owing to the contamination crisis of 2007/8. This unfortunate incident was described as one of the most dreadful episodes of a toxic drug product, especially for the United States market (Liu et al., 2009; Szajek et al., 2016). Furthermore, the contamination issue highlighted the necessity of regulated protocols to control the **quality** of heparin drugs and turned the attention of scientists back towards the optimisation of analytical methods (Devlin et al., 2019; Dionex Corporation, 2008; Guerrini et al., 2009; Pharmacopeial Forum, 2009; Volpi et al., 2012; Ye et al., 2013).

The heparin **production** process of has also been revised. Due to the complexity of source material, the industrial purification is a sophisticated and expensive operation, which involves harsh treatments over extended periods of time. Purification steps include digestion of crude sample (enzymatic or chemical), initial purification, bleaching and isolation. All of the steps summarised in **Figure 1.8** could alter the quality of final product, affecting its safety and consequently jeopardizing the reliability of the manufacturing process. Therefore, it is not surprising that heparin producers are interested in the optimisation of the whole process as well as searching for alternative (to the most popular source of porcine mucus) natural sources of heparin (Monakhova, Diehl, et al., 2018; St Ange et al., 2016; Van Der Meer et al., 2017).

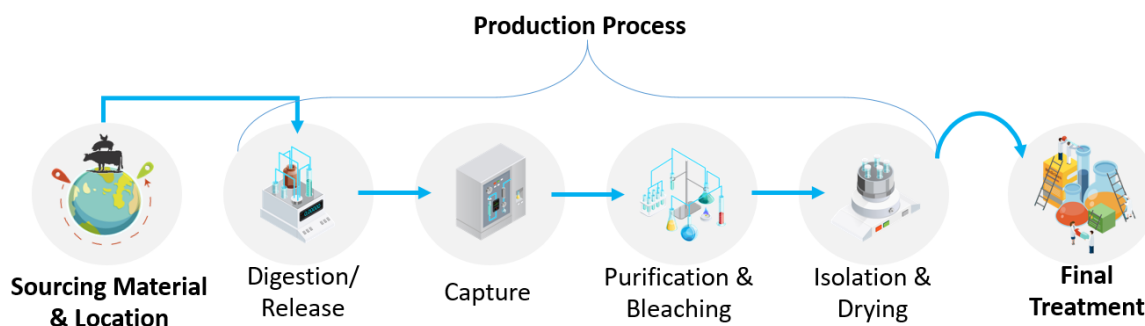


**Figure 1.8** Simplified diagram showing the major stages of the heparin manufacturing process.

On the other hand, the **stability** of heparin has been explored to a lesser extent, particularly the stability of the molecule in aqueous media and the effect of external conditions (*e.g.*, temperature, pH and pH controlling media, organic solvents, *etc.*) on its detailed substitution patterns and molecular weight. To emphasise the importance of such study, it needs to be highlighted that heparin purification is for the most part carried out in aqueous environments under the wide variety of extreme conditions (Van Der Meer et al., 2017). Moreover, heparin therapeutics are aqueous solutions that require optimal environments to sustain activity and remain safe for designed applications (LEO Pharma A/S, 2016; Pharmacopeial Forum, 2009). At the same time, nucleophilic water attack ('hydrolysis') is perhaps the most critical degradative process to biomacromolecules in aqueous systems (Bauer et al., 2012; Loftsson, 2013; Zhou et al., 2016). In most polysaccharides hydrolysis leads to cleavage of glycosidic bond(s) and changes in molecular integrity, which causes deviation from drug specifications (Bauer et al., 2012; Loftsson, 2013; Zhou et al., 2016).

Therefore, the hydrolytic stability studies on heparin are certainly of great importance equally for manufacturers – due to their potential contribution to optimisation of current processes or in recognition of alternative molecular modification routes; regulators – as it could help to standardise the production/ analysis/ storage conditions of heparin products; and users – whose safety is of the upmost importance among all the potential benefits.

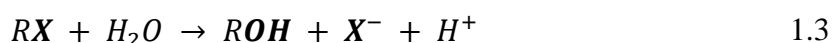
#### 1.4 GENERAL APPROACH TO HYDROLYTIC STABILITY STUDY OF PHARMACEUTICALLY ACTIVE SUBSTANCES

##### 1.4.1 Introduction

The essence of stability of pharmaceutically active substances was captured perfectly by Thorsteinn Loftsson (2013) as “(...) *the capacity of the product or a given drug substance to remain within established specifications of identity, potency, and purity during a specified time period.*” The evaluation of the stability of pharmaceutical products (or candidates) is performed through degradation studies. Depending upon the type of studied category, *i.e.*, chemical stability, physical stability and microbial stability (Loftsson, 2013), stressing factors are deliberately applied to initiate the degradation of studied substance, while the nature of changes is examined in a timely manner. Pharmaceuticals exhibit higher degradation potency in solution than in their solid form and degrade at much faster rate in aqueous than in non-aqueous medium. Consequently the hydrolysis reactions are by far the most commonly studied degradation pathways (Bauer et al., 2012; Loftsson, 2013; Zhou et al., 2016).

##### 1.4.2 General reaction of hydrolysis

Hydrolysis is a transformation process upon which a carbon-X bond of an organic molecule RX is cleaved through the nucleophilic attack of water and forms carbon-oxygen bond. The net hydrolysis reaction is commonly exemplified as a direct substitution of -X for a hydroxide group (-OH), *i.e.*:



The products of hydrolytic reaction might exhibit different physicochemical properties to parental compound, which in light of pharmacological security raises the significance of hydrolytic stability study.

### 1.4.3 Mechanisms of hydrolytic reaction

Scientists have recognised multiple reaction mechanisms that could be classified as hydrolysis, for example, March (2020) lists as many as eight different mechanisms for ester hydrolysis. In case of the complex molecules, like polysaccharides, the simplest mechanical approach assumes the classification of hydrolytic degradation upon pH, usually applied to catalyse the reaction (Cui, 2005; Finch, 1999; Tanford, 1961), *i.e.*:

- *Acid-catalysed hydrolysis*, during which protons ( $H^+$ ) catalyse the nucleophilic attack of water towards the molecular bonds; usually dominant below pH 6
- *Base-catalysed hydrolysis* where hydroxide groups ( $OH^-$ ) are consumed during the nucleophilic reaction; generally dominant above pH 8
- *Neutral hydrolysis*, which describes the spontaneous nucleophilic attack of water towards molecular bonds, without the need for catalysts; pH independent

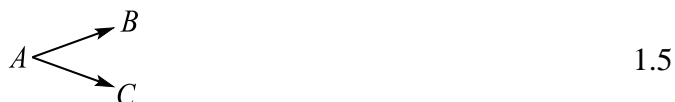
Furthermore, the hydrolysis of many pharmaceuticals, especially complex ones, usually involves more than a single degradative step. In such cases, the degradative process cannot be presented as a simple, one-term reaction but rather as an overall expression that considers all possible pathways (Bauer et al., 2012; Loftsson, 2013). Each degradation mechanism is characteristic for the studied molecule. There is no general method that can be applied for the *complex reactions*. There are, however, some general mechanisms that simplify the description of such complex systems, namely:

- *Reversible reactions* the simplest reversible reaction is the process, for which the reaction rate is considered at both directions, normally summarised as:



- *Parallel reactions* very often associated with the reactions between the studied compound and medium species (like buffer) that might lead to different degradants.

The mechanism of parallel reaction can be written as:



- *Consecutive reactions* that assume the formation of intermediate further degraded to the final product. The simplest example of consecutive reaction is the degradation of reactant *A* to product *C* along transition state *B*, as:



The assumptions about the nature of the mechanisms of a studied reaction are often based upon kinetics (Tanford, 1961); these are summarised in the following paragraph.

#### 1.4.4 Kinetics concept of hydrolytic degradation

Chemical kinetics is a powerful tool used to understand the reaction state as a function of time. The kinetics of hydrolytic changes that are taking place in an examined system (over time) can be described with mathematical functions that represent easy to measure characteristic properties of the system components *e.g.*, concentration or molecular weight (Smith, 2020; Tanford, 1961). This approach allows the researcher to understand and interpret conditions of hydrolytic instability and further propose the solutions to stabilise the studied substance.

##### 1.4.4.1 Apparent kinetic order of hydrolytic reaction

An arbitrary hydrolytic reaction can be expressed as:



where  $a$  and  $p$  represent number of the molecules of reactant  $A$  and product  $P$ , respectively. Usually for the reaction to proceed the collision of two reactant molecules is required. Hydrolysis is an exceptional example. During hydrolysis one of the reactants (water) is so largely in excess that the change of its concentration over the reaction course is negligible. In other words, the concentration of water is constant (const.) in given system and the system itself is described by “apparent” or “pseudo”-order (Bauer et al., 2012; Loftsson, 2013). Assuming that  $[H_2O] = \text{const.}$ , the rate of the reaction presented in equation 1.7 depends upon the change of concentration (or other measurable quantity) of reactant  $A$  and over a particular period is expressed as:

$$\text{rate} = -\frac{d[A]}{dt} = k_{obs} \cdot [A] \quad 1.8$$

where  $k_{obs}$  is called pseudo- (or observed) rate constant. The equation assumes degradation of only the reactant molecule in solution, implying pseudo first-order kinetics of the hydrolytic change. The separation of variables of above equation leads to:

$$\frac{d[A]}{[A]} = -k_{obs} dt \quad 1.9$$

Further integration of the equation 1.9 (over the chosen intervals) enables practical application of the rate law and the calculation of rate constant value from experimental data:

$$\int_{[A]_0}^{[A]_t} \frac{d[A]}{[A]} = -k_{obs} \int_{t_0}^t dt \quad 1.10$$

where  $[A]_0$  and  $t_0$  are the conditions at the beginning of the reaction, while  $[A]_t$  refers to the concentration of reactant measured at the time  $t$ . From the differential calculus and evaluation over the limits the equation 1.10 is expressed:

$$\int \frac{1}{x} dx = \ln x \quad \text{and} \quad \int dx = x \quad 1.11$$

$$\ln[A] \Big|_{[A]_0}^{[A]_t} = -k_{obs}t \Big|_{t_0}^t \Rightarrow \ln[A]_t - \ln[A]_0 = -k_{obs}(t - t_0)$$

and if  $t_0 = 0$  the equation 1.11 takes form(s):

$$\ln \frac{[A]_t}{[A]_0} = -k_{obs}t \quad \text{or} \quad \ln[A]_t = -k_{obs}t + \ln [A]_0 \quad 1.12$$

The logarithm of experimentally measured  $[A]_t$  value can be plotted against  $t$  giving the line of a slope corresponding to the negative pseudo-rate constant. The relation 1.12 shows that the rate of the reaction is clearly dependent upon the change of concentration of the reactant.

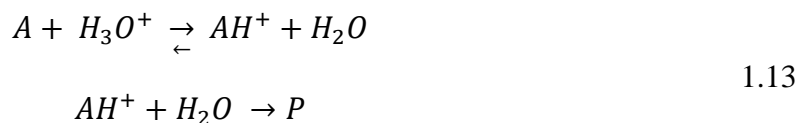
#### 1.4.4.2 Hydrolytic catalysts and catalysis rate

Hydrolytic degradation is commonly accelerated by the addition of acids or bases. Stable conditions that allow the proper examination of the reaction of a substance at applied pH are usually secured through the buffer systems that are not susceptible to rapid pH changes. The rate of aqueous reactions may therefore be accelerated by either the concentration of acidic/ basic components of buffer and in addition to the solvated hydrogen and/or hydroxide ion (*general acid-base catalysis*), follows only from the direct catalysis of hydrogen and/or hydroxide (*specific acid-base catalysis*) or occurs simultaneously when un-ionized water is recognised as the reacting agent (*solvent catalysis*) (Bauer et al., 2012; Loftsson, 2013; Zhou et al., 2016).

##### 1.4.4.2.1 Specific acid-base catalysis

Usually, the concentration of conjugated buffer components is assumed as constant and settles the buffered system under the definition of apparent kinetic law. In such cases the hydrolysis is considered as *specific acid-based catalysed*, with the degradation kinetics described by the pseudo-first order law.

The general reaction scheme of *acidic catalysed* solutions can be written as:



The ionisation of the initial species  $A$  is very fast. Thus, the rate of product formation of generalised reaction 1.13 is based on the second, slower stage and given by:

$$\frac{d[P]}{dt} = k \cdot [AH^+][H_2O] \quad 1.14$$

The concentration of conjugate acid  $AH^+$  can be defined from the measurable quantities, in accordance with rapid pre-equilibrium protonation, *i.e.*:

$$K_{a,AH^+} = \frac{[AH^+]}{[A][H_3O^+]} \Rightarrow [AH^+] = K_{a,AH^+} \cdot [A][H_3O^+] \quad 1.15$$

After substitution of equation 1.15 to 1.14, the reaction rate can be expressed as:

$$\frac{dP}{dt} = k \cdot K_{a,AH^+} \cdot [A][H_3O^+][H_2O] \quad 1.16$$

Remembering that in the hydrolytic systems water is present in great excess, and its concentration is assumed to be constant, the equation 1.16 takes form of apparent rate law:

$$\frac{d[P]}{dt} = k_{H^+} \cdot [A][H_3O^+] \quad 1.17$$

where  $k_{H^+}$  summarises ‘contributions’ of each reaction including the rate determining step (*i.e.*, the slowest reaction step) of acid catalysed hydrolysis and equals:

$$k_{H^+} = k \cdot K_{a,AH^+} \quad 1.18$$

On the other hand, the general scheme of *base catalysed* reaction can be summarised as:

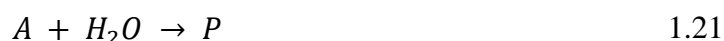


During base hydrolysis, the hydroxide ion acts as a nucleophile, whose attack towards the reagent very often leads to creation of a negatively charged intermediate (transition state that depends over the reaction mechanism). The transition state product reverts (or partially reverts) to the initial reagent; therefore, the step is excluded from the kinetic calculation and the rate equation is based on the overall scheme, *i.e.*:

$$\frac{d[P]}{dt} = k_{OH^-} \cdot [A][OH^-] \quad 1.20$$

#### 1.4.4.2.2 Solvent catalysis

The *solvent catalysis* can occur simultaneously to specific acid-base catalysis, particularly if the reaction is initiated in the environment at which the definitive catalytic influence of hydrogen or hydroxide ions is downgraded. The reaction, during which the un-ionised water is considered as the forcing agent, can be written as:



with the rate law equation given by:

$$\frac{d[P]}{dt} = k_{H_2O} \cdot [A][H_2O] \quad 1.22$$

Assuming the great excess of the water and its constant concentration, the apparent form of equation 1.22 is given by:

$$\frac{d[P]}{dt} = k_{H_2O} \cdot [A] \quad 1.23$$

The kinetic equations of *specific acid-based* and *solvent catalysis* refer to the same constituents of the hydrolytic system. Thus, these can be summarised into the general rate law:

$$\frac{d[P]}{dt} = (k_{H^+} \cdot [H^+] + k_{OH^-} [OH^-] + k_{H_2O})[A] \quad 1.24$$

The notation of equation 1.24 can be change for the experimental data, *i.e.*:  $P \rightarrow A_t$  that is the concentration of reactant measured at time  $t$  and assumed to be equal to the concentration of product, and  $A \rightarrow A_0$  that is the initial concentration of reactant. With the experimental notation, the equation 1.24 can be expressed as:

$$\frac{d[A]_t}{dt} = (k_{H^+} \cdot [H^+] + k_{OH^-} [OH^-] + k_{H_2O})[A]_0 \quad 1.25$$

The separation of variables of equation 1.25 leads to:

$$\frac{d[A]_t}{d[A]_0} = (k_{H^+} \cdot [H^+] + k_{OH^-} [OH^-] + k_{H_2O})dt \quad 1.26$$

The integration of equation 1.26 followed by differential calculus (as in equation 1.11) and logarithmic implementation results in:

$$\ln \frac{[A]_0}{[A]_t} = (k_{H^+} \cdot [H^+] + k_{OH^-} \cdot [OH^-] + k_{H_2O})t \quad 1.27$$

The substitution of above logarithmic function with the equation 1.12 gives:

$$\begin{aligned} k_{obs}t &= (k_{H^+} \cdot [H^+] + k_{OH^-} \cdot [OH^-] + k_{H_2O})t \Rightarrow \\ k_{obs} &= (k_{H^+} \cdot [H^+] + k_{OH^-} \cdot [OH^-] + k_{H_2O}) \end{aligned} \quad 1.28$$

And knowing that the water dissociation equilibrium constant  $K_w$  equals:

$$K_W = [H^+][OH^-] \Rightarrow [OH^-] = \frac{K_W}{[H^+]} \quad 1.29$$

The equation 1.28 can be written as:

$$k_{obs} = \left( k_{H^+} \cdot [H^+] + k_{OH^-} \cdot \frac{K_W}{[H^+]} + k_{H_2O} \right) \quad 1.30$$

Equation 1.30 shows that the overall rate of hydrolytic reaction is strongly dependent on concentration of protons, and therefore pH. It can be deduced that at low or high pH the first two constituents of the equation are dominant, while at neutral pH the solvolytic effect is preeminent. The stoichiometric relation between each specific rate constant provides the opportunity to understand the influence of acid, base or water towards the hydrolytic degradation of studied compound and elucidate the picture of its stability at pH range.

#### 1.4.4.2.3 General acid-base catalysis

As mentioned at the beginning of this section (1.4.4), the function of buffers applied in the hydrolytic stability study is to sustain the pH of the system. However, the charge-bearing buffer components may exhibit catalytic features and influence the reaction rate. To reveal the *general acid-base* catalytic impact of buffer species one should examine the degradation rate of studied molecule (in particular system) over the increasing concentration of (applied) buffering components (Bauer et al., 2012; Zhou et al., 2016). The deviation from reaction rate caused by the concentration changes indicates the general acid-base catalysis. In such cases the overall reaction rate should consider both acid and base components of the buffer and be written as follows:

$$\frac{d[P]}{dt} = (k_{H^+} \cdot [H^+] + k_{OH^-} [OH^-] + k_{H_2O} + k_1 \cdot [\text{buffer species 1}] + \dots) [A] \quad 1.31$$

where  $k_I$  is rate constant associated with the influence of *buffering species I* towards the analysed system. As in equation 1.24, the notation of equation 1.31 can be change for the experimental data, *i.e.*:  $P \rightarrow A_t$  that is the concentration of reactant measured at time  $t$  and assumed to be equal to the concentration of product, and  $A \rightarrow A_0$  that is the initial

concentration of reactant. With the experimental notation the equation 1.31 can be expressed as:

$$\frac{d[A]_t}{dt} = (k_{H^+} \cdot [H^+] + k_{OH^-} [OH^-] + k_{H_2O} + k_1 \cdot [\text{buffer species 1}] + \dots) [A]_0 \quad 1.32$$

After the separation of variables, integration and differential calculus (as in equation 1.11) the logarithmic form of equation 1.32 can be written as:

$$\ln \frac{[A]_0}{[A]_t} = (k_{H^+} \cdot [H^+] + k_{OH^-} [OH^-] + k_{H_2O} + k_1 \cdot [\text{buffer species 1}] + \dots) t \quad 1.33$$

After the substitution of equation 1.12 into the logarithmic function of equation 1.33 gives:

$$k_{obs} = (k_{H^+} \cdot [H^+] + k_{OH^-} [OH^-] + k_{H_2O} + k_1 \cdot [\text{buffer species 1}] + \dots) \quad 1.34$$

Equation 1.34 shows that the overall rate of hydrolytic reaction assuming the influence of *general acid-base catalysis* is strongly dependent on both concentration of protons and concentration of buffering species. In practice, the pH of examined system is very often controlled over the reaction time (with interval pH checking), while the buffering systems are carefully selected by virtue of their chemical stability, so the influence of buffering species towards the reaction rate could be neglected (Bauer et al., 2012; Loftsson, 2013; Zhou et al., 2016). This allows the introduction of the apparent theory to the investigated system, and although with approximations, to verify the stability of complex compounds in aqueous environments, omitting overcomplicated mathematical functions.

#### 1.4.4.3 Concentration- activity relation of hydrolytic reaction

The law of mass action assumes that at constant temperature chemical reaction is spontaneous and initially proceeds in one direction until ratio of products and reactants is constant. The ratio of concentrations of the generic reaction:



is expressed as:

$$Q = \frac{[C]^c [D]^d}{[A]^a [B]^b} \quad 1.36$$

and called *the mass action expression* (Bauer et al., 2012; Smith, 2020). Symbol  $Q$  is generally known as *the instantaneous reaction quotient* that signifies spontaneous chemical process. Once the reaction reaches a state of dynamic equilibrium, with the ratio of products and reactants being constant, the relation 1.36 can be represented by *the equilibrium constant  $K$* .

Generally, the laws of equilibrium constants and mass action assumes that studied system is ideal. For instance, in solutions the molarities of reactants are used to express the mass-action relation. However, to be thermodynamically correct, the activities of reactive species should be included in the mass-action equation. In contrast to concentrations, activities give information on how the solvents and surrounding species affect the behaviour of studied particles. The activity of a reactant can be estimated from its concentration  $[C]$ , *i.e.*:

$$a = \gamma \cdot [C] \quad 1.37$$

where  $\gamma$  is the *activity coefficient* that is related to the substance nature, temperature of studied system and concentration of all reacting particles (Loftsson, 2013). Nevertheless, the activity is very often excluded from the thermodynamic equilibria and consequently disregarded in kinetic calculations, assuming that approximation based on concentrations of studied species is close enough to the true value. However, the following assumption should be strictly associated with studied system rather than based on general postulations.

Consequently, the following equations justify the application of reactant concentrations in estimations considering hydrolytic system discussed in this study. Starting with the general hydrolytic reaction:



the mass-action relation based on activity of reaction 1.38 can be written as:

$$Q = \frac{a_{ROH}a_{XH}}{a_{RX}a_{H_2O}} = \frac{a_{ROH}a_{XH}}{a_{RX}} \quad 1.39$$

As the water serves as a solvent of studied system, which is present largely in excess, its activity is assumed as  $a_{H_2O} \approx 1$ . In addition, substitution of equation 1.37 into 1.39 gives:

$$Q = \frac{\gamma_{ROH} \gamma_{XH}}{\gamma_{RX}} \cdot \frac{[ROH][XH]}{[RX]} \quad 1.40$$

Due to the considerable excess of water the concentrations of reactive species in the hydrolytic system are very low. The lower the concentrations of reactants the faster the activity coefficient of each species approaches 1, *i.e.*:

$$\lim_{[C] \rightarrow 0} \gamma \rightarrow 1 \quad 1.41$$

Consequently, as the activity coefficients approach unity the activity values of considered reactants approach their concentrations, *i.e.*:

$$\lim_{\gamma \rightarrow 1} a \rightarrow [C] \quad 1.42$$

The reactants of hydrolytic system are considerably diluted. Therefore, the relation between their activity coefficients can be approximated to 1. Ergo, the activities of hydrolytic reactants approach their concentrations. In consequence, the thermodynamic and following kinetic models of the hydrolytic system are based upon the concentration of reactive species, as in final mass-action equation:

$$Q = \frac{[ROH][XH]}{[RX]} \quad 1.43$$

#### 1.4.4.4 Effect of temperature

After catalysts, temperature is another very important factor affecting the rate of hydrolytic reaction. The relation between the reaction rate and absolute temperature (expressed in Kelvin) applied over the process is commonly described by the *Arrhenius equation* (Sun, 2004; Tanford, 1961):

$$k = A \cdot e^{-\frac{E_a}{RT}} \quad 1.44$$

where  $e$  component describes the fraction of colliding molecule at temperature  $T$  (K) that has a minimum amount of energy  $E_a$  (activation energy, J/mol) to initiate the reaction and form the product. The component  $A$  is called the frequency factor and indicates the minimum number of collisions of molecules oriented in the right direction for the reaction to proceed (unit from the equation), while  $R$  is the universal gas constant (8.314 J/K·mol).

According to relation 1.44, the fraction of molecules of ‘sufficient-to-react’ energy will increase together with temperature ( $T$ ) and consequently cause an increase of the reaction rate constant ( $k$ ). The *Arrhenius equation* indicates that the reaction proceeds faster at higher temperature, therefore understandably, temperature is an important variable examined during the stability study (Loftsson, 2013; Sun, 2004; Tanford, 1961). The logarithmic form of *Arrhenius equation* provides an opportunity to experimentally explain how the solution stability of studied molecule is affected by applied temperature. The plot of the natural logarithm of equation 1.45 is a straight line, as shown in **Figure 1.9**.

$$\ln k = \ln A - \frac{E_a}{R \cdot T} \quad 1.45$$

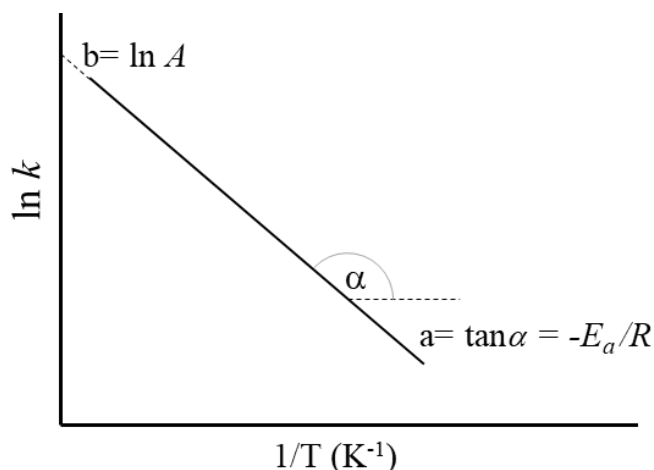


**Figure 1.9** An example of Arrhenius plot applied for experimental data to determine activation energy ( $E_a$ ) and to extrapolate the reaction rates at studied temperatures.

The activation energy ( $E_a$ ) can be calculated from the slope, while frequency factor ( $A$ ) from intercept of the straight line, being a plot of rates of the same reaction, carried at several different temperatures.

#### 1.4.5 Practical approach to hydrolytic degradation study of pharmacologically active substances

Degradation studies are vital to understand and interpret conditions that may jeopardise the functionality of active pharmacological ingredients. The experiments evaluating the behaviour of pharmacological compounds under the various stressing factors are in the first instance undertaken to protect the health of potential users. In addition, degradation studies are employed by pharmaceutical manufacturers and scientists to optimise production processes or develop new analytical pathways (Bauer et al., 2012; Zhou et al., 2016).

The application of certain conditions in forced degradation studies give the benefit of predicting the behaviour of molecule with a reasonable accuracy (Sinko, 2011; Zhou et al., 2016). For most of the pharmacologically active substances, including polysaccharides, aqueous solutions permit such estimations (Banks & Greenwood, 1963; Finch, 1999; Whistler, 1973; Zhou et al., 2016). Plus, as mentioned in the introduction to this section (1.4.1), pharmacological substances degrade at much faster rate in aqueous than in non-aqueous media. Thus, the aqueous solutions of drug compounds are routinely exposed to stressing factors like range of pHs, extreme temperatures, intensive light or action of other reactants, the effect of which is studied over time (Sinko, 2011; Zhou et al., 2016). The

choice of testing conditions is commonly associated with environments similar to these of production or prolonged storage with benefit for both manufactures and consumers. The experimental examination of potential degradative pathways is not a simple task, especially in case of polysaccharides, the functionality of which strongly relies on their physical properties, easily altered by stressing environments (Harding et al., 2017; Whistler, 1973). Therefore, a careful approach is essential to sketch a crisp picture of hydrolytic stability of pharmacologically active substances. Generally, the degradation studies can be categorised into 3 stages (Bauer et al., 2012; Loftsson, 2013; Sinko, 2011), *i.e.*:

- I. timed degradation pursued *via* thermolytic, oxidative or photolytic pathways
- II. careful analysis of physicochemical and functionality changes
- III. summary of findings *via* kinetics and the proposal of the reaction mechanism

This well-established model of degradation studies was a platform for the undertaken hydrolytic stability studies of heparin in alkaline and acidic environments.

## 1.5 RESEARCH SCOPE

### 1.5.1 Research motivation

The complexity of physiochemical properties of heparin, multiplied by the non-templated biosynthetic pathway, added to the multi-staged manufacturing process with the variety of factors applied over each of these steps (*i.e.*, temperature, chemicals, time, pressure, *etc.*) gives a very sophisticated mixture of scientific unknowns concerning one of the most important drugs in the world. Temperatures applied during the purification of the raw porcine mucosa varies. It can be as low as 4 °C during precipitation, elevated to 60 °C for alkalase digestion and up to ~80 °C during the isolation and drying (Van Der Meer et al., 2017). Furthermore, the analysis of pharmacologically active unfractionated heparin and its digestion to low molecular weight products is also associated with heat application, in range from 40 °C to 80 °C (Gray et al., 2008; Racine, 2001; Van Der Meer et al., 2017). Both treatment of raw material for heparin extraction and depolymerisation of unfractionated products require environments of specific pH that vary between pH 1 and pH 12 (depending on treatment stage, see for example (Bienkowski & Conrad, 1985;

Racine, 2001; Van Der Meer et al., 2017)). Therefore, it was considered crucial to examine chemical stability of heparin in the environment it is normally found in (as finished pharmaceutical product) and processed in (as raw material), *i.e.*, aqueous medium in a wide pH range, subjected to different temperatures as a function of time. Furthermore, it should be emphasised that a thorough search of the relevant literature revealed that until now stability studies of aqueous solutions of heparin have been relatively limited in terms of applied stressing factors.

### 1.5.2 Research aim

The aim of this research project was to study the hydrolytic degradation of finished, pharmaceutically active heparin sodium in the extended range of acidic (pH 1 – pH 6) and alkaline (pH 7 – pH 12) environments, under the influence of increased temperature (40, 60 and 80 °C) over time (up to 168 h) to reveal and understand the possible intramolecular changes on the polysaccharide chains. The graphical abstract of the research aim is presented in **Figure 1.10**.

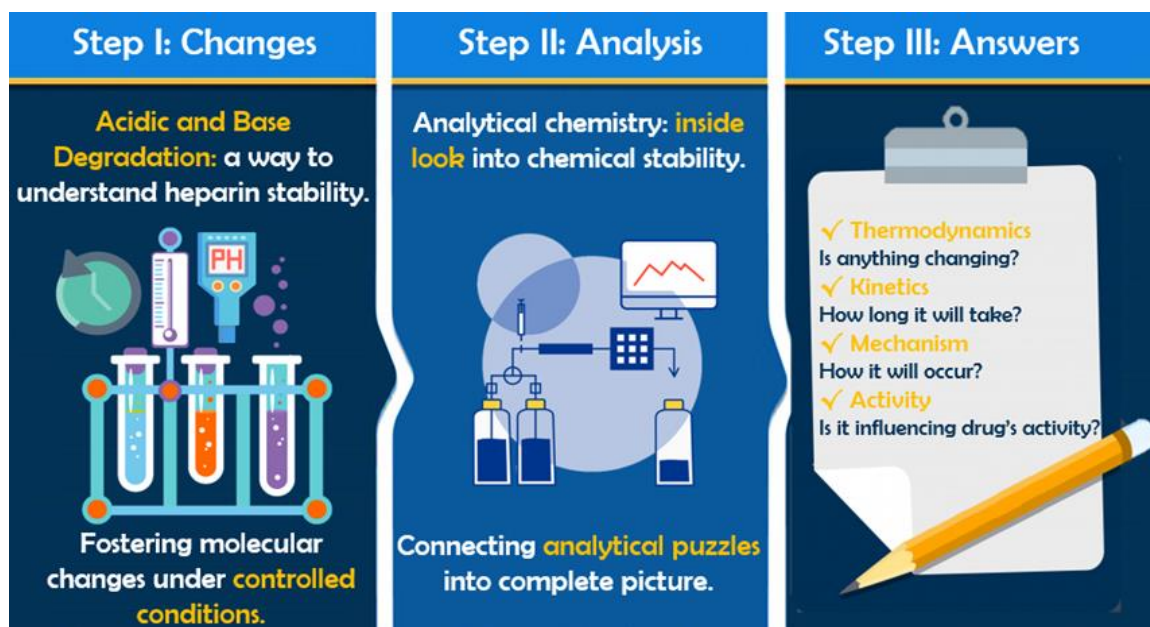


**Figure 1.10** Graphical abstract of research aim presented at mini symposium organised by study sponsor LEO Pharma A/S in Copenhagen/ Ballerup, Denmark, May 2019.

### **1.5.3 Outline of presented work**

To achieve the research goal, the undertaken study has been broken down into the specific tasks, considering the analysis of hydrolytic samples of heparin. The hydrolytic process itself and further applied analytical methods have been described in Chapter 2. The first objective was to understand the behaviour of heparin in acidic conditions. The findings of undertaken analysis have been described in Chapter 3. The results of following investigation of alkaline environments towards the heparin modifications have been summarised in Chapter 4. Furthermore, the kinetic interpretation of degradative reactions observed in acidic and alkali system has been presented at the end of Chapters 3 and 4, respectively. Finally, the research conclusions and ideas for future work have been presented in Chapter 5.

### **1.5.4 Research ambitions**

From a theoretical point of view, the proposed profile of structural modifications is a step forward in visualising the degradation mechanism and general understanding of the chemical stability of heparin. From the practical perspective, the collected data constituted a valuable body of knowledge that could have a great impact on, for example, the optimal formulation, manufacturing, and storage of products containing pharmaceutically active heparin.

## 1.5.5 Summary of research accomplishments

### 1.5.5.1 Publications

#### PUBLISHED

Kozłowski A.M., Yates E.A., Roubroeks J.P., Tømmeraas K., Smith A.M., and Morris G.A. (2021), “Hydrolytic degradation of heparin in acidic environments; NMR reveals details of selective desulfation” *ACS Appl. Mater. Interfaces*, **13**, 5551–5563

#### IN PREPARATION

Palhares L.C.G.F, London J.A., Kozłowski A.M., Chavante S.F. and Yates E.A., “Chemical Modification of Glycosaminoglycans” special edition *Macromolecules* 2021

Kozłowski A.M., A.P. Laws, Yates E.A., Gill D., Roubroeks J.P., Tømmeraas K. and Morris G.A., “Kinetic profile of acid and alkaline catalysed hydrolytic degradation of heparin”

Kozłowski A.M., Dinu V., MacCalman T., Harding S.E., Roubroeks J.P., Tømmeraas K., and Morris G.A. “Conformation of heparin after hydrolytic desulfation in acid and alkaline environments”

Kozłowski A.M., Yates E.A., Roubroeks J.P., Tømmeraas K., Smith A.M., and Morris G.A., “Degradative modifications of heparin in alkaline solutions with NMR observed rearrangements”

### 1.5.5.2 Conferences

#### ORAL PRESENTATIONS

- 15th International Conference on Polysaccharide – Glycoscience, November 2019, Prague, Czech Republic; “*Mapping the Stability: a view on the mechanism of heparin degradation in acid and alkaline environments*”

#### POSTERS

- 4th UK Hydrocolloids Symposium, September 2019, Leeds, UK; “*Physicochemical and Rheological Properties of Heparin*”
- XXth European Carbohydrate Symposium, July 2019, Leiden The Netherlands; “*Profiling the stability of heparin in acidic environments*”
- RSC Carbohydrate Group Meeting, April 2019, Reading, UK; “*New Insight into Heparin Degradation in Acidic Environments-the Influence of Time and Temperature*”; poster prize winner

# 2

## EXPERIMENTAL

---

### 2.1 INTRODUCTION

Stability of heparin in aqueous solutions could be considerably altered by numerous experimental factors. In this research the effects of pH and temperature upon heparin solutions have been studied overtime. To investigate the influence of these stressing factors on a molecular level, appropriate analytical techniques are needed. This chapter describes the methodology applied to investigate the stability of heparin in acid and alkaline solutions. Each section of this chapter introduces an individual analytical technique, presents the reasoning behind its application, and provides a detailed description of the analytical protocol. The information in **Table 2.1** summarise experimental methodologies.

**Table 2.1** Summary of analytical methods used during presented research study.

Analytical technique	<ul style="list-style-type: none"> <li>• Measured value               <ul style="list-style-type: none"> <li>○ Aim</li> </ul> </li> </ul>	Samples
Size Exclusion Chromatography (SEC) with Multi-Angle Laser Light Scattering (MALS) and Refractive Index (RI) detector	<ul style="list-style-type: none"> <li>• Weight-average molecular weight <math>M_w</math> <ul style="list-style-type: none"> <li>○ Effect of hydrolytic conditions on <math>M_w</math></li> </ul> </li> </ul>	<ul style="list-style-type: none"> <li>✓ Reference<sup>a</sup></li> <li>✓ pH 1 – 12<sup>b</sup></li> </ul>
Polyacrylamide Gel Electrophoresis (PAGE) with fluorescent tag and ionic dye	<ul style="list-style-type: none"> <li>• Reducing capacity               <ul style="list-style-type: none"> <li>○ Confirmation of glycosidic scission</li> <li>○ Structural changes</li> </ul> </li> </ul>	<ul style="list-style-type: none"> <li>✓ Reference</li> <li>✓ Hydrolysis standards<sup>c</sup></li> <li>✓ pH 1 – 3</li> <li>✓ pH 10 – 12</li> </ul>
UV-Vis Spectrophotometry	<ul style="list-style-type: none"> <li>• Absorbance               <ul style="list-style-type: none"> <li>○ Confirmation of glycosidic scission</li> <li>○ Structural changes</li> </ul> </li> </ul>	<ul style="list-style-type: none"> <li>✓ Reference</li> <li>✓ pH 1 – 3</li> <li>✓ pH 10 – 12</li> </ul>
High-Performance Anion-Exchange Chromatography (HPAEC) with:		
- Pulsed Amperometric Detector (PAD)	<ul style="list-style-type: none"> <li>• Saccharide composition               <ul style="list-style-type: none"> <li>○ Confirmation of glycosidic scission</li> </ul> </li> </ul>	<ul style="list-style-type: none"> <li>✓ Reference</li> <li>✓ TFA<sup>d</sup></li> <li>✓ pH 1 – 12</li> </ul>
- Conductivity Detector (CD)	<ul style="list-style-type: none"> <li>• Inorganic anions               <ul style="list-style-type: none"> <li>○ Effect of hydrolytic conditions on intramolecular sulfate</li> </ul> </li> </ul>	<ul style="list-style-type: none"> <li>✓ Reference</li> <li>✓ TFA<sup>d</sup></li> <li>pH 1 – 12</li> </ul>
Nuclear Magnetic Resonance (NMR) Spectroscopy	<ul style="list-style-type: none"> <li>• Chemical shifts               <ul style="list-style-type: none"> <li>○ Confirmation of desulfation order and degradation profile</li> </ul> </li> </ul>	<ul style="list-style-type: none"> <li>✓ Reference</li> <li>✓ pH 1: 24, 48, 96, 168 h</li> <li>✓ pH 12: 24, 48, 96, 168 h</li> </ul>

<sup>a</sup> reference aqueous solution of heparin sodium; <sup>b</sup> heparin hydrolysates aliquoted at specified pHs (various time-points, as specified per analysis) at 40, 60 & 80 °C; <sup>c</sup> oligosaccharide standards and TFA hydrolysates (complete hydrolysis standard, sample positive); <sup>d</sup> TFA hydrolysates (as earlier)

## 2.2 HEPARIN HYDROLYSIS

### 2.2.1 Introduction

The hydrolytically induced cleavage of glycosidic bond(s) has been recognised as an advantage when studying the chemical structure of polysaccharides and has been widely applied in manufacturing processes of oligosaccharides and low-molecular weight products (Cui, 2005; Linhardt, 1992; Melander & Tømmeraas, 2010; Smidsrød et al., 1966; Xie et al., 2018). At the same time, it has been identified as a major process influencing the chemical stability of the pharmacologically active substances that usually lead to a deviation from the drug specification (Bauer et al., 2012; Loftsson, 2013; Zhou et al., 2016). Considering the great medical importance of heparin, it is vital to fully understand the mechanism of its hydrolytic degradation and acknowledge the influence of the environmental factors towards the degradation rate. This section provides the experimental details applied during the hydrolytic reaction of heparin.

### 2.2.2 Aim of hydrolysis

The aim of this experiment was to create an environment that will enable the visualisation of the pH-, time- and temperature-dependent profiles on the structural changes in heparin and help understand the subsequent impact of these factors upon the functionality of molecule.

### 2.2.3 Materials

All reagents applied in this study were of analytical grade or higher. All aqueous solutions were prepared in ultrapure water of resistivity  $\geq 18.2 \text{ M}\Omega\cdot\text{cm}$  at  $25 \text{ }^\circ\text{C}$ , freshly drawn from Barnstead Nanopure Purification System (Thermo Fisher Scientific, Paisley, UK).

#### 2.2.3.1 *Heparin sodium*

Sodium salt of porcine mucosal heparin ( $M_w \approx 20\,000 \text{ g/mol}$ ,  $M_w/M_n = 1.1$ ) was provided by LEO Pharma (Cork, Ireland/ Ballerup, Denmark) and utilised without any further purification.

### 2.2.3.2 *Reagents*

Trifluoroacetic acid (TFA, 99%, ReagentPlus®), anhydrous sodium dihydrogen phosphate (LiChropur®), dibasic sodium phosphate ( $\geq 99.5\%$ , BioUltra), potassium chloride ( $\geq 99.5\%$ , BioXtra), sodium citrate dehydrate ( $\geq 99.5\%$ , BioUltra) and anhydrous citric acid ( $\geq 99.5\%$ , BioUltra) used for buffering systems were purchased from Sigma-Aldrich, Dorset, UK. Concentrated hydrochloric acid (12.1 M), sodium hydroxide (pearl), boric acid (99.9995%, Puratronic™, Alfa Aesar™) and di-sodium tetraborate decahydrate ( $\geq 99.5\%$ , Alfa Aesar™) were purchased from Fisher Scientific, Loughborough, UK

### 2.2.3.3 *Stock solutions*

#### Heparin sodium stock

Prior to the hydrolysis, heparin sodium was dried in the oven for 48 hours at 60 °C and subsequently stored in a desiccator. The aqueous solution of heparin was prepared by dissolving 10 g of accurately weighed oven-dried heparin sodium salt in 1000 ml of ultrapure water with stirring for 12 h. This solution will be referred to as ‘heparin stock’ and had a final concentration of 10 mg/ml.

#### Acid stocks

Aqueous solutions of TFA at a concentration of 2.0 M were prepared from the concentrated reagent. Hydrochloric acid of 1.0 M to adjust buffering systems was diluted from the concentrated acid.

#### Alkaline stock

Aqueous solution of sodium hydroxide, used for neutralisation of post-hydrolysed samples and adjustment of buffers pH, was prepared from the solid base at concentration of 1.0 M.

### 2.2.3.4 *Buffering systems*

Buffering systems were prepared by mixing the known amount of primary salt with 100 ml of heparin stock to a final concentration of 0.1 M. This approach allowed the full control over the concentration and volume of subsequently hydrolysed samples, since required only

minimal (if any) pH adjustment with HCl/NaOH solutions. Composition details of buffering systems are summarised in **Table 2.2**.

**Table 2.2** Details of buffering systems applied in heparin hydrolysis protocol.

Buffering System	Formula	pH buffering range	Application
Hydrochloric acid-Potassium chloride <sup>a</sup>	HCl + KCl	1.0 – 2.2	Acid hydrolysis: pH 1 – pH 2
Citrate buffer <sup>a</sup>	$C_6H_5O_7H_2$ + $C_6H_5O_7Na_2 \cdot 2H_2O$	3.0 – 6.2	Acid hydrolysis: pH 3 – pH 6
Sodium phosphate buffer <sup>a</sup>	$NaH_2PO_4$ + $Na_2HPO_4$	5.8 – 8.0	Base hydrolysis: pH 7 – pH 8
Boric acid buffer <sup>b</sup>	$H_3BO_4$ + NaOH	7.6 – 9.2	Base hydrolysis: pH 9
Borax buffer <sup>c</sup>	$Na_2B_4O_7 \cdot 10H_2O$ + NaOH	9.2 – 10.80	Base hydrolysis: pH 10
Phosphate buffer <sup>c</sup>	$NaH_2PO_4$ + NaOH	10.90 – 12.00	Base hydrolysis: pH 11 – pH 12

<sup>a</sup> Mohan (2003); <sup>b</sup> Makkar, Siddhuraju, & Becker (2010); <sup>c</sup> *Preparation of Buffer Solutions* (2018)

## 2.2.4 Hydrolysis protocols

The following sections (2.2.4.1 - 2.2.4.3) describe in detail the protocols of heparin hydrolysis applied in this study.

### 2.2.4.1 Acidic environments

The applied method of acid hydrolysis is a slightly modified version of hydrolysis of other glycosaminoglycans, previously described by Tømmeraas (2008). Herein, heparin sodium was thermally stressed over time at several acidic pHs. Samples buffered at the pH range from 1 to 6 were prepared in separate, sealable glass bottles (250 ml), according to procedure outlined in 2.2.3.4. The bottles were further incubated in a water bath at 40 °C, 60 °C and 80 °C (separate runs) and pH controlled. Aliquots (5 ml per pH) were collected at 0, 0.25, 1, 3, 6, 9, 12, 24, 48 h time points, immediately cooled down in an ice bath and neutralised with 1.0 M NaOH to pH 7.0 - 7.5. The neutralised hydrolysates were further diluted with water to final concentration of 5 mg/ml, split into 2.5 ml aliquots and stored

frozen at  $-20\text{ }^{\circ}\text{C}$  for further analysis. The procedure was repeated for samples buffered at pH 1 at single temperature of  $80\text{ }^{\circ}\text{C}$ , with an extended incubation time of up to 168 h. The following time points were collected: 60, 72, 96, 120, 144, 168 h. The analytical methods applied during the stability investigations are briefly summarised in **Table 2.1**, with detailed description given in following sections of this chapter.

#### 2.2.4.2 *Alkaline environments*

The hydrolysis process was repeated in alkaline environments, following the procedure of degradation in Acidic environments (**2.2.4.1**). Samples were prepared at pH range from 7 to 12, according to method given in **2.2.3.4**. The bottles were further incubated in a water bath at  $40\text{ }^{\circ}\text{C}$ ,  $60\text{ }^{\circ}\text{C}$  and  $80\text{ }^{\circ}\text{C}$  (separate runs) and pH controlled. Aliquots (5 ml per pH) were collected at 0, 0.25, 1, 3, 6, 9, 12, 24, 48 h time points, immediately cooled down in an ice bath and neutralised with 1.0 M HCl to pH 7.0 - 7.5. Furthermore, the hydrolysis of sample buffered at pH 12 was prolonged to 168.0 h (same time point as in the acid procedure) at single temperature of  $80\text{ }^{\circ}\text{C}$ .

#### 2.2.4.3 *TFA degradation*

TFA hydrolysis is an effective method to degrade polysaccharides into component mono- and oligosaccharides, through efficient glycosidic scission. This method has been mainly appreciated for smaller losses in analysed material, due to simple removal of acid excess by evaporation, and adaptation to complete hydrolysis, if applied appropriately (Morrison, 1988; Uçar & Balaban, 2003). In the past TFA hydrolysis has been successfully adapted for heparin depolymerisation (Liu et al., 2014; Zhang et al., 2012). Therefore herein, the advantage of TFA hydrolysis was taken in preparation of a “completely” hydrolysed heparin standard (as far as possible, without jeopardising the structure of released units), which served as hydrolytic sample positive in further analysis.

The heparin sodium salt was hydrolysed in 2.0 M aqueous solution of TFA. The oven-dried sample (25 mg, drying conditions described in **2.2.3.3**) was dissolved in 2.5 ml of acid to a final concentration of 10 mg/ml. The reaction was carried out in pressure tubes heated to  $100\text{ }^{\circ}\text{C}$ , over 24 h. The hydrolysis progress was monitored on TLC (thin layer chromatography) plates, according to procedure described in **section 2.2.4.3.1**. Aliquots

were taken out after 0 h, 1 h, 3 h, 6, 12 and 24 h and cooled down in an ice bath. The excess of TFA was removed at 40 °C, under the constant stream of nitrogen (TurboVap® LV Caliper Life Sciences, Waltham, Massachusetts, USA). Initially dried samples were re-dissolved in water, neutralised with 1.0 M NaOH and freeze-dried (Christ Alpha 2-4 LSC freeze-dryer, Martin Christ, Osterode am Harz Germany). Lyophilised samples were accurately weighed and dissolved in an appropriate volume of water such that the final concentration was 5 mg/ml. Samples were stored frozen at -20 °C until the analysis.

#### 2.2.4.3.1 Thin Layer Chromatography for the control of TFA hydrolysis of heparin

Thin layer chromatography has been used as a qualitative technique, in the visualisation of post-hydrolytic GAG-derived saccharide bands (Anderson et al., 2000; Zhang et al., 2006, 2007). In this study, the TLC was optimised towards monitoring the TFA hydrolysis of heparin (until in completion). Details of TLC protocol are summarised below.

##### Reagents

Diphenylamine ((C<sub>6</sub>H<sub>5</sub>)<sub>2</sub>NH;  $M_w = 169.23$  g/mol,  $d = 1.2$  g/cm<sup>3</sup>), aniline ((C<sub>6</sub>H<sub>5</sub>)NH;  $M_w = 93.13$  g/mol,  $d = 1.02$  g/cm<sup>3</sup>), 85% phosphoric acid (H<sub>3</sub>PO<sub>4</sub>;  $M_w = 97.99$  g/mol,  $d = 1.88$  g/cm<sup>3</sup>), formic acid (CH<sub>2</sub>O<sub>2</sub>;  $M_w = 46.03$  g/mol,  $d = 1.22$  g/cm<sup>3</sup>), acetone (C<sub>3</sub>H<sub>6</sub>O;  $M_w = 58.08$  g/mol,  $d = 0.79$  g/cm<sup>3</sup>) and n-butanol (C<sub>4</sub>H<sub>10</sub>O;  $M_w = 74.123$  g/mol,  $d = 0.81$  g/cm<sup>3</sup>) were purchased from Fisher Scientific, Loughborough, UK. Aluminium-backed TLC plates, precoated with silica gel 60 (5 x 3.5 cm) were from Sigma-Aldrich, Dorset, UK

##### Developing Solvent System/ Mobile Phase

The mobile phase consisted of n-butanol/ formic acid/ ultrapure water mixed together in 4:8:1 (v/v/v) ratio (Zhang et al., 2007).

##### Staining Reagent

For the staining reagent 2 g of diphenylamine were dissolved in about 10-20 ml of acetone (from total volume of 90 ml), while gently swirling, 2 ml of aniline and a remainder of acetone were added (Vázquez-Martínez & G. López, 2019). Thereafter, 10 ml of 85% H<sub>3</sub>PO<sub>4</sub> was added in portions, to avoid the creation of insoluble particles (Kocourek et al., 1966).

### Loading and developing protocol

Before each serialization, the TLC chamber was saturated with mobile phase for at least 10 min. In the meantime, 0.5 µl of heparin hydrolysates (5 mg/ml) were loaded onto TLC aluminium plates and air dried. The plates were developed in mobile phase (complete run until the plate edge) and dried at 105 °C for 5 min. The oven-dried, developed plates were further stained by dipping in diphenylamine-aniline-phosphoric acid reagent (DAP) (Zhang et al., 2007). Once air dried (Vázquez-Martínez & G. López, 2019), the plates were heated in oven at 105 °C for 20 min. The analysed plates were further store in freezer at -20 °C (can be stored for up to 6 months, without significant reduction in colour intensity)(Anderson et al., 2000).

## 2.3 ANALYSIS OF THE MOLECULAR WEIGHT OF HEPARIN HYDROLYSATES IN HYDROLYTIC ENVIRONMENTS

### 2.3.1 Introduction

Polysaccharide behaviour and functionality are driven by various physical properties, among which the molecular weight has been recognised as one of the most important (Harding et al., 1991, 2017). There is no exception in significance of molecular weight of heparin, upon which the specific medical response has been based (Lima et al., 2017; Mulloy et al., 2015; Onishi et al., 2016). Consequently, the identification of factors that may potentially influence the molecular weight of pharmacologically active heparin has taken on new guises. Therefore, the first analytical step in this research has been directed towards understanding the temporal relation between pH and temperature, applied in hydrolytic degradation, and the molecular weight of polymer. In this section, the details of analytical approach are summarised.

### 2.3.2 General aim of analytical method

Size exclusion chromatography (SEC) is an analytical technique applied for a routine molecular weight determination of macromolecules based on their hydrodynamic volume (size) (Brady et al., 2016; Morris et al., 2014; Podzimek, 2009). Once coupled with multi-angle light scattering (MALS) and refractive index (RI) detectors, SEC gains an advantage

of being an *absolute* method (no calibration curve needed). Hence is being employed as a method of choice for the characterisation of polysaccharides from various natural sources, including heparin (Bertini et al., 2017; Mulloy et al., 2014; Ouyang et al., 2017). In this study the advantage of SEC-MALS-RI chromatographic system has also been taken. The molecular weight of each hydrolytic fraction was evaluated according to the protocols described below.

### 2.3.3 Materials

All reagents applied in this study were of analytical grade or higher. All aqueous solutions were prepared in ultrapure water of resistivity  $\geq 18.2 \text{ M}\Omega\cdot\text{cm}$  at 25 °C, freshly drawn from Barnstead Nanopure Purification System (Thermo Fisher Scientific, Paisley, UK).

#### 2.3.3.1 Reagents

Mobile phase reagents, *i.e.*, ammonium acetate and sodium azide, together with Bovine Serum Albumin (BSA,  $M_w = 66 \text{ kDa}$ , Fisher Bioreagents™) applied as a system normalization standard were purchased from Fisher Scientific, Loughborough, UK.

#### 2.3.3.2 Standard solutions

##### Heparin sodium

The molecular weight reference standard of heparin sodium was prepared in the mobile phase at concentration of 5 mg/ml, following the procedure described in 2.2.3.3.

##### Bovine Serum Albumin

The system normalization standards (BSA) were prepared in the identical solvents to those of experimental samples (neutralized buffers pH 1 - 12). For this an accurately weighed BSA was dissolved with stirring (approx. 1 h) in appropriate buffering medium to prepare solution at concentration of 2 mg/ml. The standards were prepared fresh prior to each analytical sequence (Center for Macromolecular Interactions - University of Harvard).

*NOTE:* Bovine Serum Albumin has been applied as the system normalization standard to normalize detectors (relates the scattering at each individual detector to the right angle (90 °) detector) and align the peaks (this takes in to account the volume of solvent in the connectors between the detectors). The normalization of Size Exclusion Chromatography system with Multi-Angle Light-Scattering and Refractive Index detectors is a standard procedure, needed for each combination of column, buffer or changes in flow rate to minimise measurement error. It should be performed with well-behaved, monodisperse and relatively small macromolecule. BSA is an isotropic scatterer (*i.e.*, scatters light evenly in all directions) with a root-mean square radius <10 nm. These features are vital for MALS normalisation and consequently, BSA was the molecule of choice in this study. (Center for Macromolecular Interactions- University of Harvard, n.d.; Center for Macromolecular Interactions, n.d.; Mehn et al., 2016). BSA has been used previously as a normalization standard in heparin analysis (see for example Bertini et al., 2017; Mulloy et al., 2014; Ouyang et al., 2017; Pharmacopeial Forum, 2009) and under the studied conditions there was no evidence of denaturation. SEC-MALS-RI is *absolute* method and as such, it does not require the application of standard (*e.g.*, dextran) to generate molecular weight data (for more details see for example (Harding et al., 1991, 2017; Morris et al., 2014).

#### 2.3.3.3 *Sample preparation*

Heparin hydrolysates (acid, alkaline & TFA, see **2.2.4** for hydrolytic protocols) were thawed at room temperature prior to analysis (approx. thawing time 45 min). The concentrations of samples were equal to 5 mg/ml. Each analytical sample (including standards and blank) was filtered through 0.45 µm regenerated cellulose (RC) syringe filter (17 mm, Target2™, Thermo Fisher Scientific, Paisley, UK) directly in to an autosampler vial (9 mm, Screw Thread Vials, Thermo Scientific™).

#### 2.3.3.4 *Mobile phase*

The mobile phase of 0.1 M ammonium acetate and 0.05 % (w/v) sodium azide was prepared *via* direct dissolution of accurately weight salts in ultrapure water. The mobile phase was filtered under the vacuum (this also gives the advantage of degassing) through 0.45 µm pore-size nitrocellulose membrane.

### 2.3.4 Instrumental details

The average weight molecular weight and molecular weight distribution of heparin sodium were absolutely measured using size exclusion chromatography with an on-line light scattering module. The analytical compartment was composed from Agilent 1200 Infinity Series Analytical LC System (Agilent Technologies LDA UK Limited, Stockport, UK) connected to Wyatt Technology MALS (DAWN 8+) and RI (T-REX) detectors (Wyatt Technology Corporation, Santa Barbara, USA). Instrumental details and details of the connections between the particular components are shown in **Figure 2.1**. The system was coupled to TSK G4000 SW<sub>XL</sub> and TSK G3000 SW<sub>XL</sub> columns (7.8 mm × 30 cm, each) connected in series and protected by similarly packed guard column (6 mm × 4 cm) (Tosoh Bioscience, Tokyo, Japan).

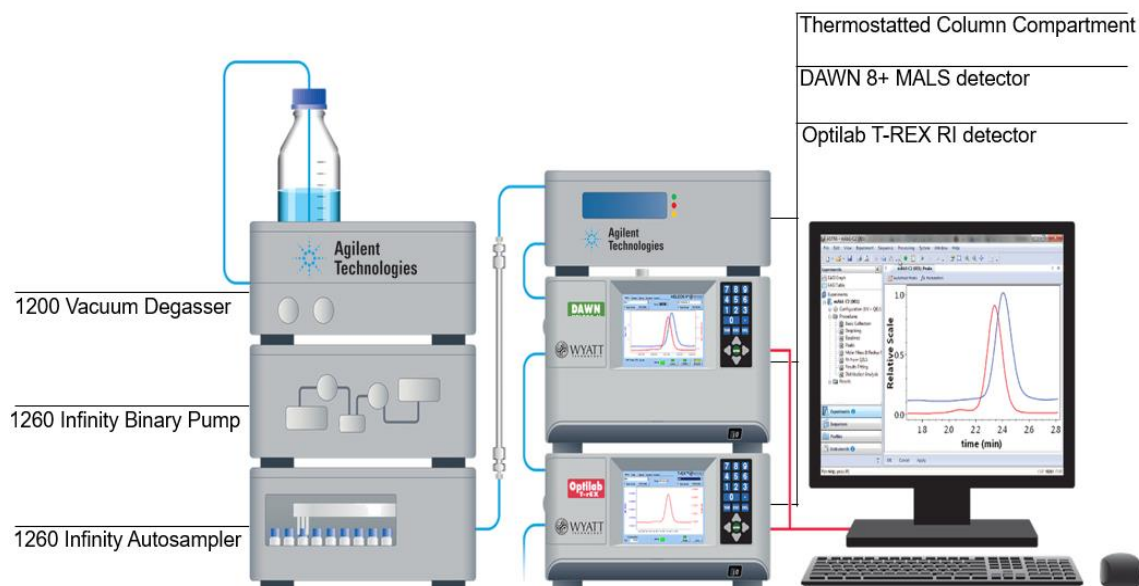


**Figure 2.1** SEC-MALS-RI system for molecular weight analysis includes HPLC instruments (Agilent Technologies), MALS and RI detectors (Wyatt Technology) and ASTRA® software loaded to computer receiver. Diagram adapted from Wyatt Technology (Wyatt Technology, n.d.).

### 2.3.5 Chromatographic protocol

The analytical columns were eluted with a 0.1 M NH<sub>4</sub>OAc + 0.05% (w/v) Na<sub>3</sub>N mobile phase at flow rate of 0.6 ml/min and temperature of 30 °C. The injection volume was set to 100 µl. The duration of a single run was set to 50 min.

### 2.3.5.1 *System normalization*

The normalization of the chromatographic system was performed prior to each analytical sequence, using a monodisperse BSA standard dissolved in identical solvents to those of experimental samples (Center for Macromolecular Interactions- University of Harvard, n.d.). Signal alignment, band broadening and detector normalization parameters were optimised for each individual buffering medium (x 12) and saved as methods. The methods were further applied in analysis of heparin hydrolysates, grouped per temperature and per pH (as described below).

### 2.3.5.2 *Analysis*

#### Heparin standard

The molecular weight reference standard of heparin sodium was analysed in separate sequence, under adequately normalized conditions.

#### Acid heparin hydrolysates

Heparin hydrolysates were divided into 3 lots, per temperature (40, 60 and 80 °C) and into 6 groups based on the pH (1 - 6) to which they were subjected. Each group consisted of 9 hydrolysed samples, arranged in order of ascending hydrolysis time (time points: 0, 0.25, 1, 3, 6, 9, 12, 24, 48 h) and sample blank (buffer analysed with regards to salt peak elution). Each group was analysed in separate sequence, under adequately normalized conditions. The hydrolysates acquired during the extended hydrolysis at pH 1/ 80 °C (60, 72, 96, 120, 144, 168 h) were also analysed in separate sequence, under adequately normalized conditions.

#### Alkaline heparin hydrolysates

The samples hydrolysed at alkaline conditions were also divided into 3 lots, per temperature (40, 60 and 80 °C) and into 6 groups based on the pH (7 - 12) to which they were subjected. The analysis followed the 'acid heparin hydrolysates' protocol described above.

### TFA heparin hydrolysates

Heparin samples degraded in TFA acid were arranged in order of ascending hydrolysis time (time points: 0, 1, 3, 6, 12, 24 h) and analysed in separate sequence, under adequately normalized conditions.

#### **2.3.6 Data processing**

The chromatograms were recorded with Astra software v. 6.1.5 (Wyatt Technology Corporation, Santa Barbara, USA). The refractive index increment ( $dn/dc$ ) applied for data processing equalled 0.131 ml/g for heparin and heparin hydrolysates (Mulloy et al., 2014) and 0.185 ml/g for BSA (Theisen et al., 2000). Numerical data were copied and organised in Microsoft Excel. The chromatograms were plotted in GraphPad Prism v. 8.4.1 (GraphPad Software, San Diego, USA).

## 2.4 CONFIRMATION OF HEPARIN CHAIN DEGRADATION - GEL ELECTROPHORESIS AS THE REDUCING ENDS ASSAY

### **2.4.1 Introduction**

In polysaccharides, one end of the chain possesses the reducing capacity, while the other end has a non-reducing character. Once subjected to degradation, the reducing power of polymer is usually reported to be inversely proportional to its weight-average molecular weight and is associated with the chain fragmentation (Harding et al., 2017). Therefore, measuring the change in reducing capacity of polysaccharide or proving the appearance of new reducing ends can be applied as confirmation assay of the glycosidic linkage scission. Herein, the reducing ends assay was employed to confirm the scission of heparin chain at studied hydrolytic conditions.

### **2.4.2 General aim of analytical method**

For the purpose of this study the polyacrylamide electrophoresis (PAGE) was adapted as the reducing ends assay. The method enables direct indication of saccharides in a degraded sample by labelling their reducing terminus with a fluorescence tag and further separation on acrylamide/bis-acrylamide gel during the electrophoretic run. The positions of the

potential hydrolytic digests are detected through the excitation of fluorescence tag in analytical transilluminator (Drummond et al., 2001; Turnbull, 2009) and often compared with a ladder of known standards. The materials and method applied in sequencing the potential post-hydrolytic heparin products are specified below.

### 2.4.3 Materials

All reagents applied in this study were of analytical grade or higher. All aqueous solutions were prepared in ultrapure water of resistivity  $\geq 18.2 \text{ M}\Omega\cdot\text{cm}$  at  $25 \text{ }^\circ\text{C}$ , freshly drawn from Barnstead Nanopure Purification System (Thermo Fisher Scientific, Paisley, UK).

#### 2.4.3.1 Reagents

##### Chemicals

Acrylamide/Bis-acrylamide dry powder blend (19:1, T50% - C5%, BioReagent), 2-amino-2-(hydroxymethyl)-1,3-propanediol (Trizma®,  $\geq 99.9\%$ ), 2-(N-morpholino)ethanesulfonic acid hydrate (MES,  $\geq 99\%$ , BioXtra), N,N,N',N'-tetramethylethylenediamine (TEMED,  $\sim 99\%$ , BioReagent), 7-amino-1,3-naphthalenedisulfonic acid monopotassium salt monohydrate (ANDSA,  $\geq 98\%$  BioReagent), glycerol ( $\geq 99\%$ ) and Azure A chloride were purchased from Sigma-Aldrich, Dorset, UK. Ethylene glycol (99.5%, ACROS Organics), ammonium persulfate (APS,  $\geq 99\%$ ), formamide (99.5%, ACROS Organics), tris(hydroxymethyl)aminomethane acetate salt (Tris-Acetate, 99%, ACROS Organics) and LDS sample buffer (NuPAGE™, ThermoFisher Scientific, UK) mixed with marker samples were purchased from Fisher Scientific, Loughborough, UK.

##### Oligosaccharide standards

Unsaturated oligosaccharides standards of disaccharide (dp2), tetrasaccharide (dp4) and hexasaccharide (dp6) derived from heparin by nitrous acid cleavage were kindly provided by Dr Edwin A. Yates (University of Liverpool). Unsaturated oligosaccharide standards of octasaccharide (dp8), decasaccharide (dp10) and tetradecasaccharide (dp14) derived from heparin by enzyme cleavage were purchased from Dextra (Reading, UK).

### 2.4.3.2 *Standard preparation*

#### Oligosaccharide standards

Each of six oligosaccharide standards was accurately weighed and dissolved (with 12 h stirring) in an appropriate volume of ultrapure water such that the final concentration was 2 mg/ml. Afterwards, 15 µl of each standard was transferred into an Eppendorf safe-lock tube, mixed together, frozen at -80 °C and lyophilized. The dry mixture of standards was further applied for fluorescence labelling (as described in **2.4.4.1**).

#### Heparin sodium standard

Heparin standard at concentration of 5 mg/ml was diluted from stock and prepared according to procedure described in **2.2.3.3**. The aqueous solution (20 µl) was transferred into an Eppendorf safe-lock tube, frozen at -80 °C and lyophilized. Dry sample was further applied for fluorescence labelling (as described below).

### 2.4.3.3 *Sample preparation*

#### Acidic heparin hydrolysates

The samples of heparin, hydrolysed at pH 1, pH 2 and pH 3 at temperatures of 40, 60 and 80 °C (see **2.2.4.1** for hydrolysis details) were thawed at room temperature (~ 45 min) and arranged in 9 groups (per pH, per temperature), in order of ascending hydrolysis time (0, 0.25, 1, 3, 6, 9, 12, 24, 48 h + extended hydrolysis samples pH 1/ 80 °C: 60, 72, 96, 120, 144 and 168 h). Each sample (2.5 ml) was loaded onto PD-10 desalting column, prepacked with Sephadex™ G-25 Medium (GE Healthcare Life Sciences, Little Chalfont, UK) and desalted with water according to spin protocol (GE Healthcare, 2007). The eluates were collected, freeze-dried, accurately weighed (various masses) and re-dissolved in appropriate volumes of ultrapure water for a final concentration of 5 mg/ml. Desalted hydrolysates (20 µl) were transferred to separate Eppendorf safe-lock tubes, frozen at -80°C and lyophilized. Dry samples were further applied for fluorescence labelling (as described below).

### Alkaline heparin hydrolysates

The samples of heparin, hydrolysed at pH 10, pH 11 and pH 12 at temperatures of 40, 60 and 80 °C (see 2.2.4.2 for hydrolysis details) were treated in the same way as acid heparin hydrolysates. The hydrolysates acquired during the extended hydrolysis at pH 12/ 80 °C (60.0, 72.0, 96.0, 120.0, 144.0 and 168.0 h) were desalted separately according to the same protocol.

### TFA heparin hydrolysates

The samples of heparin degraded in aqueous solutions of TFA (see 2.2.4.3 for degradation protocol) were thawed at room temperature (~ 45 min). Hydrolysates (20 µl) were transferred to separate Eppendorf safe-lock tubes, frozen at -80 °C and lyophilized. Dry samples were further applied for fluorescence labelling (as described below).

#### *2.4.3.4 Preparation of electrophoretic buffers and gel intermediates*

### Acrylamide/bis- acrylamide solution

The dry powder blend of acrylamide/bis- acrylamide (19:1) was reconstituted by slow addition of 43 ml of ultrapure water directly to the container and gently stirred for approx. 2 h (Turnbull, 2009).

### Tris-Acetate buffer

Tris-Acetate buffer at a concentration of 895 mM was prepared by dissolving the accurately weighed salt in appropriate volume of ultrapure water. The pH of buffer equalled 7 (no adjustment required).

### GlycoMap (GM) buffer

The GlycoMap buffer consisted of ethylene glycol/ ultrapure water/ 895 mM Tris-Acetate buffer (pH 7), mixed in 1.75: 1.75: 1.0 (v/v/v) ratio.

### Running buffer (10x)

Concentrated (10x) Tris-MES running buffer of pH 7.5 was prepared by dissolving accurately weighted Trizma and MES compounds in ultrapure water. For the pH 7.5, the mixing ratios were 1.0: 1.1: 27.5 (w/w/v), respectively.

### Overlay buffer

The overlay buffer consisted of GM buffer/ ultrapure water mixed in 1.0: 1.2 (v/v) ratio.

### Ammonium Persulfate (APS)

The aqueous solution of 10% (w/v) APS was prepared daily by dissolving the accurately weighed salt in ultrapure water.

### Loading buffer (2x)

Loading buffer consisted of ultrapure water/ 80% glycerol/ 895 mM Tris-Acetate mixed in 1.0: 1.25: 2.5 (v/v/v) ratio.

#### 2.4.3.5 *Degradation indicators*

### ANDSA solution

Saturated solution of 7-amino-1,3-naphthalenedisulfonic acid monopotassium salt monohydrate (ANDSA) was prepared daily by dissolving 80 mg of salt in 1000  $\mu$ l formamide (Turnbull, 2009).

### Azure A solution

The stock solution of 1% (w/v) Azure A chloride was prepared by dissolving the accurately weighed salt in ultrapure water.

## **2.4.4 Electrophoresis protocol**

### 2.4.4.1 *Fluorescent labelling*

The lyophilised samples of heparin hydrolysates (~100  $\mu$ g), heparin standard (~100  $\mu$ g) and oligosaccharides mix (~30  $\mu$ g per dp) were mixed with 25  $\mu$ l of saturated solution of

7-amino-1,3-naphthalenedisulfonic acid monopotassium monohydrate (ANDSA) in formamide and incubated for 16 h at 25 °C. The 33% acrylamide Tris-Acetate gels were cast prior to electrophoresis in 1.5 mm Invitrogen™ mini cassettes (80 mm x 80 mm, Thermo Fisher Scientific, Paisley, UK) with 10 well comb.

The mechanism of tagging, upon which the fluorescently active  $\alpha$ - and  $\beta$ -glycosylamines are formed, is presented in **Figure 2.2** below. The mechanism show attachment of the fluorescence label (ANDSA) to reducing terminus of saccharide *via* reductive amination, through the imine that can be reversibly reduced to a fluorescently responsive amine (Drummond et al., 2001; Vuong et al., 2017; Yan et al., 2015).

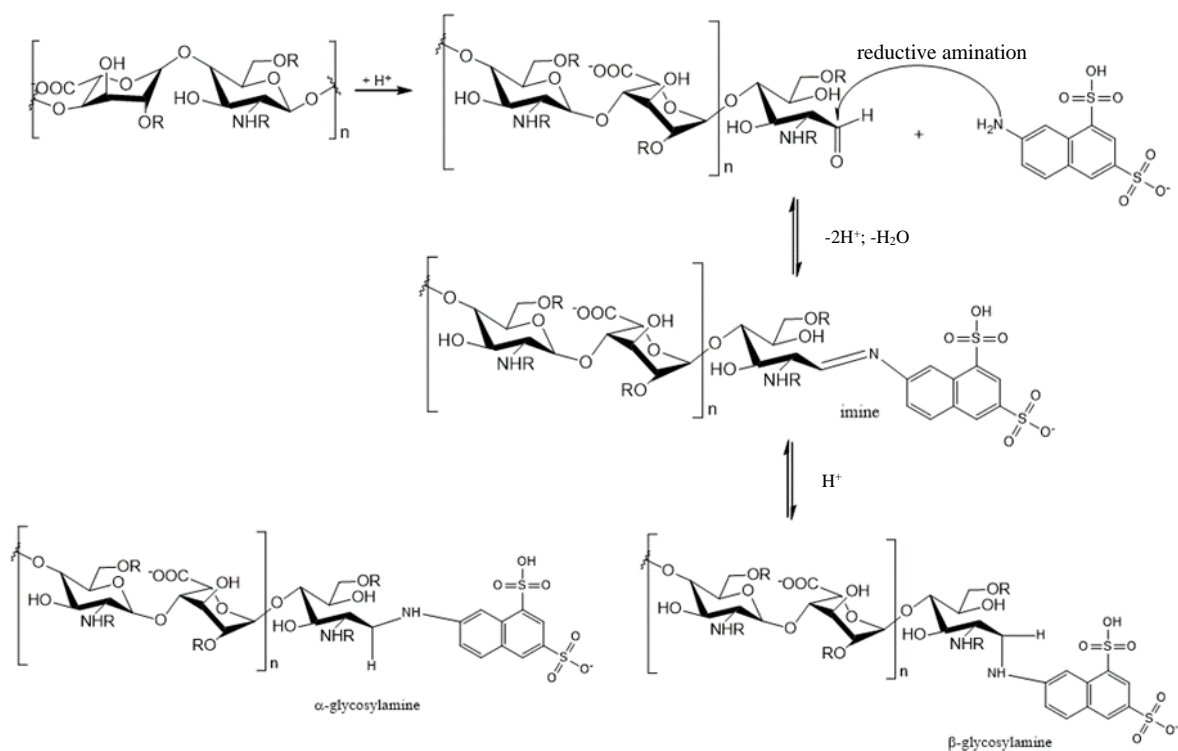


**Figure 2.2** Simplified mechanism of heparin saccharides labelling with ANDSA fluorophore. See for example, (Drummond et al., 2001; Vuong et al., 2017; Yan et al., 2015).

#### 2.4.4.2 *Acrylamide gel casting*

##### Resolving gel

For the resolving gel, the solutions of GM buffer (4.5 ml) and acrylamide (5.5 ml) were very gently mixed in a Falcon tube. Next, 10% (w/v) of APS (28  $\mu$ l) and TEMED (6.6  $\mu$ l) were added and mixed well. The resolving solution was immediately poured into the gel unit and overlaid with the overlay buffer (150  $\mu$ l) to block oxygen from inhibiting polymerization of the resolving gel. The gel polymerization was signalled/ visualized within approximately 30–45 min, by very sharp liquid-gel interface (Turnbull, 2009). After pouring away the overlay buffer and rinsing the top of the gel with water (remaining liquid blotted with paper filter), the stacking gel was casted.

##### Stacking gel

For the stacking gel the solutions of GM buffer (1.8 ml), acrylamide (0.6 ml) and ultrapure water (1.6 ml) were very gently mixed in a Falcon tube. Next, 10% (w/v) of APS (5  $\mu$ l) and TEMED (5  $\mu$ l) were added and mixed well. The stacking gel solution was poured directly over the resolving gel and the well-forming comb was insert immediately. The gel was left to polymerise for approximately 60 minutes. Afterwards, the comb was carefully removed, the gel's wells were washed with running buffer (1x) and the cassettes were placed in electrophoresis tank, ready to load.

#### 2.4.4.3 *Electrophoresis*

The electrophoresis tank was placed in the ice water-bath, to dissipate the heat generated during the run. The tank chambers with the gel units were filled with the Tris-MES running buffer (1x). The samples of fluorescently labelled heparin hydrolysate standards and oligosaccharides were mixed with loading buffer (1:1 ratio). The samples (20  $\mu$ l) were carefully loaded onto the gel wells. The oligosaccharides mixed with LDS sample buffer, containing phenol red and Coomassie G250 dyes, were loaded into separate wells to track the separation progress. The electrophoresis was terminated when the marker reached about 5 cm from the gel bottom (Turnbull, 2009). The electrophoresis protocol is graphically summarised in **Figure 2.3**.

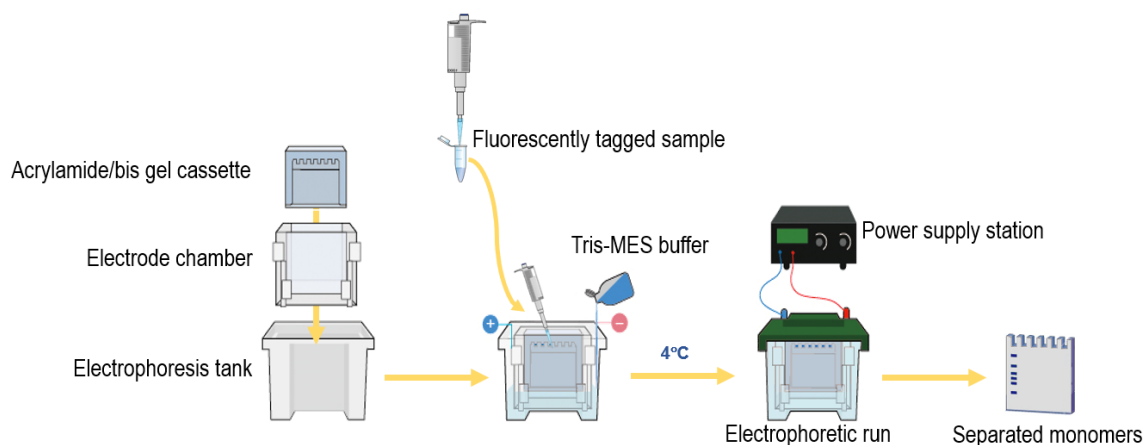


**Figure 2.3** Graphical summary of the PAGE electrophoresis protocol, applied as the reducing ends assay to confirm the scission of heparin chain, at studied hydrolytic conditions.

#### 2.4.4.4 Azure A staining

Once the terminated PAGE (polyacrylamide gel electrophoresis) gels were fluorescently visualised and digitalized. The sets were stained with a 0.08% solution of Azure A, diluted directly from stock, for 1 h at room temperature (Powell et al., 2010). The excess of the blue stain was washed overnight with deionised H<sub>2</sub>O on the orbital shaker (VWR Standard).

Metachromatic dyes, such as Azure A, interact with polyanionic polysaccharides due to an electrostatic interaction, creating non-covalently bound complexes (Ehrlich & Stivala, 1973; Mulloy, 2012; Warttinger et al., 2017). The schematic mechanism of heparin complexation with Azure A is presented in **Figure 2.4**. As the colour intensity of heparin-Azure A complex is directly proportional to charge density (and therefore sulfation), it is easy to assess changes in sulfation pattern of polysaccharide. Therefore, Azure A staining was not only applied in spectrophotometric analysis, but also for quick, naked-eye estimations of desulfation.

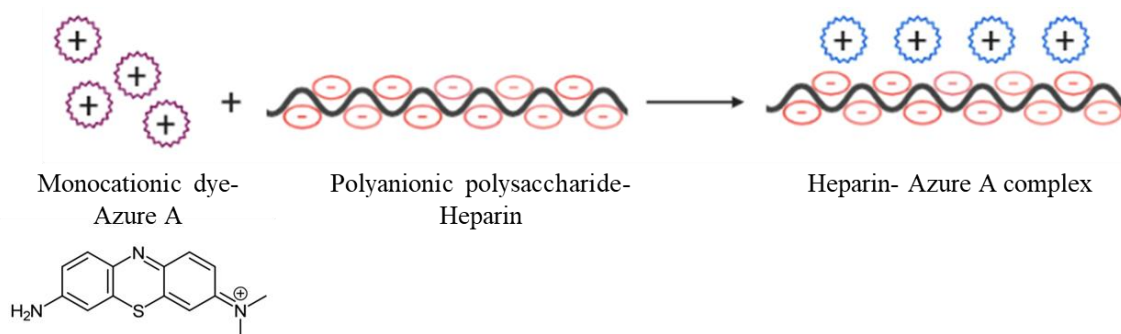


**Figure 2.4** Schematic representation of Azure A dye heparin staining (Ehrlich & Stivala, 1973; Mulloy, 2012; Warttinger et al., 2017).

### 2.4.5 Data processing

The terminated PAGE gels were pulled out from the casting cassettes and viewed on a UV transilluminator ( $\lambda_{\max} = 302 \text{ nm}$ ). The images were recorded using GeneSnap software with a gel imaging camera (G-BOX fluorescence system, Syngene, Cambridge, UK). The Azure A-stained gels were recorded with 12 MP f/1.7 1.4-micron pixels OIS camera (Samsung Galaxy S7) with the light adjustment.

## 2.5 UV-VIS SPECTROPHOTOMETRY FOR THE DETECTION OF COLOUR CHANGE OF HYDROLYSED SAMPLES

### 2.5.1 Introduction

Spectrophotometry employs light to interact with molecule, which gives an opportunity to vet the sample and examine its coherence or structure. The visible (Vis) and ultraviolet (UV) radiation have been systematically applied to probe the features of biomacromolecules (Hofmann, 2010; Murray et al., 1994). Polysaccharides are generally invisible in UV-Vis, due to the lack of interactive chromophores that absorb light (Harding, 2005). Spectrophotometric scanning usually requires derivatisation of samples and/or their interaction with UV-Vis active reagents (Cui, 2005; Hofmann, 2010). The assays designed for this purpose give a chance to apply the UV-Vis analysis in quantitative studies of carbohydrates structures, although, the assays themselves often require the application of very harsh conditions, which may be incompatible with experimental questions. In such cases UV-VIS spectroscopy has been applied as qualitative techniques, especially in catalysed hydrolytic studies, where one looks at the development of absorption capabilities

of polysaccharide, as a result of environmentally influenced structural changes (Cui, 2005; Finch, 1999; Zhou et al., 2016).

### **2.5.2 General aim of analytical method**

In the past, strong alkaline environments have been proved to cleave the glycosidic bond between the sugar and hexuronic acid units of polysaccharides, releasing the 4,5-unsaturated acid unit at the non-reducing end (Jaseja et al., 1989; Rej & Perlin, 1990; Zhang et al., 2006). The unsaturated centre constitutes a natural UV chromophore (232 nm), advantageous for the qualitative UV-Vis detection. To confirm if similar modification took place in this study, the absorbance of chosen alkaline heparin hydrolysates was measured according to protocol summarised below. On the other hand, since aqueous solutions of heparin exposed to strong acidic environments have been shown to have affinity toward the colour change (Jandik et al., 1996), acid hydrolysed samples were also examined using UV-Vis spectrophotometry.

### **2.5.3 Materials**

All aqueous solutions were prepared in ultrapure water of resistivity  $\geq 18.2$  M $\Omega$ .cm at 25 °C, freshly drawn from Barnstead Nanopure Purification System (Thermo Fisher Scientific, Paisley, UK).

#### *2.5.3.1 Sample preparation*

The aqueous solutions of heparin, hydrolysed at pH 1 - 3, pH 10 - 12 at 40, 60 and 80 °C (time points: 0, 0.25, 1, 3, 6, 9, 12, 24, 48 h + extended hydrolysis: 60, 72, 96, 120, 144 and 168 h) and TFA hydrolysates (see **2.2.4** for hydrolytic protocols) submitted to UV-Vis analysis were prepared at concentration of 500 ppm from concentrated, desalted samples (5000 ppm/ 5 mg/ml, see **2.4.3.3** for desalting protocol) and left overnight at 4 °C. Each sample was centrifuged prior to analysis, to minimise the influence of aggregates in carried measurements.

#### **2.5.4 Measurements**

All spectrophotometric measurements were made with Agilent Cary 60 UV-Vis spectrophotometer (Agilent Technologies, Cheadle, UK). The spectra were recorded at wavelength range between 200 and 800 nm, against a water blank, at rate of 4800 nm/ min with 1.5 nm resolution. The measurements were taken in high precision silica cells (1.4 ml, Hellma Analytics, UK) at room temperature. The analytical protocol was triplicated for each sample.

#### **2.5.5 Data processing**

The spectra were recorded with WinUV software v. 5.0.0. Numerical data were copied and organised in Microsoft Excel. The graphs were transformed in GraphPad Prism v. 8.4.1 (GraphPad Software, San Diego, CA, USA).

### **2.6 THE COMPLETE SACCHARIDE ANALYSIS OF POST-HYDROLYTIC SAMPLES OF HEPARIN**

#### **2.6.1 Introduction**

The complete saccharide analysis of degraded samples has been successfully applied in structural characterisation of various complex polysaccharides (Cui, 2005; Robyt, 1998). Besides the advantage of structure elucidation, the compositional study of post-hydrolytic samples can be certainly adapted as an effective tool to understand the reactivity/ stability of compound at the applied conditions. This section provides experimental details of the saccharide analysis of heparin hydrolysates, employed to supplement the picture of the successive degradation mechanism of molecule.

#### **2.6.2 General aim of analytical method**

High-performance anion-exchange chromatography coupled with a pulsed amperometric detector (HPAEC-PAD) has been found invaluable in analysis of all classes of monosaccharides and oligosaccharides, without the need of prior derivatisation. The application of appropriate elution method (isocratic or gradient) with the mobile phase of adequate ionic strength and alkaline pH, expands the saccharides ionisation range.

Consequently, the neutral, amino and acidic sugars can be separated in a single run (Alyassin et al., 2020; Hardy & Reid Townsend, 1994; Zhang et al., 2012). The advantage of a single chromatographic separation of various saccharides was taken during the analysis of post-hydrolytic samples of heparin. The analytical procedures applied in this study are described in following sections.

### 2.6.3 Materials

All reagents applied in this study were of analytical grade or higher. All aqueous solutions were prepared in ultrapure water of resistivity  $\geq 18.2 \text{ M}\Omega\cdot\text{cm}$  at 25 °C, freshly drawn from Barnstead Nanopure Purification System (Thermo Fisher Scientific, Paisley, UK).

#### 2.6.3.1 Reagents

##### Chemicals

Aqueous solution of concentrated sodium hydroxide (NaOH, 50% w/v,) was purchased from Fisher Scientific, Loughborough, UK. Anhydrous salt of sodium acetate (NaOAc,  $\geq 99\%$ ) was purchased from Sigma-Aldrich, Dorset, UK.

##### Monosaccharide standards

The standards of D-galactosamine hydrochloride (GalN, 99%, Acros Organics), D-glucosamine hydrochloride (GlcN, 98+%, Acros Organics), D-fucose (Fuc, 98%, Alfa Aesar), D-glucuronic acid (GlcA, 98+%, Alfa Aesar) and D-galacturonic acid monohydrate (GalA, 97%, Alfa Aesar) were purchased from Fisher Scientific, Loughborough, UK. *N*-acetyl-D-glucosamine (GlcNAc,  $\geq 99\%$ ), *N*-acetyl-D-glucosamine-6-sulfate sodium salt (GlcNAc(6S),  $\geq 97\%$ ) were purchased from Sigma-Aldrich, Dorset, UK. Sodium salts of D-glucosamine-3-*O*-sulfate (GlcN(3S)), D-glucosamine-6-*O*-sulfate (GlcN(6S)), D-glucosamine-2-*N*-6-*O*-disulfate (GlcNS(6S)) and D-glucosamine-2-*N*-3-*O*-disulfate (GlcNS(3S)) were ordered from Dextra Laboratories Ltd, Reading, UK. Sodium salts of D-glucosamine-2-*N*-sulfate (GlcNS) was purchased from Carbosynth Limited, Compton, UK. L-iduronic acid (IdoA) was ordered from Synthose, Ontario, Canada.

### 2.6.3.2 Standards preparation

#### Monosaccharide standards

The monosaccharide standards of Fuc, GluA, GalA, IduA, GalN, GlcN, GlcN(3S), GlcN(6S), GlcNS, GlcNS(3S), GlcNS(6S), GlcNAc and GlcNAc(6S), were accurately weighed (various masses) and dissolved in appropriate amount of ultrapure water with 12 h stirring. The final concentration was equal to 5000 ppm (5 mg/ml, stock solutions) per monosaccharide. Each stock solution was further diluted to 650 ppm and used in the preparation of series of multi-saccharides solutions at concentrations of 0.5, 1.0, 5.0, 10.0, 25, 50 ppm per saccharide, to be used as analytical standards. Each monosaccharide was also prepared at individual concentration of 50 ppm.

### 2.6.3.3 Sample preparation

The aqueous solutions of heparin hydrolysates (acid, alkaline & TFA, see 2.2.4 for hydrolytic protocols) submitted to HPAEC-PAD analysis were prepared at concentration of 500 ppm from concentrated samples (5000 ppm/ 5 mg/ml), thawed at room temperature prior to the analysis (~ 45 min). Samples were spiked with internal standard of D-fucose, to its final concentration of 50 ppm.

Each analytical sample (including standards) was filtered through a 0.45 µm regenerated cellulose (RC) syringe filter (17 mm, Target2™, Thermo Fisher Scientific, Paisley, UK) directly to autosampler vial (9 mm, Screw Thread Vials, Thermo Scientific™).

### 2.6.3.4 Mobile phases

The stock of sodium acetate (0.6 M) was prepared in advance, *via* direct dissolution of accurately weighed salts in ultrapure water. The solution was sonicated and filtered under the vacuum (degassing) through 0.45 µm pore-size nitrocellulose membrane. Concentrated sodium hydroxide (50%, w/v, *aq*) was used as supplied.

The multi-step gradient protocol used in this method required preparation of two different mobile phases at various concentrations of NaOH and NaOAc. Thus, mobile phase A was

prepared at single concentration of NaOH equal to 15 mM, while mobile phase B consisted of 15 mM NaOH fixed with 150 mM NaOAc (Zhang et al., 2012).

#### **2.6.4 Instrumental details**

The analysis was proceeded on Dionex ICS-3000 Ion Chromatography System (Dionex Corporation, USA) with Reagent-Free Eluent Generation. The analytical compartment was composed from Eluent Organiser with Dual Pump Channel, Detector Module, Autosampler and Pulsed Amperometric Detector with disposable gold working electrode. The saccharides separation was carried out on CarboPac PA20 analytical column (3 x 150 mm), protected by similarly packed guard column (3 x 30 mm, BioLac™, Thermo Fisher Scientific, Paisley, UK) at room temperature.

#### **2.6.5 Chromatographic protocol**

Mobile phases were delivered at 0.3 ml/min, with isocratic flow of mobile phase A (15 mM NaOH) for the first 15 min, followed by linear gradient of mobile phase B (150 mM NaOAc + 15 mM NaOH) for the next 45 min (Zhang et al., 2012). Helium was applied as a carrier gas at pressure of 50 - 60 psi. The injection volume was set to 25 µl.

The standards and TFA hydrolysates were analysed in triplicate. The analytical repetition of heparin hydrolysates varied and is specified in appropriate sections. The individual analysis of monosaccharides confirmed the retention times of each standard in the mixture. The acquisition time was set to 60 min.

##### *2.6.5.1 Analysis of standards*

Firstly, to identify the retention time of an individual standard, the samples at single monosaccharide concentration of 50 ppm were injected. Once the retention times were determined, the set of multi-saccharide standards (concentrations given in **2.6.3.2**) were analysed in triplicate, for the purpose of qualitative and quantitative evaluation of the applied method. The analysis of standards was repeated with each analytical sequence of heparin hydrolysates, for the purpose of qualitative study. The quantitative calculations were based on the internal standard method (D-fucose).

### 2.6.5.2 *Analysis of heparin samples*

#### Acid heparin hydrolysates

The heparin samples hydrolysed in acidic environments were organised similarly to those submitted to SEC-MALS-RI analysis, described in 2.3.5. The hydrolysates were analysed per temperature, from the highest to the lowest pH (pH 6 → pH 1), with ascending hydrolysis time (time points: 0, 0.25, 1, 3, 6, 9, 12, 24, 48 h + extended hydrolysis samples pH 1/ 80 °C: 60, 72, 96, 120, 144 and 168 h). The samples hydrolysed at pH 1 were run in triplicate, while samples hydrolysed at pH 2 – 6 were analysed in duplicate.

#### Alkaline heparin hydrolysates

The alkaline hydrolysates were analysed in the same manner as heparin samples degraded in acidic environments). The hydrolysates were analysed per temperature, from the lowest to the highest pH (pH 7 → pH 12) with ascending hydrolysis time (time points: 0, 0.25, 1, 3, 6, 9, 12, 24, 48 h + extended hydrolysis samples pH 12/ 80 °C: 60, 72, 96, 120, 144 and 168 h). The samples hydrolysed at pH 12 were run in triplicate, while samples hydrolysed at pH 7 – 11 were analysed in duplicate.

#### TFA heparin hydrolysates

Heparin samples degraded in TFA acid were arranged in order of ascending hydrolysis time (time points: 0, 1, 3, 6, 12, 24 h) and analysed in triplicate in separate sequence.

### **2.6.6 Data processing**

The chromatograms were recorded with Chromeleon software v. 6.8. (Thermo Fisher Scientific, Paisley, UK). Numerical data were copied and organised in Microsoft Excel. The chromatographic plots and statistical analysis were performed in GraphPad Prism v. 8.4.1 (GraphPad Software, San Diego, USA).

## 2.7 THE QUANTITATIVE ANALYSIS OF ANIONS IN POST-HYDROLYTIC SAMPLES OF HEPARIN

### 2.7.1 Introduction

Amongst the family of glycosaminoglycans, heparin carries the title of the most highly sulfated (Linhardt, 2003). However, the sulfo groups covalently linked to heparin are relatively labile and can be removed from the polymer chain when exposed to acidic or alkaline treatments (Bedini et al., 2017; Liu et al., 2014). Changes in sulfation pattern most certainly affects the pharmacological activity of the compound (Jorpes & Bergström, 1939; Mulloy et al., 2015; Raman et al., 2013), but the information regarding the influence of sulfate loss on molecular weight is limited. Therefore, this study aimed to clarify how the amount of released sulfate influences the total molecular weight of polysaccharide in regard to applied conditions. The following sections include detailed information on the analytical procedure adopted to quantify the sulfate discharged from the heparin chain.

### 2.7.2 General aim of analytical method

In aqueous solutions, the sulfate groups liberated from heparin chain are present in form of free inorganic anions and therefore can be considered as the individual components of the mixture. Once the column of appropriate matrix is chosen, the high-performance anion exchange chromatography (HPAEC) gives the opportunity to separate negatively charged sulfate ions from the polymer residues. Furthermore, coupling the chromatographic system with conductivity detector (CD) allows accurate quantification of the inorganic anions. The instrumental and methodological specification of HPAEC-CD system used for the quantitative analysis of heparin anions are given in the following sections.

### 2.7.3 Materials

All reagents applied in this study were of analytical grade or higher. All aqueous solutions were prepared in ultrapure water of resistivity  $\geq 18.2 \text{ M}\Omega\cdot\text{cm}$  at  $25 \text{ }^\circ\text{C}$ , freshly drawn from Barnstead Nanopure Purification System (Thermo Fisher Scientific, Paisley, UK).

### 2.7.3.1 Reagents

Certified multi-anion ( $F^-$ ,  $Cl^-$ ,  $Br^-$ ,  $NO_3^-$ ,  $SO_4^{2-}$ ,  $PO_4^{3-}$ ; 10 ppm  $\pm$  0.2% per each anion), as well as acetate and citrate anions (1000 ppm, TraceCERT®) standards were purchased from Sigma-Aldrich, Dorset, UK and treated as the stock solutions. Sodium carbonate ( $\geq$  99.0%, BioXtra) and sodium bicarbonate (99.5%, Acros Organics) used for mobile phase preparation were ordered from Fisher Scientific, Loughborough, UK.

### 2.7.3.2 Standards preparation

#### Anion standards

All standards used in this study were prepared from certified stocks. The solutions of multi-anion standard, as well as solutions of sodium acetate (separate) were prepared at concentrations of 0.1, 0.5, 1.0, 3.0 and 5.0 ppm per each anion. The solution of sodium citrate was prepared at single concentration of 10.0 ppm.

#### Heparin standard for free anion detection

Heparin standard was prepared at the concentration of 10.0 ppm from stock (see 2.2.3.3 for more details regarding stock) and analysed for the content of free anions.

### 2.7.3.3 Sample preparation

Heparin hydrolysates (acid, alkaline & TFA, see 2.2.4 for hydrolytic protocols) submitted to HPAEC-CD analysis were prepared at concentration of 10.0 ppm from concentrated samples (5 mg/ml), thawed at room temperature prior to the analysis (~ 45 min).

Each analytical sample (including standards and blank) was filtered through 0.45  $\mu$ m polyethersulfone membrane (PES) syringe filters (13 mm, Azure, Gilson Scientific, UK) prior to the injection.

### 2.7.3.4 Mobile phase

The mobile phase consisted of a mixture of 3.2 mM sodium carbonate and 1.0 mM sodium bicarbonate was prepared *via* direct dissolution of accurately weighed salts in ultrapure

water. The eluent was sonicated, and vacuum filtered (degassing) through 0.45 µm pore-size nitrocellulose membrane.

#### **2.7.4 Instrumental details**

The HPAEC-CD analysis was performed on Dionex ICS 1500 ion chromatography system with Self Regenerating Suppressor (SRS) and DS6 conductivity detector (Dionex, Camberley, UK). The separation was carried out on Dionex™ IonPac™ AS14 IC column (4 x 250 mm), protected by similarly packed guard column (4 x 50 mm, Thermo Fisher Scientific, Hemel Hempstead, UK) at 30 °C.

#### **2.7.5 Chromatographic protocol**

Mobile phase was delivered at 1.2 ml/min with isocratic flow. Samples were injected manually at volume of 25 µl.

##### *2.7.5.1 Analysis of standards*

##### Inorganic anions

The set of multi-anion and acetate anion standards were analysed in triplicate. The acquisition time was set to 15 min. The analysis of standards was repeated with each buffer (pH 1 – 12) prior to analysis of heparin hydrolysates, for the purpose of qualitative study.

##### Organic anions

According to information provided by chromatographic column supplier, citrate anions should not interfere with the detection of inorganic peaks of interest (Thermo Fisher Scientific, personal correspondence). However, if the concentration is too high, these may be strongly retained, influencing the baseline and/or eluting late from the column. Citrate salts were used for the preparation of buffers at pH from 3 to 6 (see 2.2.3.4). Thus, the compatibility of chromatographic system was verified (in triplicate) using 10 ppm sodium citrate standard. The acquisition time was set to 45 min.

### Heparin standard

The heparin standard analysed for free anion content was run in triplicate. The acquisition time was set to 15 min.

#### 2.7.5.2 *Analysis of heparin hydrolysates*

Hydrolysed heparin samples were injected per pH/ per temperature with ascending hydrolysis time (time points: 0, 0.25, 1, 3, 6, 9, 12, 24, 48 h + extended hydrolysis samples pH 1 and pH 12/ 80 °C: 60, 72, 96, 120, 144 and 168 h). The acquisition time was set to 15 min for samples buffered at pH 1 - 2, pH 7 - 12 and TFA degraded heparins, while samples buffered at pH 3 - 6 were run for 30 min. All samples were analysed in triplicate. The system was washed overnight with mobile phase between the analyses of samples buffered at different pHs.

#### **2.7.6 Data processing**

The chromatograms were recorded with Chromeleon software v. 6.8. (Thermo Fisher Scientific, Paisley, UK). Numerical data were copied and organised in Microsoft Excel. The chromatographic plots and statistical analysis were performed in GraphPad Prism v. 8.4.1 (GraphPad Software, San Diego, CA, USA).

## 2.8 AN INSIDE LOOK INTO STRUCTURAL CHANGES OF HEPARIN WITHIN THE CONTEXT OF HYDROLYTIC CONDITIONS

### **2.8.1 Introduction**

Presumably, a technique that would enable the ‘real-time’ observation of changes taking the place within the structure of macromolecule would resolve the difficulties with interpretations of influences of various environmental factors toward their stability. Unfortunately, the possibilities to run the experiment with a simultaneous observation of intramolecular modifications are (for now) very limited, especially when a compound as complex as heparin is being considered. Nevertheless, there are indirect ways to get an inside look into the structural changes of molecule. In this respect, nuclear magnetic resonance (NMR) spectroscopy is (in the author’s opinion) one of the most adaptable

techniques. This section summarises the utilisation of NMR to follow the structural changes within the heparin molecule in the context of (chosen) hydrolytic conditions.

### **2.8.2 General aim of analytical method**

NMR spectroscopy measures the absorbance of electromagnetic energy at radio frequencies, characteristic for certain 'NMR active' isotopes, which are further expressed in form of chemical shifts (Murray et al., 1994). The chemical shift is a function of the chemical group that contains the absorbing isotope and neighbouring active nuclei. Consequently, NMR spectra not only fingerprints the structure of molecule, but also allows the reconstruction of its three-dimensional arrangement.

Accessing the structure of heparin through the high-resolution instruments considerably expanded knowledge on the elemental building blocks of molecule. Nowadays, besides the major saccharide units, the minor residues in polysaccharide chain are being recognised (Guerrini et al., 2001; Zhang et al., 2011). The advanced NMR analysis has been applied to access other structural features, like the sulfation/ acetylation patterns, to understand the conformation and dynamics of heparin, to model the configuration of glycosidic linkages, and understand the protein binding region (Hricovíni, 2015; Mulloy et al., 2012; Yates et al., 2000). Among information that may be gathered *via* NMR, details of the structural features of molecule (such as sulfation/ acetylation patterns) and configuration of glycosidic linkages are the essential ones, when studying the intramolecular changes invoked by the external conditions. The comparison of spectra acquired before and after the application of stressing factors allows not only the detection of structural modifications, but also to ascertain the moment of change.

In cases where the complexity of heparin solution interferes with a quality of 1D NMR spectra (due to the peak overlap), multidimensional techniques can be applied. In certain circumstances, applying the frequency in two dimensions under the optimised carefully chosen conditions reveals more information than one-dimensional data. Apart from structural and impurity identification, 2D NMR experiments permit quantitative analysis of monosaccharide units (with a tolerable error), recognition of heparin in crude half-product or differentiation between the heparin (animal) origin (Guerrini et al., 2009; Guerrini et al., 2005; Keire et al., 2013; Mauri, Boccardi, et al., 2017; Mauri, Marinozzi, et

al., 2017; Nidhi et al., 2011; St Ange et al., 2016). Among various multidimensional techniques Heteronuclear Single Quantum Coherence (HSQC), that directly expresses  $^{13}\text{C}$ – $^1\text{H}$  coupling, is the most frequently applied technique in heparin research (Monakhova, Fareed, et al., 2018).

The common application of HSQC method resulted in well-established peak library, which was utilised in subsequent experiments. To understand the structural transformation within the heparin molecule, the NMR spectra of various post-hydrolytic samples were compared with the heparin standard. Details of the experimental protocols applied in this study are specified in following sections.

### 2.8.3 Materials

#### 2.8.3.1 Reagents

##### Chemicals

Deuterium oxide ( $\text{D}_2\text{O}$ ,  $\geq 99.96\%$  D, MagniSolv<sup>TM</sup>), deuterium oxide containing sodium salt of 3-(trimethylsilyl) propionic-2,2,3,3- $\text{d}_4$  acid (TPS, 0.05 wt.% in  $\text{D}_2\text{O}$ , 99.9% D) for NMR spectroscopy were purchased from Sigma-Aldrich, Dorset, UK.

##### Heparin Standards

Details regarding the heparin sodium used as the reference standard are given in 2.2.3.1. The standard of N-desulfated heparin was kindly provided by Dr Edwin A. Yates (University of Liverpool).

#### 2.8.3.2 Heparin standard preparation

Prior to NMR analysis, 50 mg of heparin sodium was dissolved in 0.5 ml  $\text{D}_2\text{O}$  and freeze-dried repeatedly to remove the exchangeable protons. The thoroughly dried sample was redissolved in ~0.6 ml  $\text{D}_2\text{O}$  mixed with internal NMR standard (acetone 10  $\mu\text{l}$ /100 ml  $\text{D}_2\text{O}$  or TPS, specified per sample in protocol and/or in the results chapter) and transferred to the precision grade NMR tube (OD 5 mm, borosilicate glass, Sigma-Aldrich, Dorset, UK) for analysis. As the NMR studies were carried for qualitative purpose, the internal standards were used for referencing spectra, with  $\delta$  (chemical shift) TPS of 0.00/0.00 ppm ( $^1\text{H}/^{13}\text{C}$ )

and  $\delta$  Acetone of 2.22/32.93 ppm (*Human Metabolome Database*, n.d.-a). The desulfated standards were treated similarly, although with less material (20 mg).

### 2.8.3.3 *Hydrolysed samples preparation*

Heparin hydrolysates aliquoted at pH 1 and pH 12 at 24, 48, 96 and 168 hours of degradation at 40, 60 and 80 °C (see **2.2.4** for the hydrolysis details) were desalted according to protocol given in **section 2.4.3.3** and freeze-dried. Dry samples were accurately weighed (various masses) and repeatedly lyophilized against D<sub>2</sub>O. Proton-exchanged hydrolysates were further redissolved in ~0.6 ml of solvent with internal standard and transferred to the precision grade NMR tube for analysis.

## 2.8.4 **NMR system details**

### 2.8.4.1 *Instrumental details*

NMR measurements were performed on Bruker Advance Neo 600 MHz spectrometer (Bruker Biospin, Rheinstetten, Germany) equipped with Bruker Prodigy Cryoprobe and 24-position SampleCase autosampler.

### 2.8.4.2 *Acquisition details*

#### One-dimensional NMR

The one-dimensional <sup>1</sup>H spectra were recorded at 60 °C (333 K) with a standard pulse program (zg30), 2 sec delay for 16 scans (if not stated otherwise) and total acquisition time of 2.75 sec. The carbon <sup>13</sup>C analysis, based on standard pulse program (zgpg30), was approached with 1 sec delay, 512 scans (if not stated otherwise) and total acquisition time of 1.61 sec.

#### Two-dimensional NMR

The two-dimensional <sup>1</sup>H-<sup>13</sup>C heteronuclear single quantum coherence (HSQC) spectra were recorded at 60 °C (333 K) using Bruker library pulse program (hsqcedetgppsp.3), with 1.44 sec delay for single scan (if not stated otherwise) and total acquisition time of 0.129

sec. The transmitter frequency offset was equal to 5.305 ppm for  $^1\text{H}$  and 62 ppm for  $^{13}\text{C}$ , while the  $^1J_{\text{C-H}}$  coupling constant was set to 150 Hz.

### **2.8.5 Analytical protocols**

The one- and two-dimensional NMR spectra of heparin standards and hydrolysates (prepared according to protocol given in **sections 2.8.3.2** and **2.8.3.3**, above) were recorded at 60 °C (333 K). The acquisition setups are given in **section 2.8.4.2**, above.

### **2.8.6 Data processing**

NMR data were recorded automatically using Bruker's TopSpin software v 4.0.6. Spectra were manually phased, and baseline corrected. Chemical shifts were indicated in *ppm* units, relatively to an internal reference standard.

# 3

## STABILITY OF HEPARIN IN ACIDIC ENVIRONMENTS

---

This chapter has been reproduced in part with permission from *ACS Appl. Mater. Interfaces* 2021, 13, 4, 5551–5563. Copyright 2021 American Chemical Society.

<https://doi.org/10.1021/acsami.0c20198>

### 3.1 INTRODUCTION

The fundamentals of chemical stability of heparin in mild acidic conditions are based on the work of Danishefsky et al. (1960), who examined its hydrolytic behaviour in such conditions. This early study already suggested the lability of heparin to hydrolytic sulfate loss and questioned the capacity of glycosidic scission, which would usually be expected as a result of acid catalysed hydrolytic attack towards the polysaccharide chain (Cui, 2005; Danishefsky et al., 1960; Galanos et al., 1969). Fifteen years later, Inoue and Nagasawa (1976) expanded the scope of degradative conditions and continued desulfation studies in hydrolytic and solvolytic environments. Their work was a proof of concept of ordered N-/O-desulfation, mentioned by Danishefsky et al. (1960), and a key to further, deliberately performed solvolytic modifications of heparin (Baumann et al., 1998; Kariya et al., 2000; Nagasawa et al., 1977). Although solvolytic-induced, these studies established the high lability of N-sulfate (NS-) of heparin to mild acidic conditions and specified the environments necessary to selectively target 6-O-sulfate (6OS-), with the following (although less sufficient) 2-O-desulfation (2OS-). Without detracting from the importance of these findings, the side-effect of solvolytic studies was the generalisation, regardless of surrounding medium, of the desulfation order of heparin to N-desulfation as first and most

rapid, 6-O-desulfation as next, much slower process and at last, 2-O-desulfation, which can be schematically written as: 2OS < 6OS << NS.

On the other hand, the resistance of heparin chains to acid catalysed glycosidic scission, also mentioned by Danishefsky et al. (1960), remained as a challenge for those focusing on structural studies or seeking a way to LMW products. It even led to a confusion regarding the identity of uronic acid residue of the major disaccharide block, which was for a long time believed to be D-glucuronic acid rather than L-iduronic acid (Casu, 1989). Ultimately, the resistance of heparin to mild acidic environments was thought of as ‘inconvenient’ and became ‘a step’ in more advantageous deaminative cleavage with nitrous acid (Casu, 1989; Conrad, 1980; Linhardt, 1992). Consequently, the studies focussing on the hydrolytic stability of heparin in these environments were narrowed down, with the most recent article being from 1996, which generally discussed (or rather revised) the stability of heparin, however, without any *in-depth* analysis (Jandik et al., 1996).

To better understand the behaviour of heparin in mild acidic aqueous environments, the stability of molecule in such conditions has been re-examined in this chapter. To complement the pioneering work of Danishefsky et al. (1960), the acidic and temperature ranges examined herein were extended to pH 1 - 6 and 40, 60 & 80 °C and examined as a function of time (up to 168 h). The choice of analytical techniques summarised in **section 3.2**, allowed the investigation of a variety of heparin features. The results of the undertaken study are presented in **section 3.3** and critically examined, with regards to applied conditions. The kinetic model describing the studied system is proposed in **section 3.4**. The major findings are summarised in **section 3.5**, where also a view on a proposed, updated acid catalysed degradation mechanism of heparin has been presented.

## 3.2 SUMMARY OF APPLIED ANALYTICAL METHODS

The complete experimental procedure of acid hydrolysis of sodium salt porcine mucosal heparin ( $M_{w,0} \approx 20,000$  g/mol,  $M_w/M_n = 1.1$ ) is presented in **section 2.1**, while **Figure 3.1** summarises the hydrolytic protocol. The analytical methods applied to investigate the physicochemical changes caused by hydrolytic conditions are summarised in **Table 3.1**,

while more detailed description of each technique is given in **Experimental Chapter 2**.

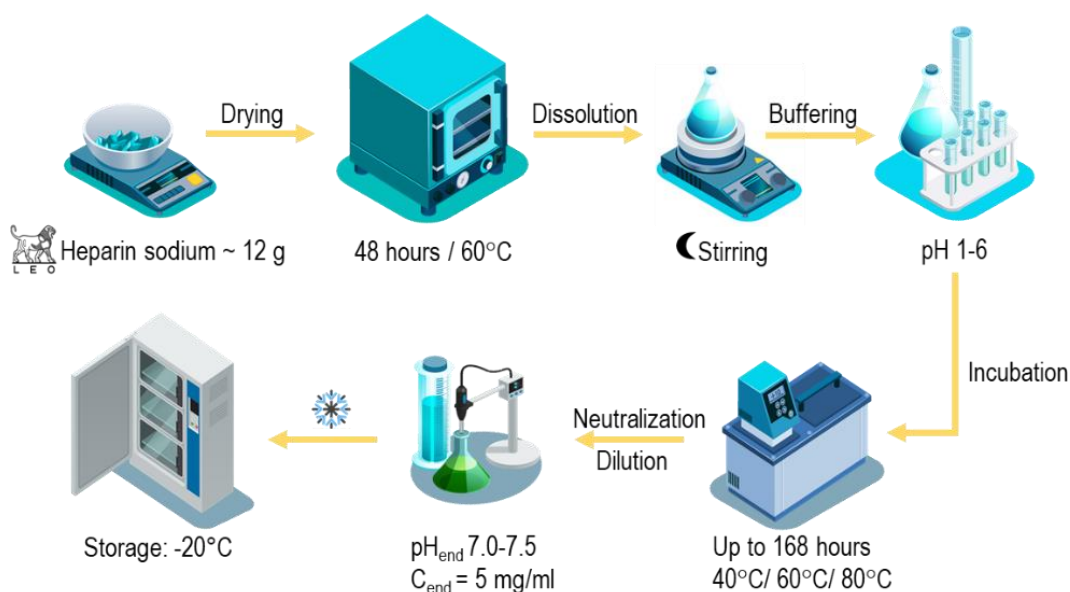


**Figure 3.1** Graphical illustration of heparin hydrolysis process in acidic environments.

**Table 3.1** Summary of the analytical methods applied in acid hydrolysis study of heparin.

Method	Objectives	Data Type	Details <sup>a</sup>
Size Exclusion Chromatography	Confirmation of molecular weight change of acid hydrolysed samples	Quantitative	2.3
Gel Electrophoresis	Verification of glycosidic bond scission <i>via</i> PAGE reducing ends analysis	Qualitative	2.4
UV-Vis Spectrophotometry	Verification of glycosidic bond scission based on the absorbance change	Qualitative	2.5
Anion Exchange Chromatography	Pulsed Amperometric Detector: total compositional analysis of hydrolysates	Qualitative	2.6
	Conductivity Detector: confirmation of sulfate hydrolysis (sulfate scission)	Quantitative	2.7
NMR Spectroscopy	Investigation of desulfation order and confirmation of glycosidic bond scission	Qualitative	2.8

<sup>a</sup> section number in Experimental Chapter 2.

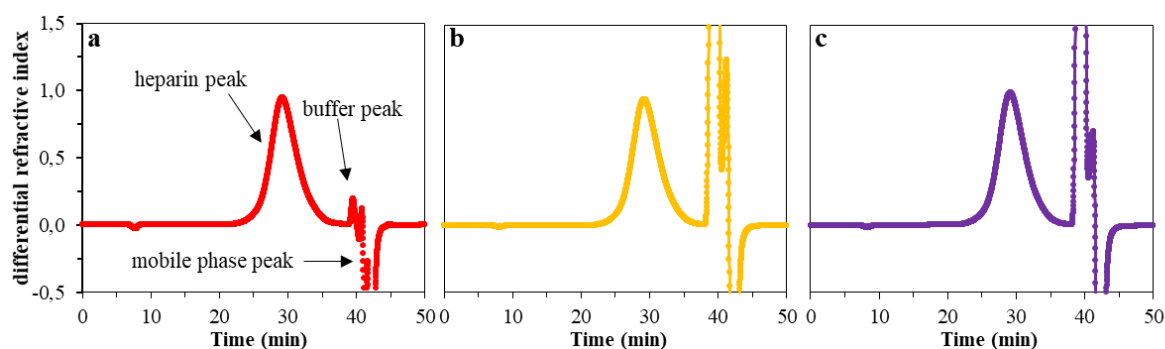
### 3.3 RESULTS AND DISCUSSION

#### 3.3.1 The effect of acidic environments on molecular weight of heparin as a function of time and temperature

The changes of molecular weight of natural polymers are usually attributed to stressing factors (chemical or physical) or enzymatic action (Cui, 2005; Murray et al., 1994). Regardless of the cause, the change of polysaccharide molecular weight generally signifies an alteration of its structure, and thus, functionality (Harding et al., 1991, 2017). The specific medical response of heparin is directly associated with its molecular weight and chemical structure (Lima et al., 2017; Mulloy et al., 2015; Onishi et al., 2016). Consequently, posing the question how (or if) the applied experimental conditions affected heparin molecular weight was considered as a natural starting point for stability studies.

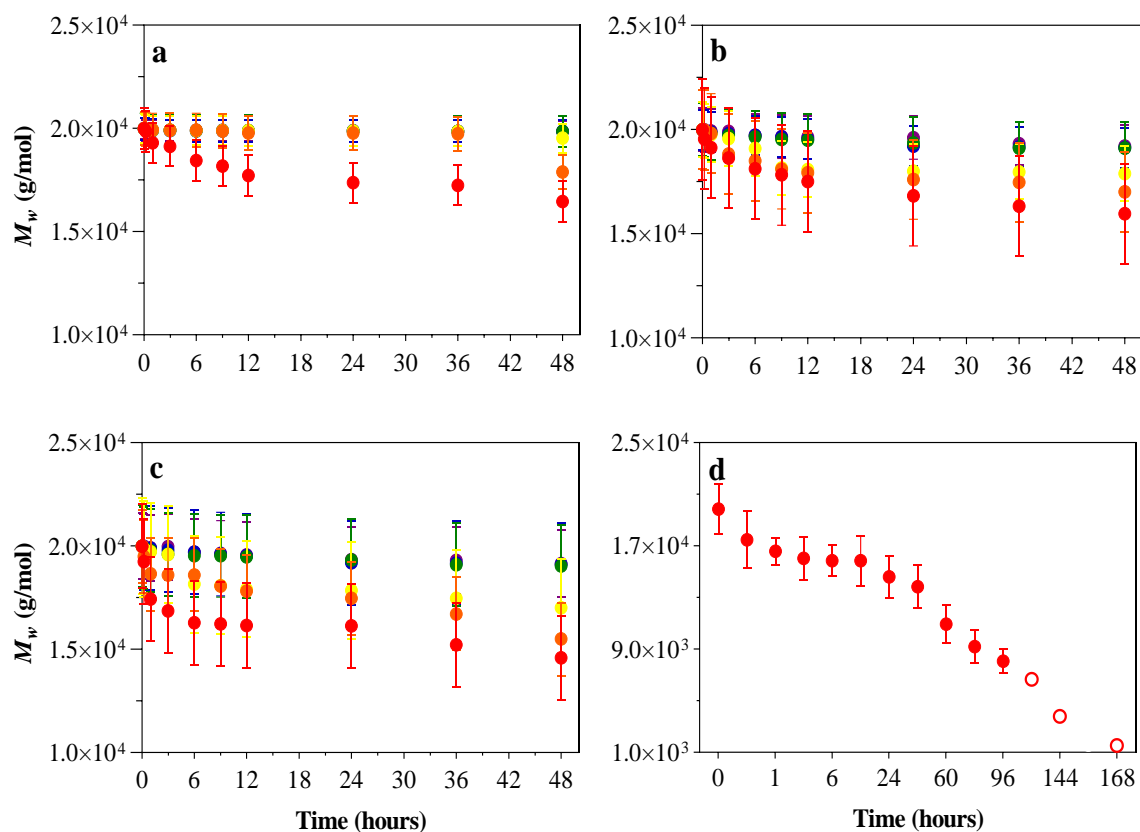
##### 3.3.1.1 The results of average weight molecular weight analysis

The most convenient way to characterise the heterogeneous polysaccharides, like heparin, is by means of number-average molecular weight ( $M_n$ ) and/or weight-average molecular weight ( $M_w$ ). For this reason, size exclusion chromatography was applied (for analytical details see 2.3). The changes of  $M_w$  of thermally stressed heparin (40, 60, 80 °C) in acidic environments (pH 1 - 6) were followed over time. Elution profiles of selected samples are presented below in **Figure 3.2**.



**Figure 3.2** Elution profiles of heparins hydrolysed at **a)** pH 1/ 40 °C after 24 h, **b)** pH 3/ 60 °C after 24 h, and **c)** pH 6/ 80 °C after 24 h. Samples were analysed *via* size exclusion chromatography with multi-angle-light-scattering detector and refractive index detector. Presented chromatograms are results of normalized refractive index detector signal.

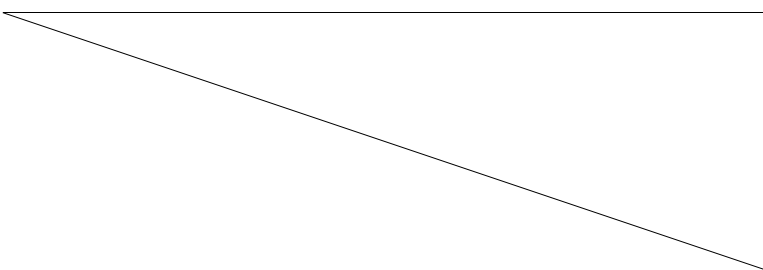
The collected molecular weights were plotted as a function of time (up to 168 h) in **Figure 3.3**, with averaged uncertainties defined as 95% confidence intervals of triplicated measurements. The approximate decrease of  $M_w$  (%), calculated for chosen hydrolysates, are summarised in **Table 3.2**.



**Figure 3.3** Average weight molecular weight of heparin hydrolysed at **a)** 40 °C, **b)** 60 °C, and **c-d)** 80 °C, plotted as function of time at pH 1 - 6. The extrapolated  $M_w$  (120, 144 & 168 h) in **d** are marked by  $\circ$  data point. The averaged uncertainty defines the 95% confidence interval.  $\bullet$  pH 1,  $\bullet$  pH 2,  $\bullet$  pH 3,  $\bullet$  pH 4,  $\bullet$  pH 5,  $\bullet$  pH 6

As illustrated in **Figure 3.3a-c**, the relation between the molecular weight loss and pH was inversely correlated (lower pH = more prominent molecular weight loss), whilst the rate of degradation increased with temperature (higher temperature = faster decrease). The collected results imply a lack of significant change in molecular weight ( $\leq 5\%$ ) for heparins hydrolysed between pH 4 and pH 6 at all studied temperatures (examples in **Table 3.2**). On the other hand, the maximum molecular weight loss at pH 1, pH 2 and pH 3 was reached at 80 °C and calculated to 27, 23 and 15%, respectively. For these environments, the decrease was also observed at milder temperatures (*i.e.*: 40 and 60 °C), however, to a lesser degree (**Table 3.2**).

**Table 3.2** Summary of approximate average weight molecular weight decrease (%) of acid hydrolysed heparins (chosen time-points) in respect to the initial heparin standard.

Heparin Hydrolysates		Approximate weight-average molecular weight decrease <sup>a</sup>					
		pH 1	pH 2	pH 3	pH 4	pH 5	pH 6
40 ° C	0.25 h	1%	< 1%	< 1%	< 1%	< 1%	< 1%
	6 h	8%	< 1%	< 1%	< 1%	< 1%	< 1%
	12 h	11%	1%	1%	1%	1%	< 1%
	24 h	13%	1%	1%	1%	1%	1%
	48 h	18%	11%	2%	1%	1%	1%
60 ° C	0.25 h	2%	< 1%	< 1%	< 1%	< 1%	< 1%
	6 h	9%	7%	4%	2%	1%	1%
	12 h	12%	10%	10%	2%	2%	1%
	24 h	16%	12%	10%	3%	2%	2%
	48 h	20%	15%	11%	4%	4%	4%
80 ° C	0.25 h	4%	< 1%	< 1%	< 1%	< 1%	< 1%
	6 h	19%	7%	9%	2%	1%	1%
	12 h	19%	11%	10%	3%	2%	2%
	24 h	19%	13%	11%	3%	4%	3%
	48 h	27%	23%	15%	5%	4%	4%
	96 h	59%					
	120 h <sup>b</sup>	66%					
	168 h <sup>b</sup>	92%					

<sup>a</sup> Calculated by subtracting  $M_w$  (g/mol) of hydrolysate from the  $M_w$  (g/mol) of initial heparin standard.

<sup>b</sup> value estimated *via* nonlinear, fitted extrapolation of data presented in **Figure 3.3d**

The results collected for hydrolysis at pH 4 - 6 suggest the resistance of heparin to these conditions. Based on the previous literature (Danishefsky et al., 1960; Jandik et al., 1996), the stability of molecule at such mild acidic environments was expected. However, the 27% molecular weight loss observed after 48 h incubation in pH 1/ 80 °C was considered relatively modest, especially since similar conditions have been applied in the preparation of heparin oligomers and low molecular weight products. Therefore it was expected that applied conditions would cause relatively high molecular weight loss (Linhardt, 1992; Xie et al., 2018). Furthermore, the pseudo-plateau observed between the 6<sup>th</sup> and 24<sup>th</sup> hour of hydrolysis (pH 1/ 80 °C), with a more prominent molecular weight drop between the 24<sup>th</sup> to 48<sup>th</sup> hour was unexpected (**Figure 3.3c**; **Table 3.2**). To investigate if continuous hydrolysis at these conditions is more effective (in terms of molecular weight loss) and to further evaluate the rate of change, the hydrolysis at pH 1/ 80 °C was extended to 168 h.

The molecular weight change results from the prolonged hydrolysis are summarised in **Figure 3.3d**. As illustrated, the prolonged hydrolytic conditions caused further, more definite (from 24<sup>th</sup> hour onward) loss in molecular weight (**Table 3.2**). In fact, after 120 h, the hydrolytic fraction was too small to be measured by size-exclusion chromatography (see **APPENDIX A** for illustrative data), therefore  $M_w$  at 120, 144 and 168 h points were extrapolated using a fitted, nonlinear regression method. The pseudo-plateau region was observed again, this time more prominently between 3<sup>rd</sup> and 12<sup>th</sup> hour time- point.

### 3.3.1.2 Concluding remarks

In summary, the hydrolysis carried out between pH 1 and pH 3 at 40, 60 and 80 °C resulted in loss of weight-average molecular weight of heparin, especially under the harshest of applied environments, *i.e.*, pH 1/ 80°C. Furthermore, the shape of plot of  $M_w$  (g/mol) vs time (h) for these particular conditions could reflect different degradative processes happening at structural level of polymer. The first degradative process reaching the plateau after approximately 24 h of hydrolysis, as in **Figure 3.3c-d**, with a further reaction of more prominent molecular weight loss, as in **Figure 3.3d**. In order to reveal the possible mechanisms of these processes, the hydrolytic samples were analysed further.

### 3.3.2 The influence of applied conditions on glycosidic bonds of heparin – verification of chain fragmentation

#### 3.3.2.1 PAGE-based reducing-ends assay

The appearance of new reducing ends was previously used as direct evidence of polysaccharide degradation (Jandik et al., 1996; Taylor et al., 2019; Tommeraas et al., 2001). Here, to estimate the extent of chain scission of acid hydrolysed heparin, PAGE electrophoresis with fluorescent reducing-end labelling was employed. The appearance of new reducing ends (which would mark chain scission) in heparin hydrolysates was assessed directly from the band illuminated on acrylamide gel (for method details see **section 2.4**).

##### 3.3.2.1.1 Summary of method optimisation

The electrophoretic conditions needed to be optimized towards readable, unambiguous assay of a good reproducibility between the replicates. The optimization of the loading of the dp standards ladder was addressed by creating the matrix of reactions between the mix of unsaturated heparin oligosaccharides standards and 7-amino-1,3-naphthalenedisulfonic acid monopotassium salt monohydrate (ANDSA) fluorophore (for experimental details see **2.4.4.1**). The heparin hydrolysates load was optimised on the basis of reaction of ANDSA with heparin polymer hydrolysed in TFA (sample positive, prepared according to protocol given in **section 2.2.4.3**).

As illustrated in **Figure 3.4**, good readability of dp standards (arranged in ladder) was delivered at 30 µg/ per dp, while as much as 100 µg of heparin hydrolysate was required for similar clarity. The loading of higher amounts of polymer (*e.g.*, 500 µg, **Figure 3.4b**) did not enhance visualisation, but resulted in a ‘smile’, blurred band. Thus, 100 µg of hydrolysates was loaded in following analysis.

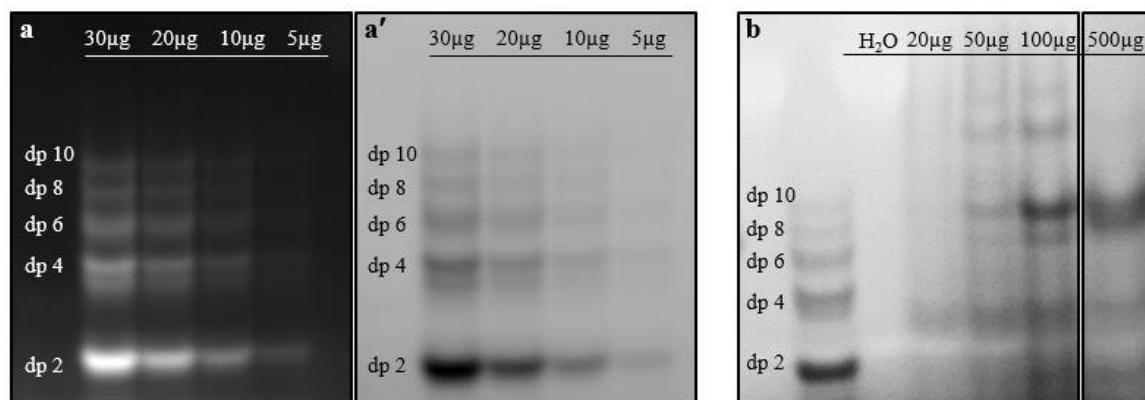


**Figure 3.4** Results of load optimisation for the reducing-ends assay. Pictures **a/a'**) present acrylamide gels of electrophoretic-separated, ANDSA tagged dp oligosaccharides, used as ladder of standards during the PAGE analysis of acid hydrolysed heparin, while at **b)** bands of TFA hydrolysed heparin unit are visualised (sample positive); H<sub>2</sub>O- blank load.

#### 3.3.2.1.2 Fluorescent analysis of acid hydrolysates of heparin

Following the optimization process, heparin hydrolysates were examined to confirm/exclude capacity of applied hydrolytic conditions to catalyze glycosidic scission along the polysaccharide chain. Samples were assigned to PAGE analysis upon the considerable molecular weight loss, based on data presented in **section 3.3.1**. Thus, ANDSA-labelled heparins (100 µg), hydrolysed at pH 1 - 3, at 40 °C, 60 °C and 80 °C (various time-points) were loaded onto the separate gels and submitted to electrophoresis (for details of electrophoresis run see **2.4**). Illustrative images of fluorescently visualized gels are shown in **Figure 3.5**.

As illustrated, no bands were eluted (besides standards) from gels corresponding to hydrolysis carried at pH 2 and pH 3, at any of the studied temperatures. The same was true for hydrolysates prepared at pH 1/ 40 and 60 °C (**Figure 3.5**). The lack of bands suggested that these conditions were insufficient to break the glycosidic linkages between heparin units to any significant extent.

In contrast, new bands were observed at 24 h and 48 h time-points for pH 1/ 80 °C hydrolysis (highlighted by the yellow box, **Figure 3.5**). With reference to (dp) standard ladder, the bands were located between the dp 8 and dp 2 oligosaccharides and their intensity increased with time (**Figure 3.5**). It can therefore be assumed that after 24 h incubation at pH 1/ 80 °C, heparin chains started to gradually degrade, *i.e.*, the

hydrolytically induced, glycosidic scission had started. To confirm that the chain scission continued, the electrophoretic assay was repeated for aliquots withdrawn during the extended hydrolysis at pH 1/ 80 °C. Examples of gels are shown in **Figure 3.6**.

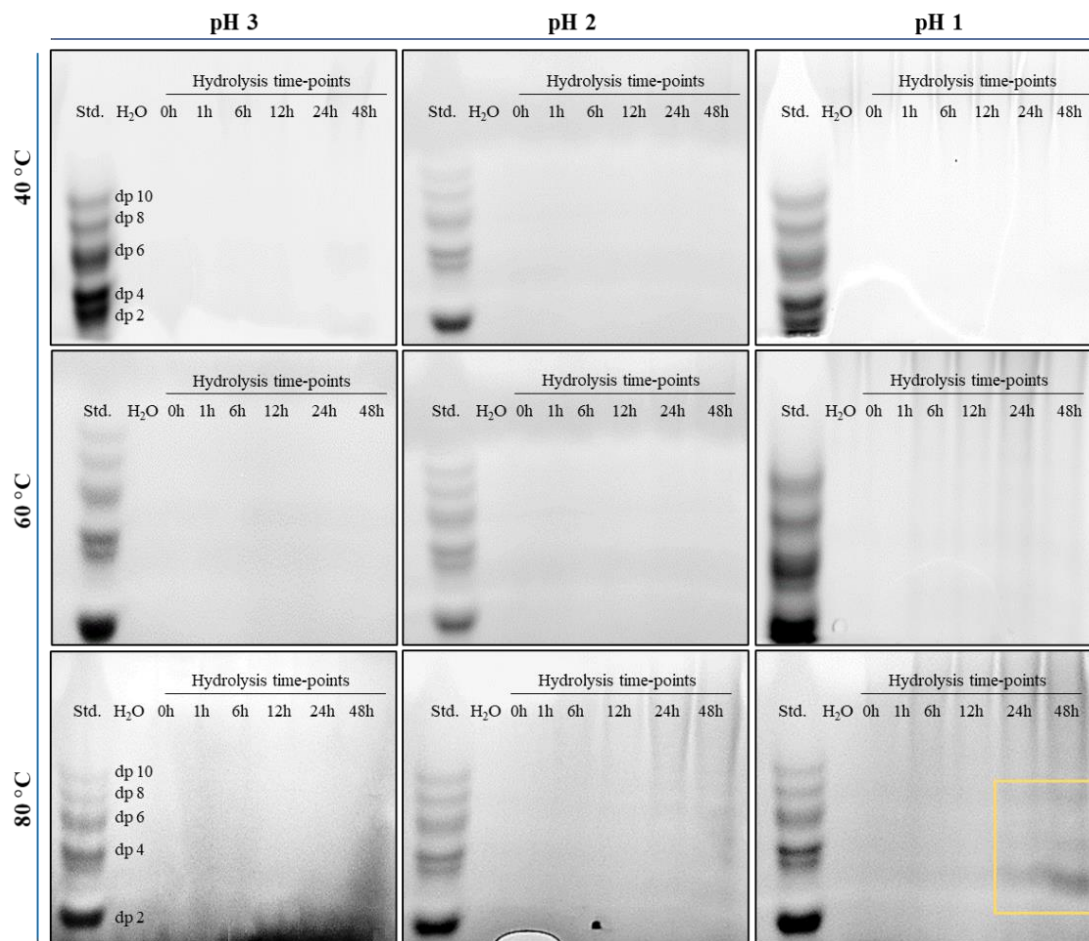


**Figure 3.5** Fluorescent images of acrylamide gels of acid degraded heparins. Comparison of samples aliquoted at various time-points at pH 3, pH 2 and pH 1 degradation, at 40, 60 and 80 °C. Weak, newly formed bands observed at 24 h and 48 h time-point on pH 1/ 80 °C gel are highlighted in yellow; Std- standard dp ladder, H<sub>2</sub>O- blank load.

As shown in **Figure 3.6**, the multiple bands were eluted on gel mirroring the extended hydrolysis of heparin at pH 1/ 80 °C. The bands observed between 24 h and 72 h are of low intensity and within dp standard range (dp 2 - 10). The bands of samples aliquoted  $\leq 96$  h are sharper and exhibit greater diversity in terms of polymerisation degree. Furthermore, the samples hydrolysed between 96 h and 168 h seem to reflect a similar band pattern (although with lower intensity at the beginning of run; dp range < dp 10). To assess more closely the composition of post-hydrolytic samples, these were analysed further by chromatographic and spectroscopic techniques, described in following sections.

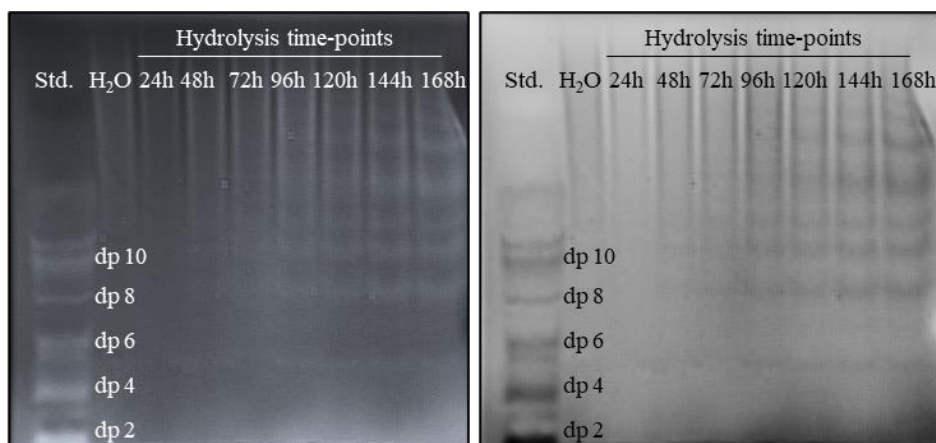


**Figure 3.6** Fluorescent image of acrylamide gel, showed in inverted colours, of extended acid hydrolysis of heparin (chosen time- points), carried out at pH 1 and 80 °C.

### 3.3.2.1.3 Cationic dye staining of acid hydrolysates of heparin

When subjected to specific catalysed hydrolysis, sulfated polysaccharides, like heparin, exhibit the potential to lose sulfate groups prior to depolymerisation (Bedini et al., 2017; Danishefsky et al., 1960; Finch, 1999; Karlsson & Singh, 1999). The sulfate group of glycosaminoglycans bind the cationic dyes, like Azure A. Thus, cationic dye staining is an alternative method to measure desulfation magnitude (Ehrlich & Stivala, 1973; Finch, 1999; Mulloy et al., 2015; Powell et al., 2010).

Benefiting from acrylamide gels with heparin hydrolysates loaded for the first part of this study, the straightforward Azure A staining was applied to qualitatively assess desulfation progress (for experimental details see **section 2.4.4.4**). The analysis showed that colour intensity of cationic dye decreased as a function of time and temperature and inversely to pH. The illustrative results of samples hydrolysed at pH 1, at 40, 60 and 80 °C are presented in **Figure 3.7**. The results collected for pH 2 and pH 3 closely resembled the pH 1/ 40 & 60 °C gels (**Figure 3.7a-b**), regardless of applied temperature. On the other hand, at pH 1/ 80 °C, the stain intensity decreases rapidly, with 24 h aliquot being the least coloured sample. As illustrated in **Figure 3.7c-d**, the blue staining disappeared after 48 h, for gel loaded with pH 1/ 80 °C hydrolysates.

The colour intensity of Azure A-saccharide complex reflects sulfate content of the polysaccharide (Mulloy et al., 2015; Powell et al., 2010). Thus, the complete absence of colour signifies considerable sulfate loss. It may therefore be assumed that pH 1/ 80 °C

hydrolysis led to extensive desulfation of heparin, while milder conditions (*e.g.*, pH 1 - 3/ 40 °C) mark a lower sulfate loss, visualised by a gradual fading of the cationic dye. The quantitative capacity of this process was verified *via* ion chromatography, described in the following **section 3.3.3**.

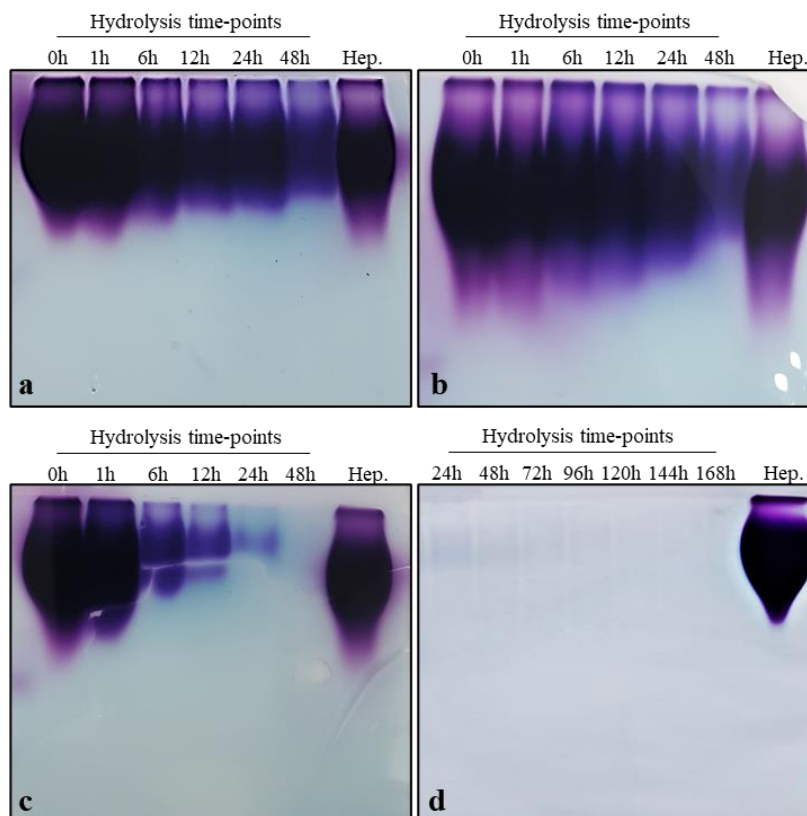


**Figure 3.7** Images of acrylamide gels of heparin hydrolysed at pH 1 at **a)** 40 °C, **b)** 60 °C and **c-d)** 80 °C (chosen aliquots), stained with Azure A dye; Hep- unhydrolysed heparin reference standard.

#### 3.3.2.1.4 PAGE electrophoresis concluding remarks

Both fluorescent tagging and cationic staining of post-hydrolytic samples initially portrayed behaviour of heparin in acidic environments. Two processes could be distinguished from gel profiles, *i.e.*, glycosidic scission - most probably requiring long processing time under harsh acidic conditions (here, at least 24 h at pH 1 / 80 °C) and desulfation, which has been observed at milder pH and temperature. These two mechanisms could justify a two-staged molecular weight loss demonstrated using SEC-MALS and described in **section 3.3.1**. To further explore this hypothesis a more comprehensive analysis of hydrolysed heparin samples was undertaken.

### 3.3.2.2 UV-Vis spectrophotometry

UV-VIS spectroscopy has been previously used in the qualitative study of GAGs (subjected to alkaline or enzymatic treatment) to prove scission of glycosidic bonds, by characterising the unsaturated iduronic residues at new reducing terminus *via* the absorbance of electromagnetic radiation at 232 nm. (Deakin & Lyon, 2008; Limtiaco et al., 2011; Ucakturk et al., 2014). Although a similar rearrangement would not be expected in acid environments, the absorbance of samples after treatment at pH 1 - 3, at 40, 60 and 80 °C, was verified. After all, an increasing absorption potential of polysaccharides has been generally associated with their structural changes (Cui, 2005; Finch, 1999; Zhou et al., 2016).

The spectroscopically analysed hydrolysates (according to protocol given in **2.5.4**) of pH 2 - 3 (all three temperatures) and pH 1/ 40 and 60 °C did not demonstrate any UV-Vis absorbance. The lack of absorbance surely followed from the stability of molecule at above conditions and is in line with previous results (*i.e.*, molecular weight analysis in **3.3.1** and reducing ends assay in **3.3.2.1**). On the other hand, as illustrated in **Figure 3.8**, the absorbance (240 nm) of samples hydrolysed at pH 1/ 80 °C/ 24 h  $\leq$  increased over time.

In contrast to characteristic absorbance at 232 nm, which has been consistently proven to be the result of iduronate unsaturation (Deakin & Lyon, 2008; Lima et al., 2011; Limtiaco et al., 2011; Mourier et al., 2015; Ucakturk et al., 2014), the absorbance at 240 nm may signify structural changes. Groisman & de Lederkremer (1987) suggested that 240 nm absorbance follows from the glycosidic scission between the saccharide and serine residues and reflects rearrangements of broken O-glycosidic bond to absorbing specie. Similar conclusions were more recently presented by Shi et al. (2017), although, none of these studies actually focused on heparin but rather on other glycans also initially linked to serine. Furthermore, in both examples, the rearrangements were catalysed by alkaline environments.

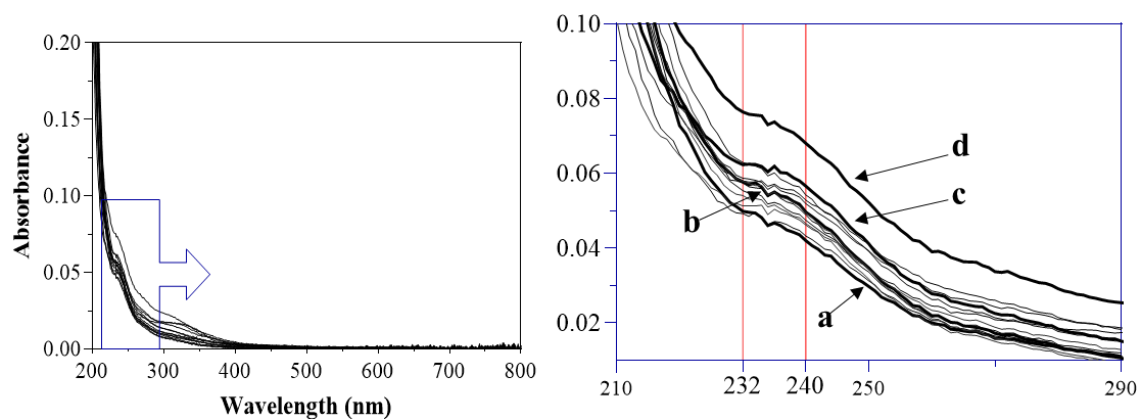


**Figure 3.8** The absorbance spectra of sample hydrolysed at pH 1/ 80 °C over the 168 h. Each line represents hydrolytic time-point, plotted in ascending manner, *i.e.*: **a**) 0.25 (the lowest), 1, 3, 6, 9, 12, 24, **b**) 48, 72, **c**) 96, 144, **c**) 168 h (the highest).

An interesting explanation was presented by Rcaud et al. (2009), who paired the 240 nm absorbance with excitation of sulfate electrons of SO<sub>3</sub> groups, covalently bound to heparin-derived disaccharides. Surapaneni et al. (2014) went a step further, proving that the 240 nm absorbance of 6-O-sulfated oligosaccharides (derived from other GAG - chondroitin sulfate) increased proportionally to chain length. Following the acrylamide elution pattern of pH 1/ 80 °C sample (**Figure 3.6**), it was considered that more oligosaccharides (of longer chain) were severed from heparin overtime. Perhaps, the isolated products were still O-sulfated which was further reflected in absorbance of spectra. Both the composition and sulfation profile of hydrolysates were further investigated.

### 3.3.2.3 The complete saccharide analysis

The PAGE electrophoresis, described in the previous section (3.3.2.1), sketched a raw picture of heparin subjected to acidic environments (pH 1 - 3) at increased temperature (40, 60 & 80 °C). Upon the elution profile of fluorescently tagged samples (**Figure 3.5** & **Figure 3.6**) it was concluded that glycosidic scission concerned samples exposed to pH 1 and 80 °C, while milder conditions were most probably associated with the desulfation of molecule (as discussed 3.3.2.1.3). Furthermore, UV-Vis spectroscopy suggested that cleaved oligosaccharides could still be O-sulfated (see above section 3.3.2.2). To assess more closely the composition of post-hydrolytic samples, these were analysed *via* ion exchange chromatography, coupled with a pulsed amperometric detector (for analytical details see section 2.6). Taking the advantage of instrument being connected to an autosampler all

hydrolytic samples (pH 1 - 6, all studied temperatures) were examined, to empirically prove the initial hypothesis of the stability of heparin at pH 4 - 6, presented in **section 3.3.1**.

### 3.3.2.3.1 Summary of method optimisation

The applied protocol of ion chromatography was developed according to previous literature, describing a single chromatographic method for the analysis of neutral and amino sugars, together with uronic acids (for protocol details see **section 2.6.5**) (Alyassin et al., 2020; Zhang et al., 2012). To recognise the elution profile of possible heparin saccharides, a mixture of ten monosaccharide standards, *i.e.*: Fuc (as an internal standard), GalN, GlcN, GlcNS, GlcNAc, GlcNS(3S), GlcNS(6S), GlcA, GalA and IdoA was analysed at the series of concentrations, ranging between 0.5 ppm and 100.0 ppm. The retention times of individual standards, specified in **Table 3.3**, were assigned by the analysis of separate monosaccharides (50 ppm) (as described in the protocol in **2.6.5**). Apart from GlcN and GlcNS, which had the same retention time, the remaining 9 monosaccharides were well separated, as presented in an illustrative elution chromatogram in **Figure 3.9**. The calibration curves of each standard plotted using peak area are shown in **Figure 3.10**.

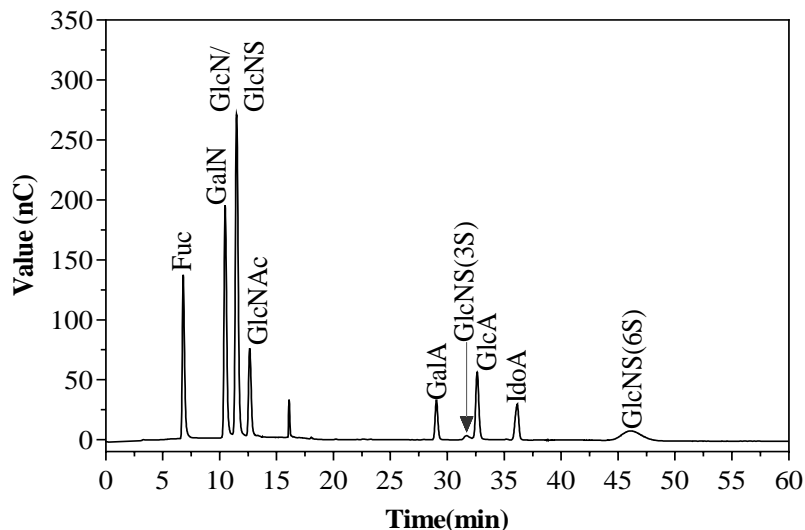


**Figure 3.9** The illustrative elution profile of monosaccharide standards at concentration of 100 ppm, chosen for the complete saccharide analysis of acid hydrolysed heparin.

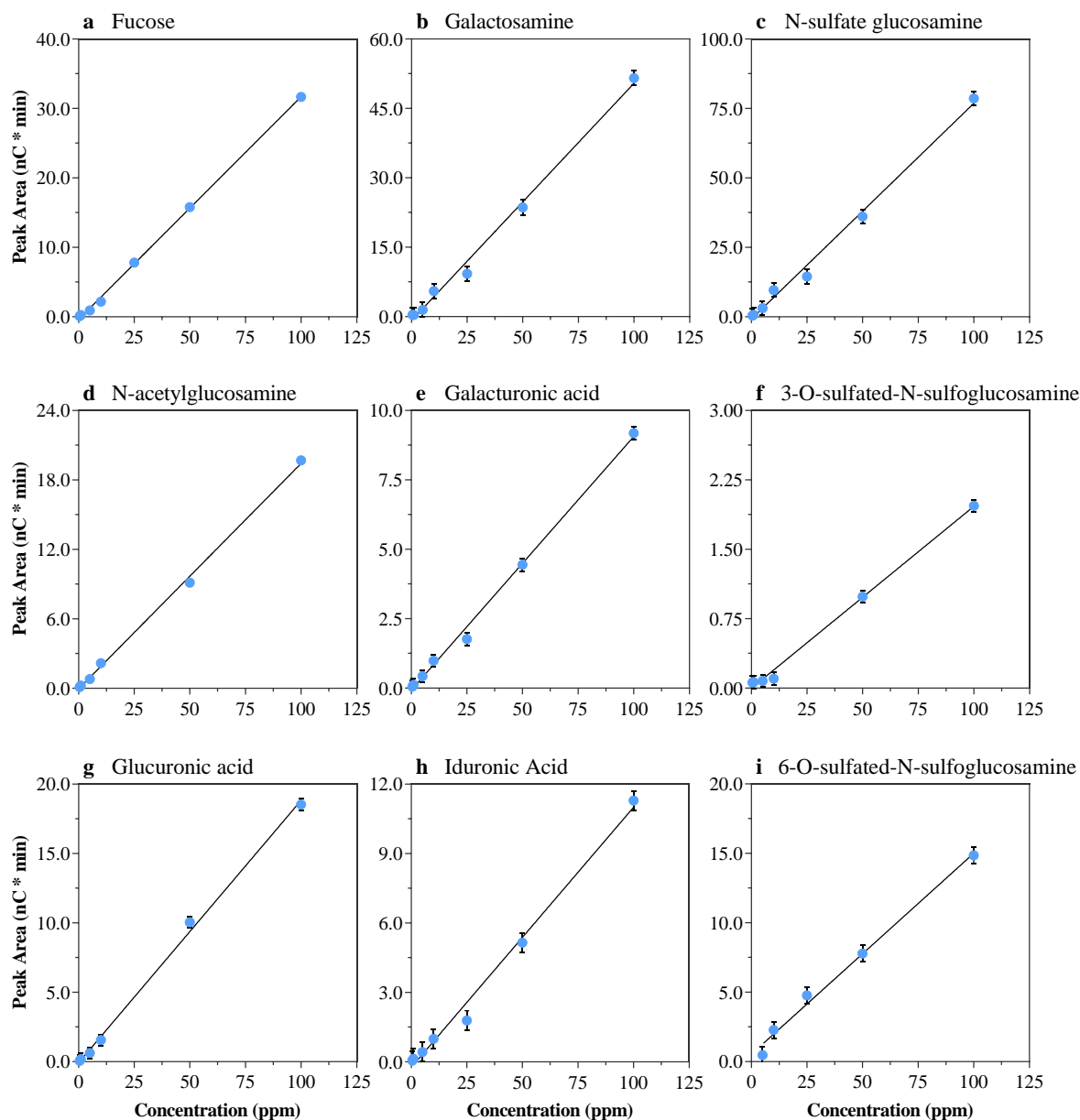


**Figure 3.10** The representative calibration curves of **a)** Fuc, **b)** Gal, **c)** GlcNS, **d)** GlcNAc, **e)** GalA, **f)** GlcNS(3S), **g)** GlcA, **h)** IdoA and **i)** GlcNS(6S) plotted as a function of concentration (ppm), against the peak area (nC\*min). The vertical error bars (where visible) represent standard error of regression, calculated for each analytical range.

As summarised in **Table 3.3**, correlation coefficients ( $R^2$ ), calculated for each monosaccharide, were generally greater than 99.1%, which demonstrate good linearity over the range of studied concentrations. Linearity of curves of GlcNAc, GlcNS(3S) and GlcA standards were affected by a peak corresponding to the sample at concentration of 25.0 ppm (correlation coefficient  $\leq 98\%$ ). Therefore, 25.0 ppm data were excluded from calibration plots of these three standards. The values of detection and quantification limits,

given in **Table 3.3**, were calculated from the signal-to-noise (S/N) ratio of the lowest injected concentration of individually standard. The relative response factor (RRF) of each standard was calculated with respect to the fucose (internal standard) peak area, referenced as 1.00 (at 100 ppm, **Table 3.3**). The advantage of response factors and internal standard can be taken in quantitative study. However, in polysaccharide research, the quantitative analysis usually requires to treat sugar standards at the same manner as unknown sample, and in case of hydrolysis, assumption regarding the total amount of monomers of polysaccharide chain (Cui, 2005; Dionex Corporation, 2008). Considering the range of conditions applied in this study, as well as heterogeneity of heparin, here, the ion chromatography was appreciated for its qualitative features. The quantitative calculations were undertaken to assess statistical abilities of the method itself.

**Table 3.3** The summary of statistical data of monosaccharide standards.

Standard	RT (min)	R <sup>2</sup> (%)	Slope	Intercept	LOD	LOQ	RRF
Fuc	6.8 ± 0.6	99.91	0.320	-0.434	0.14	0.48	1.00
GalN	9.5 ± 0.8	99.39	0.513	-0.856	0.50	1.67	1.63
GlcN/ GlcNS	10.2 ± 0.7	99.35	0.777	-0.814	0.50	1.66	2.48
GlcNAc	11.6 ± 0.6	99.84	0.195	-0.050	0.12	0.39	0.62
GalA	29.6 ± 0.4	99.62	0.091	-0.073	0.07	0.22	0.29
GlcNS(3S)	32.4 ± 0.6	99.55	0.020	-0.002	0.03	0.11	0.06
GlcA	33.3 ± 0.5	99.77	0.189	-0.075	0.76	0.25	0.59
IdoA	37.0 ± 0.4	99.13	0.113	-0.242	0.64	0.21	0.36
GlcNS(6S)	46.1 ± 0.4	99.14	0.145	0.532	0.30	1.00	0.47

RT- retention time, average of RT of all standard mixtures; R<sup>2</sup> - correlation coefficient, RRF- relative response factor, calculated by setting the peak area of fucose to 1.00 in the experiment with 100 ppm standards, LOD- limit of detection; LOQ- limit of quantitation

In addition to monosaccharide elution analysis, the aqueous solution of heparin sodium standard was examined, to rule out presence of free monosaccharides in initial sample (sample negative). On the other hand, the final TFA hydrolysate of heparin (24 h hydrolysis) was used to mirror its complete degradation profile (sample positive). An illustrative chromatogram of sample positive is presented in **Figure 3.11**. The GlcN (no GlcNS- due to N-desulfation), GlcA and IdoA peaks were assigned according to retention time of standards shown in **Figure 3.9**. The remaining peaks, eluted between 20 and 35 min, most likely resemble heparin oligosaccharides. Their appearance is consistent with the PAGE profile of TFA hydrolysates (**Figure 3.4b**) and with results from a previous study that was used in preparation of presented analytical protocol (Zhang et al., 2012).

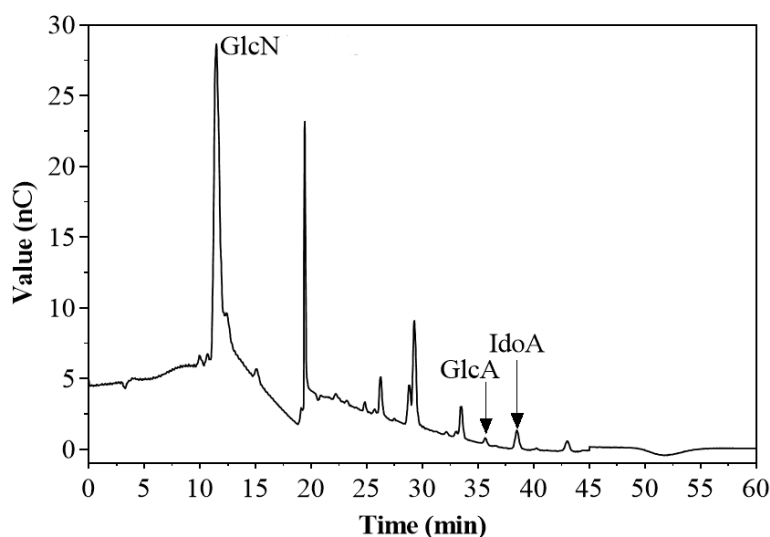


**Figure 3.11** The illustrative chromatogram of final TFA hydrolysate of heparin used to mirror its degradation profile. The presence of GlcN, GlcA and IdoA peaks was based on the assignment of standards shown in **Figure 3.9**. The unidentified peaks most probably represent the post-hydrolytic heparin oligosaccharides. The narrow peak at ~ 20 min marks system peak, characteristic for gradient elution.

#### 3.3.2.3.2 Hydrolysates analysis

The hydrolysates of heparin were analysed to profile the composition of polymer exposed to acidic environments (pH 1 - 6) at three different temperatures (40, 60, 80 °C) as a function of time. Although samples exposed to pH range between 4 and 6 showed relative stability at all three temperatures, manifested by minimal molecular weight loss ( $\leq 5\%$ , as discussed in **section 3.3.1**), and therefore were not expected to show any indication of decomposition, they were analysed to empirically confirm the initial hypothesis.

The chromatographic peaks, representing the units released during the glycosidic scission of heparin, were observed no earlier than after 24 h of processing at pH 1 and 80 °C. The absence of peaks in samples subjected to the milder hydrolytic conditions demonstrate their inability to break glycosidic bonds between heparin monomers. By contrast, prolonged incubation at pH 1/ 80 ° enhanced polymer degradation, as reflected in **Figure 3.12**.

The results of HPAEC-PAD analysis were in close agreement with PAGE profiles of heparin hydrolysates. No bands were eluted on acrylamide gels for samples hydrolysed between pH 2 and pH 3, at all studied temperatures (**Figure 3.5**). Chromatographic analysis also did not show post-degradation peaks for these samples. Under harsher conditions of pH 1, the PAGE bands were not visible prior to 24 h of incubation at 80 °C (**Figure 3.5**) and this sample was also the first one to show presence of peaks in HPAEC-PAD analysis (**Figure 3.12a**). Furthermore, the elution profiles of samples aliquoted between 96 h and 168 h seem to reflect similar elution pattern, with peaks height (and area) increasing as a function of time (**Figure 3.12c-f**).

As shown in **Figure 3.12** GlcN/GlcNS was the earliest monomer released from heparin chain, with following scission of unidentified components, which were most probably heparin oligosaccharides of various degree of polymerisation, consistent with PAGE gels in **Figure 3.6**. The structure of the repeating disaccharide unit of heparin is composed of glucosamine and uronic acid residues at a ratio of 1:1, therefore hydrolytic release should lead to detection of similar amounts of both units. However, this was not the case for samples analysed in this study. The deviation from the expected ratio (various numbers, generally unfavourable for IdoA) caused the questioning of IdoA detection (ergo, the question mark in **Figure 3.12**). The detection uncertainty of IdoA could be a result of poor scission of glycosidic linkages of uronic acids that are highly resistant to low pH (Cui, 2005) or an outcome of degradation of initially released acid units, as suggested in different study (Zhang et al., 2012). In the latter case, the detected peak might mark IdoA, as well as its adducts. Furthermore, in **Figure 3.12f** the missing peak of GlcN/GlcNS is marked with \*. Disappearance of signal is very likely associated with decomposition of sugar unit, caused by prolonged exposure to harsh environments, *e.g.*, pH 1/ 80 °C/ 168 h (Zhang et al., 2018; Zhang & Sutheerawattananonda, 2020).

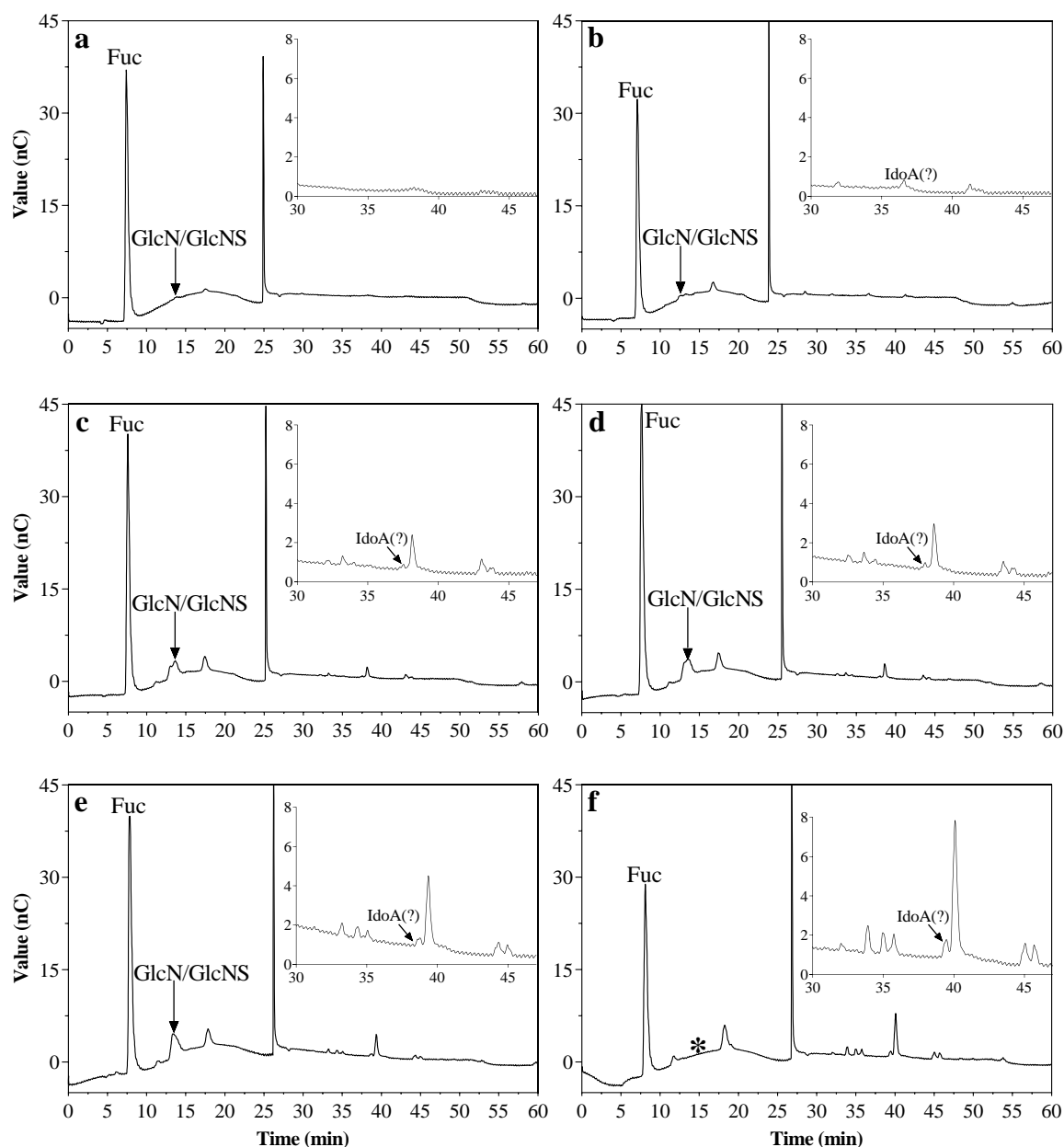


**Figure 3.12** The illustrative elution profiles of heparin hydrolysed at pH 1/ 80 °C over a) 24h, b) 48 h, c) 96 h, d) 120 h, e) 144 h and f) 168 h. The GlcN/GlcNS and (most probably) IdoA peaks were assigned according to elution of calibration standards, shown in **Figure 3.9**. The position missing peak of GlcN/GlcNS in **f**) is marked by \*. The narrow peak at ~ 27 min marks system peak, characteristic for gradient elution. The elevation of chromatographic baseline before the system peak is a result of chromatogram magnification, common in analysis of saccharides at low concentration *via* gradient elution (see for example (Hardy & Reid Townsend, 1994)). Fuc- internal standard.

### 3.3.2.3.3 The complete monosaccharides analysis concluding remarks

The complete monosaccharide analysis of acid hydrolysed heparin was used to assess if (and from when) the degradation of polymer chain was a result of glycosidic scission, as had been hypothesised after PAGE electrophoresis (see **3.3.2.1**), and to examine profiles of post-hydrolytic samples, based on comparison with standards. Ion chromatography results demonstrated the stability of heparin to milder acidic environments (pH 2 - 6, all studied temperatures). At the same time, it was confirmed that glycosidic bonds started to gradually break from 24 h processing at pH 1/ 80 °C and depolymerisation continued over time. These results were consistent with the outcome of PAGE analysis. However, the resistance of heparin to milder hydrolysis, especially those carried out at pH 2 - 3 (all temperatures) and pH 1 (40 and 60 °C) brings into the question the molecular weight loss observed under these conditions (as presented in **3.3.1**). The Azure A staining discussed earlier in **section 3.3.2.1.3** shed some light on desulfation caused by the hydrolytic environments. Therefore, the hydrolytic desulfation of heparin and its effect on molecular weight was investigated.

### 3.3.3 The effect of degradative environments on heparin sulfate groups

Considering that small amounts of mono- and oligosaccharides were detected only in samples hydrolysed under harsh conditions (pH 1/ 80 °C/ 24 h<sub>≤</sub>), the origin of the molecular weight loss observed at milder hydrolytic environments remained unresolved. As previously demonstrated, sulfated polysaccharides, like heparin, have the potential to lose sulfate groups prior to depolymerisation (Bedini et al., 2017; Finch, 1999; Karlsson & Singh, 1999). Thus, the presence of sulfate anions in post-hydrolytic samples was ascertained using ion chromatography, coupled with a conductivity detector (for analytical protocol, see **section 2.7**). The samples of heparin subjected to different temperatures (40 °C, 60 °C and 80 °C) at a range of acidic pH (pH 1 - 6) and over prolonged period (up to 168 hours) were analysed. The principles of adapted analysis were based on two questions that were raised upon the results of previous analysis, *i.e.*, is the desulfation process occurring under the applied conditions and how is the sulfate loss influencing the molecular weight of heparin? The latest of these questions is of particular relevance to molecule stability, as the percentage of sulfate of completely sulfated heparin disaccharide (IdoA(2S)-GlcNS(6S)  $M_w = 577.6$  g/mol) is approximately 38% (see for example Mulloy, 2012).

### 3.3.3.1 Quantitative analysis of inorganic sulfate in post-hydrolytic samples

#### 3.3.3.1.1 Summary of method optimisation

The analytical protocol of analysis of inorganic sulfate in post-hydrolytic samples of heparin was an adaptation of method described in Liu et al. (2014), taking advantage of ion chromatography to study content of inorganic anions in glycosaminoglycan samples. Liu et al. (2014) suggested the presence of acetate ( $\text{Ac}^-$ ) and other inorganic anions (besides sulfate) in acid-treated heparin. In the presented study the inorganic anions standards of  $\text{F}^-$ ,  $\text{Ac}^-$ ,  $\text{Cl}^-$ ,  $\text{Br}^-$ ,  $\text{NO}_3^-$ ,  $\text{PO}_4^{3-}$  and  $\text{SO}_4^{2-}$  were analysed (according to protocol described in **section 2.7.5**) at series of concentrations, ranging between 0.1 ppm and 5.0 ppm. The five anion components of multi-elemental standard, *i.e.*:  $\text{F}^-$ ,  $\text{Cl}^-$ ,  $\text{Br}^-$ ,  $\text{NO}_3^-$ ,  $\text{PO}_4^{3-}$  and  $\text{SO}_4^{2-}$  were well separated. The illustrative elution chromatograms are presented below, in **Figure 3.13**.

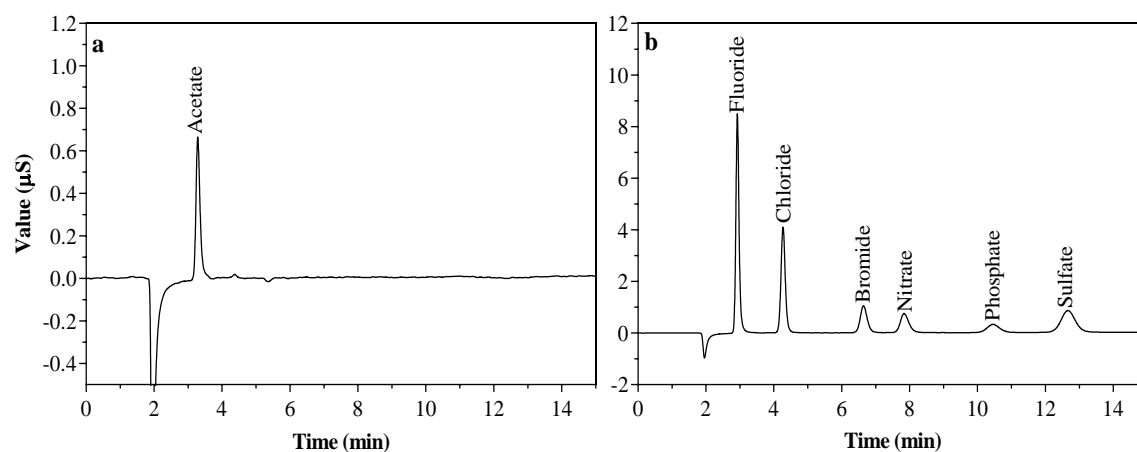


**Figure 3.13** Chromatograms of **a)** acetate standard and **b)** multi-anion standard applied in anion analysis of acid hydrolysed heparin, collected at concentration of 5 ppm.

Citrate salts were used for the preparation of buffers at pH from 3 to 6 (see **2.2.3.4**). Thus, the compatibility of chromatographic system was verified using sodium citrate standard at single concentration of 10 ppm (as advised by column supplier, private correspondence, see **2.7.5.1**). It was confirmed that citrate anions are not separated by chosen column and would not interfere with the detection of inorganic peaks.

The calibration curves, plotted for each anion by the peak area, gave very good linearity at studied concentration range. Illustrative calibration plots are presented in **Figure 3.14**. As

summarised in **Table 3.4**, correlation coefficients, calculated for each anion were generally greater than 99.9%. The values of detection and quantification limits, calculated in relation to standard deviation of the y-intercept of the regression line (Shrivastava & Gupta, 2011), confirmed the applicability of method for quantification of minor amount of each anion (see **Table 3.4**). Low values of both LOD and LOQ allowed the chromatographic analysis at low concentrations, without jeopardizing the analytical column life that could have occurred by polysaccharide contamination and column bedding (Karlsson & Singh, 1999).

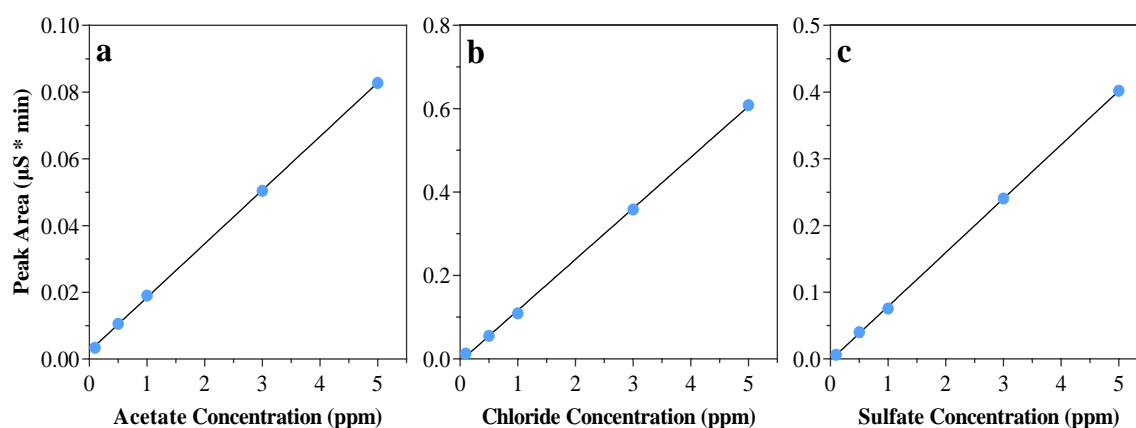


**Figure 3.14** The representative calibration curves of **a)** acetate, **b)** chloride and **c)** sulfate anions plotted as a function of concentration (ppm), against peak area ( $\mu\text{S}\cdot\text{min}$ ). The vertical error bars (too small to see) represent standard deviation from the mean of plotted peak area (triplicated run).

In addition to anion analysis, the aqueous solution of heparin sodium standard was examined, to rule out presence of free sulfate anions in initial sample. During the analysis free chloride anion was detected ( $45 \pm 2$  ppm). Sodium chloride is added during the manufacturing process of heparin. Hence, the trace amounts of chloride anion are usually present in finished product, despite the desalting process (Liu et al., 2014; Van Der Meer et al., 2017). Besides chloride, no other free anions were eluted from the heparin sodium standard.

**Table 3.4** The summary of statistical data of anion standards.

Anion	RT (min)	R <sup>2</sup> (%)	Slope	Intercept	LOD <sup>a</sup> (ppm)	LOQ <sup>b</sup> (ppm)	S <sub>yx</sub>
F <sup>-</sup>	3.0 ± 0.1	99.93	0.269	-0.018	0.19	0.63	0.017
Ac <sup>-</sup>	3.2 ± 0.1	100.0	0.016	0.002	0.09	0.30	0.001
Cl <sup>-</sup>	4.2 ± 0.1	99.96	0.122	-0.006	0.15	0.50	0.006
Br <sup>-</sup>	6.4 ± 0.1	100.0	0.067	-0.003	0.06	0.22	0.001
NO <sub>3</sub> <sup>3-</sup>	7.9 ± 0.1	99.97	0.081	-0.016	0.42	1.40	0.011
PO <sub>4</sub> <sup>3-</sup>	10.3 ± 0.1	100.0	0.043	-0.005	0.14	0.45	0.002
SO <sub>4</sub> <sup>2-</sup>	12.6 ± 0.1	99.99	0.081	-0.002	0.08	0.26	0.002

RT- retention time, average of RT of all standard mixtures; R<sup>2</sup> - correlation coefficient; S<sub>yx</sub> – standard error of estimate; calculated as <sup>a</sup>LOD- limit of detection <sup>b</sup>LOQ- limit of quantification measured respectively as 3x and 10x standard deviation of the y-intercept of the regression line divided by slope (Shrivastava & Gupta 2011)

#### 3.3.3.1.2 Analysis of hydrolysates

The analysis of the heparin standard confirmed the absence of free sulfate in the starting material, consequently, the subsequent detection of anions was associated with the hydrolytic desulfation of molecule. The hydrolysed sulfate anions were detected in heparin samples treated under the following conditions: 40 °C: pH 1 - 2, 60 °C: pH 1 - 3 and 80 °C: pH 1 - 4. Illustrative chromatograms of maximum detection (pH 1/ 80 °C) and lack of detection (pH 5/ 80 °C) are presented in **Figure 3.15 a** and **b**, respectively. The results of ion chromatography resemble the results of Azure A staining, discussed in **section 3.3.2.1.3**, which also suggested desulfation (through the change of dye intensity, as in **Figure 3.7**) for the same samples. On the other hand, no anions were detected in the samples exposed to 40 °C: pH 3 - 6, 60 °C: pH 4 - 6 and 80 °C: pH 5 – 6, which with respect to earlier results, is consistent with negligible changes in  $M_w$  (as in **3.3.1**).

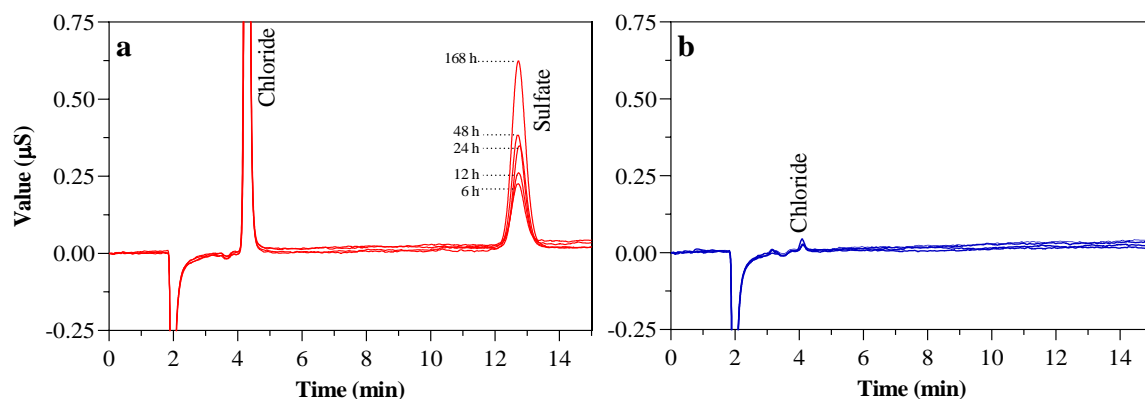


**Figure 3.15** The illustrative chromatograms of sulfate anion, detected in heparin samples hydrolysed at **a)** pH 1/ 80 °C, with peaks corresponding to chosen time points (6, 12, 24, 48 and 168 h) and **b)** pH 5/ 80 °C. The large chloride peak in **a)** corresponds to buffering salt (KCl + HCl), while in **b)** it represents free anion detected in initial sample. Sample concentration equal to 10 ppm.

Besides sulfate and free chloride (eluted from starting material or buffering system), no other anions were detected in acid hydrolysed samples, at any of the studied temperatures, although, as mentioned at the beginning of this section, the earlier study of Liu et al. (2014) suggested the possibility of detection of acetate anions in acid treated heparin samples. The deacetylation of heparin is a process that requires an action of very harsh conditions (strong acids like H<sub>2</sub>SO<sub>4</sub> or HNO<sub>3</sub> at 100 °C) (Bienkowski & Conrad, 1985; Hook, 1974; Riesenfeld & Roden, 1990). Therefore, the observation of acetate anion in sample treated by 0.1 M HCl, like in Liu's (2014), is puzzling and difficult to explain. Yet, absence of acetate in this study is understandable and linked to the conditions being insufficient to break the bond between molecule and acetate group, even after a prolonged incubation at pH 1 and 80 °C.

Once plotted, as in **Figure 3.16**, the concentration of detected sulfate had an increasing trend in function of time and temperature. To be more specific, at pH 1/ 40 °C, the anion concentration increased at fairly consistent rate, while at pH 2 / 40 °C sulfate was detected at single time-point of 48 h (**Figure 3.16a**). At pH 1 - 3/ 60 °C and pH 1 - 4/ 80 °C, the anion concentration increased rapidly for the first 12 hand successively slowed down until the reaction was terminated (**Figure 3.16b-c**), apart from pH 1/ 80 °C, which featured an additional concentration increase after 24 h. The analysis of further hydrolysed samples (end point: 168 h), showed that at these conditions, desulfation could be divided into three stages, *i.e.*: 0 - 24 h, 24 - 96 h, and 96 - 168 h (**Figure 3.16d**).

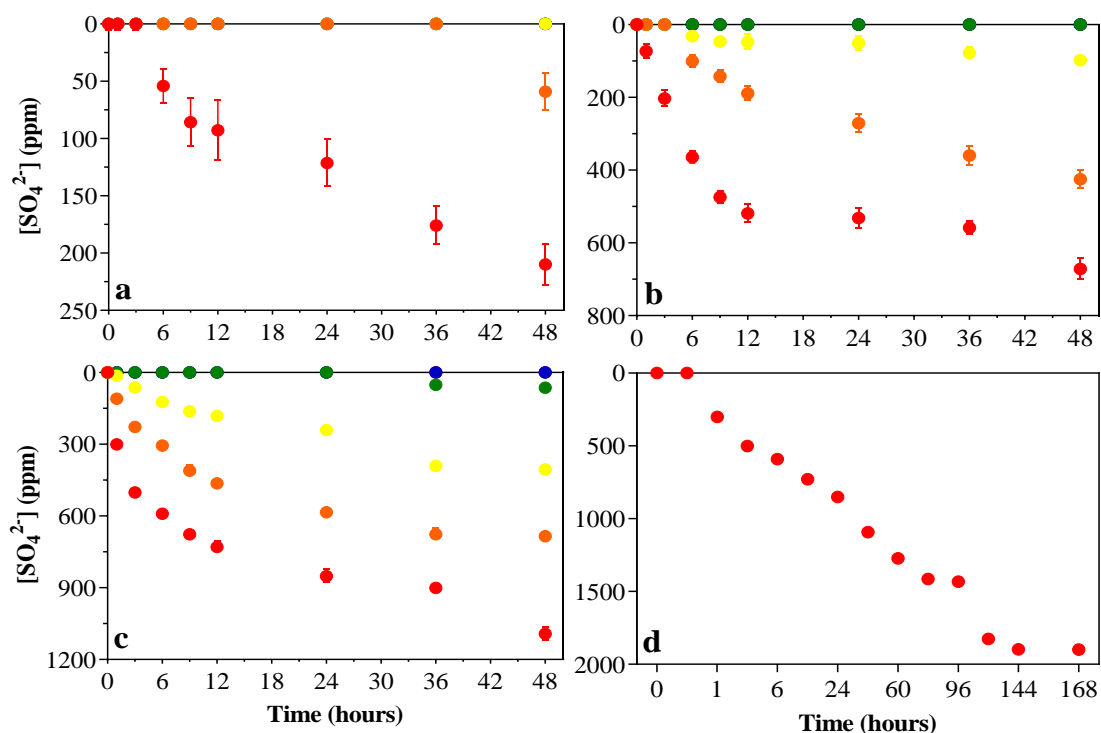


**Figure 3.16** Measured concentration of sulfate anions of thermally stressed heparin at **a)** 40 °C, **b)** 60 °C and **c-d)** 80 °C plotted as a function of time at pH 1 - 6. The vertical error bars (not visible) represent standard deviation from concentrations, calculated from peak area *via* calibration curve method. ● pH 1, ● pH 2, ● pH 3, ● pH 4, ● pH 5, ● pH 6

The hydrolytic scission of different sulfate groups (*i.e.*, these from positions NS-, 2OS-, 6OS-) is most probably associated with different reaction mechanisms characterised by specific reaction rates. Perhaps, the variation in **Figure 3.16d** could be regarded as a direct consequence of changes between the desulfation rates of individual groups, probably liberated in order. The last assumption would be in agreement with earlier studies focusing on heparin stability, discussed in introduction to this chapter (see **3.1**) (Danishefsky et al., 1960; Inoue & Nagasawa, 1976; Jandik et al., 1996). Thus, to investigate further, the chosen hydrolysates were subjected to detailed NMR analysis, described further in **section 3.3.4**. The hypothesis regarding the different reaction rate accounted for a basis of the kinetic approximation presented in **section 3.4**.

### 3.3.3.2 The influence of desulfation on molecular weight of heparin

Acknowledging the prominent sulfate loss, discussed in section above (**3.3.3.1**), the relation between desulfation and molecular weight of heparin was examined. The samples hydrolysed  $\geq 48$  h, at pH 1/ 80 °C had a tendency to glycosidic scission (as discussed in

sections 3.3.2.1.4 & 3.3.2.3.3), hence, the hydrolysates aliquoted during the prolonged processing (48 h<) were excluded from calculations. Attention was directed towards samples that demonstrated depolymerisation resistance, *i.e.*, these hydrolysed at pH 2 - 3/ all temperatures and pH 1/ 40 and 60 °C, which still have demonstrated a considerable molecular weight loss (as discussed in 3.3.1). The aim of the undertaken estimation was to answer if under these conditions desulfation could be accountable as the sole source of heparin molecular weight change.

The concentrations of hydrolysed sulfate ( $C_{\text{sulfate}}$ ; ppm or mg/dm<sup>3</sup>), detected via HPAEC-CD, as well as calculated molecular weight of hydrolysed sulfate ( $M_{\text{sulfate}}$ ; g/mol) are summarized below in **Table 3.5** (chosen examples).

**Table 3.5** Hydrolysed sulfate data of chosen acid-treated heparin samples.

Heparin Hydrolysates		Hydrolysed Sulfate Data					
		40 °C		60 °C		80 °C	
		$C_{\text{sulfate}}$ (ppm) <sup>a</sup>	$M_{\text{sulfate}}$ (g/mol)	$C_{\text{sulfate}}$ (ppm) <sup>a</sup>	$M_{\text{sulfate}}$ (g/mol)	$C_{\text{sulfate}}$ (ppm) <sup>a</sup>	$M_{\text{sulfate}}$ (g/mol)
pH 1	6 h	54 ± 15 <sup>b</sup>	216	364 ± 17	1457	590 ± 17	2361
	12 h	93 ± 26	371	519 ± 21	2075	730 ± 24	2918
	24 h	121 ± 20	484	532 ± 25	2125	852 ± 27	3406
	48 h	210 ± 18	840	671 ± 21	2685	1092 ± 28	4368
pH 2	6 h	n.d.	n.a. <sup>d</sup>	101 ± 18	402	305 ± 19	1223
	12 h	n.d.	n.a.	189 ± 19	756	463 ± 16	1855
	24 h	n.d.	n.a.	271 ± 25	1085	584 ± 18	2337
	48 h	59 ± 16	236	425 ± 26	1700	685 ± 21	2739
pH 3	6 h	n.d.	n.a.	31 ± 14	127	123 ± 17	493
	12 h	n.d.	n.a.	47 ± 19	190	182 ± 16	728
	24 h	n.d.	n.a.	51 ± 19	204	241 ± 17	963
	48 h	n.d.	n.a.	98 ± 15	392	406 ± 20	1622

<sup>a</sup> Concentration calculated by calibration curve using peak area in ppm (parts per million) unit, that is equivalent to 1 milligram of inorganic sulfate anion per litre of solution (mg/dm<sup>3</sup>); <sup>b</sup> Error calculated from standard deviation of triplicated reading; <sup>c</sup> n.d.= not detected; <sup>d</sup> n.a.= not applicable

The  $M_{sulfate}$  ( $g/mol$ ) were calculated to estimate the influence of sulfate loss (in  $g/mol$ ) upon total molecular weight of heparin (also in  $g/mol$  units). This was assessed by substitution of the concentrations of detected sulfate ( $C_{sulfate}$ ;  $ppm$  or  $mg/dm^3$ ) in equation 3.1, *i.e.*:

$$M_{sulfate} = \bar{M}_{w,0} \text{ Hp} \left( \frac{g}{mol} \right) \times \frac{C_{sulfate} (ppm \text{ or } mg/dm^3)}{C_{initial} (ppm \text{ or } mg/dm^3)} \quad 3.1$$

where  $M_{w,0}$  equals average weight molecular weight of untreated heparin sample ( $M_{w,0} \text{ Hp} \approx 20,000 \text{ g/mol}$ ) and  $C_{initial}$  equals initial concentration of chromatographically analysed hydrolytic sample of heparin ( $C_{initial} = 5000 \text{ ppm or } mg/dm^3$ ; for details see protocol in 2.7).

The molecular weights of hydrolytically released sulfate ( $M_{sulfate}$ ;  $g/mol$ ) (Table 3.5) were further subtracted from the average weight molecular weight of heparin subjected to specific conditions at hydrolytic time of 0 h ( $M_{w,t=0} \text{ Hp}_{hyd}$ ;  $g/mol$ ), ” (measured via size exclusion chromatography, see 3.3.1), *i.e.*:

$$\text{Calculated } M_w = M_{w,t=0} \text{ Hp}_{hyd} \left( \frac{g}{mol} \right) - M_{sulfate} \left( \frac{g}{mol} \right) \quad 3.2$$

The values of “calculated  $M_w$ ” and “measured  $M_w$ ” (measured via size exclusion chromatography, see 3.3.1) of selected hydrolytic samples are summarised in Table 3.6. The numbers were statistically compared using non-parametric Wilcoxon matched pairs signed rank test. In this non-parametric statistical approach, the differences between each set of matched data were computed and ranked, while the difference medians were tested against zero. As the p values of all paired data were greater than 0.05 ( $p > 0.05$ , per pH, per temperature), it was concluded that overall medians did not vary, therefore the values of matched  $M_w$  pairs were not significantly different. Consequently, it was deduced that under hydrolytic conditions of pH 1 - 3, 40, 60 and 80 °C, over 48h, desulfation could account for most of the observed decrease in molecular weight of heparin. As shown in Table 3.6, at pH 1/ 80 °C/ 48 h, the detected  $C_{sulfate}$  equalled 1092 ppm, which accounts for ~ 1/5 of total concentration of initial sample ( $C_{initial} = 5000 \text{ ppm}$ ). Thus, although electrophoretic and chromatographic studies (see sections 3.3.2.1.4 & 3.3.2.3.3) showed the presence of mono-/oligosaccharides in samples aliquoted at 24<sup>th</sup> and 48<sup>th</sup> hours of incubation in pH 1/ 80 °C, the extent of observed glycosidic scission must be very low. At these points, in

contrast to desulfation, glycosidic scission must not substantially influence the molecular weight of heparin. Furthermore, since the acrylamide elution pattern of oligosaccharides (**Figure 3.12**) did not precisely match their sulfated oligo-standards, it could be assumed that severed residues themselves were desulfated, which would additionally diminish their impact towards the heparin molecular weight loss, although, following both Azure A staining (see **3.3.2.1.3**) and UV-Vis results (discussed in **3.3.2.2**), this would rather concern N- sulfate than different (O-) sulfate groups.

**Table 3.6** Summary of calculated and measured  $M_w$  of selected heparin hydrolysates.

Heparin Hydrolysates		Calculated $M_w$ (g/mol) <sup>a</sup> $\times 10^4$ vs Measured $M_w$ (g/mol) $\times 10^4$		
		40 °C	60 °C	80 °C
pH 1	6 h	1.98 vs 1.84	1.85 vs 1.81	1.76 vs 1.63
	12 h	1.96 vs 1.77	1.79 vs 1.75	1.71 vs 1.62
	24 h	1.95 vs 1.74	1.79 vs 1.68	1.66 vs 1.61
	48 h	1.92 vs 1.65 <sup>b</sup>	1.73 vs 1.60	1.56 vs 1.46 <sup>c</sup>
		$p^d = 0.1250$	$p = 0.1250$	$p = 0.2500$
pH 2	6 h	1.99 vs 1.99	1.96 vs 1.85	1.88 vs 1.86
	12 h	1.99 vs 1.98	1.92 vs 1.79	1.81 vs 1.78
	24 h	1.99 vs 1.98	1.89 vs 1.76	1.77 vs 1.75
	48 h	1.98 vs 1.79	1.83 vs 1.70	1.73 vs 1.55
		$p = 0.1250$	$p = 0.1250$	$p = 0.1250$
pH 3	6 h	1.99 vs 1.99	1.99 vs 1.91	1.95 vs 1.82
	12 h	1.99 vs 1.99	1.98 vs 1.81	1.93 vs 1.79
	24 h	1.99 vs 1.99	1.98 vs 1.80	1.90 vs 1.79
	48 h	1.99 vs 1.95	1.96 vs 1.79	1.84 vs 1.70
		$p = 0.1250$	$p = 0.1250$	$p = 0.1250$

<sup>a</sup> Calculated  $M_w$  (g/mol) calculated by subtracting the amount of released sulfate anions (g/mol), measured by HPAEC-CD, from the  $M_w$  of heparin sodium standard, measure by SEC-MALS-RI. <sup>b, c</sup> pairs of calculated and measured that  $M_w$  (g/mol) and demonstrated not significantly effective pairing; <sup>d</sup> calculated value, if  $p > 0.05$ , compared data are not significantly different

### 3.3.3.3 *The effect of sulfate loss on anticoagulant activity of heparin*

The anion analysis of heparin hydrolysates showed that acid and temperature treatment released a substantial amount of sulfate ions from the heparin chain. It has been previously demonstrated that an alteration in heparin's sulfation sequence affects its biochemical activity while, for example, 2/6-O-desulfated heparin has shown antifibrotic and anti-inflammatory properties (Lundin et al., 2000; Mulloy et al., 2015; Sugaya et al., 2008), the removal of N- and 3-O-sulfate had had negative consequences to heparin anticoagulation activity (Jorpes & Bergström, 1939; Mulloy et al., 2015; Skidmore et al., 2008). Consequently, the effect of sulfate loss observed in this study upon the anticoagulant activity of heparin was questioned.

The close collaboration with Dr Edwin A. Yates (University of Liverpool) created an opportunity to test the anticoagulation properties of heparin acid hydrolysates. The examined samples were carefully chosen, to maximise diversity of sulfation pattern, *i.e.*: pH 1/ 80 °C/ 48 h; pH 2/ 40 °C/ 48 h; pH 3/ 60 °C/ 12 h; pH 4/ 80 °C/ 6 h; pH 5/ 40 °C/ 24 h; pH 6/ 60 °C/ 48 h. The analysis was kindly performed by the practitioners of The Royal Liverpool University Hospital. The samples were tested against results of Activated Partial Thromboplastin Time (aPTT) and Partial Thromboplastin Time (PTT).

The aPTT and PTT are routine tests performed for patients who have experienced an unexplained bleeding or thrombosis, are long term users of heparin or sometimes as a presurgical screening (Rountree et al., 2020). Both tests examine how fast the patient's blood produces clots, as measured in seconds. The aPTT assess the activity of the intrinsic and common pathways of coagulation that usually takes around 35 s (*Screening Tests in Haemostasis: The APTT*, n.d.), while PPT focuses on intrinsic pathway, with a clotting time of approximately 15 s (*Partial Thromboplastin Time (PTT) Test: MedlinePlus Medical Test*, n.d.). The aPTT and PTT can be adjusted to confirm the anticoagulant properties of heparin, since the addition of active GAG will delay the clotting time.

As presented in **Figure 3.17**, both aPTT and PTT tests demonstrated that anticoagulation properties of samples hydrolysed between pH 2 and pH 5 (chosen aliquots, specified in figure caption) aligned with intact standard. The activity of pH 6 sample, in both assays,

appeared to be around 10-fold weaker than that of heparin standard. The pH 1 hydrolysate did not show anticoagulant action in either test, so consequently, has not been plotted.

Among all samples submitted to anticoagulation check, only heparin hydrolysed at pH 1/ 80 °C completely lost its activity. In fact, the activity of samples subjected to milder conditions (besides pH 6), did not change to any significant extent. With reference to desulfation, the aPTT and PTT assays showed that anticoagulation atrophy is generally a result of very drastic sulfate loss (like in pH 1/ 80°C). To understand what type of sulfate (N- or O- or combination) so radically influenced the activity, the sample was analysed further. On the other hand, the modest desulfation, fortunately, would not really jeopardise the anticoagulation performance that should ensure the safety of the drug.

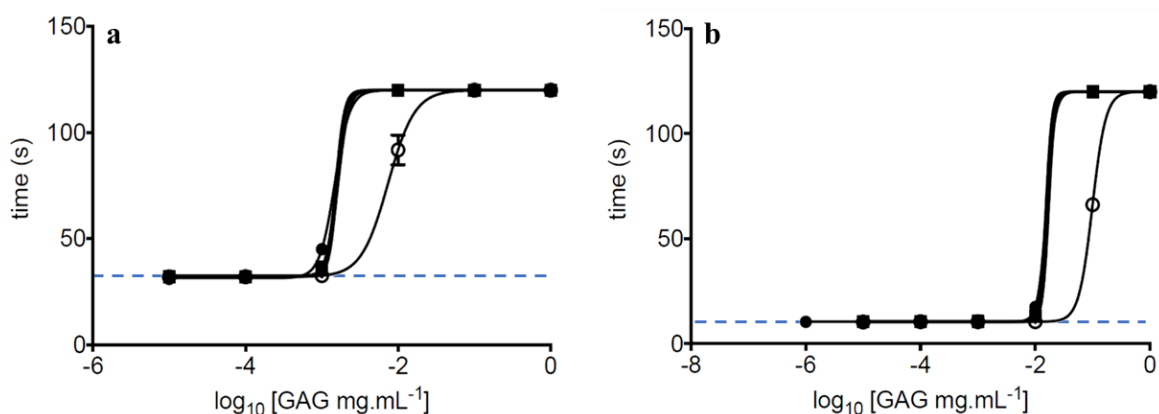


**Figure 3.17** The results of **a)** Activated Partial Thromboplastin Time (aPTT) and **b)** Partial Thromboplastin Time (PTT) tests of heparin acid hydrolysates, showing the change in clogging time (s) (delay of clogging time) due to addition of GAG (mg/ml). The blue line marks the normal clogging time that for **a)** aPTT test is ~ 35 s, and **b)** PTT test is ~ 15 s. Plot markers, *i.e.*: ●- heparin standard; ■- pH 2/ 40 °C/ 48 h; ▲- pH 3/ 60 °C/ 12 h; ▼- pH 4/ 80 °C/ 6 h; ◆- pH 5/ 40 °C/ 24 h; ○- pH 6/ 60 °C/ 48 h are overlapping due to negligible differences between the anticoagulation times of tested samples. Courtesy of The Royal Liverpool University Hospital.

#### 3.3.3.4 Concluding remarks

The anion analysis of the hydrolytic samples helped to establish that applied conditions were sufficient to release the covalently bonded sulfate from the heparin chain. The desulfation was particularly evident during the reaction carried at pH 1 - 3, especially at 80 °C. In fact, the statistical analysis showed that between pH 1 and pH 3, at all three studied temperatures, the reduction of molecular weight of heparin was primarily caused by

hydrolytic sulfate loss, rather than chain scission. Once to a significant extent (like at pH 1/ 80 °C), the desulfation could jeopardise the anticoagulant activity of heparin. The change of desulfation rate (over time) at harsher conditions (pH 1/ 80 °C/ up to 168 h) suggested that the process could involve different sulfate groups. To further investigate the last assumption, the hydrolysed samples were subjected to NMR analysis.

### **3.3.4 Inside look at acid-catalysed, hydrolytic desulfation of heparin, its selectivity, and a follow up to molecule chain fragmentation**

NMR spectroscopy has become one of the most comprehensive techniques for examining the detailed structure of glycosaminoglycans (see for example: Mulloy et al., 2012; Pomin, 2012, 2014b, 2014a; Rudd et al., 2019). It also offers an opportunity to follow structural alteration of the polymer chain, by either monitoring the modifications in spectra, like changes of chemical shifts of  $^1\text{H}$  and  $^{13}\text{C}$  signals in perspective to standard spectra, or by the appearance of new peaks (see for example: Panagos et al., 2016; Tømmeraas & Melander, 2008; Yates et al., 1996). In case of heparin, the positions of  $^1\text{H}$  and  $^{13}\text{C}$  signals are sensitive to the neighbouring groups like hydroxyl, carboxylate and amine, glycosidic oxygen, and O- or N-sulfate (Pomin, 2012, 2014b). In particular, the positions of  $^{13}\text{C}$  nuclei, adjacent to hydroxyl and amine groups are displaced downfield, that is, to higher chemical shift values because of substitution with sulfate groups, which are strongly electron-withdrawing. Logically, the removal of a covalently bound sulfate from these (hydroxyl and amine groups) results in their upfield move, towards lower chemical shift values.

The NMR shift patterns of heparin signals have been systematically studied and considered variants of each combination of sulfation and desulfation at IdoA and GlcN residues (see for example: Mulloy et al., 1993; Taylor et al., 2019; Yates et al., 1996). The redeployment of characteristic signals has been acknowledged (and assigned), following the sulfation changes. Here, the signals library created by earlier studies was treated as a tool to recognise the desulfation order of hydrolysed heparin readily from the NMR spectra. The desulfation profile of heparin, sketched in **section 3.3.3.1**, characterised the changed in desulfation rate (which probably mirrored removal of different sulfate groups) during the hydrolysis at pH 1. Therefore, this sample was used to model the desulfation order of molecule.

#### 3.3.4.1 *Standard spectra acquirement and analysis*

The one- $(^1\text{H}/^{13}\text{C})$  and two-dimensional (HSQC) spectra of heparin standard are presented in **Figure 3.18** and **Figure 3.19**, respectively. The spectra were acquired at the beginning of analysis, according to protocol described in **section 2.8.4**. The signals were labelled based on the comparative assignments of Keire et al. (2013) and Mauri et al. (2017). Generally, the heparin polysaccharide signals are divided into three NMR spectral groups that correspond to anomeric (5.0- 5.7 ppm), aliphatic (2.9- 4.5 ppm) and acetamidomethyl (1.9- 2.2 ppm) regions (see for example Monakhova & Diehl, 2018; Pomin, 2014b). Here, the glucosamine and iduronate characteristic regions has been highlighted in 2D spectrum of **Figure 3.19**, as these are crucial to track desulfation associated rearrangements discussed further in this section. At the same time the intensity of  $\beta$ -glucuronate and linkage region in **Figure 3.19b** is associated with high resolution of two-dimensional NMR reading (in comparison with one-dimensional in **Figure 3.19a**) and should not be considered as vital reference point for structure related discussion. The structure and chemical shift details of numbered peaks are given in **Table 3.7**. The spectra were treated as a reference for the following desulfation study, approached by comparative analysis between chemical shifts of chosen standard and hydrolysed signal.

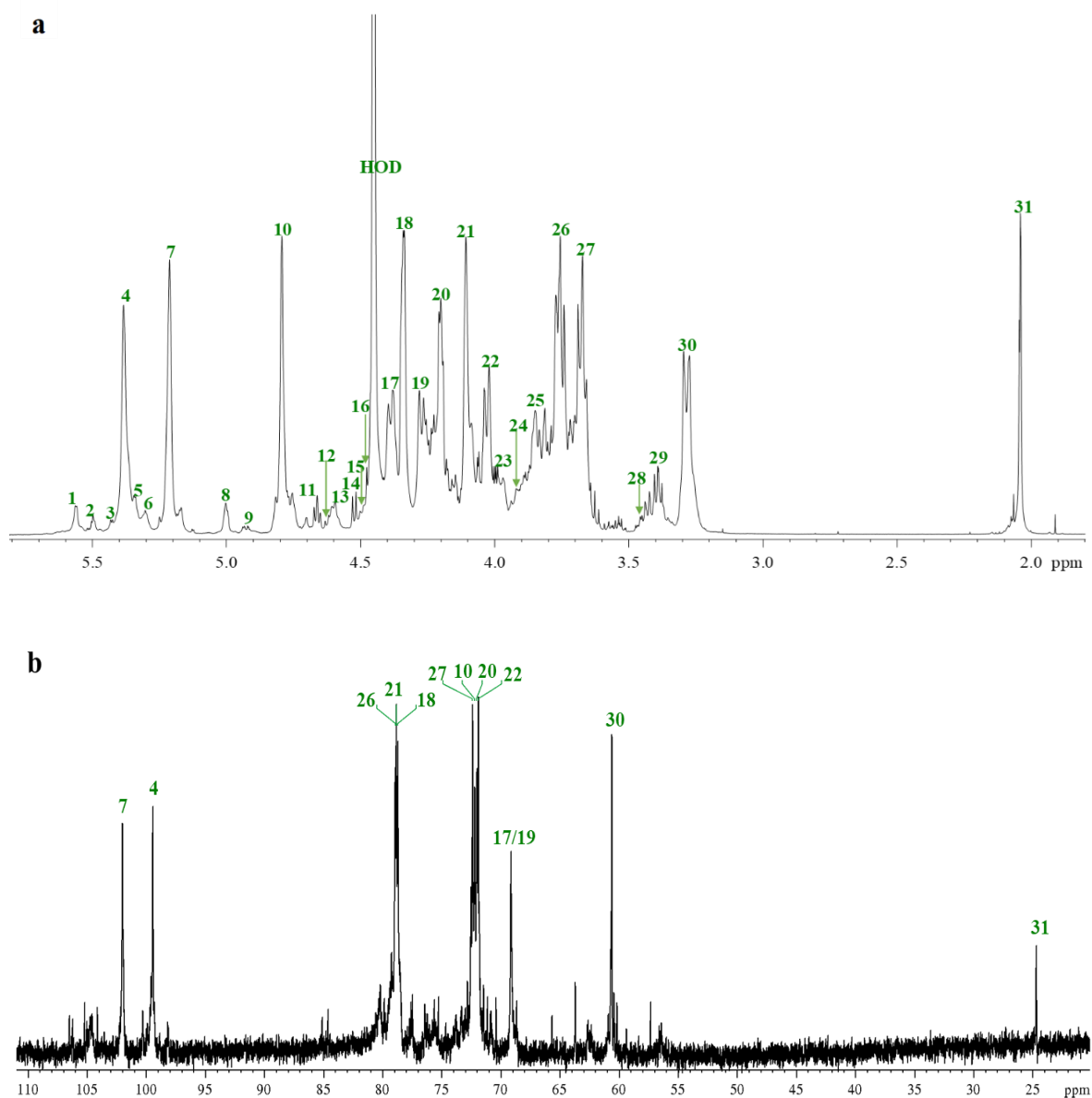


**Figure 3.18** One dimensional a) proton (<sup>1</sup>H) and b) carbon (<sup>13</sup>C) NMR spectra of heparin standard in D<sub>2</sub>O acquired according to protocol described in section 2.8.4. The details of labelled peaks are given in Table 3.7. The standard spectra were treated as a reference for following desulfation study (based on chemical shift differences between chosen peaks).

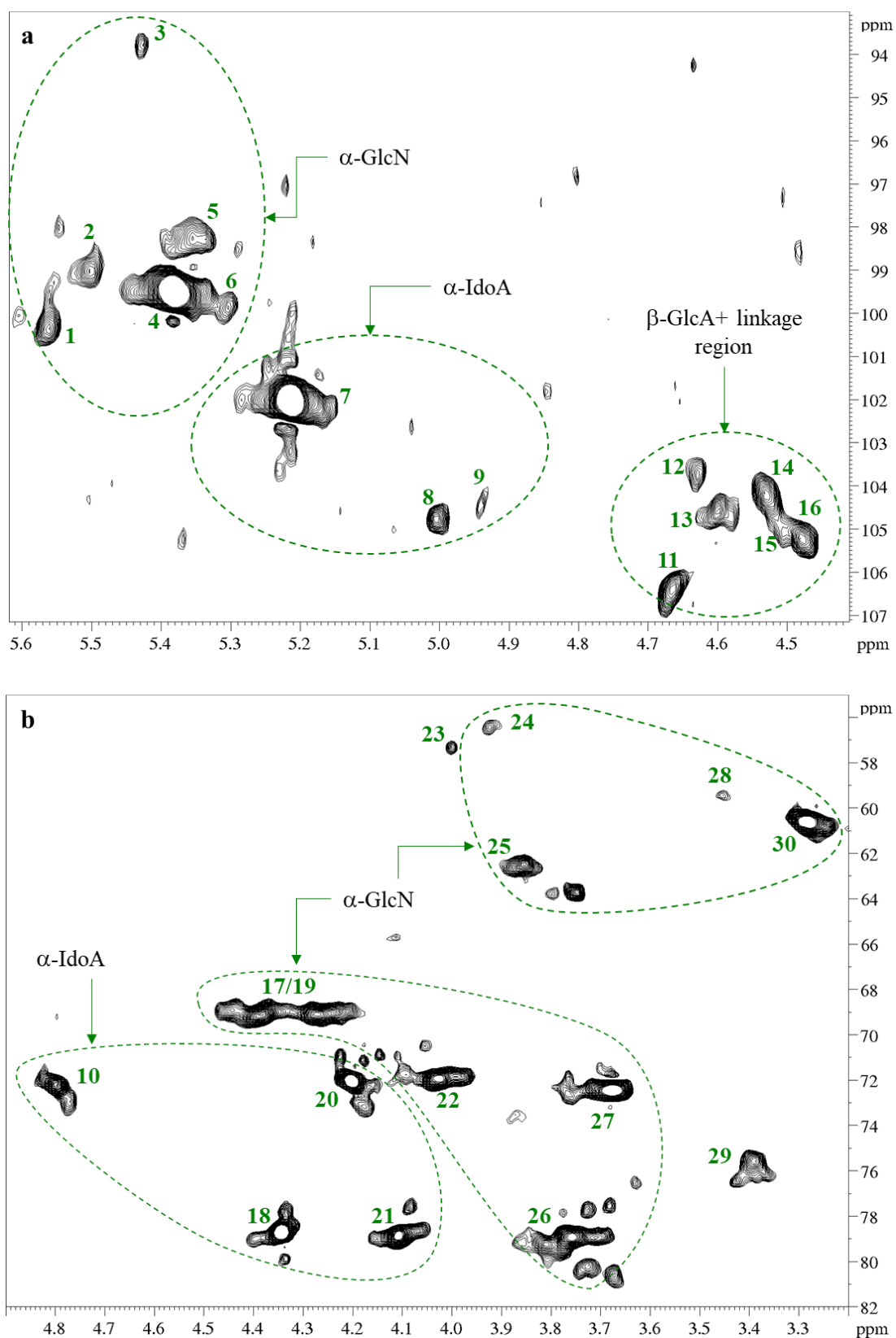


**Figure 3.19** Two-dimensional HSQC spectra of heparin standard, also used as reference for the following desulfation study. Picture a) and b) represents anomeric and aliphatic regions of polysaccharide, respectively.

**Table 3.7** Details of NMR signals of heparin standard, shown in **Figure 3.18 - Figure 3.19**.

N <sup>o</sup>	Carbon number <sup>a</sup>	Structure <sup>b</sup>	<sup>1</sup> H <sup>c</sup> (ppm)	<sup>13</sup> C <sup>d</sup> (ppm)	N <sup>o</sup>	Carbon number	Structure	<sup>1</sup> H (ppm)	<sup>13</sup> C (ppm)
$\alpha$ -Glucosamine units					$\alpha$ -Iduronic acid units				
1	A-1	A <sub>NS,6X</sub> -(G)	5.56	100.3	7	I-1	I <sub>2S</sub> -(A <sub>NS,6X</sub> )	5.21	102.0
2	A-1	A <sub>NS,3S,6X</sub>	5.51	99.0	8	I-1	I <sub>2OH</sub> -(A <sub>6S</sub> )	5.00	104.7
3	A-1	A <sub>NS</sub> - $\alpha$ Red	5.43	93.7	9	I-1	I <sub>2OH</sub> -(A <sub>6OH</sub> )	4.94	104.3
4	A-1	A <sub>NS,6X</sub> -(I <sub>2S</sub> ) + A <sub>NAc</sub> -(G)	5.38	99.4	10	I-5	<sup>5</sup> I <sub>2S</sub>	4.79	72.2
5	A-1	A <sub>NS,6X</sub> -(I)	5.36	98.2	18	I-2	<sup>2</sup> I <sub>2S</sub>	4.34	78.7
6	A-1	A <sub>NS</sub>	5.31	99.8	20	I-3	<sup>3</sup> I <sub>2S</sub>	4.20	72.0
17	A-6	A <sub>NY,3X,6S</sub> or A <sub>NX,6S</sub>	4.38	69.1	21	I-4	<sup>4</sup> I <sub>2S</sub>	4.11	78.8
19	A-6	A <sub>NY,3X,6S</sub> or A <sub>NX,6X</sub>	4.28	69.1	$\beta$ -Glucuronic acid + linkage region				
22	A-5	A <sub>NS,6S</sub>	4.02	71.9	11	G-1	<sup>1</sup> G-(Gal) + <sup>1</sup> Gal-(Gal)	4.66	106.3
24	A-2	A <sub>NAc,6X</sub>	3.92	56.5	12	G-1	<sup>1</sup> G-(A <sub>NS,3S</sub> )	4.63	103.7
25	A-6	A <sub>NS,6OH</sub>	3.85	62.4	13	G-1	<sup>1</sup> G-(A <sub>NS</sub> )	4.60	104.5
26	A-4	A <sub>NS,6S</sub>	3.76	78.9	14	G-1	<sup>1</sup> Gal-(Xyl)	4.53	104.1
27	A-3	A <sub>NS,6X</sub>	3.67	72.4	15	G-1	<sup>1</sup> G-(A <sub>NAc</sub> )	4.50	105.0
28	A-2	A <sub>NS,3S,6X</sub>	3.45	59.4	16	Xyl-1	Xyl-(Ser)	4.48	105.2
30	A-2	A <sub>NS,6X</sub>	3.27	60.6	29	G-2	<sup>2</sup> G + <sup>2</sup> A <sub>3S</sub>	3.39	75.6
31	A-2	A <sub>NAc</sub>	2.04	24.7	23		Ser	4.00	57.4

N<sup>o</sup>- peak number on NMR spectrum; <sup>a</sup> carbon number of monosaccharide unit; <sup>b</sup> structure of monosaccharide unit (+ linkage region, if applicable); <sup>c</sup> chemical shift value on proton spectrum; <sup>d</sup> chemical shift value on carbon spectrum; A- glucosamine residues; I- iduronic acid residues, G-glucuronic acid residues; S- sulfated; Ac- acetylated; X= H<sup>+</sup> or SO<sub>3</sub><sup>-</sup>; Y= H<sup>+</sup> or Ac<sup>-</sup> or SO<sub>3</sub><sup>-</sup>; Ser- serine

## 3.3.4.2 NMR- based model of heparin desulfation order and selectivity

The one- ( $^1\text{H}/^{13}\text{C}$ ) and two-dimensional (HSQC) spectra of heparin pH 1 hydrolysates, aliquoted at 40/ 60 °C: 24 and 48 h, as well as at 80 °C: 24, 48, 96 and 168 h, were compared with spectra of heparin standard, presented in **section 3.3.4.1**. The data used for comparative analysis, discussed in following sections are summarized below, in **Table 3.8**.

**Table 3.8**  $^{13}\text{C}$  and  $^1\text{H}$  chemical shifts of heparin standards and pH 1 hydrolysates.

pH 1 aliquot		$^1\text{H}/^{13}\text{C}$ chemical shift (ppm)											
		Peak <sup>a</sup> A-1 I <sub>2S</sub> - ANS(6X)	A-2 ANS(6X)	A-3 ANS(6X)	A-4 ANS(6S)	A-5 ANS(6S)	A-6 ANX(6OH)	A-6 ANY(3X,6S) OR ANX(6X)	I-1 I <sub>2S</sub> - ANS(6X)	I-2 I <sub>2S</sub>	I-3 I <sub>2S</sub>	I-4 I <sub>2S</sub>	I-5 I <sub>2S</sub>
Heparin standard		5.38	3.27	3.67	3.76	4.02	3.85	4.28-4.38	5.21	4.34	4.20	4.11	4.79
		99.4	60.6	72.4	78.9	71.9	n.d.	69.1	102.0	78.7	72.0	78.8	72.2
40 ° C	24 h	5.41	3.40	3.66	3.75	4.01	3.84	4.27-4.38	5.21	4.35	4.37	4.10	4.90
		93.7	56.9	72.5	79.2	71.9	n.d.	69.1	102.0	78.7	65.4	78.8	69.9
	48 h	5.41	3.40	3.68	3.75	4.01	3.84	4.27	5.21	4.35	4.37	4.10	4.90
		93.7	56.9	72.5	79.2	71.8	n.d.	69.1	102.0	75.5	65.4	78.6	69.9
60 ° C	24 h	5.41	3.40	3.96	3.80	4.02	3.85	4.29	4.96	4.36	4.36	4.19	4.90
		93.8	57.0	71.1	79.2	72.2	n.d.	68.8	104.7	75.6	65.6	77.2	70.0
	48 h	5.42	3.40	3.96	3.80	4.02	3.85	4.29	4.95	4.37	4.37	4.19	4.90
		93.8	57.0	71.1	79.2	72.2	n.d.	68.8	104.7	75.6	65.6	77.2	70.0
80 ° C	24 h	5.42	3.40	3.96	3.80	4.03	3.85	4.29	4.95	4.36	4.34	4.17	4.88
		93.8	57.0	71.0	79.2	74.2	62.3	68.8	104.7	75.6	65.6	77.2	70.0
	48 h	5.40	3.37	3.86	3.75	3.96	3.82	4.29	4.95	4.34	4.34	4.17	4.88
		93.8	57.0	71.0	79.4	74.2	62.3	68.9	104.7	75.5	65.5	77.0	69.7
	96 h	5.42	3.37	3.88	3.83	3.97	3.86	4.27	4.96	4.35	4.34	4.18	4.88
		93.9	57.2	71.2	79.5	74.3	62.4	68.8	104.7	75.6	65.7	77.2	69.9
	168 h	5.42	3.37	3.88	3.83	3.97	3.85	4.27	4.96	4.35	4.34	4.17	4.89
		94.1	57.2	71.3	79.7	74.4	62.4	68.8	105.2	75.6	65.7	77.2	69.9

<sup>a</sup> numbers next to monomer signal mark the carbon number; n.d.– not detected in  $^{13}\text{C}$  spectrum, but observed in 2D HSQC; various colours mark most prominent changes in 40 ° C, 60 ° C and 80 ° C NMR spectra

## 3.3.4.2.1 NMR confirmed lability of N-linked sulfate of heparin

In 1996, Yates et al. (1996) presented a comprehensive study of NMR spectra of heparin, discussing the changes of chemical shifts in reference to the species of different sulfation patterns. Therein, the discharge of an N-linked sulfate group from the glucosamine unit caused the upfield shift at the carbon from which the anionic group was detached (A-2), as a result of decreased deshielding effect (Yates et al., 1996). Following the A-2 displacement, the I-3 signal was free to resonate further upfield (that was a consequence of terminated interaction between the hydroxyl at position 3 of IdoA and the N-sulfate of GlcNS) (Yates et al., 1996). Therefore, both A-2 and I-3 signals can serve as indicators of N-desulfation.

When comparing standard heparin with the pH 1/ 40 °C/ 24 h sample, as in **Table 3.8**, the partial upfield shift from 72.0 to 65.4 ppm ( $\Delta = 6.6$  ppm) and partial downfield shift from 4.20 to 4.37 ppm ( $\Delta = 0.17$  ppm) were noted respectively in  $^{13}\text{C}$  and  $^1\text{H}$  spectrum for signal I-3. Additionally, the I-5 signal started to move upfield, from 72.2 to 69.9 ppm ( $\Delta = 2.3$  ppm) in carbon and downfield from 4.20 to 4.37 ppm ( $\Delta = 0.17$  ppm) in proton (**Table 3.8**, yellow highlight). The positions of A-1 and A-2 signals started to shift upfield as follows: 99.4  $\rightarrow$  93.7 ppm ( $\Delta = 5.7$  ppm), 60.6  $\rightarrow$  56.9 ppm ( $\Delta = 3.7$  ppm) in  $^{13}\text{C}$ , while in  $^1\text{H}$  signals of these moved only by 0.03 and 0.13 ppm downfield, respectively for A-1 and A-2 (**Table 3.8**, yellow highlight). The spectrum of pH 1/ 40 °C/ 48 h sample resembles the pH 1/ 40 °C/ 24 h spectrum, with an additional upfield change of I-2, from 78.7 to 75.5 ppm ( $\Delta = 3.2$  ppm) in  $^{13}\text{C}$  and little downfield move of 0.01 ppm in  $^1\text{H}$ , it is presented in **Figure 3.20**.

Following the discussed literature (Yates et al., 1996), the move of A-2 and I-3 peaks marked the beginning of heparin N-desulfation. Clearly, the N-desulfation was the only degradative process observed at these conditions. Therefore, it could be assumed that the change of molecular weight of heparin, observed at pH 1/ 40 °C (discussed in **section 3.3.1**), was completely due to sulfate loss. Furthermore, the presented results provide experimental evidence of heparin susceptibility to N-sulfate loss in hydrolytic conditions, initially founded on proximate studies and indirect analysis (Danishefsky et al., 1960; Inoue & Nagasawa, 1976; Jandik et al., 1996).

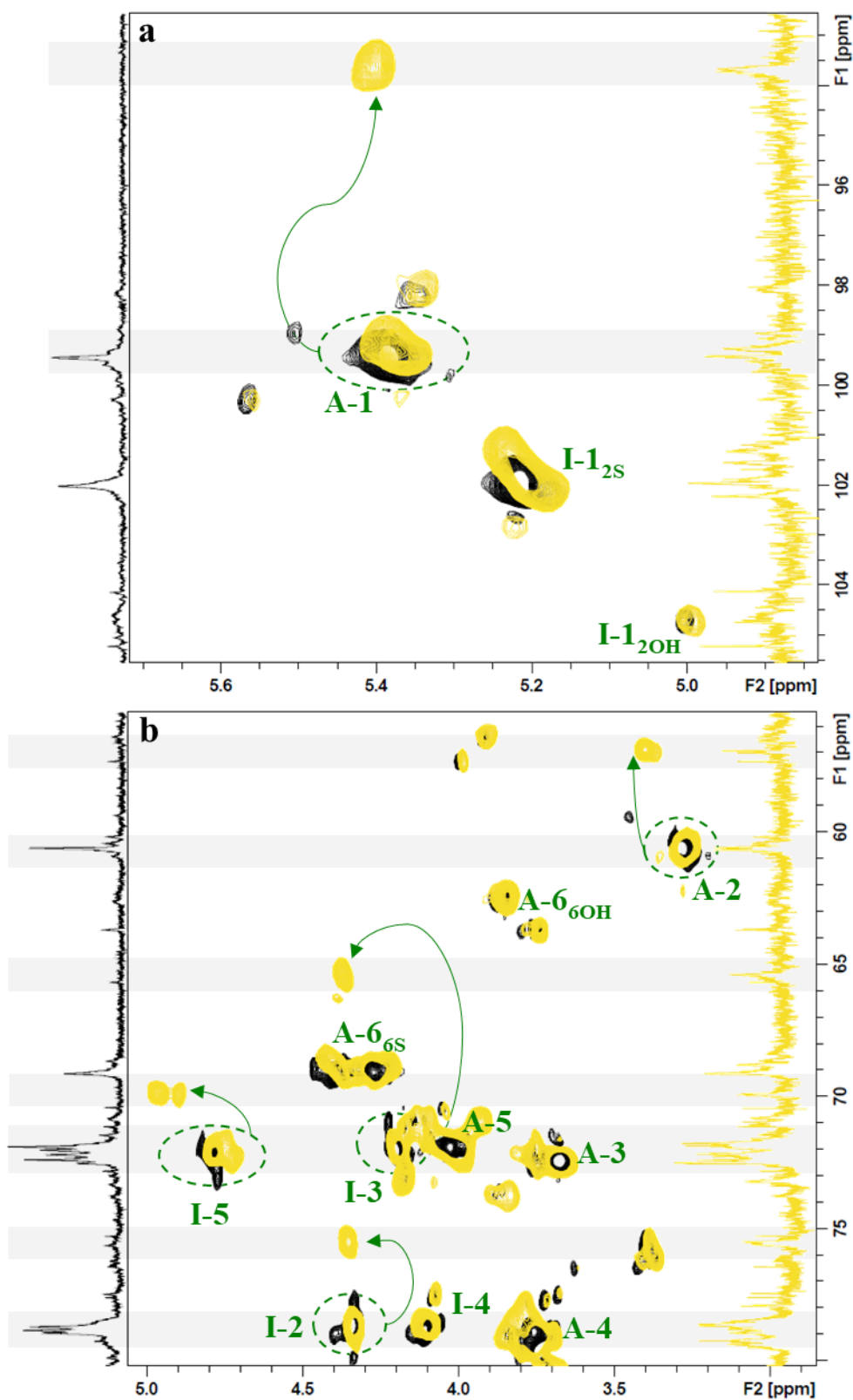


**Figure 3.20** The NMR spectra (HSQC) of heparin hydrolysed at pH 1/ 80 °C/ 48 h (yellow) over the standard sample (black). The green arrows and grey region mark the shift of peaks in **a)** anomeric and **b)** aliphatic regions, which reflects (the beginning of) N-desulfation of the molecule under applied conditions.

## 3.3.4.2.2 Unexpected order of reactivity of O-linked sulfates of heparin

The analysis of samples hydrolysed at pH 1/ 60 °C showed that signals A-1, A-2, I-2, I-3 and I-5 were completely shifted to the positions discussed in the paragraph above (3.3.4.2.1) after 24 h of processing (Table 3.8, orange highlight). The ‘shift termination’ of peaks associated with N-desulfation (as discussed in 3.3.4.2.1) suggested completion of N-desulfation process. Following this assumption, the pH 1/ 60 °C spectra were checked against a N-desulfated heparin standard. The resemblance between compared spectra and match between the  $^1\text{H}/^{13}\text{C}$  positions of the glucosamine and iduronate peaks (Table 3.8, orange highlight), indicated that hydrolytic degradation at pH 1/ 60 °C indeed led to completely N-desulfation of heparin, after 24 hours.

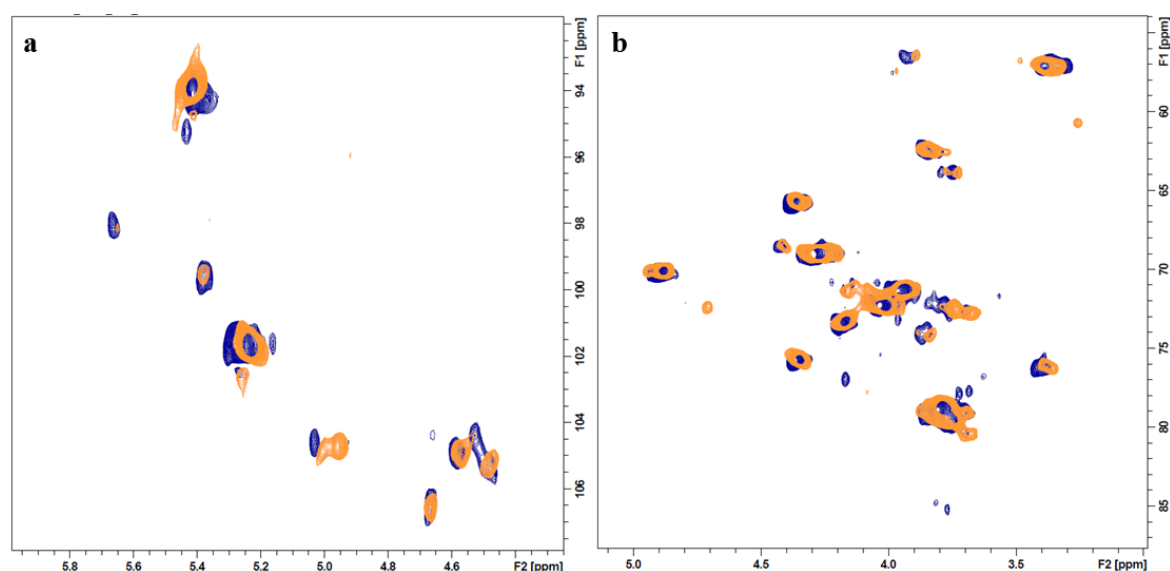


**Figure 3.21** The NMR spectra (HSQC) of heparin hydrolysed at pH 1/ 60 °C/ 24 h (orange) over the N-desulfated standard (blue), showing the resemblance of spectra in **a**) anomeric and **b**) aliphatic regions.

The analysis of pH 1/ 60 °C sample revealed another interesting phenomenon. The change of I-1 signal, which started to move downfield in  $^{13}\text{C}$  from 102.0 to 104.7 ppm ( $\Delta = 2.7$  ppm), and upfield in  $^1\text{H}$  from 5.21 to 4.96 ppm ( $\Delta = 0.25$  ppm) (Table 3.8, orange highlight), marked beginning of O-desulfation at carbon 2- of IdoA (Yates et al., 1996). At the same time, as shown in Figure 3.22, the  $^1\text{H}/^{13}\text{C}$  positions of signal A-6 remained unchanged (Table 3.8). This suggests that under applied conditions 2-O-desulfation is in preference to 6-O-desulfation. To highlight the importance of this finding, it should be recapped that until

now, the hydrolytic desulfation of heparin was generalised as OS<<NS (Danishefsky et al., 1960; Inoue & Nagasawa, 1976), with confidence that O-desulfation follows 2OS< 6OS order, as in solvolytic environments (Baumann et al., 1998; Kariya et al., 2000; Nagasawa et al., 1977). In fact, the selectivity of hydrolytic process leaned towards 2-O-sulfate rather than to 6-O-sulfate.

To get more perspective at 6-O-desulfation, the spectra of pH 1/ 80 °C hydrolysate were analysed. The previous studies demonstrated that loss of 6-O-sulfate is associated with the major chemical shift of A-6 and A-5 carbon signals (Taylor et al., 2019; Yates et al., 1996). The <sup>13</sup>C spectra comparison of heparin standard and pH 1/ 80 °C, indeed, exposed the upfield changes from 69.1 to 62.3 ppm ( $\Delta= 6.9$  ppm) at positions A-6 and downfield move of the A-5 signal, from 71.9 to 74.2 ppm ( $\Delta= 2.3$  ppm). The proton positions of both peaks moved upfield by 0.03 and 0.06 ppm, respectively (**Table 3.8**). As illustrated in **Figure 3.23**, the progressive movement of I-1 signal (102.0  $\rightarrow$  104.7 ppm), marking the continuing 2-O-desulfation, was also observed. This suggests that the acid-catalysed, hydrolytic 6-O-desulfation is not conditional upon 2-O-sulfate loss, and therefore, not selective.

The selectivity of hydrolytic O-desulfation of heparin needs to be discussed further. To do so, the integral ratios of chosen signals were studied. The following analysis showed that, at pH 1/ 60°C, the approximate integrals ratio of I-1 signals,  $I_{2S} : I_{OH}$ , is 6.7:1, while the ratio of integrated A-6 signals,  $A_{6S} : A_{OH}$ , is 4.1:1. Therefore, at these conditions, heparin exhibits preference towards hydrolytic secondary sulfate (2-O-S-) loss. In comparison, at pH 1/ 80 °C, the same estimation favours 6-O-sulfate by 1.5 greater fold than at 60 °C. Furthermore, the pH 1/ 80 °C conditions triggered glycosidic scission, which would additionally compromise the judgment of the O-desulfation order. In addition, the results of UV-Vis analysis (summarised in **section 3.3.2.2**) suggested that the cleaved units might still hold O-sulfate groups. Nevertheless, the presented findings demonstrated that the acid-catalysed hydrolytic desulfation of heparin is strongly dependent upon the applied conditions and should certainly not be considered to follow the same mechanism as solvolytic degradation.

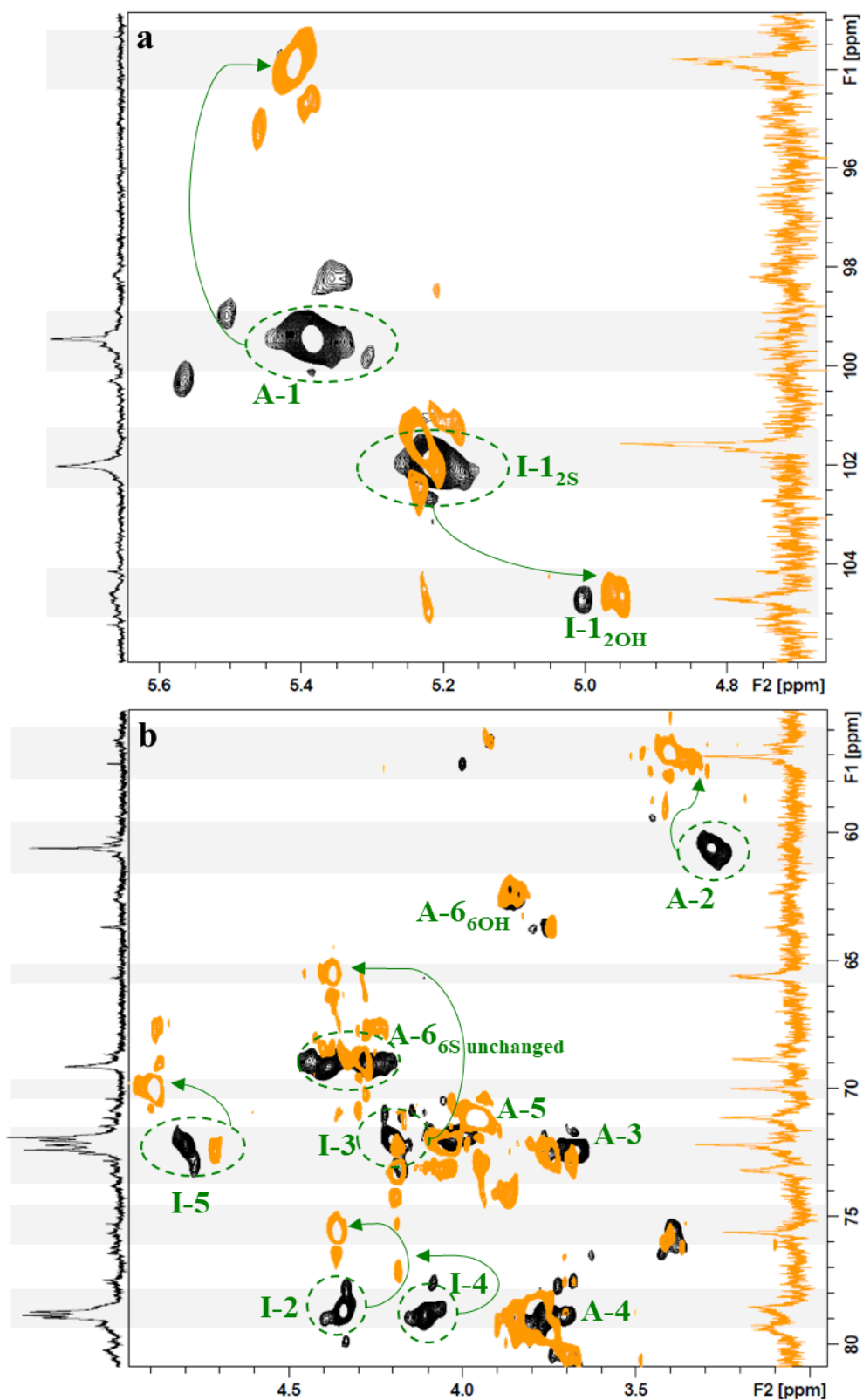


**Figure 3.22** The NMR spectra (HSQC) of heparin hydrolysed at pH 1/ 60 °C/ 48 h (orange) over the standard sample (black). The green arrows and grey region mark the shift of peaks in **a)** anomeric and **b)** aliphatic regions. The shift of A-1 and A-2 marks completed N-desulfation, while changes of I-I reflect 2-O-desulfation.

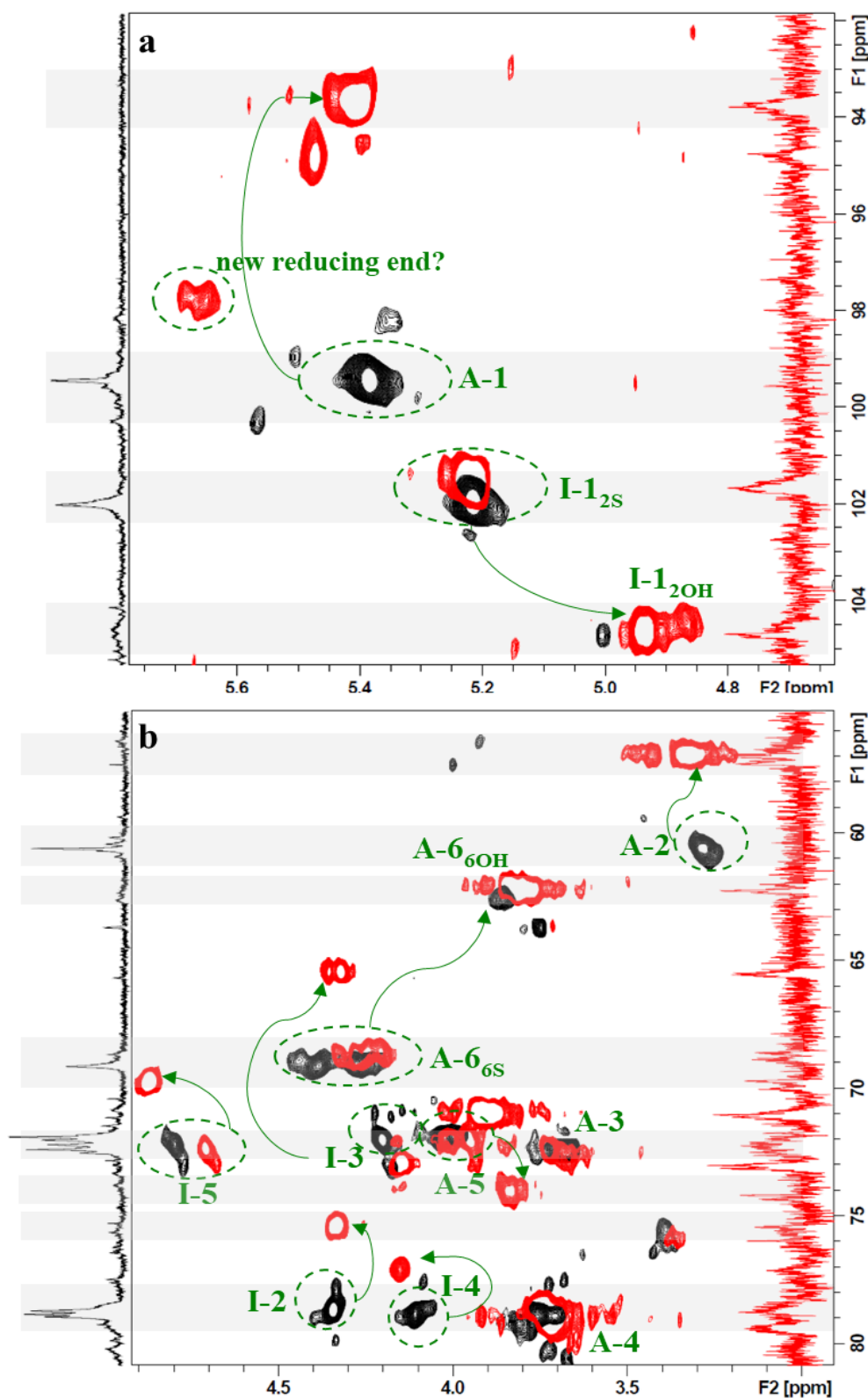


**Figure 3.23** The NMR spectra (HSQC) of heparin hydrolysed at pH 1/ 80 °C/ 48 h (**red**) over the standard sample (**black**). The green arrows and grey region mark the shift of peaks in **a**) anomeric and **b**) aliphatic regions. The shift of A-6 marks the beginning of 6-O-desulfation, while I-I reflect continuous 2-O-desulfation. The new peak signed and circled in **a**) probably reflects C-1 of severed glucosamine unit.

In addition, a new peak of coordinates 5.48 ppm/  $^1\text{H}$ ; 94.8 ppm/  $^{13}\text{C}$  was observed in pH 1/ 80 °C/ 48 h spectrum, as circled in **Figure 3.23**. Bearing in mind that these conditions are sufficient to initiate glycosidic scission (see **3.3.2.1** and **3.3.2.3**), the signal may represent C-1 of free glucosamine (Pomin, 2012; Tommeraas et al., 2001). As shown in **Figure 3.23**, this was the ‘only’ new signal characterised in the NMR spectrum, while the elution profile of ion chromatography indicated the presence of other residues in pH 1/ 80 °C/ 48 h sample (see **Figure 3.12**). Yet, the prolonged hydrolysis at pH 1/ 80 °C created an opportunity to check if the NMR profile would reflect further degradation (observed by electrophoresis in **3.3.2.1** and chromatography in **3.3.2.3**) of polymeric chain. However, it would be challenging to distinguish the low levels cleaved oligosaccharides, since their NMR spectra most probably resemble the original heparin spectrum (Guerrini et al., 2005).

#### 3.3.4.2.3 Inside look at continuous desulfation and degradation of heparin

In electrophoretic and quantitative anion analysis (discussed in **sections 3.3.2.1.4** and **3.3.3.1**, respectively) samples aliquoted at 96 h and 168 h were associated with the most characteristic changes, *i.e.*, in electrophoresis, these were identified with depolymerisation limits, based on elution profiles; in anion chromatography, these were thought as boundaries between different, released sulfate groups. Therefore, both samples were chosen to further investigate the desulfation and degradation progress of pH 1/ 80 °C hydrolysed heparin. As previously, the NMR spectra of each sample were compared with heparin standard. The outcome of HSQC comparison is presented in **Figure 3.24** and **Figure 3.25**, respectively for 96 h and 168 h hydrolysates.

The aliphatic regions of both samples still very much resembled the original heparin (**Figure 3.24** and **Figure 3.25**). Of course, the signals were shifted to the positions reflecting changes in sulfation pattern (discussed in previous sections). Surprisingly, the A-6 signal was still observed at its original (68.8 ppm/  $^{13}\text{C}$ ) and shifted (62.4 ppm/  $^{13}\text{C}$ ) locations, confirming the ongoing 6-O-desulfation (**Figure 3.24** and **Figure 3.25**). Furthermore, I-1 signal that mirrored the continuing 2-O-desulfation was also observed. On the other hand, glycosidic scission would be expected to occur at the reducing end of polymeric chain, and logically, be reflected by changes in anomeric region. In fact, as marked in yellow in **Figure 3.24** and **Figure 3.25** it was the case in both samples.

Considering the location of new peaks, depolymerisation most probably resulted in short oligosaccharides, composed of glucosamine and iduronate residues of different sulfation profiles. Slow O-desulfation, pictured *via* NMR (and UV-Vis in **section 3.3.2.2**) suggests that some of cleaved units could still hold 2-O- and 6-O-sulfate groups. Furthermore, the degradation could alter the iduronate units, which would explain low ratio of GlcN to IdoA observed during the monosaccharide analysis discussed in **section 3.3.2.3**. However, this assumption requires more detailed analysis.

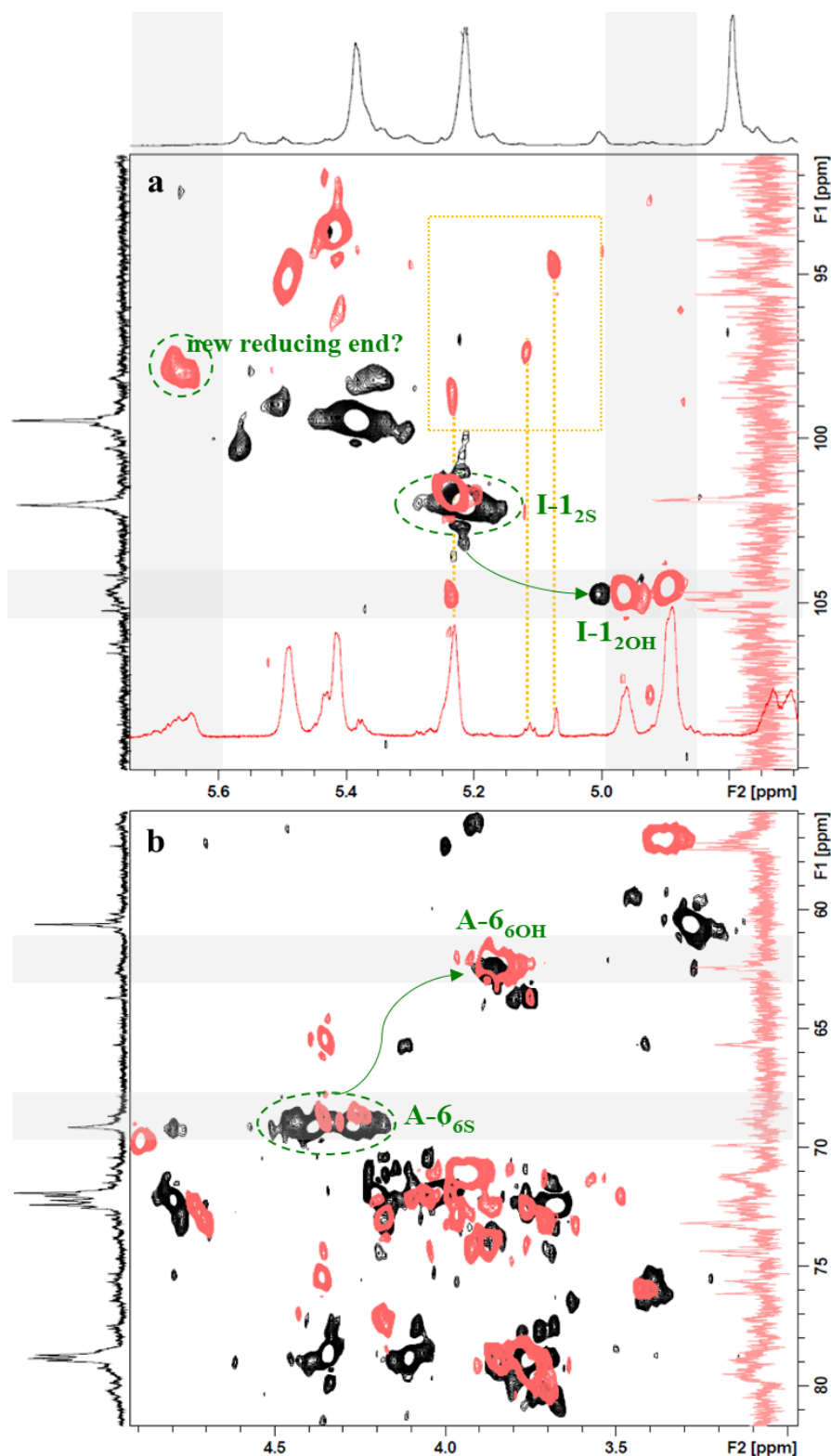


**Figure 3.24** The NMR spectra (HSQC) of heparin hydrolysed at pH 1 / 80 °C / 96 h (red) over the standard sample (black). The green arrows mark the continuous 2-O-desulfation in **a**) anomeric and 6-O-desulfation in **b**) aliphatic regions. In **a**) the new, unidentified peaks are highlighted in yellow square, while signed and green-circled probably reflects C-1 of hydrolytically liberated GlcN unit.

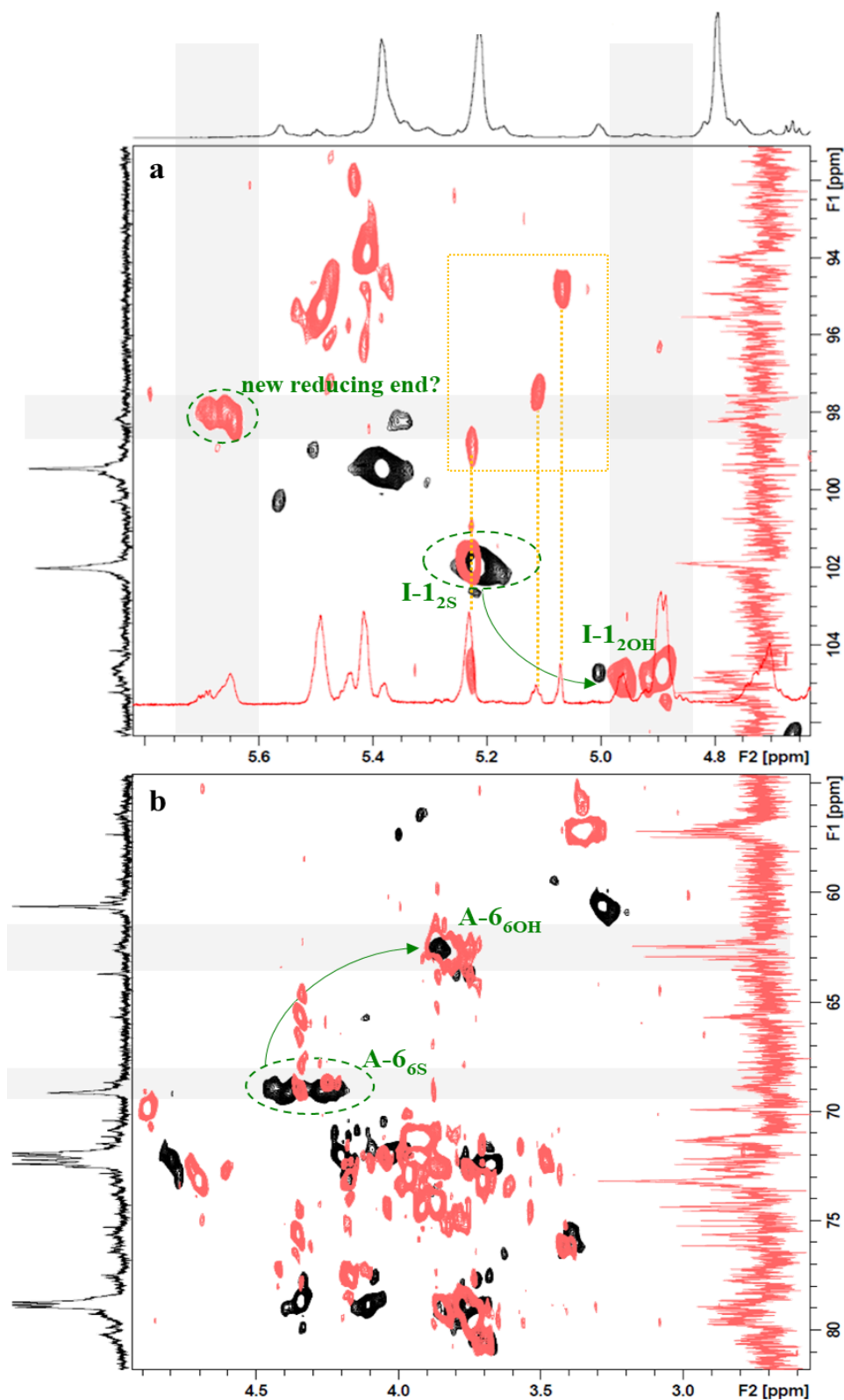


**Figure 3.25** The NMR spectra (HSQC) of heparin hydrolysed at pH 1/ 80 °C/ 168 h (red) over the standard sample (black). The green arrows mark the continuous 2-O-desulfation in **a)** anomeric and 6-O-desulfation in **b)** aliphatic regions. In **a)** the new, unidentified peaks are highlighted in yellow square, while signed and green-circled probably reflects C-1 of hydrolytically liberated GlcN unit.

## 3.3.4.2.4 NMR model of hydrolytic desulfation of heparin - concluding remarks

Although Danishefsky et al. (1960) and Inoue/Nagasawa (1976) established the hydrolytic priority of heparin to N-desulfation over the O-desulfation in acidic pH (Danishefsky et al., 1960; Inoue & Nagasawa, 1976), the order of the latter has not been fully studied. Based on solvolytic degradation, examined in more detail (for general summary see Baumann et al., 1998; or Bedini et al., 2017), the hydrolytic sulfate loss at acidic pH was believed to follow  $2OS < 6OS \ll NS$  order. However, the NMR analysis presented herein, demonstrated that O-desulfation order of heparin dissolved in aqueous media is strongly dependent upon applied conditions (both pH and temperature), and if brought to any ordered equation, it should rather be written as  $6OS \leq 2OS \ll NS$ . Furthermore, NMR analysis provided an experimental evidence of N-desulfation priority. It was also shown that N-sulfate group could be completely removed from heparin chain, without jeopardising the glycosidic bonds (at pH 1/ 60 °C). Although this alteration would most probably lead to loss of anticoagulant activity (as discussed in **3.3.3.3**), which may be attractive for those who seeks to create heparin substitutes of such reduced anticoagulation power. In contrast to N-group, the 2-/6-O-sulfates exhibited low lability to applied conditions, and even when exposed to harsh environments (pH 1/ 80 °C) over the long periods of time (up to 168 h) were still detected in heparin chain. This creates the potential to adjust heparin structure and design compound of different (to anticoagulant) functionality. Considering the reviewed order of desulfation and significance of sulfate loss towards the character and functionality of the molecule, the desulfation process should certainly be included in mechanism of hydrolytic degradation of heparin in aqueous acidic environments. Hence, **Figure 3.26** presents a refinement to the mechanism previously suggested by Jandik et al. (1996).

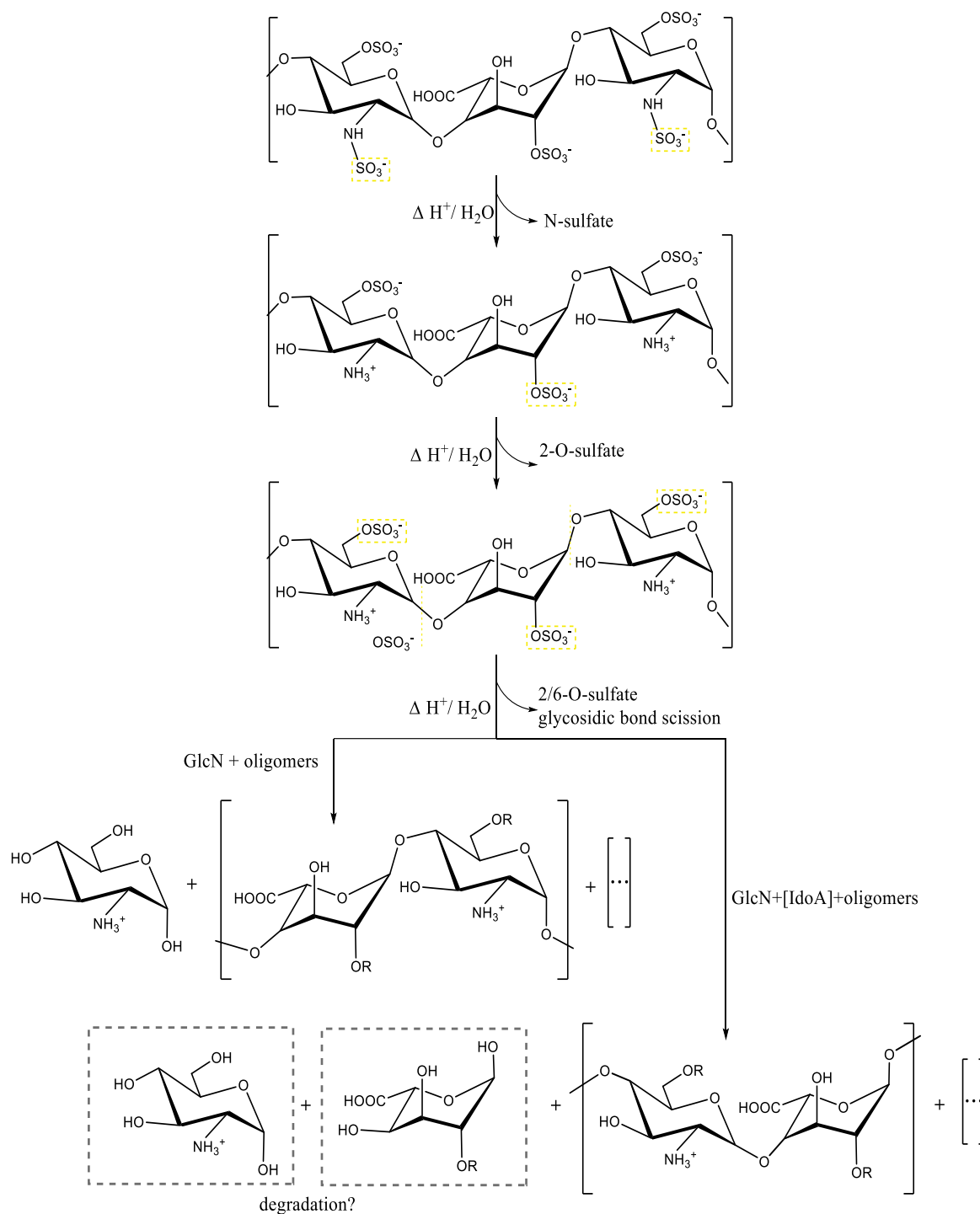


**Figure 3.26** Proposed mechanism of hydrolytic degradation of heparin in acidic environments based on the conclusions drawn from the experimental study presented in Chapter 3. The individual sulfate groups liberated at each characteristic stage of the mechanism, were highlighted in yellow. The last stage of the mechanism assumes two pathways: one targeting the GlcN/GlcNS-(1 $\rightarrow$  bond and resulting in GlcN monomer and heparin oligomers (left) and one that assumes the additional scission of IdoA and further degradation of monomeric-units (right). The bracket left after the final arrow indicates the (probable) subsequent degradation of the polymer chain. R= H or  $SO_3^-$  (conditional upon applied factors).

#### 3.3.4.3 A second (NMR) glance at pharmacological activity of hydrolysed heparin

The results of anticoagulation tests (discussed in **section 3.3.3.3**) demonstrated that the activity of samples hydrolysed between pH 2 and 6 (various aliquots) was not affected by applied conditions. Samples hydrolysed at pH 6/ 60 °C/ 48 h showed 10-fold weaker responses to both aPTT and PTT tests than other samples (**Figure 3.17**). To investigate if the lowered activity was a consequence of structural alterations, triggered by this particular environment, the pH 6 sample was subjected to NMR analysis (according to protocol described in **section 2.8.5**). The comparative analysis of NMR spectra (heparin sample vs. hydrolysate, spectrum not shown) did not display any structural changes in pH 6 sample.

However, as illustrated in  $^1\text{H}$  spectra in **Figure 3.27**, citric acid, characterised by doublet of doublets in 2.7 - 2.5 pm region (*Human Metabolome Database*, n.d.-b) was detected in tested sample, regardless desalting performed primarily (as per protocol in **section 2.4.3.3**) to each anticoagulant activity check.

The traces of citric acid are the results of insufficient desalting of hydrolytic sample, buffered at pH 6 in citrate buffer (details of hydrolytic buffer systems are given in **2.2.3.4**). The aPTT and PTT procedures refer to activity in time. Therefore, measured from the moment of addition of calcium cations (which catalyse clotting pathway) to the experimental samples, the presence of citrate anions, which would be expected to chelate calcium and prevent spontaneous clotting, has therefore most probably resulted in an underestimation of the response of both tests (*Partial Thromboplastin Time (PTT) Test: MedlinePlus Medical Test*, n.d.; *Screening Tests in Haemostasis: The APTT*, n.d.). Thus, the decreased activity of samples subjected to pH 6/ 60 °C/ 48 h is a result of incomplete sample clean-up during the preparation, rather than any change within the heparin structure.

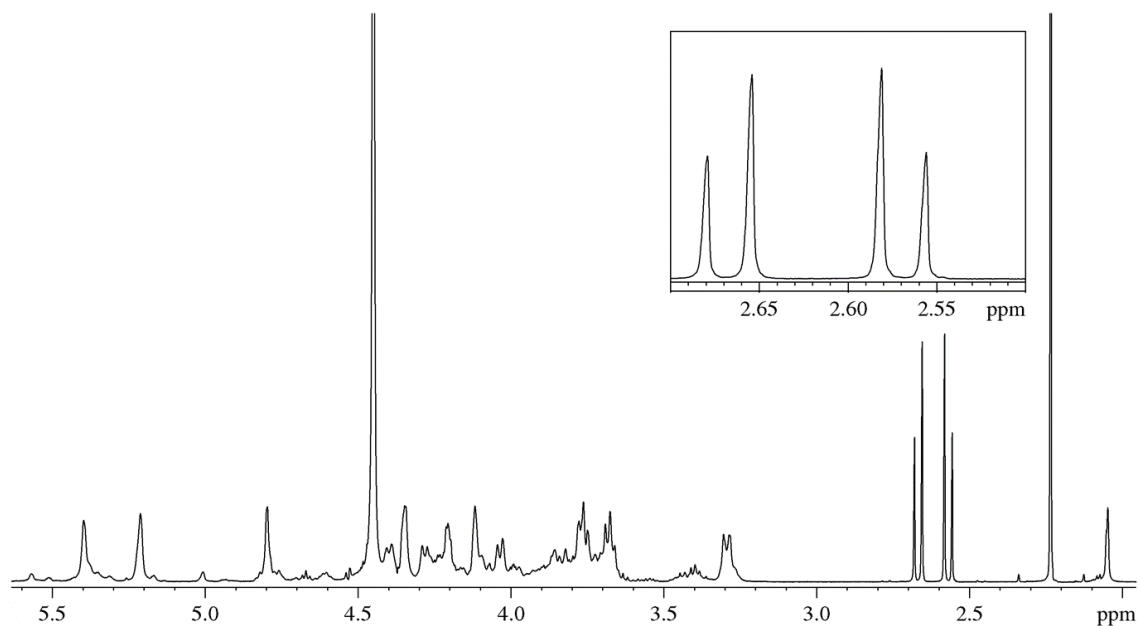


**Figure 3.27** Proton NMR spectrum of pH 6/ 60 °C/ 48 h sample, which showed low(er) anticoagulant activity in aPTT and PTT study, with zoomed in doublet of doublets typical of citric acid.

### 3.4 THE KINETIC APPROXIMATION OF HYDROLYTIC DEGRADATION OF HEPARIN IN ACIDIC ENVIRONMENTS

#### 3.4.1 Introduction

Once described, kinetics is a powerful tool that can be used to control or manipulate a chemical reaction. In order to do so, one will have to understand the rate with which the reaction proceeds as well as the influence of factors, such as the reaction temperature, concentration of reactants, action of catalysts or the nature of reaction medium (Sun, 2004; Tanford, 1961). The study of reaction kinetics usually goes hand in hand with the elucidation of the reaction mechanism, especially in case of degradation studies (Bauer et al., 2012; Loftsson, 2013; Sinko, 2011). In case of macromolecules, like polysaccharides, it is hard to specify their exact behaviour in a studied system, particularly if the degradation of heterogenous compounds is considered. Consequently, the kinetic description of many macromolecules could not be distinguished at all, or in best case scenario, would be approximated to random scission (Bradley & Mitchell, 1988; Karlsson & Singh, 1999; Melander & Tømmerraas, 2010; Morris et al., 2009; Tømmerraas & Melander, 2008)

The objective of this section is to formulate a kinetics approximation for degradative reactions of heparin, catalysed by acidic pH in aqueous systems. The platform for this task were results discussed in **section 3.3** of this chapter. Considering system complexity, the “approximation” concept needs to be emphasised, while the presented model should be considered as theoretical. Yet, to strengthen the presented idea, chosen data were plotted **Figure 3.28** and **Figure 3.29** according to standard kinetic law, as demonstrated in **section 3.4.3**. The ‘lack of kinetic fit’ emphasised that the standard kinetics approach was not appropriate to accurately describe degradative process of heparin, observed in acidic environments.

### 3.4.2 Proposed kinetic model of hydrolytic degradation of heparin in acidic environments

To support the estimation of kinetic equation describing the hydrolytic degradation of heparin in acidic environments, it was found useful to summarise the changes discussed in **section 3.3** in a schematic reaction flow.

Firstly, the cationic dye staining (summarised in **3.3.2.1.3**), sulfate anion analysis (discussed in **3.3.3**) and comprehensive NMR study (discussed in **3.3.4.2.1**) helped to establish the primary lability of N-sulfate groups of heparin to aqueous acidic environments. In fact, it has been shown that heparin, subjected to pH 1/ 60 °C, could be completely N-desulfated (for details, see **section 3.3.4.2.1**). Thus, the N-desulfation was proposed as a first stage of degradative mechanism, presented in Scheme 3.1. N-desulfation has been considered as a “completed” reaction, hence, it was kinetically separated (to simplify the estimation) and summarised in scheme 3.1:



where,  $k_{-NS}$  is the N-desulfation rate constant of heparin.

Before approaching the kinetic estimation, the following assumptions were noted. Firstly, as discussed in **section 1.4.4**, the hydrolytic reaction was run so largely in excess of solvent (water) that its concentration was considered constant in given system and the system itself was described by “apparent” or “pseudo” first order. Ergo, the further discussed rate

constants should be considered as “observed”. Secondly, the studied system was buffered, with the pH controlled over the reaction time. Therefore, the *general acid-base* catalytic impact of buffering species was neglected (as discussed in **1.4.4.2.3**). On the other hand, considering the *specific acid-base* catalysis (discussed in **1.4.4.2.1**), the estimated rate constants would be strongly dependent upon the concentration of protons, and therefore pH, as shown in **equation 1.30**. Finally, the reactions of discussed schemes were treated as homogeneous.

Following the kinetic assumptions, the rate of N-desulfation of heparin in Scheme 3.1, was summarised as:

$$\frac{d[Hep]}{dt} = -k_{-NS} \cdot [Hep] \quad 3.3$$

where  $k_{-NS}$  is a pseudo- N-desulfation rate constant, while  $Hep$  is the concentration (or other easily measurable characteristic properties, *e.g.*, molecular weight) of heparin at the reaction time  $t$ . By integrating the equation 3.3 in line with rearrangements presented from **equation 1.10** to **equation 1.12**, it can be written as:

$$\ln \frac{[Hep]_t}{[Hep]_0} = -k_{-NS}t \quad \text{or} \quad \frac{[Hep]_t}{[Hep]_0} = \exp(-k_{-NS}t) \quad 3.4$$

and changing the notation to match Scheme 3.1, *i.e.*:  $Hep_t \rightarrow Hep_{-NS}$ ;  $Hep_0 \rightarrow Hep$ , the equation 3.4 can be re-written as:

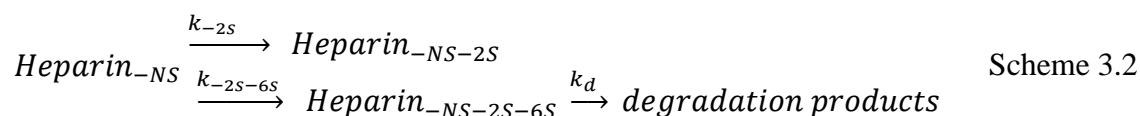
$$\ln \frac{[Hep]_{-NS}}{[Hep]} = -k_{NS}t \quad \text{or} \quad \frac{[Hep]_{-NS}}{[Hep]} = \exp(-k_{NS}t) \quad 3.5$$

If the rate constant  $k_{-NS}$  is known, the equation 3.5 could be used to predict how the concentration (or molecular weight) of heparin is changing with respect to time  $t$ . Furthermore, as discussed in **section 1.4.4.4**, the reaction rate was assumed to follow the Arrhenius dependence of temperature. Thus, using the Arrhenius relation, shown in **equation 1.22**, equation 3.5 can be re-written to include the influence of temperature:

$$\frac{[Hep]_{-NS}}{[Hep]} = \exp\left(A \cdot \exp\left(\frac{E_a}{RT}\right) t\right) \quad 3.6$$

where  $T$  is temperature (K),  $E_a$  is activation energy (J/mol),  $A$  is called the frequency factor and  $R$  is the universal gas constant (8.314 J/K·mol).

NMR analysis of acid hydrolysed heparin, discussed in **section 3.3.4.2.2**, showed that the process following N-desulfation is 2-O-desulfation. At the same time, it was shown that the selectivity between 2-O-desulfation and subsequent 6-O-desulfation was relatively low (**3.3.4.2.2**). Therefore, it could be assumed that the 2-O-desulfated and 2/6-O-desulfated products would be simultaneously present in the studied system. Furthermore, none of these reactions were completed before an actual depolymerisation of glycosidic bonds between the elementary units of heparin, caused by prolonged acid treatment, as shown in **section 3.3.4.2.3**. In essence, the state of such system could be written as:



where  $k_{-2S}$  is a pseudo-2-O-desulfation rate constant,  $k_{-2S-6S}$  is a pseudo-2/6-O-desulfation rate constant and  $k_d$  is a pseudo-degradation rate constant.

Without doubt, the sequence of reactions summarised in Scheme 3.2 is extremely complicated to be kinetically described. Obviously, none of the above reactants would reach their concentration maximum in examined system. Rather, the concentration of N-desulfated heparin, *Heparin -NS*, would only decrease, the concentrations of N-2-O-desulfated heparin, *Heparin -NS-2S*, and *degradation products* would only increase, while the concentration of N-2/6-O-desulfated heparin, *Heparin -NS-2S-6S*, would be exposed to both changes.

Focussing only on desulfation, presented in Scheme 3.2, the kinetics of these reactions could be described *via* parallel model (Loftsson, 2013; Yablonsky et al., 2010; Zhou et al., 2016, this work 1.3.3), *i.e.*:

$$\frac{d[Hep]_{-NS}}{dt} = -(k_{-2S} + k_{-2S-6S}) \cdot [Hep]_{-NS} \quad 3.7$$

$$\frac{d[Hep]_{-NS-2S}}{dt} = k_{-2S} \cdot [Hep]_{-NS} \quad 3.8$$

$$\frac{d[Hep]_{-NS-2S-6S}}{dt} = k_{-2S-6S} \cdot [Hep]_{-NS} \quad 3.9$$

To solve equation 3.6, the integration and differential calculus as in **equations 1.10 - 1.12** apply, which gives:

$$[Hep]_{-NS} = [Hep]_{-NS,0} \exp(-(k_{-2S} + k_{-2S-6S})t) \quad 3.10$$

The substitution of equation 3.10 to 3.8 allows to solve the latter, *i.e.*:

$$\frac{d[Hep]_{-NS-2S}}{dt} = k_{-2S} \cdot [Hep]_{-NS}$$

$$\frac{d[Hep]_{-NS-2S}}{dt} = k_{-2S} \cdot \{[Hep]_{-NS,0} \exp(-(k_{-2S} + k_{-2S-6S})t)\}$$

$$\int_0^{[Hep]_{-NS-2S}} d[Hep]_{-NS-2S} = \int_0^{[Hep]_{-NS-2S}} k_{-2S} \cdot \{[Hep]_{-NS,0} \exp(-(k_{-2S} + k_{-2S-6S})t)\} dt \quad 3.11$$

$$[Hep]_{-NS-2S} = [Hep]_{-NS,0} \cdot \frac{k_{-2S}}{k_{-2S} + k_{-2S-6S}} \cdot (1 - \exp(-(k_{-2S} + k_{-2S-6S})t))$$

similarly, equation 3.9 gives:

$$[Hep]_{-NS-2S-6S} = [Hep]_{-NS,0} \cdot \frac{k_{-2S-6S}}{k_{-2S} + k_{-2S-6S}} \cdot (1 - \exp(-(k_{-2S} + k_{-2S-6S})t)) \quad 3.12$$

and therefore:

$$\frac{[Hep]_{-NS-2S}}{[Hep]_{-NS-2S-6S}} = \frac{k_{-2S}}{k_{-2S-6S}} \quad 3.13$$

Through the equation 3.12, the changes of reaction rates could be estimated accordingly to reagents concentrations, and *vice versa*, concentrations could be calculated based on known reaction rate.

The equations 3.7 - 3.9 apply if desulfation is the sole process in hydrolytic system. However, the NMR studies of heparin sample degraded in acidic pH 1 and 80 °C for longer than 48 h showed that N-2/6-O-desulfated products were a subject of further degradation, as shown in Scheme 3.2. To include this step in kinetic approximation, the equation 3.8 would be change accordingly (Loftsson, 2013; Yablonsky et al., 2010, this work 1.3.3):

$$\frac{d[Hep]_{-NS-2S-6S}}{dt} = (k_{-2S-6S} \cdot [Hep]_{-NS}) - (k_d \cdot [Hep]_{-NS-2S-6S}) \quad 3.14$$

and

$$\frac{d[P]}{dt} = k_d \cdot [Hep]_{-NS-2S-6S} \quad 3.15$$

where  $P$  equals to concentration of degraded products.

The value of  $[Hep -NS]$  was substituted from equation 3.10 (Einbu & Vårum, 2008) , thus the equation 3.14 solves as:

$$\begin{aligned}
& \int_0^{[Hep]_{-NS-2S-6S}} [Hep]_{-NS-2S-6S} = \\
& \int_0^{[Hep]_{-NS}} (k_{-2S-6S} \cdot [Hep]_{-NS}) dt - \int_0^{[Hep]_{-NS-2S-6S}} (k_d \cdot [Hep]_{-NS-2S-6S}) dt \quad 3.16
\end{aligned}$$

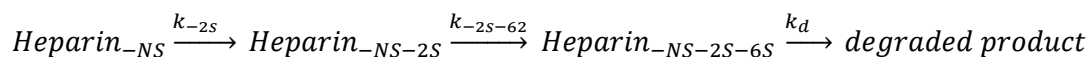
$$\begin{aligned}
& [Hep]_{-NS-2S-6S}] = \\
& \exp(-t \cdot k_d) + \left( [Hep]_{-NS-2S-6S}]_0 + \frac{(k_{-2S-6S} \cdot [Hep]_{-NS}]_0 \cdot (1 - \exp((k_d - k_{-2S-6S} - k_{-2S})t))}{k_{-2S} + k_{-2S-6S} - k_d} \right)
\end{aligned}$$

As the lower part of Scheme 3.2, that includes degradation product, follows the steps of consecutive reactions, *i.e.*:  $[Hep-NS] \rightarrow [Hep-NS-2S-6S] \rightarrow [P]$ , the relation between the concentrations of reagents could be related (Loftsson, 2013; Yablonsky et al., 2010):

$$\begin{aligned}
[Hep]_{-NS}] &= [Hep]_{-NS}] + [Hep]_{-NS-2S-6S}] + [P]; \quad \text{thus} \\
[P] &= [Hep]_{-NS}] - [Hep]_{-NS}] - [Hep]_{-NS-2S-6S}] \quad 3.17
\end{aligned}$$

The relation 3.17 allows the omission of the complicated integration and differential calculus of equation 3.15. Instead, the concentration of degradative products  $[P]$  could be estimated by subtraction of values of  $[Hep-NS]$  and  $[Hep-NS-2S-6S]$ , calculated *via* equations 3.10 and 3.16, respectively, from the initial concentration of  $[Hep-NS]$ . With known  $[P]$ , the degradation rate constant  $k_d$  can be determined according to equation 3.15. Additionally, to estimate the influence of temperature towards any of discussed steps, the equations 3.10 - 3.16 could be re-written with Arrhenius relation, as in example 3.6.

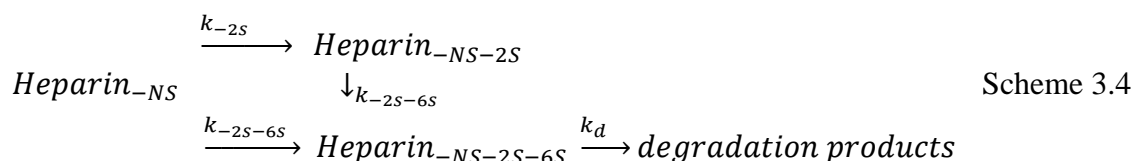
Before closing the section concerning kinetics of acid catalysed hydrolytic degradation of heparin, the short note regarding the Scheme 3.2 is required. Although such presentation of hydrolytic reactions may not be perfectly accurate, it was considered as the best theoretical match. If, for example, all reactions would be written in consecutive flow, *i.e.*:



Scheme 3.3

This suggests that 6-O-desulfation is conditional upon 2-O-desulfation. Furthermore, Scheme 3.3 implies that the 2-O-desulfated and 6-O-desulfated products would reach concentration maximum prior to following step (Loftsson, 2013; Sinko, 2011; Yablonsky et al., 2010; Zhou et al., 2016), which according to analysis summarised in **section 3.3.4** is not true. Under applied conditions, 2-O-desulfation and 6-O-desulfation of heparin were continuous processes (**3.3.4**). The flow presented in Scheme 3.2 allows such an assumption and give a chance to estimate how the concentrations of one species influence the others.

Furthermore, to simplify calculations, the relation between 2-O-desulfated and 6-O-desulfated product was summarised in Scheme 3.2. As mentioned (for details, see **3.3.4.2.2**), loss of 6-O-sulfate group follows 2-O-desulfation, but is not selective. Of course, the extra step could be added to Scheme 3.2:



To solve this relation matrix modelling would be required (Korobov & Ochkov, 2011b, 2011a). As the parallel reactions of Scheme 3.2 also assume the relation between 2-O-desulfated and 6-O-desulfated heparins (according to equation 3.13), at this point of experimental approach it was found satisfying.

### 3.4.3 The choice of kinetic plots in a proof-of-concept verification of presented kinetic approximation of acid hydrolysed heparin

Without a doubt the kinetics approximation of hydrolytic degradation of heparin in acidic environments, presented in previous **section 3.4.2**, does not represent the simplest model. Faced with the complicated estimations that require further modelling and deeper numerical analysis one could question if the observed rearrangements, summarised in **section 3.4.2**, would not fit simpler kinetic equations. The easiest way to extract rate laws of

intramolecular processes, like degradation, is certainly the graphical method. If the collected data, plotted as a function of time according to tested rate law, are linear, it means that assumed kinetic model of investigated system fits the rate law hypothesis (Loftsson, 2013; Sinko, 2011; Tanford, 1961; Zhou et al., 2016).

Taking into account the excess of water the hydrolytic reaction of heparin was assumed to follow the pseudo-first order kinetic law. If the degradation of heparin in acidic aqueous solutions (desulfation and following depolymerisation) could be described by single rate law equation, it would take a form of **equation 1.12**, which once plotted with experimental data, would be a straight line. As the change of molecular weight of heparin over time reflected all the degradative processes (desulfation and depolymerisation), it could be used to test above hypothesis. Accordingly, **equation 1.12** could be re-written as:

$$\ln M_{w,Hep_t} = -k_{obs}t + \ln M_{w,Hep_0} \quad 3.18$$

where  $M_{w,Hep_t}$  equals molecular weight of heparin at the reaction time  $t$  and  $M_{w,Hep_0}$  equals initial molecular weight of heparin (at reaction time  $t = 0$ ). To create the plot, the equation 3.18 could be written as:

$$\begin{aligned} \ln M_{w,Hep_t} &= -k_{obs}t + \ln M_{w,Hep_0} \\ &\downarrow \\ y &= -mx + b \end{aligned} \quad 3.19$$

Following the above hypothesis, molecular weight data of hydrolysed heparin collected *via* SEC-MALS-RI (see **3.3.1**) were applied for kinetic plots presented in below figures. Yet, it should be taken in to account that molecular weights of heparins analysed by size exclusion chromatography were estimated with relatively high measurement error (see **Figure 3.3**), therefore presented plots should be treated as approximated estimations of limited accuracy. Nevertheless, as shown in **Figure 3.28**, the plot of natural logarithm of molecular weight of heparin, measured after hydrolysis at pH 1/ 80 °C/ from up to 168 h, and presented as a function of time is far from being a linear function. The shape of the plot

suggests that description of hydrolytic degradation of heparin *via* single first-order kinetics equation, like in 3.19, would be inadequate estimation.

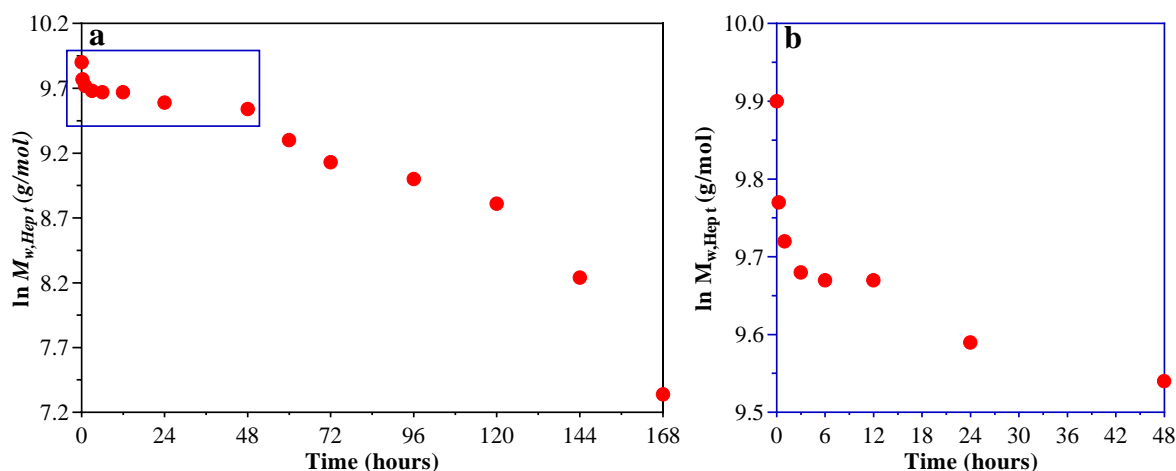


**Figure 3.28** The natural logarithm of molecular weight of heparin, measured after hydrolysis **a)** pH 1/ 80 °C over 168 h, plotted as a function of time according to first-order kinetics equation. Figure **b)** shows the magnification of the first 48 h in **a)**.

To test if the shape of the plot in **Figure 3.28** was not a result of an incorrect assumption regarding the reaction (pseudo-first) order, the data were also plotted following the pseudo-second order kinetics (for mathematical principals of second-order law see for example Bauer et al., 2012; Loftsson, 2013), the equation of which was rearranged as:

$$\frac{1}{M_{w,Hept}} = k_{obs}t + \frac{1}{M_{w,Hept_0}} \quad 3.20$$

$$\downarrow$$

$$y = mx + b$$

However, as presented in **Figure 3.29**, changing the order rate did not improve plot shape.

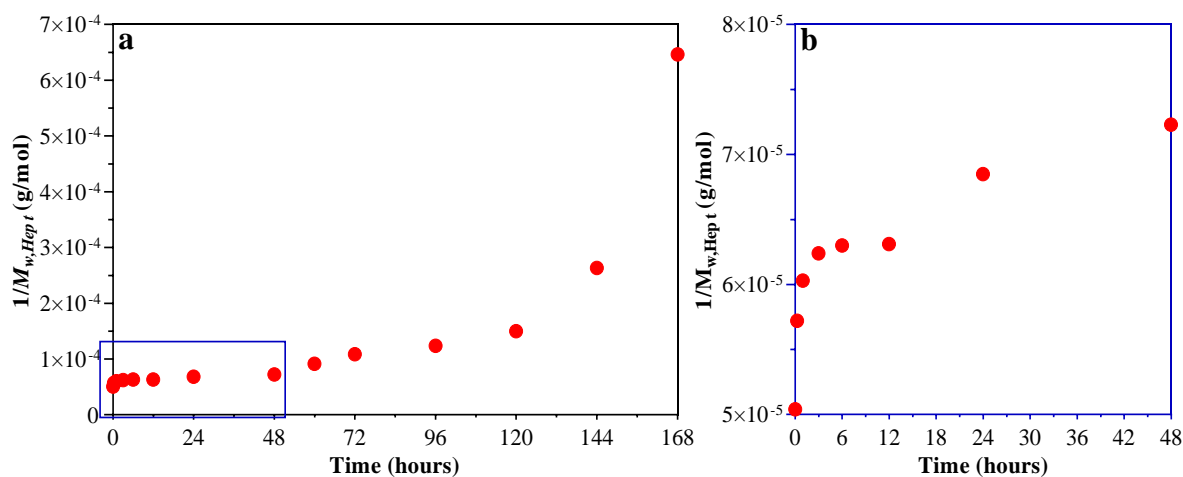


**Figure 3.29** The fraction of molecular weight of heparin, measured after hydrolysis at pH a) 1/ 80 °C/ 168 h, plotted as a function of time according to second-order kinetics equation. Figure b) shows the magnification of the first 48 h in a)

The deviation from linearity in **Figure 3.28** strengthens the hypothesis regarding the approximated kinetics presented in **section 3.4.2**, and prior to a full test of equations 3.10 - 3.17 against the numerical data, which would be an interesting task for future study, can serve as proof-of-concept of assumed kinetic model of heparin degradation in acidic environments.

#### 3.4.4 Concluding remarks

The kinetic approximation concerning the hydrolytic desulfation (NS-, 2OS-, 6OS-) and following glycosidic scission of heparin chain, catalysed by acidic treatment, was designed according to parallel and consecutive-based reaction scheme. The presented approximation was based on experimental results; however, it was not tested against the numerical data. The first-order and second-order kinetic plots for molecular weights of heparin measured at pH 1/ 80 °C over 168 h were applied to support kinetic hypothesis. Yet, until testing, the presented models should be as theoretical concept. Due to the complexity of approximated equations, these ideally would require matrix or graphical modelling against experimental data that could be approached *via* Mathcad, Maple or MATLAB software (Einbu & Vårum, 2008; Korobov & Ochkov, 2011) and would be an excellent challenge for future work.

### 3.5 CHAPTER CONCLUSIONS

This chapter has focused on the physicochemical changes of heparin in aqueous media, catalysed by acid environments (pH 1 - 6) and temperature (40, 60 and 80 °C), which were followed over time (up to 168 h) through a variety of analytical techniques.

Heparin appeared to be resistant to glycosidic scission when subjected to hydrolysis at pH from 1 to 6, at 40 °C and 60 °C. On the other hand, under the following conditions: pH 1 – 2/ 40 °C; pH 1 – 3/ 60 °C; pH 1 – 4/ 80 °C the amount of hydrolytically cleaved sulfate could alone account for the molecular weight loss of polymer. Actual chain depolymerisation was initiated around the 24<sup>th</sup> hydrolytic hour in pH 1/ 80 °C and proceeded with time, although at limited rate. The following conditions: pH 3 – 6/ 40 °C; pH 4 – 6/ 60 °C; pH 5 – 6/ 80 °C did not induce any critical intramolecular changes of heparin. Thus, when applied in industrial or research applications, these environments can be considered as safe, regarding stability or functionality of the molecule.

Monosaccharide analysis and NMR spectra of prolonged hydrolysates (pH 1/ 80 °C) suggested that through the partial chain degradation the glucosamine, iduronate and unknown oligosaccharide units could be released, of which the first two may undergo further degradation. Nevertheless, the crucial finding of this study, which marks 60 years since pioneering work of Danishefsky et al. (1960) on hydrolytic desulfation of heparin, was to experimentally confirm that desulfation in fact is a primary degradative process of heparin in aqueous media, with a selectivity strongly dependent upon applied conditions that could be generally summarised as  $6OS \leq 2OS \ll NS$ .

Furthermore, the processes of hydrolytic desulfation (NS-, 2OS-, 6OS-) and glycosidic scission of the heparin chain, catalysed by acidic treatment, were presented *via* the parallel and consecutive-based reaction scheme. This allowed the approximation of kinetic model that could fit the analysed system and be further used to characterise the thermochemical degradation of heparin for new, pharmacological derivatives. However, the applicability of estimated model required closer examination against numerical data.

# 4

## STABILITY OF HEPARIN IN ALKALINE ENVIRONMENTS

---

### 4.1 INTRODUCTION

Although the anticoagulant and antithrombic properties of heparin have been mostly utilised in clinical practice (Jaffer & Weitz, 2014; Mulloy, 2012; Onishi et al., 2016), during the century of use, many additional pharmacological features of the molecule have been investigated (for detailed review see, for example Lima et al., 2017; Meneghetti et al., 2015; Mulloy et al., 2015). The thorough analysis has helped to establish the relationship between the pharmacological response of heparin and its physicochemical parameters, including molecular weight, conformation, and charge distribution (as discussed in **section 1.2.3**). Among these, the charge distribution, more specifically- the distribution of sulfate groups, has been found to drive the diverse activities of heparin (Raman et al., 2013; Skidmore et al., 2008). Thus, the strategy to develop heparin derivatives with different pharmacological properties and to expand its therapeutical profile strongly relies on modification of sulfation patterns.

The selectivity of hydrolytic desulfation in acidic environments was considered as limited to N-sulfate (as discussed in introduction to **Chapter 3**). Hence, the influence of alkaline conditions on sulfation and general conformation of heparin gained more attention. It has been reported that alkaline treatments (sodium hydroxide; pH 11- 13) not only alter the sulfation parameters, but also led to various structural modifications, dependent upon applied environments. Previous studies revealed that strong alkali (NaOH) causes the rearrangement of the 2-O-sulfated iduronate (IdoA(2S)) into 2,3-epoxy- $\alpha$ -L-guluronate (2,3-epiGulA) or desulfated  $\alpha$ -L-galacturonate (GalA) or 2-O-desulfation of acid residue

(IdoA), in relation to applied conditions specified in **Figure 4.1** (Casu & Lindahl, 2001; Jaseja et al., 1989; Rej & Perlin, 1990). Furthermore, it was shown that at high pH, the 3-O-sulfate group of N,3-sulfated (GlcNS(3S)) and oversulfated (GlcNS(3,6S)) glucosamine exhibit an unusual closure to 2,3-N-sulfoaziridine ring (Santini et al., 1997), as in **Figure 4.1**. Each of these possible modifications altered the sulfation pattern, conformation and molecular weight of heparin, which naturally resulted in activity changes.

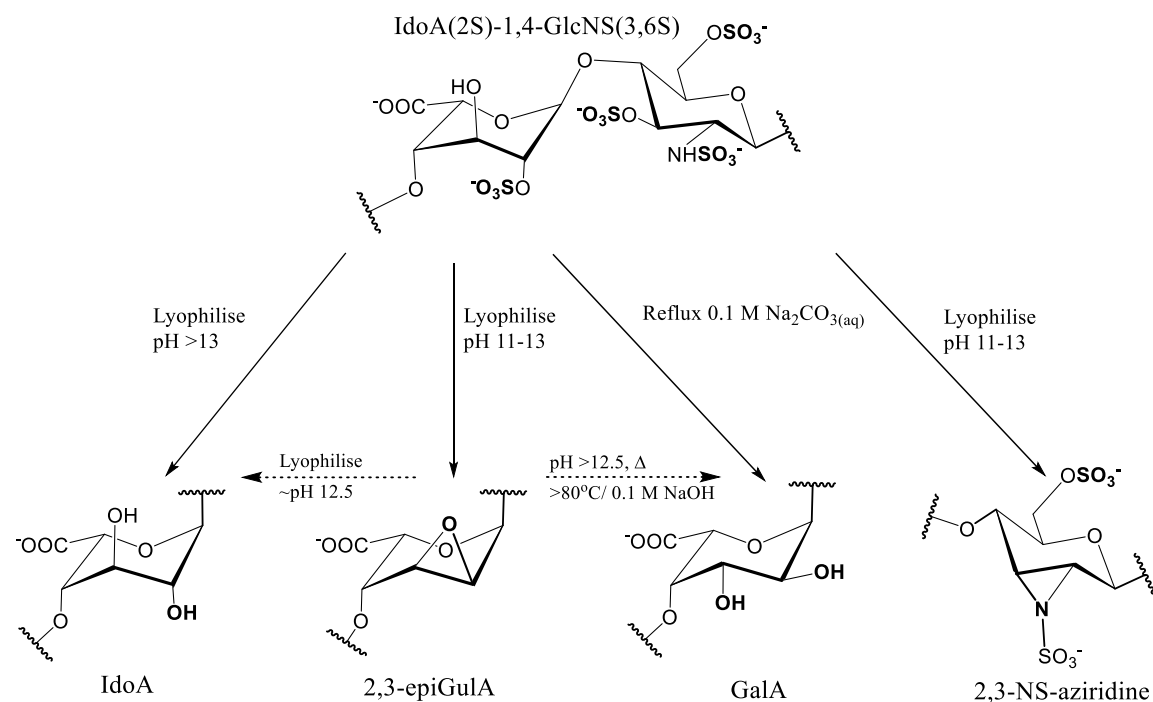


**Figure 4.1** Reaction scheme summarising the structural changes of the 2-O-sulfated iduronate and N,3,6-sulfated glucosamine units of heparin chain, catalysed by various alkaline conditions. Figure based upon the literature discussed in text above, *i.e.*, (Casu & Lindahl, 2001; Jaseja et al., 1989; Rej & Perlin, 1990; Santini et al., 1997).

During the development of alkali-catalysed heparin derivatives both iduronate and glucosamine residues have demonstrated lability to alternative modifications shown in **Figure 4.1**. Base hydrolysis of heparin benzyl ester, industrially applied in the production of low molecular weight products (Enoxaparin), usually leads to the formation of 2,3-epoxyuronic acid (unsaturated uronic acid) at the non-reducing end (Gray et al., 2008; Lima et al., 2011; Linhardt, 1992; Linhardt & Gunay, 1999). The same mechanism may also result in alterations at reducing terminus, which promotes two bicyclic forms of amino-sugars, *i.e.*, 1,6-anhydro-glucosamine and 1,6-anhydro-mannosamine (Fareed et al., 2005; Mascellani et al., 2007). The alkali-catalysed epimerisation to 2-deoxy-6-O-sulfo-2-

sulfamino-D-mannose has also been reported at N,6-sulfated glucosamine (GlcNS(6S)) (the Lobry de Bruyn – van Eckenstein rearrangement) (Yamada et al., 1998), as well as at N-acetylated terminus (Toida et al., 1996).

Undoubtedly, each of the discussed studies examined the effect of harsh alkaline environments upon the structural features of heparin and contributed to the general knowledge about its molecular stability. However, the ‘harsh’ conditions had been the key to these rearrangements. Besides the research that specifically focuses on such structurally altered units, the reviewed environments have a limited applicability in purification, preparation, and storage of pharmacologically active heparin. During the extraction of heparin from porcine mucosa the maximal pH is around 11, the temperature generally does not exceed 80 °C and the product would be never left unneutralised prior to lyophilisation (Linhardt et al., 1990; Van Der Meer et al., 2017). Furthermore, the pH of the final heparin solution is between 5.0 – 7.5, with maximum storage temperature of 40 °C (LEO Pharma A/S, 2016; LEO Pharma Inc & LEO Pharma A/S, 2016; Pharmacopeial Forum, 2009). From the industrial perspective, the stability studies of heparin at less harsh alkaline environments would be more beneficial, as more relevant to applied manufacturing process. Also, the extension of studies to milder conditions would complement the stability picture of heparin in alkaline environments and assess the scope of rearrangements presented in **Figure 4.1**.

Considering the discussed analytical gap, in this project the stability of heparin was examined in alkaline environments at pH7-12, at 40, 60 & 80 °C, as a function of time (up to 168 h). The choice of analytical techniques summarised in **section 4.2**, allowed the investigation of a variety of heparin features. The results of undertaken studies are presented in **section 4.3** and were critically examined with respect to the applied conditions. The kinetic model describing the studied system is proposed in **section 4.4**. The major findings are finally summarised at the end of chapter, in **section 4.5**.

## 4.2 SUMMARY OF APPLIED ANALYTICAL METHODS

The complete experimental procedure of alkaline hydrolysis of sodium salt porcine mucosal heparin ( $M_{w,0} \approx 20,000$  g/mol,  $M_w/M_n = 1.1$ ) is presented in **section 2.1**, while

**Figure 4.2** below briefly summarises the hydrolytic protocol. The analytical methods applied to investigate the physicochemical changes caused by hydrolytic conditions are summarised in **Table 3.1** in previous chapter (Chapter 3), while more detailed description of each technique is given in the **Experimental Chapter (Chapter 2)**.

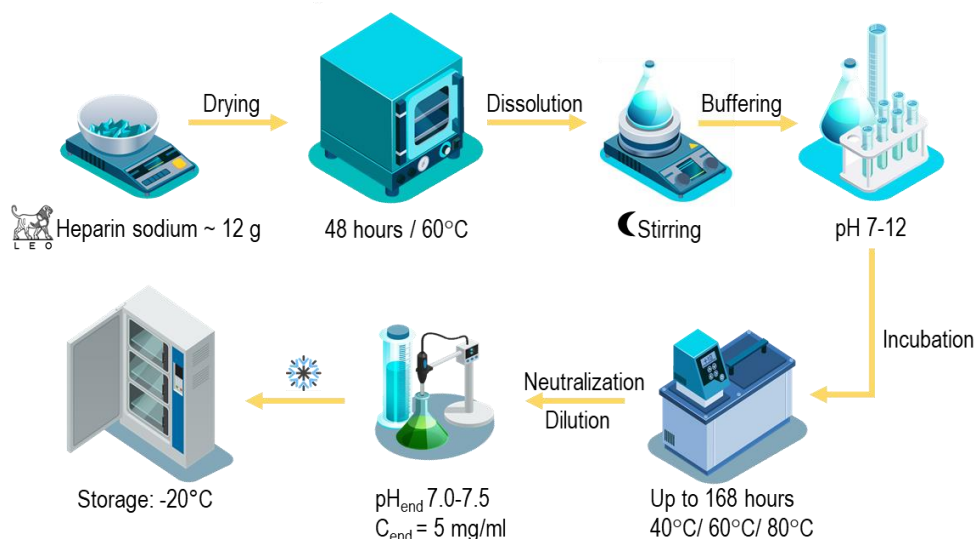


**Figure 4.2** Graphical illustration of heparin hydrolysis process in alkaline environments.

## 4.3 RESULTS AND DISCUSSION

### 4.3.1 The effect of alkaline environments on molecular weight of heparin as a function of time and temperature

#### 4.3.1.1 Results of average weight molecular weight analysis

The first analytical step was directed towards understanding the effect of alkaline environments on molecular weight of heparin, similarly to the previous chapter, which focused on heparin stability in acidic environments (**Chapter 3**). The average weight molecular weight ( $M_w$ ) of thermally stressed heparin (40, 60, 80 °C) in alkaline environments (pH 7 - 12) were followed *via* size exclusion chromatography (for analytical details see **2.3**). Elution profiles of selected samples are presented below in **Figure 4.3**. The collected molecular weights were plotted as a function of time (up to 168 h) in **Figure 4.4.**, with averaged uncertainties defined as 95% confidence intervals of triplicated measurements. Subsequently, the approximate decrease of  $M_w$  (%) were calculated (chosen hydrolysates), with data summarised in **Table 4.1**

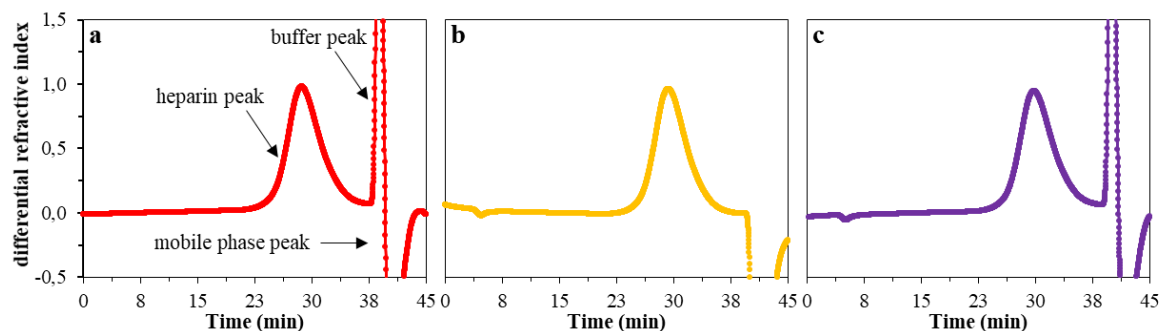


**Figure 4.3** Elution profiles of heparins hydrolysed at **a)** pH 7/ 80 °C after 24 h, **b)** pH 9/ 60 °C after 24 h, and **c)** pH 12/ 40 °C after 24 h. The sample buffer in **b)** (boric acid buffer for pH 9) was eluted with mobile phase, thus buffer peak is not visible. Samples were analysed *via* size exclusion chromatography with multi-angle-light-scattering detector and refractive index detector. Presented chromatograms are results of normalized (against the highest value) refractive index assessment.

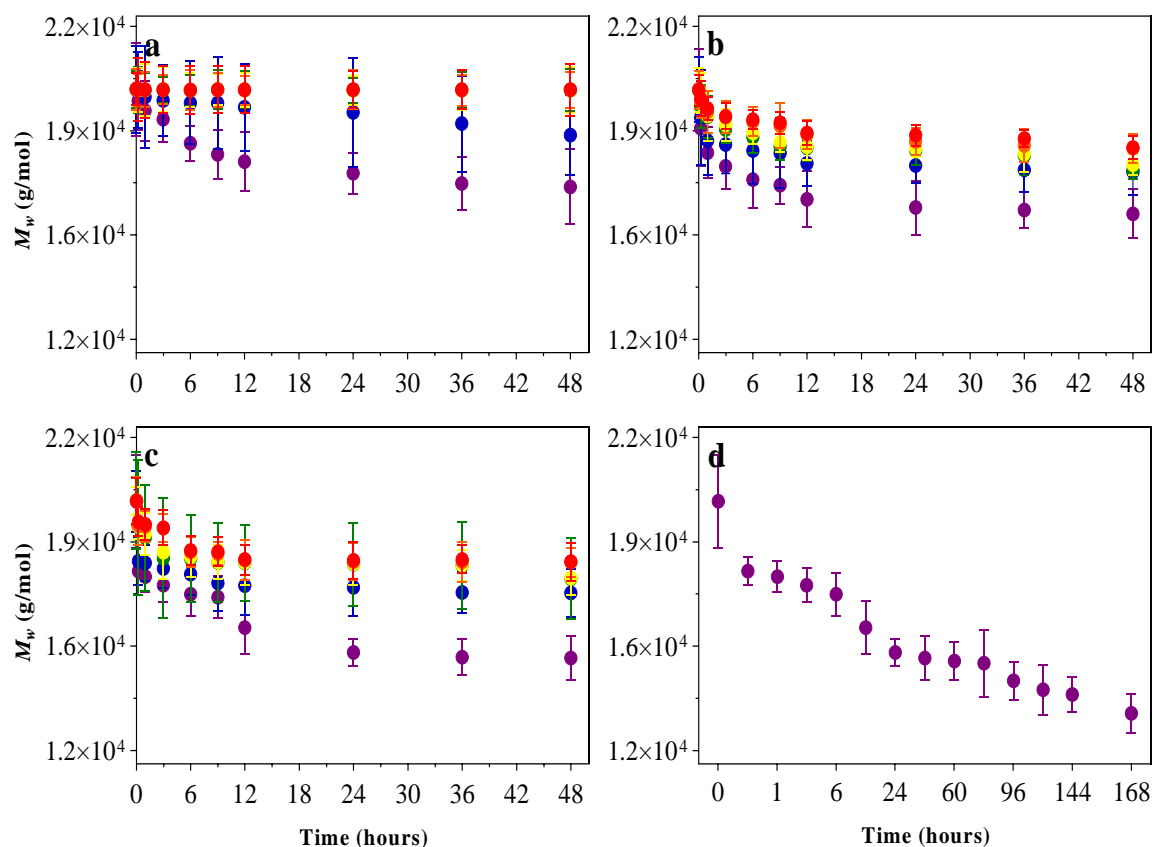


**Figure 4.4** Average weight molecular weight of heparin hydrolysed at **a)** 40 °C, **b)** 60 °C, and **c-d)** 80 °C, plotted as function of time at pH 7 - 12. The averaged uncertainty defines the 95% confidence interval. ● pH 7, ● pH 8, ● pH 9, ● pH 10, ● pH 11, ● pH 12

The negligible changes of molecular weight of heparin hydrolysed between pH 7 and pH 11, at 40 °C, characterised by almost straight line (over the analysed time) in **Figure 4.4a**, marks the stability of molecule at these conditions. The maximal, 15% loss in average weight molecular weight, observed at this temperature (40 °C), was noted for heparin subjected to pH 12/ 48 h (**Table 4.1**).

The incubation at 60 °C led to a steady decrease of molecular weight of heparin over the studied time, at each of tested alkaline pH, as visualised by **Figure 4.4b**, with maximum reaching 19% at pH 12/ 48 h, and approximately 11% loss at the same time-point (48 h) from pH 7 to pH 11. Interestingly, the temperature increase from 60 to 80 °C did not significantly accelerate the molecular weight loss at pH ranging from 7 and 11, increasing it only by 2% (on average) per-time point (**Table 4.1**), with a plateau observed between 12 h and 48 h, as in **Figure 4.4c**. A considerable, 10% drop in molecular weight was observed after only 0.25 h at pH 12/ 80 °C, as shown in **Figure 4.4d** and **Table 4.1**. Afterwards, the rate of molecular weight loss at these conditions was consistent, with maximum decrease of 32%, noted after 168 h (**Table 4.1**).

#### 4.3.1.2 Concluding remarks

In contrast to acidic environments, discussed in **section 3.3.1**, the alkaline conditions catalysed steady decrease of molecular weight of heparin. The most significant changes in molecular weights of polymer were observed at the harshest of applied conditions, *i.e.*, pH 12/ 80 °C, while at pH 1/ 80°C/ 168 h the molecule lost approximately 92% of initial molecular weight, which was further associated with chain fragmentation and almost total desulfation (see chapter concluding remarks **3.5**), here (pH 12/ 80 °C/ 168 h) only 32% decrease was observed. In the past similar modest reductions of molecular weight of heparin (under alkaline environments) was associated with the intramolecular conversion of iduronate proceeded by desulfation (2-O-desulfation), rather than depolymerisation of polysaccharide chain (Holme et al., 1996; Jaseja et al., 1989). The following analysis aimed to examine this theory in the light of applied conditions.

**Table 4.1** Summary of approximate average weight molecular weight decrease (%) of alkaline hydrolysed heparins (chosen time-points) in respect to the initial heparin standard.

Heparin Hydrolysates		Approximate weight-average molecular weight decrease <sup>a</sup>						
		pH 7	pH 8	pH 9	pH 10	pH 11	pH 12	
40 ° C	0.25 h	<1%	<1%	<1%	<1%	< 1%	2%	
	6 h	<1%	<1%	<1%	<1%	2%	8%	
	12 h	<1%	<1%	<1%	<1%	3%	11%	
	24 h	<1%	<1%	<1%	<1%	3%	13%	
	48 h	<1%	<1%	<1%	<1%	7%	15%	
60 ° C	0.25 h	<1%	<1%	< 1%	3%	4%	6%	
	6 h	4%	5%	6%	7%	9%	13%	
	12 h	6%	7%	9%	9%	11%	16%	
	24 h	7%	8%	9%	10%	11%	18%	
	48 h	9%	9%	11%	12%	12%	19%	
80 ° C	0.25 h	3%	4%	4%	4%	9%	10%	
	6 h	7%	8%	8%	9%	11%	14%	
	12 h	9%	9%	9%	9%	13%	19%	
	24 h	9%	9%	9%	10%	13%	23%	
	48 h	9%	9%	12%	12%	14%	24%	
	96 h							27%
	120 h							28%
	168 h							32%

<sup>a</sup> Calculated by subtracting  $M_w$  (g/mol) of hydrolysate from the  $M_w$  (g/mol) of initial heparin standard

### 4.3.2 The influence of applied alkaline conditions on glycosidic bonds of polysaccharide – verification of chain fragmentation

#### 4.3.2.1 PAGE-based reducing-ends assay

PAGE electrophoresis-based reducing-end assays previously confirmed/excluded the hydrolytic scission of glycosidic bonds of heparin in acidic environments, as presented in **section 3.3.2.1**. The main advantage of this straightforward technique was direct indication of heparin chain depolymerisation from the fluorescent bands illuminated on acrylamide gel while the cationic dye (Azure A) staining allowed the preliminary assessment of molecular desulfation of studied samples according to the changes of colour intensity (for more details, see **section 2.4**). Both features (depolymerisation and desulfation) of heparin in alkaline conditions were questioned after the molecular weight analysis (discussed in **4.3.1**). Hence, advantage of PAGE-based reducing-ends assay was taken again.

##### 4.3.2.1.1 Fluorescent analysis of alkaline hydrolysates of heparin

Taking the advantage of optimisation process, described in **section 3.3.2.1.1**, heparin samples (100 µg), hydrolysed at pH 10 – 12, at 40, 60 and 80 °C (various time-points), which were characterised by noticeable molecular weight loss (as discussed in **section 4.3.1**), were ANDSA-labelled, loaded onto the separate gels and submitted to electrophoresis (for details of electrophoresis see **2.4**). Illustrative images of fluorescently visualized gels are shown in **Figure 4.5** and **Figure 4.6**. As presented in **Figure 4.5**, no bands were eluted (besides standards) from gels corresponding to hydrolysis carried at pH 10 – 12, up to 48 h, at any of the studied temperatures. Furthermore, the prolonged (to 168 h) incubation at pH 12/ 80 °C also did not result in band visualisation, as shown in **Figure 4.6**. The collected results suggested that these conditions were insufficient to break the glycosidic linkages between heparin units to any significant extent, while this was expected to be true for pH 10 and pH 11 (considering the limited molecular weight loss), the results collected for prolonged pH 12 hydrolysis were certainly very interesting. The lack of bands, ergo, the lack of new reducing ends, implies the lack (or very limited) depolymerisation. Thus, it could be initially assumed that the 32% loss of molecular weight observed at these conditions was not associated with depolymerisation of polysaccharide chain.

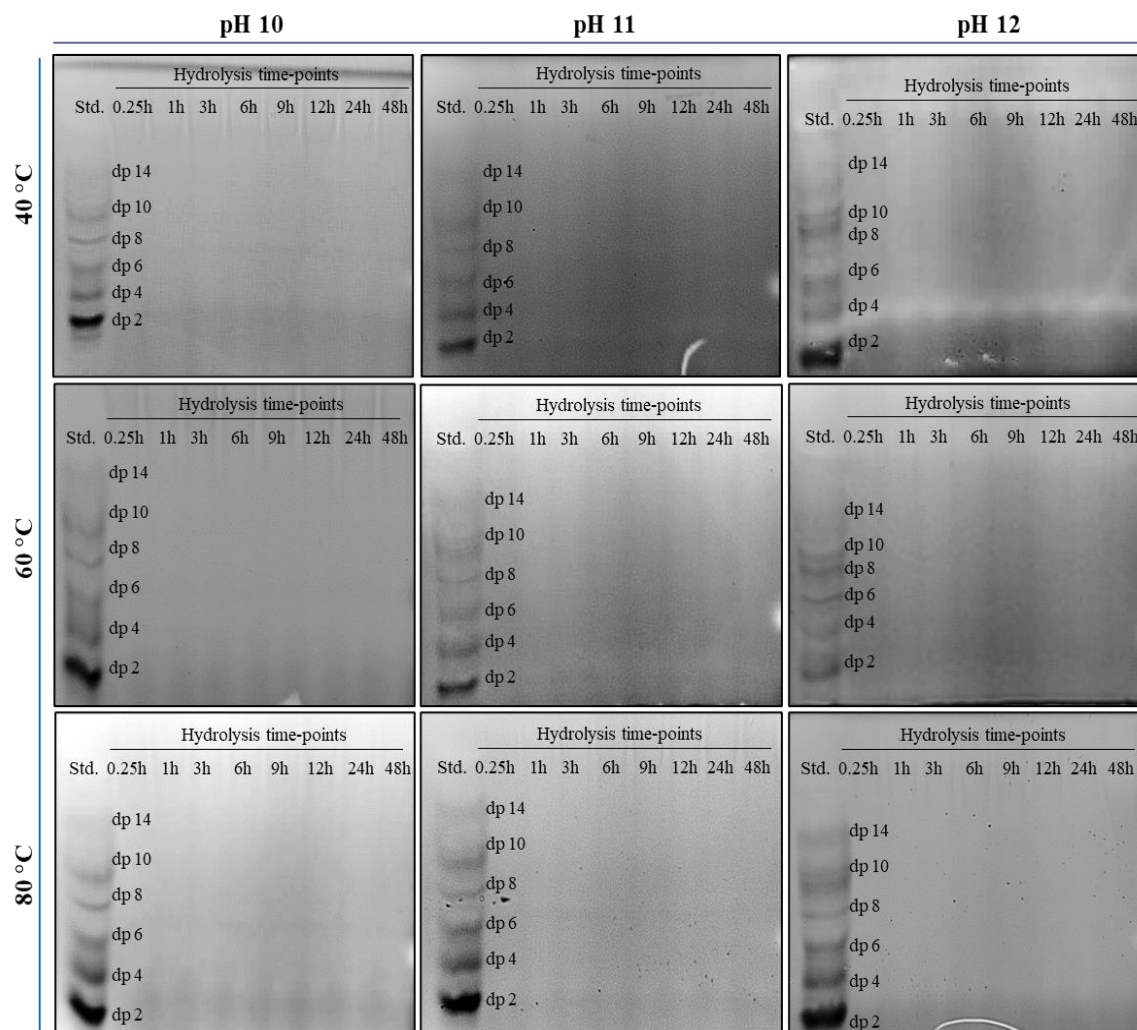


**Figure 4.5** Fluorescent images of acrylamide gels of alkaline degraded heparins. Comparison of samples aliquoted at various time-points at pH 10, pH 11 and pH 12 degradation, at 40, 60 and 80 °C. Std- standard dp ladder.

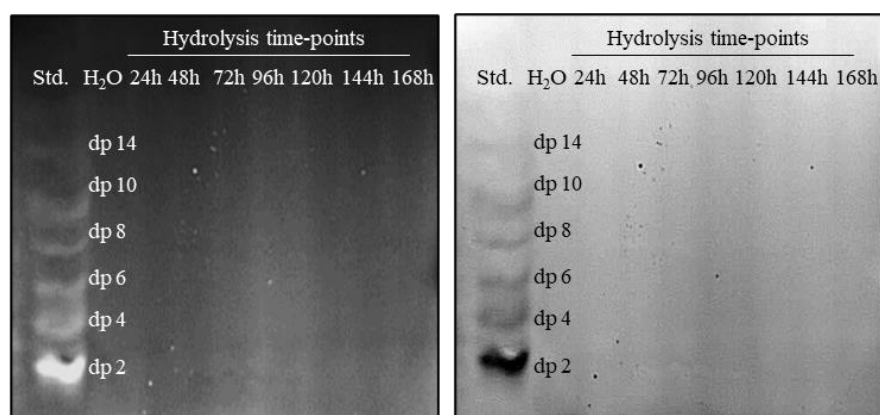


**Figure 4.6** Fluorescent image of acrylamide gel, showed in inverted colours, of extended alkaline hydrolysis of heparin (chosen time- points), carried in pH 12 at 80 °C. Std- standard dp ladder.

#### 4.3.2.1.2 Cationic dye staining of alkaline hydrolysates of heparin

Data collected in the first stage of the PAGE assay suggested the limitation of applied alkaline conditions to catalyse the scission of heparin glycosidic bonds. Earlier analysis demonstrated the lability of the sulfate groups on heparin to aqueous acid environments (as discussed in **3.3.2.1.3**). Thus, the advantage of cationic dye staining (protocol given in **2.4.4.4**) was taken to initially assess the desulfation capacity of heparin at alkaline conditions. However, no considerable changes in colour intensity of cationic dye were observed for samples hydrolysed at pH 10 – 12, up to 48 h, at all three studied temperatures. Again, while the results of samples collected at pH 10 and pH 11 were not surprising (considering the limited molecular weight loss), these of pH 12, especially of prolonged hydrolysis, were more interesting. As shown in **Figure 4.7**, the strength of staining was neither altered over time, nor by temperature. The colour of Azure A was slightly brighter than the heparin standard between 24 and 168 h (**Figure 4.7d**), however it did not fade, like in acidic example presented in **Figure 3.7**. The colour intensity of Azure A-saccharide complex mirrors the sulfation content of the latter (Mulloy et al., 2015; Powell et al., 2010), therefore, its limited change would justify limited sulfate loss. It may therefore be assumed that alkaline hydrolysis did not alter the sulfation profile of heparin to any significant extent, which would most probably exclude desulfation as a major factor affecting the molecular weight of heparin.

#### 4.3.2.1.3 PAGE electrophoresis concluding remarks

The aim of PAGE based reducing-ends assay was to qualitatively assess the extent of hydrolytic depolymerisation and desulfation of heparin in alkaline conditions. The analysis was thought of as a first step towards explanation of molecular weight loss of polysaccharide, demonstrated in previous **section 4.3.1**. The fluorescent and cationic dye tagging of hydrolysates exposed the limitation of degradative processes (glycosidic scission and desulfation, respectively) at the studied alkaline conditions. The collected results return the attention towards the hypothesis of alkali-catalysed intramolecular changes of heparin (iduronate, specifically) and their effect upon the molecular weight of heparin, regardless to depolymerisation (stated at the end of previous section, see **4.3.1.2**) (based on Holme et al., 1996; Jaseja et al., 1989). The following analysis intended to take a closer look at this theory.

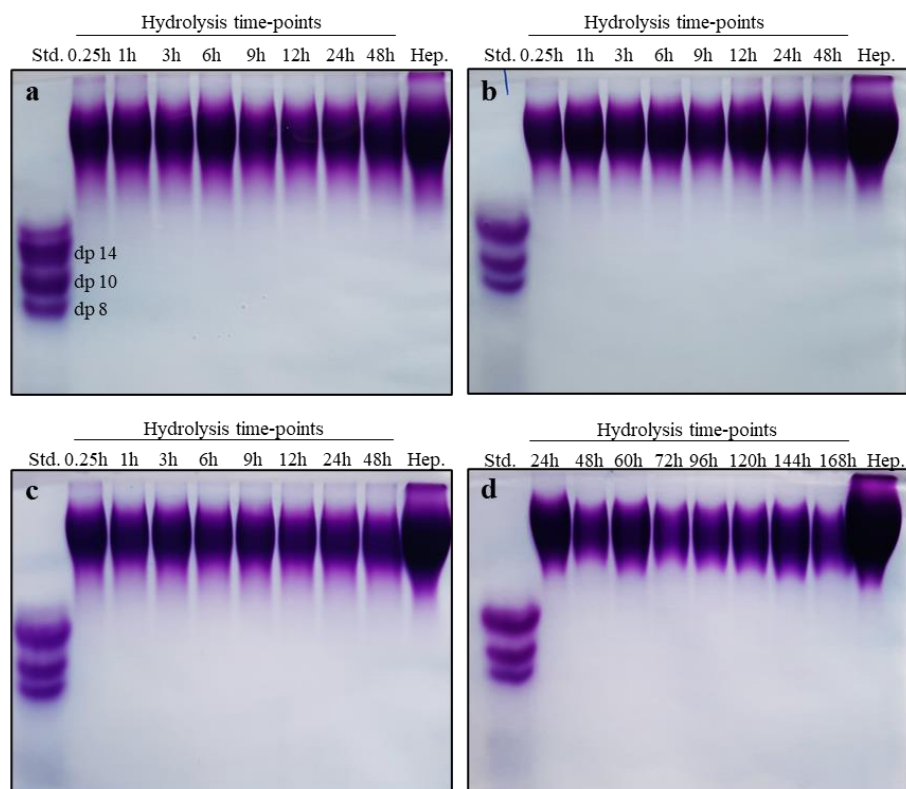


**Figure 4.7** Images of acrylamide gels of heparin hydrolysed at pH 12 at **a)** 40 °C, **b)** 60 °C and **c-d)** 80 °C (chosen aliquots), stained with Azure A dye; Hep- unhydrolysed heparin reference standard. Std- standard dp ladder.

#### 4.3.2.2 UV-Vis spectrophotometry

UV-Vis spectroscopy has been used to highlight the scope of alkaline and enzymatic hydrolysis of GAGs, by measuring the absorbance of electromagnetic radiation at 232 nm, characteristic for unsaturated iduronate at new reducing terminus of alkali/enzymatically treated samples (Deakin & Lyon, 2008; Limtiaco et al., 2011; Powell et al., 2010; Ucakturk et al., 2014). Although the reducing-ends assay indicated the limitation of applied alkaline conditions towards glycosidic scission of heparin bonds, it cannot be excluded that the imposition of these environments affected iduronate. Therefore, the absorbance of post-hydrolytic alkaline samples of heparin was verified.

Samples subjected to UV-Vis examination were chosen upon the considerable molecular weight loss, according to data summarised in **section 4.3.1**. Thus, samples hydrolysed at pH 10 - 12, at 40 °C, 60 °C and 80 °C (various time-points) were checked (according to protocol given in **section 2.5.4**). The lack of 232 nm absorbance in any of analysed samples, even after prolonged hydrolysis at pH 12/ 80 °C, as illustrated in **Figure 4.8**, suggests

absence of absorbing units, ruling out the depolymerization and rearrangements of reducing IdoA to unsaturated specie. The differences between the plotted absorbance spectra are result of systematic error (instrument acquisition) and magnification rather than the result of increasing absorbance. The peaks, similar to these observed in **Figure 3.8** after the acid hydrolysis, were not observed after the alkali treatment.

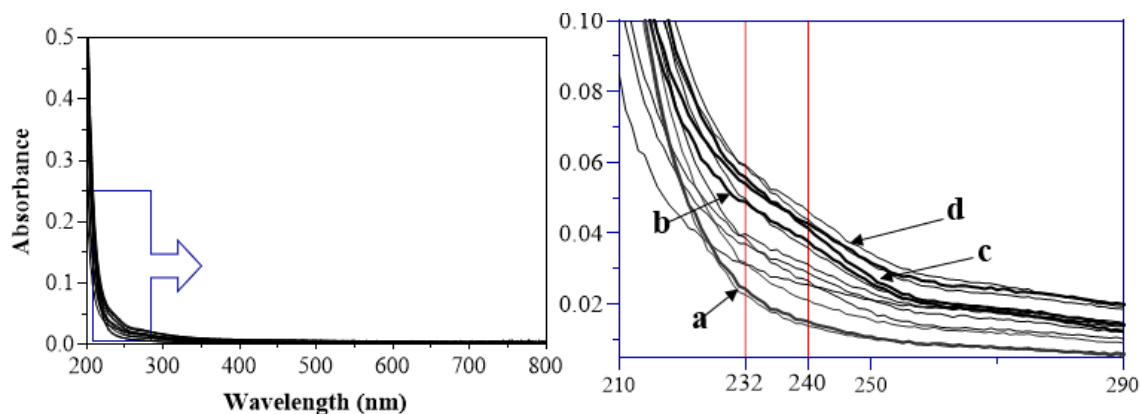


**Figure 4.8** The absorbance spectra of sample hydrolysed at pH 12/ 80 °C over the 168 h. Each line represents hydrolytic time-point, plotted in ascending manner, *i.e.*: **a**) 0.25 (the lowest), 1, 3, 6, 9, 12, 24, **b**) 48, 72, **c**) 96, 144, **d**) 168 h (the highest). The differences between the plotted absorbance spectra are result of systematic error and magnification, not a result of increasing absorbance.

Both the PAGE-based reducing-ends assay and UV-Vis spectroscopy sketched a picture of heparin as a molecule relatively resistant to applied alkaline conditions. Although the results of these two experiments presented herein are consistent, it should be remembered that in the past similar conditions (*i.e.*, 0.1 N NaOH; 60 °C; absorbance increase at 232 nm observed after ~10 h; see Jandik et al., 1996) had actually prompted depolymerization of heparin chain (analysed *via* changes in reducing power of polysaccharide) as well as unsaturation of IdoA (demonstrated by UV-Vis) (Jandik et al., 1996). Perhaps, the nature of these changes depends not only on applied pH, but also on the pH maintaining species. Jandik and co-workers (1996), who reported alkali-catalyzed depolymerization and changes in 232 nm absorption of heparin used sodium hydroxide, while in presented studies phosphate buffer was applied to maintain pH 12. Furthermore, a short study carried out alongside this research project also demonstrated an absorbance increase in a sodium hydroxide system (pH 12), although at 271 nm (Xiong, Z. (2020). “*Effect of pH, salt and temperature on the conformation of heparin.*” UG dissertation, University of Huddersfield, data not published). As summarized in introduction to this chapter (see **4.1**), NaOH is very

reactive compound, causing heparin chain degradation and series of IdoA rearrangements. Considering the results collected up to this point, one could assume that heparin is relatively stable in applied buffering system, or perhaps, the studied environments catalyze different rearrangements to those studied previously. With an aim to answer these questions, the alkali hydrolysates of heparin were analysed further.

#### 4.3.2.3 *The complete saccharide analysis*

Although PAGE electrophoresis and UV-Vis spectroscopy initially ruled out the possibility of glycosidic scission of heparin chain in aqueous alkaline conditions, both of these methods provided qualitative data. Taking the quantitative advantage of ion chromatography, which was previously optimised towards relatively low limit of detection (general LOD  $\leq$  0.5 ppm, see **3.3.2.3**), the composition of post-hydrolytic samples was assessed. The technique created an opportunity for quick (autosampler connection) and in-depth analysis of all of alkali hydrolysed samples (pH 7 - 12, all studied temperatures), to confirm assumption of heparin resistivity to these conditions. Furthermore, if small units of severed saccharides diffused out of the PAGE gels and evaded detection, these would be eluted in chromatograms (if within limit of detection).

##### 4.3.2.3.1 Summary of method optimisation

The detailed summary of method optimisation is given in **section 3.3.2.3.1**. The mix of chromatographic standards of Fuc, GalN, GlcN, GlcNS, GlcNAc, GlcNS(3S), GlcNS(6S), GlcA, GalA and IdoA, at the series of concentrations (0.5 - 100.0 ppm) were run prior to analysis of alkali hydrolysates (analysed in series, as described in **section 2.6**), to confirm the retention times and detection limits. The retention times of particular standards and calculated values of detection limits generally resembled these given in **Table 3.3** (retention times within previously calculated  $\pm$  range).

##### 4.3.2.3.2 Hydrolysates analysis

The hydrolysates of heparin were analysed to profile the composition of polymer exposed to alkaline environments (pH 7 – 12) at three different temperatures (40, 60, 80 °C) as a function of time (up to 168 h). Although previous qualitative methods (PAGE

electrophoresis and UV-Vis analysis discussed in **sections 4.3.2.1** and **4.3.2.2**, respectively) suggested the stability of heparin at these conditions, the HPAEC-PAD analysis has an advantage of low detection limit for monosaccharides that could potentially be released from the polysaccharide chain and evade detection using the previous methods, due to their size or/and amount. Yet, despite the low detection margin, the elution profile of alkali hydrolysed samples were blank (except for internal standard of Fuc). Matching the previous results of PAGE and UV-Vis analysis, even the prolonged processing did not result in the detection of saccharide units, as shown in **Figure 4.9**, indicating the lack of heparin chain depolymerisation. The minor peak, marked by \* in **Figure 4.9d** of the pH 12/ 80 °C/ 168 h hydrolysis sample, was the only observed change that could potentially demonstrate limited polysaccharide degradation. With the retention time of ~ 34 min, it could be one of the uronic acid residues (GlcA or IdoA, judging by RT in **Table 3.3**), severed from heparin chain after the alkali catalysed structural rearrangement (discussed in chapter introduction in **section 4.1**).

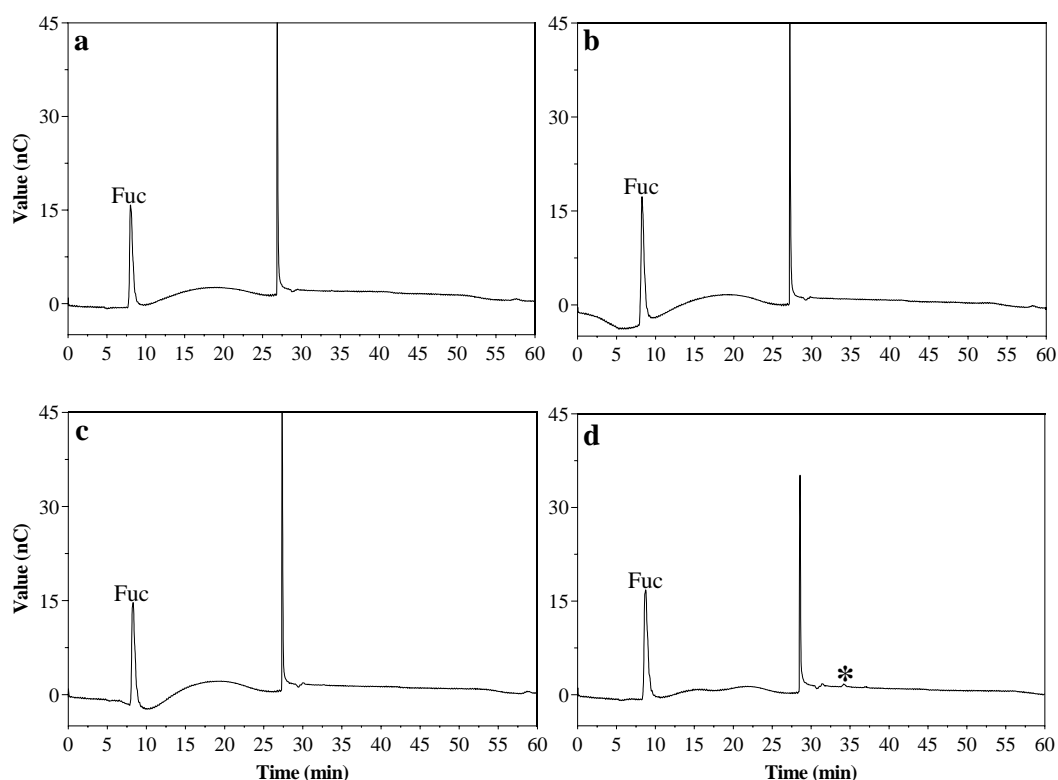


**Figure 4.9** The illustrative elution profiles of heparin hydrolysed at pH 12/ 80 °C over a) 24h, b) 48 h, c) 96 h, and d) 168 h. The small, unidentified peak is marked by \* in d). The narrow peak at ~ 27 min marks system peak, characteristic for gradient elution. Fuc-internal standard.

#### 4.3.2.3.3 The complete monosaccharides analysis concluding remarks

The alkaline hydrolysates of heparin were analysed *via* ion chromatography to assess the probability of glycosidic bond scission between the polysaccharide units. The method was considered as advantageous in comparison to PAGE electrophoresis and UV-Vis spectrophotometry, which had earlier suggested stability of heparin chain in alkaline conditions due to its low detection limit. Notwithstanding the detection limits, chromatograms of alkali treated samples showed no peaks, indicating that the applied conditions did not result in heparin chain fragmentation. Although the chromatographic results were consistent with PAGE and UV-Vis findings (discussed in in **sections 4.3.2.1** and **4.3.2.2**, respectively), they certainly did not help to explain why the molecular weight of heparin had decreased in studied environments (as discussed in **section 4.3.1**). At this point, it became more clear that the molecular weight loss would be justified by either by prominent desulfation, as in acid environments (for more details see **section 3.3.3**), or other intramolecular changes, as previously suggested by Holme (1996) and Jaseja (1989). Both hypotheses were addressed in following analysis.

### **4.3.3 The effect of degradative environments on heparin sulfate groups**

Chapter 3 demonstrated that acid-catalysed desulfation could solely affect the molecular weight of heparin to a significant extent (for more details, see **3.3.3.2**). Without having found an answer to molecular weight loss of heparin treated with alkaline environments, and after excluding the chain fragmentation (as discussed in previous sections, summarised in **4.3.2.3.3**), the hydrolysed samples were analysed from the perspective of desulfation. The analysis was carried *via* ion chromatography, coupled with a conductivity detector, according to experimental protocol summarised in **section 2.7**.

#### *4.3.3.1 Quantitative analysis of inorganic sulfate in post-hydrolytic samples*

##### 4.3.3.1.1 Summary of method optimisation

The detailed summary of method optimisation is given in **section 3.3.3.1.1**. The chromatographic standards of  $\text{Ac}^-$  and multi-elemental standard of  $\text{F}^-$ ,  $\text{Cl}^-$ ,  $\text{Br}^-$ ,  $\text{NO}_3^-$ ,  $\text{PO}_4^{3-}$  and  $\text{SO}_4^{2-}$  were analysed at the series of concentrations (0.1 - 0.5 ppm), prior to analysis of alkali hydrolysates, to confirm the retention times and detection limits of these anions. In

comparison to standards run before the acid-hydrolysed samples, the retention times of  $\text{Br}^-$ ,  $\text{NO}_3^-$ ,  $\text{PO}_4^{3-}$  and  $\text{SO}_4^{2-}$  (previously summarised in **Table 3.4**), changed to 5.7, 6.6, 8.9 and 10.6 ( $\pm 0.1$ ) min, respectively. Changes like these are common and follow strictly from the instrument operation, especially if the system has not been used for a long time (in this case the time interval between acid and alkaline measurements was 10 months) (“A Practical Guide to Ion Chromatography,” 2007; Bahadir, 2013). As earlier, anion calibration curves presented great linearity (with the lowest correlation coefficient equal to 99.97 % for  $\text{PO}_4^{3-}$ ), while the detection limits were generally calculated as lower to these summarised in **Table 3.4** (e.g.,  $\text{SO}_4^{2-}$   $\text{LOD}_{\text{acid}} = 0.08$  ppm;  $\text{LOD}_{\text{alkali}} = 0.05$  ppm). Low detection margin and good linearity of calibration curves of anion standards as well as very small standard deviations confirmed fine repeatability of ion chromatography and its applicability in following analysis.

#### 4.3.3.1.2 Hydrolysates analysis

The detection of sulfate anions was associated solely with the hydrolytic desulfation of molecule, as the analysis of heparin standard confirmed the purity of starting material (discussed in **section 3.3.3.1.1**). The sulfate anions were detected in heparin samples hydrolysed under the following conditions: 60 °C: pH 12 and 80 °C: pH 10 - 12. The illustrative chromatograms of maximum detection (pH 12/ 80 °C) and lack of detection (pH 9/ 80 °C) are presented in **Figure 4.10 a** and **b**, respectively.

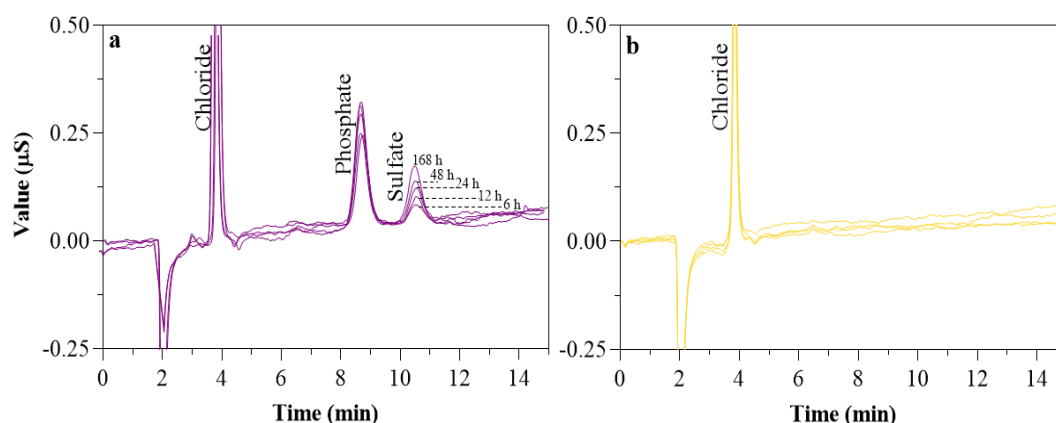


**Figure 4.10** Illustrative chromatograms of sulfate anion, detected in heparin samples hydrolysed at **a**) pH 12/ 80 °C, with peaks corresponding to chosen time points (6, 12, 24, 48 and 168 h), and **b**) pH 9/ 80 °C. The chloride and phosphate peaks correspond to neutralisation agents and buffering salts ( $\text{HCl}$  and  $\text{NaH}_2\text{PO}_4 + \text{NaOH}$ , respectively). Sample concentration equal to 10 ppm.

No anions (excluding  $\text{Cl}^-$  and  $\text{PO}_4^{3-}$  for neutralising agent and buffering salts, respectively) were detected at 40 °C, at any of applied pHs. Lack of sulfate detection suggest resistance of anion to these conditions, as well as to pH 7 – 11/ 60 °C and pH 7 – 10/ 80 °C. At 60 °C, sulfate was detected only at pH 12, while at 80 °C the small quantities of anion were observed at pH 10 and pH 11. When plotted as a function of time in **Figure 4.11**, the concentration of detected sulfate presented an increasing trend of a relatively steady rate, with pseudo-plateaus observed between 24 and 48 hours at pH 12/ 60 °C (**Figure 4.11a**) and pH 11 & 12/ 80 °C (**Figure 4.11b**). During the prolonged hydrolysis at pH 12/ 80 °C the concentration of liberated sulfate continued to rise over time, at again, systematic rate (**Figure 4.11b**).

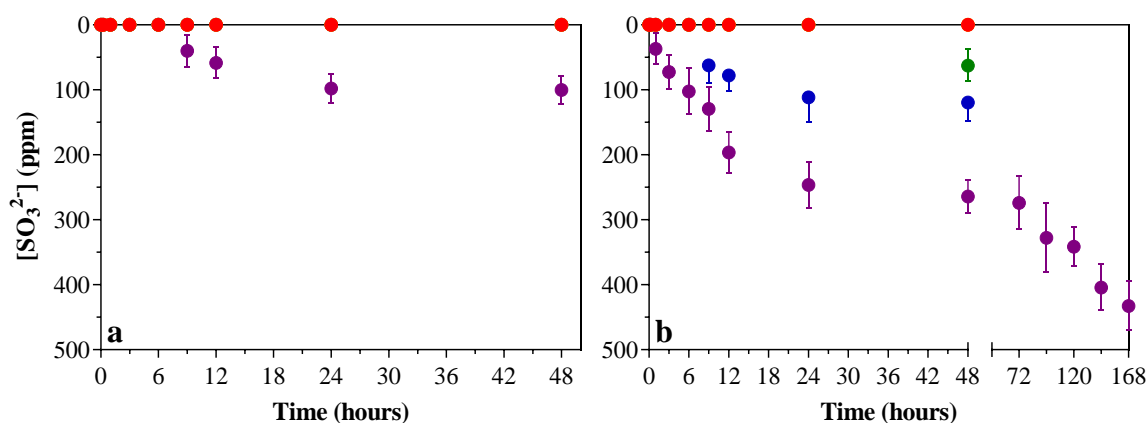


**Figure 4.11** Measured concentration of sulfate anions of thermally stressed heparin at **a)** 60 °C and **b)** 80 °C plotted for as a function of time at pH 7 - 12. The vertical error bars represent standard deviation from concentrations, calculated from peak area *via* calibration curve method. Triplicated runs. ● pH 7, ● pH 8, ● pH 9, ● pH 10, ● pH 11, ● pH 12

The pseudo-plateaus of desulfation were previously observed at acidic conditions and associated with liberation of different sulfate groups from heparin chain (*i.e.*, N-, 2O-, 6O). This assumption was confirmed by NMR analysis of acid hydrolysed samples (discussed in **3.3.3.1**). However, in this (alkaline) case, the characteristic behaviour of desulfation rate should be explained with the support of previous research. It had been established that at harsh alkaline conditions ( $\text{pH} \geq 11$ ), the 2-O-sulfated residues of iduronic acid (IdoA2S) undergoes almost quantitative desulfation, while other sulfate groups of heparin (*i.e.*, NS-, 6OS-) remain intact (Baumann et al., 1998; Casu, 1985; Jaseja et al., 1989). The 2OS-concentrated desulfation, dependent upon high pH would explain both lack of sulfate

detection at  $\text{pH} < 11$  and the limited change of colour intensity of Azure A (see **4.3.2.1.2**), which has stronger affinity toward N-sulfate, and therefore would not fade if N-sulfate was not severed from heparin (Ehrlich & Stivala, 1973; Finch, 1999; Powell et al., 2010). The observed pseudo-plateaus most probably reflect the slow kinetics of the 2-O-desulfation process rather than the ‘point’ of change between different liberated sulfate groups, like in case of acid hydrolysis. To examine this hypothesis chosen alkali hydrolysates were further looked at *via* NMR spectroscopy.

#### 4.3.3.2 The influence of desulfation on molecular weight of heparin

Following estimations presented in acid- hydrolysed **section 3.3.3.2**, the concentrations of alkali- hydrolysed sulfate ( $C_{\text{sulfate}}$ ; ppm or  $\text{mg}/\text{dm}^3$ ), detected *via* HPAEC- CD, was used to calculate molecular weight ( $M_{\text{sulfate}}$ ; g/mol). Both values, relatively modest in comparison to results of acid hydrolysis (see **Table 3.5**), are summarised in **Table 4.2**.

**Table 4.2** Hydrolysed sulfate data of chosen alkali-treated heparin samples.

Heparin Hydrolysates	Hydrolysed Sulfate Data					
	60 °C			80 °C		
	pH 12		pH 11		pH 12	
	$C_{\text{sulfate}}$ (ppm)	$M_{\text{sulfate}}$ (g/mol)	$C_{\text{sulfate}}$ (ppm)	$M_{\text{sulfate}}$ (g/mol)	$C_{\text{sulfate}}$ (ppm)	$M_{\text{sulfate}}$ (g/mol)
9 h	$40 \pm 24^b$	159	$62 \pm 27$	246	$129 \pm 34$	513
12 h	$58 \pm 24$	232	$78 \pm 25$	309	$197 \pm 32$	779
24 h	$98 \pm 22$	388	$112 \pm 39$	442	$246 \pm 35$	976
48 h	$100 \pm 21$	397	$119 \pm 29$	473	$264 \pm 25$	1047
72 h					$274 \pm 41$	1085
96 h					$328 \pm 53$	1299
120 h					$341 \pm 30$	1352
144 h					$404 \pm 36$	1601
168h					$433 \pm 37$	1714

<sup>b</sup> Error calculated from standard deviation of triplicated reading; <sup>c</sup> n.d.= not detected; <sup>d</sup> n.a.= not applicable

As previously, the weight of sulfate ( $M_{sulfate}$ ) was estimated as a fraction of initial molecular weight of heparin ( $M_{w,0} \text{ Hp} \approx 20,000 \text{ g/mol}$ ), according to **equation 3.1**. Following the procedure presented in acid- hydrolysis section (see **3.3.3.2**), the molecular weights of alkali- released sulfate ( $M_{sulfate}; \text{ g/mol}$ ) (**Table 4.2.**) were further subtracted from the average weight molecular weight of heparin subjected to specific conditions at hydrolytic time of 0 h ( $M_{w,t=0} \text{ Hp}_{hyd}; \text{ g/mol}$ ), (measured via size exclusion chromatography, see **3.3.1**), according to **equation 3.2**.

The calculated  $M_w$  and measured  $M_w$  of selected hydrolytic samples are summarized in **Table 4.3**. The numbers were statistically compared using non-parametric Wilcoxon matched pairs signed rank test. Statistically compared pairs of calculated and measured  $M_w$  of pH 12/ 60 °C and pH 11/ 80 °C sample were not significantly different ( $p > 0.05$ ) and demonstrated significantly effective pairing (**Table 4.3**). Consequently, at these conditions, desulfation could be considered as the sole source of molecular weight loss of heparin.

On the other hand, the same statistical operation indicated that pairs of calculated and measured  $M_w$  of pH 12/ 80 °C sample differed significantly ( $p < 0.05$ ). The higher number of variables (nine for pH 12/ 80°C, compared to four for pH 11/ 80°C) certainly affected the power of the p-value, but nevertheless, the strong differences between calculated and measured  $M_w$  of pH 12/ 80 °C samples are clear, regardless the statistical test (**Table 4.3**). Accordingly, it may be assumed that at applied conditions other processes and not just desulfation were responsible for the molecular weight changes in heparin. Given the results of previous analysis (reducing-ends assay, absorbance and monosaccharide profiles of hydrolysates, discussed in **section 4.3.2**), these could be indeed associated with structural rearrangements along the molecular chain rather than its scission (Holme et al., 1996; Jaseja et al., 1989). The NMR spectroscopy was the final analysis chosen to address this hypothesis.

#### 4.3.3.3 Concluding remarks

The anion analysis of alkali hydrolyses demonstrated that desulfation of heparin, triggered to the point exceeding the chromatographic limit of detection ( $\text{LOD}_{\text{SO}_4^{3-}} = 0.05 \text{ ppm}$ ), was susceptible to relatively harsh conditions, *i.e.*, pH 12/ 60 °C/9 h  $\leq$ ; pH11/ 80 °C/9 h  $\leq$ ; pH 12/ 80 °C/1 h  $\leq$ . Considering the strength of applied conditions and recalling the argument

of specific 2-O-desulfation of IdoA2S (dependent upon raised temperature and  $\text{pH} \leq 11$ ), it was assumed that observed anions originated from the C-2 of iduronate. Furthermore, the statistical analysis showed that at  $\text{pH} 12/ 60\text{ }^\circ\text{C}$  and  $\text{pH} 11/ 80\text{ }^\circ\text{C}$  the reduction of molecular weight of heparin could be accounted for hydrolytic sulfate loss, while this was not the case at  $\text{pH} 12/ 80\text{ }^\circ\text{C}$ . In light of previous analysis, which pointed out the resistance of heparin glycosidic bonds to applied alkaline conditions, and excluding the influence of desulfation, the molecular weight loss was thought to be associated with structural rearrangements along the polysaccharide chain. To finally test affinity of C-2 to sulfate loss and potential of IdoA to structural modifications, the chosen alkali hydrolysates of heparin were subjected to NMR analysis.

**Table 4.3** Summary of calculated and measured  $M_w$  of selected heparin hydrolysates.

Heparin Hydrolysates	Calculated $M_w(\text{g/mol})^a \times 10^4$ vs Measured $M_w(\text{g/mol}) \times 10^4$		
	60 °C		80 °C
	pH 12	pH 11	pH 12
9 h	1.97 vs 1.70	1.96 vs 1.74	1.93 vs 1.70
12 h	1.96 vs 1.66	1.95 vs 1.73	1.90 vs 1.61
24 h	1.94 vs 1.63	1.94 vs 1.72	1.88 vs 1.53
48 h	1.94 vs 1.61	1.93 vs 1.71	1.88 vs 1.52
	$p^b = 0.1250$	$p = 0.1250$	
72 h <sup>c</sup>			1.87 vs 1.50
96 h			1.85 vs 1.45
120 h			1.85 vs 1.42
144 h			1.82 vs 1.41
168h			1.81 vs 1.35
			$p = 0.0039$

<sup>a</sup> Calculated  $M_w(\text{g/mol})$  calculated by subtracting the amount of released sulfate anions (g/mol), measured by HPAEC-CD, from the  $M_w$  of heparin sodium standard, measure by SEC-MALS-RI; <sup>b</sup> calculated value, if  $p > 0.05$ , compared data are not significantly different; <sup>c</sup> prolonged hydrolysis time-points, *i.e.*, 72 – 168 h, applicable for  $\text{pH} 12/ 80\text{ }^\circ\text{C}$  only

#### 4.3.4 Inside look at alkaline-catalysed, hydrolytic degradation of heparin; final confirmation of iduronate modifications and desulfation

In the first part of this study the great potential of NMR spectroscopy to fingerprint acid-catalysed modifications at molecular level of heparin has been presented. By monitoring the chemical shifts of  $^1\text{H}$  and  $^{13}\text{C}$  signals of hydrolysates, in perspective to polysaccharide standard spectra, the scope and order of heparin desulfation at acidic conditions has been established (for details, see **section 3.3.4**). Following the success of previous analysis, a similar approach has been used to ascertain potential of heparin iduronate towards alkali-catalysed modifications and desulfation, which was indicated by the presence of free sulfate groups (summarised in **4.3.2.3.3** and **4.3.3.3**).

Previous NMR spectra (presented in *e.g.*, Desai et al., 1993; Holme et al., 1996; Jaseja et al., 1989; Rej & Perlin, 1990) served as the basis for following, comprehensive analysis of alkali treated heparin. The most prominent changes in the molecular weight and sulfation profiles of heparin were observed at pH 12. Therefore, this sample was used as a starting point to determine the possible intramolecular modifications.

##### 4.3.4.1 Standard spectra acquirement and analysis

The detailed description of standard spectra acquisition and assignment is presented in **section 3.3.4.1**. The one- ( $^1\text{H}/^{13}\text{C}$ ) and two-dimensional (HSQC) spectra of the heparin standard were acquired prior to the study of hydrolysates, according to protocol described in **section 2.8.4**. The spectra were treated as a reference for the following desulfation and modification study, approached by comparative analysis between chemical shifts of chosen NMR signals.

##### 4.3.4.2 NMR- illustrated 2-O-desulfation of iduronate as initial step of alkali-catalysed degradation of heparin

The one- ( $^1\text{H}/^{13}\text{C}$ ) and two-dimensional (HSQC) spectra of pH 12 hydrolysates of heparin, aliquoted at 40 and 60 °C, at 24 and 48 h were compared with these of heparin standard. Illustrative spectra of pH 12/ 40 °C and pH 12/ 60 °C samples are presented in **Figure 4.12** and **Figure 4.13**, respectively. As illustrated, the only clear difference between standard (black) and hydrolysates (pink/ purple) spectra was appearance of a ‘stretched’ signal under

the I-1 (**Figure 4.12** and **Figure 4.13**), which marks the continuous desulfation of IdoA(2S) (Casu, 1985; Fraidenraich y Waisman & Cirelli, 1992). Besides this one peak, there is a clear resemblance between anomeric and aliphatic regions of both spectra (standard vs. hydrolysates, **Figure 4.12** and **Figure 4.13**). Consequently, 2-O-desulfation was recognised as the sole intramolecular process happening at studied conditions. Ergo, treatment of heparin with pH 12, at 40 and 60 °C, up to 48 h, catalyses IdoA(2S) desulfation without breaking the glycosidic bonds between the heparin units.

As the spectra acquired at 24 h and 48 h at each temperature were identical (40 °C/ 24 h = 40 °C/ 48 h, *etc.*), the time gap between collected samples seemed not to alter additional modifications. This explains the pseudo-plateaus observed during both molecular weight (**Figure 4.4**), and in case of pH 12/ 60°C sample, sulfate analysis (**Figure 4.11**). None of sulfate was detected during ion chromatography analysis of pH 12/ 40 °C sample (as discussed in **section 4.3.3**). Thus, it may be assumed that desulfation observed at these conditions *via* NMR (of a greater sensitivity than chromatography), had only just been initiated and did not exceed the chromatographic limit of detection.

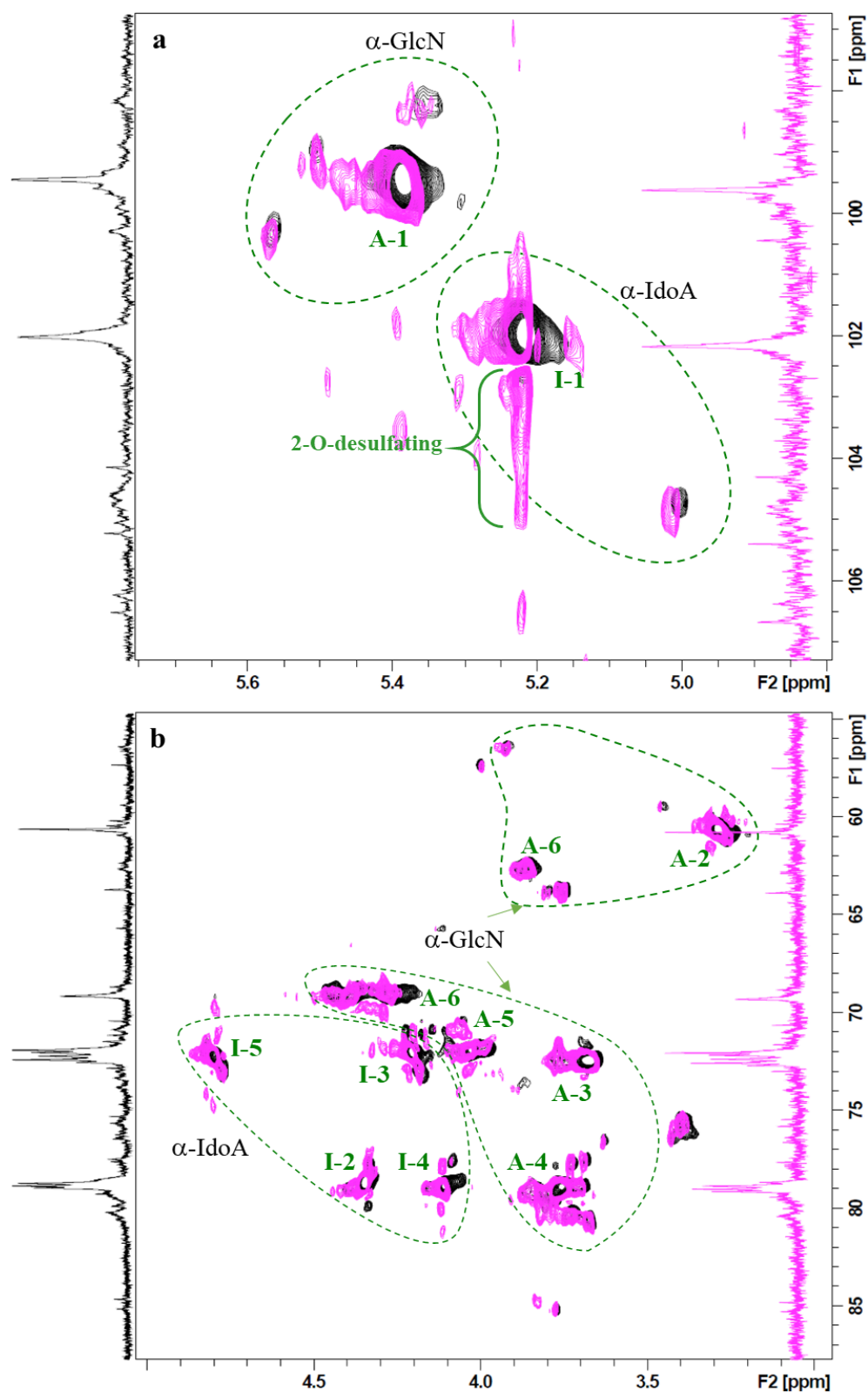


**Figure 4.12** The NMR spectra (HSQC with  $^{13}\text{C}$  projection) of heparin hydrolysed at pH 12/ 40 °C/ 24 h (pink) over the standard sample (black). The glucosamine and iduronate regions, with most important peaks are circled in both **a**) anomeric and **b**) aliphatic regions. The stretched signal under I-1 of hydrolysate marks the continuous desulfation of IdoA(2S).

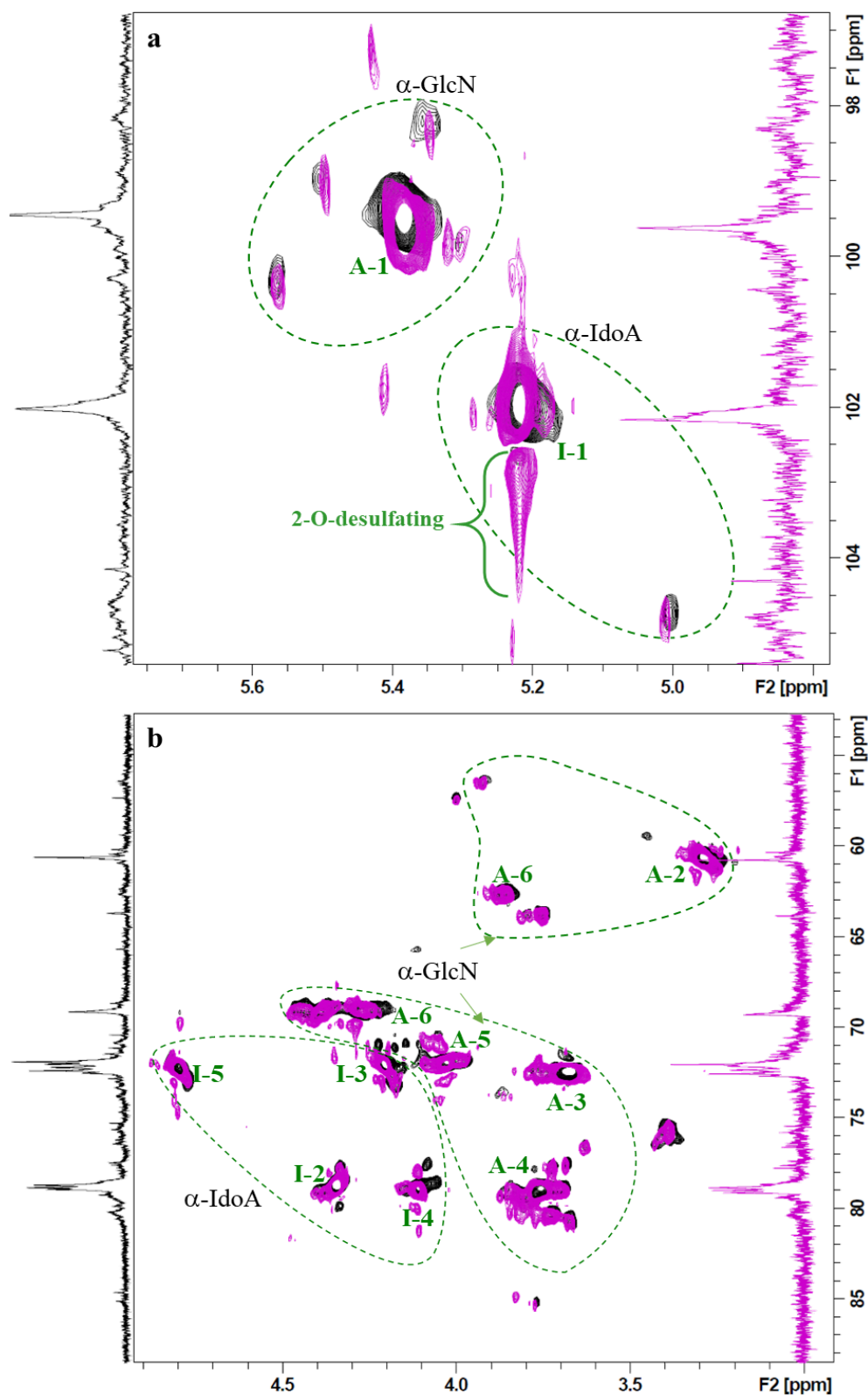


**Figure 4.13** The NMR spectra (HSQC with  $^{13}\text{C}$  projection) of heparin hydrolysed at pH 12/ 60 °C/ 24 h (purple) over the standard sample (black). The glucosamine and iduronate regions, with most important peaks are circled in both **a**) anomeric and **b**) aliphatic regions. The stretched signal under I-1 of hydrolysate marks the continuous desulfation of IdoA(2S).

#### 4.3.4.3 NMR illustrated modifications of iduronate residue of heparin at alkali-catalysed hydrolysis

The chemical shift data for heparin at pH 12/ 80 °C/ 24 h ≤, is summarised in **Table 4.4**, were accessed with the aid of a HSQC spectra where the  $^1\text{H}/^{13}\text{C}$  projection are presented in **Figure 4.14** and **Figure 4.16**. The changes observed in the aliphatic and anomeric regions of both figures indicated that during the hydrolysis of heparin under these conditions (specified in figure captions) the iduronic acid moiety was altered.

The acquisition of spectra at pH 12/ 80 °C/ 24 h in **Figure 4.14**, enabled observation of 2-O-desulfated residues of iduronic acid at 5.23/ 105.1 ppm ( $^1\text{H}/^{13}\text{C}$  chemical shifts) (Jaseja et al., 1989). Furthermore, the appearance of a 5.23/ 99.1 ppm signal (**Figure 4.14**) suggested that desulfated IdoA species were linked to an anomeric carbon of GlcNS (Casu, 1985; Fraidenraich y Waisman & Cirelli, 1992). At the same time, the sulfoamino group ( $-\text{NH}_2\text{SO}_3^{2-}$ ) of glucosamine remained intact. Had the hydrolytic cleavage of glucosamine sulfate occurred, the A-1 signal would have moved downfield in proton spectrum by only 0.01 ppm and upfield in carbon as 99.4 → 93.7 ppm (Yates et al., 1996; this work, section 3.3.4.2.1). The observed signal A-1 has moved downfield in proton spectrum from 5.38 → 5.47 ppm, as well as in carbon 99.4 → 101.3 ppm (**Figure 4.14; Table 4.4**). The change of chemical shift of A-1 was possible as the shielding effect of IdoA(2S) decreased together with its desulfation (Fraidenraich y Waisman & Cirelli, 1992; Jaseja et al., 1989). The 6-O-desulfation would have been detected by major upfield chemical shift of A-6 and A-5 carbon signals, *i.e.*: 69.1 → 62.3 ppm and 71.9 → 74.2 ppm respectively (Taylor et al., 2019; Yates et al., 1996; this work, section 3.3.4.2.3), while clearly that was not the case in discussed example (**Figure 4.14; Table 4.4**). The observation of 2-O-desulfated iduronate in **Figure 4.14** indicates that some moieties of desulfated acid retained stereochemical orientation (Desai et al., 1993), while the portion of desulfated species gave a rise to  $\alpha$ -L-galacturonate (Casu & Lindahl, 2001; Jaseja et al., 1989; Rej & Perlin, 1990). The appearance of galacturonic units was marked by new signals in anomeric region, *i.e.*: 5.16/ 101.6 ppm designated G-1 and 5.16/ 99.0 ppm that reflected the G-1 – (A-1) linkage (**Figure 4.14; Table 4.4**) (Fraidenraich y Waisman & Cirelli, 1992; Jaseja et al., 1989). The chemical shifts of other new signals were found in aliphatic region at 4.02/ 78.6 ppm, 4.48/ 80.5 ppm and 4.67/74.4 ppm, recognised as G-2/3, G-4, G-5, respectively (**Figure 4.14; Table 4.4**).

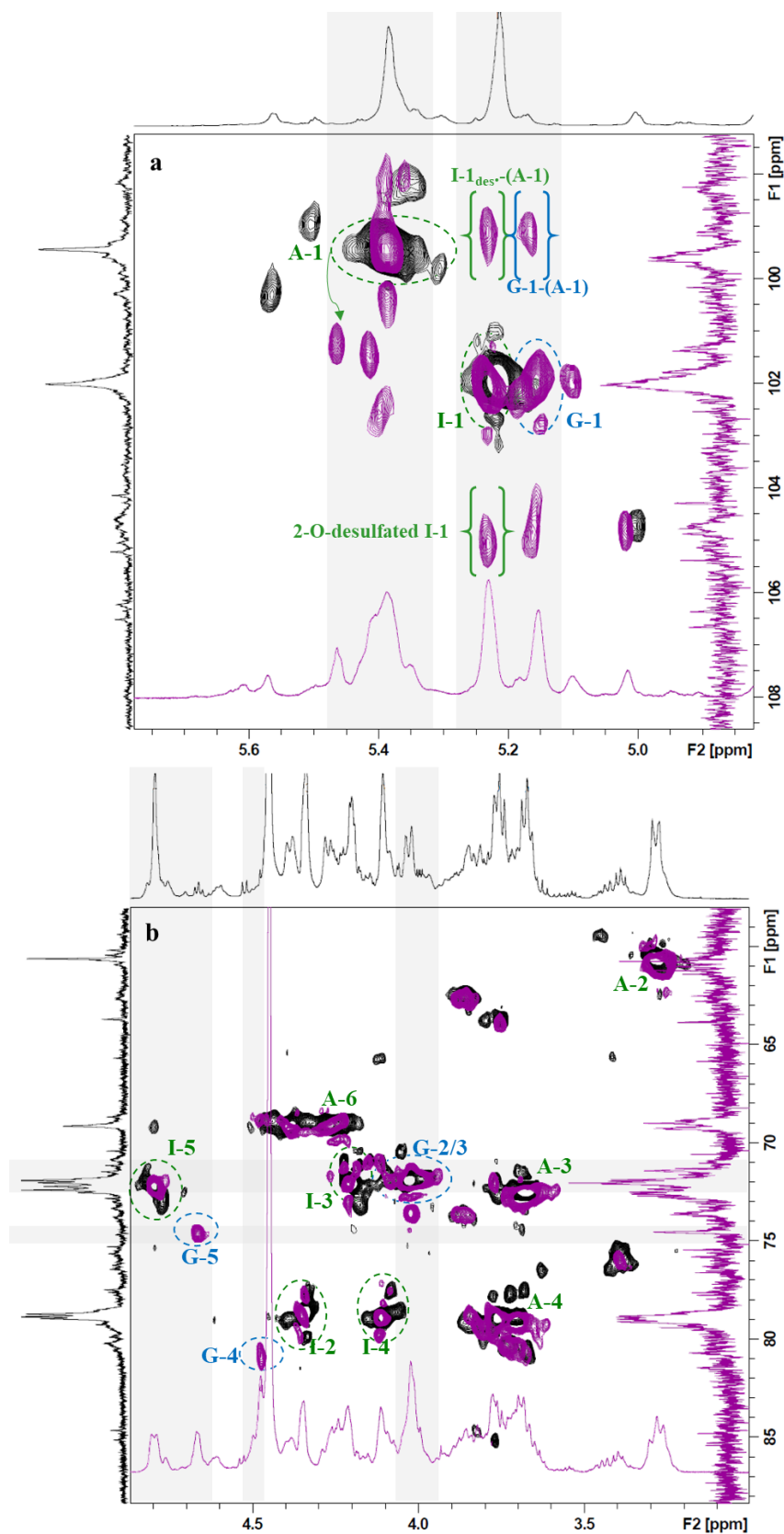


**Figure 4.14** The NMR spectra (HSQC with  $^1\text{H}/^{13}\text{C}$  projection) of heparin hydrolysed at pH 12/ 80 °C/ 24 h (purple) over the standard sample (black). The glucosamine, iduronate and new, galacturonate peaks are circled in both **a**) anomeric and **b**) aliphatic regions.

**Table 4.4**  $^{13}\text{C}$  and  $^1\text{H}$  chemical shifts of heparin standards and pH 12 hydrolysates.

Peak <sup>a</sup>	$^1\text{H}/^{13}\text{C}$ chemical shift (ppm)			References
	Heparin Standard	pH 12/ 80 °C 24 h – 48 h <sup>b</sup>	pH 12/ 80 °C 48 h < <sup>b</sup>	
A-1	5.38 99.4	5.38 → 5.47 <sup>c</sup> 99.4 → 101.3	5.38 → 5.47 99.4 → 101.3	
A-2	3.27 60.6	3.26 61.2	3.26 61.2	
A-3	3.67 72.4	3.67 72.6	3.67 72.6	Yates et al.(1996)
A-4	3.76 78.9	3.70 78.9	3.70 78.9	
A-5	4.02 71.9	4.02 71.9	n.a. <sup>d</sup> n.a.	
A-6	4.28 - 4.38 69.1	4.28 - 4.38 69.0	4.28 - 4.38 69.0	
I-1 (I-1 <sub>des</sub> – (A-1))	5.21	5.23 99.1	5.23	Yates et al.(1996) Fraidenraich (1992)
I-1 (I-1 <sub>des</sub> )	102.0	101.8 105.1	101.8	Jaseja et al. (1989) Jaseja et al. (1989)
G-1 (G-1 – (A-1))		5.16 99.0	5.16	Fraidenraich (1992)
G-1		101.6	101.6	Jaseja et al. (1989)
I-2	4.34 78.7	4.35 71.3	4.35 71.3	Yates et al.(1996)
G-2/3		4.02 78.6	4.02 78.6	Jaseja et al. (1989)
I-3	4.20 72.0	4.21 72.0	4.21 72.0	Yates et al.(1996)
I-4	4.11 78.8	4.11 78.6	4.11 78.6	Yates et al.(1996)
G-4		4.48 80.5	4.48 80.5	Jaseja et al. (1989)
I-5	4.79 72.2	4.79 72.1	4.79 72.1	Yates et al.(1996)
G-5		4.67 74.4	4.67 74.4	Fraidenraich (1992) Jaseja et al. (1989)

<sup>a</sup> number next to signal stands for carbon number of saccharide unit; <sup>b</sup> details of alkali hydrolysates of heparin; <sup>c</sup> arrow marks visibility of both peaks at original and shifted position; <sup>d</sup> not assigned; A- glucosamine residues; I- iduronic acid residues, G-galacturonic acid residues;

In **Figure 4.15** of pH 12/ 80 °C/ 96 h sample the definition of galacturonate signals was enhanced in comparison to these in **Figure 4.14**. Thus, prolonged hydrolysis at pH 12/ 80 °C must result in more prominent inversion of stereochemistry at the positions C-2 and C-3 of desulfated iduronate (Jaseja et al., 1989). Upon the approximate integral ratio of IdoA:GalA signals of spectrum pH 12/ 80 °C/ 168 h in **Figure 4.16**, *i.e.*: I-1:G-1 = 1.0:2.5; I-5:G-6 = 1.0:2.6; I-2:I-3:G-2/3 = 4.8:1.0:26.7; it was concluded that nearly all iduronate units were modified (*i.e.*, desulfated and of changed stereochemistry). At the same time, the sulfated glucosamine residues (NS-, 6OS-) remained unaltered (**Figure 4.15** and **Figure 4.16**), ergo, were considered as resistant to applied conditions. Furthermore, no alteration in any of discussed spectra have indicated the glycosidic scission. This allowed to exclude depolymerisation of heparin chain at applied conditions.

It is noteworthy that two uronic acid stereoisomers, namely  $\alpha$ -L-iduronate and  $\alpha$ -L-galacturonate were formed exclusively after or rather as a result of the alkaline hydrolysis of 2-O-sulfated  $\alpha$ -L-iduronate of heparin. In neither of investigated sample the 2,3-anhydro intermediate was captured. Earlier studies presumed that reactions promoting similar exclusive conversion required prolonged heating of heparin in 0.1 M Na<sub>2</sub>CO<sub>3</sub> under the reflux (Holme et al., 1996; Rej & Perlin, 1990). The specificity of discussed rearrangement was considered as a result of earlier desulfation of iduronate moiety that was clearly initiated prior to structural modifications (as presented by NMR spectra of acquired at lower temperatures **Figure 4.12**, **Figure 4.13** and signals in **Figure 4.14**). Previous studies suggested that desulfation mechanism of IdoA(2S) is based upon the intramolecular displacement of 2-O-sulfate that paradoxically is a vital step in 2,3-anhydride formation (Casu & Lindahl, 2001; Jaseja et al., 1989; Rej & Perlin, 1990). Perhaps the application of buffering system catalysed the IdoA(2S) desulfation in other (than intramolecular displacement) mechanism that through the kinetically favoured 2-O-desulfation decreases the probability of anhydride closure. On the other hand, the 2,3-anhydride rearrangement could simply happen at extremely fast rate, making impossible to capture its signal *via* applied NMR analysis. Nevertheless, simple heating of heparin in common phosphate buffer clearly led to almost selective hydrolysis of iduronate, and even though the reaction period was considered as a drawback, the processing in phosphate buffer should be recognised as a potential for researchers seeking similar modifications of heparin.

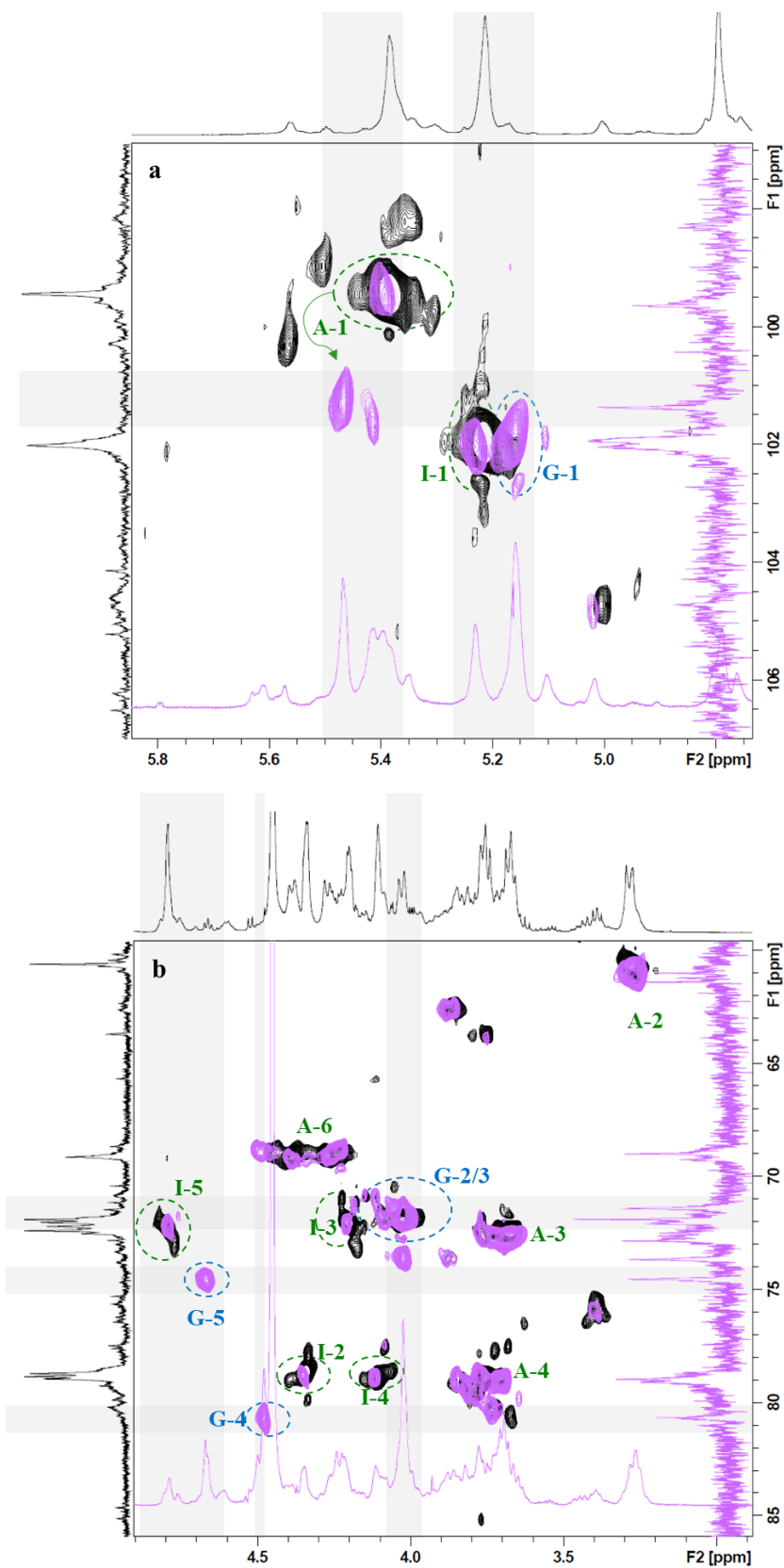


**Figure 4.15** The NMR spectra (HSQC with  $^1\text{H}/^{13}\text{C}$  projection) of heparin hydrolysed at pH 12/ 80 °C/ 96 h (violet) over the standard sample (black). The glucosamine, iduronate and new, galacturonate peaks are circled in both **a)** anomeric and **b)** aliphatic regions.

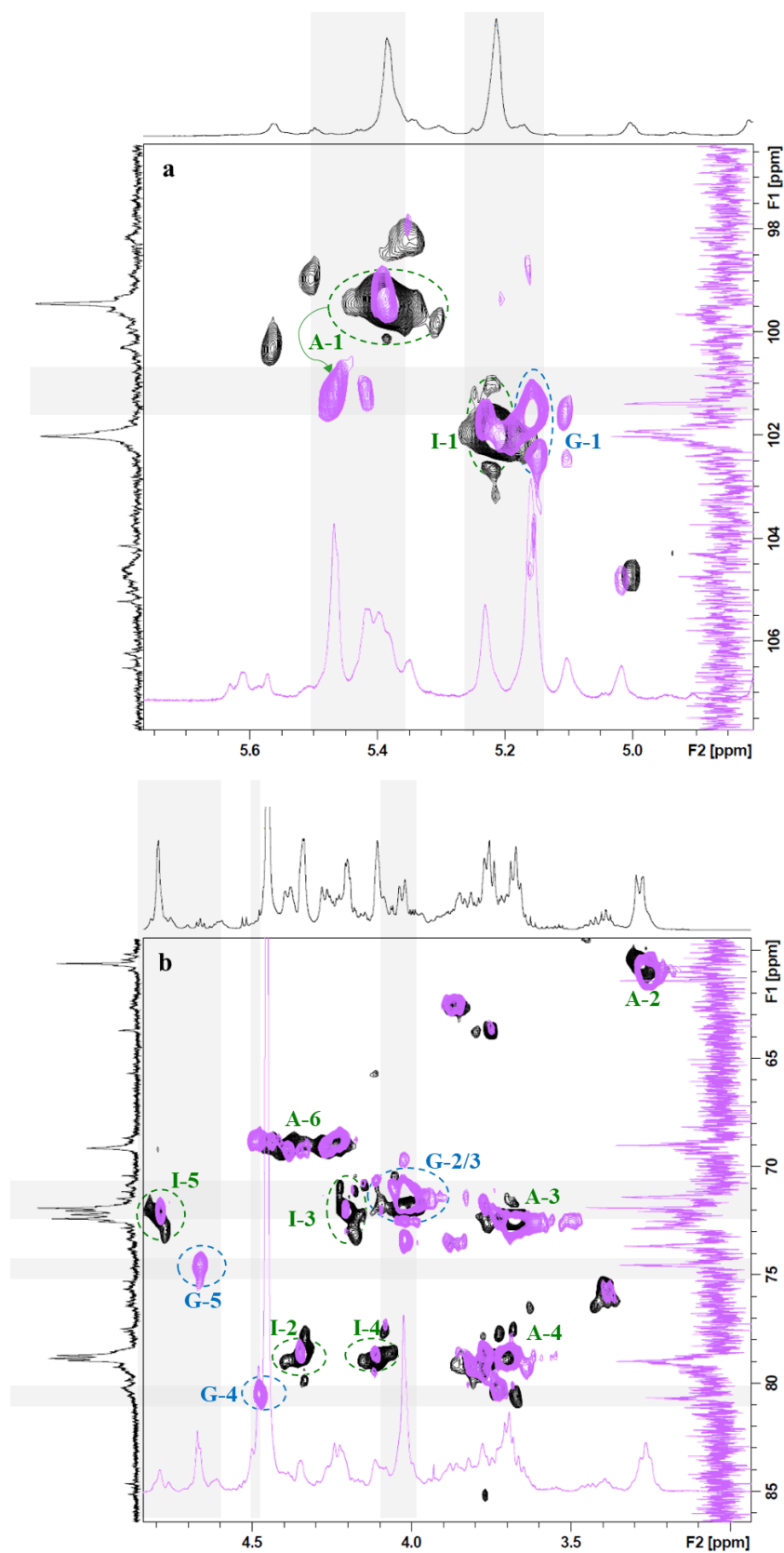


**Figure 4.16** The NMR spectra (HSQC with  $^1\text{H}/^{13}\text{C}$  projection) of heparin hydrolysed at pH 12/ 80 °C/ 168 h (violet) over the standard sample (black). The glucosamine, iduronate and new, galacturonate peaks are circled in both **a)** anomeric and **b)** aliphatic regions.

#### 4.3.4.4 NMR analysis of heparin samples treated with milder alkaline conditions

The comprehensive NMR analysis of heparin samples hydrolysed at pH 12, at all three of studied temperatures, revealed the lability of molecule to 2-O-desulfation and stereochemical rearrangements of iduronate. Both modifications clearly affected the molecular weight of heparin, as presented using various analytical techniques, discussed throughout this chapter. The changes in molecular weight of heparin were also observed after the hydrolysis of molecule at milder alkaline conditions, *i.e.*, pH 7- 11, at 60 °C and 80 °C. Among these, pH 10 and pH 11 were recognised as the most important, decreasing the heparin molecular weight by 12 % and 14 %, respectively (percentage calculated after processing in these pHs for 48 h/ 80 °C, as in **Table 4.1**). Although anion analysis demonstrated that treatment of heparin with pH 11 at 80 °C led to sulfate cleavage, which had a significant consequence towards the molecular weight of polysaccharide (discussed in **section 4.3.3**), this was not observed at pH 10/ 60 & 80 °C and pH 11/ 60 °C. Furthermore, none of the above conditions were associated with chain depolymerisation (as discussed in **section 4.3.2**), which would normally serve as an argument to explain the molecular weight loss of polysaccharide. Therefore, the pH 10/ 60 & 80 °C and pH 11/ 60 & 80 °C hydrolysates of heparin were analysed by NMR, to get a closer look at possible chain degradation.

As illustrated in **Figure 4.17 a** and **c**, no visible, structural changes were observed after the treatment of heparin sample with pH 10 and pH 11 at 60 °C. In case of hydrolysis at these pHs at 80 °C, the ‘stretched’ signal in **Figure 4.17 b**, marking the ongoing 2-O-desulfation (similar as in pH 12/ 40 and 60 °C; **Figure 4.12** and **Figure 4.13**, respectively), was noted. This observation matched the results of anion analysis, discussed in **section 4.3.3**, that identified sulfate in pH 10 and pH 11/ 80 °C hydrolysates.

The desulfation of heparin at pH 10 and pH 11, at 80 °C would be considered as a major cause of molecular weight loss. In-depth analysis of chosen samples did not identify any apparent degradative processes that could alert the molecular weight of heparin at milder conditions, like pH 10 or pH 11 and 60 °C, the observed 12% decrease need to be looked at from the perspective of measurement uncertainty, acknowledge by error bars in molecular weight plots in **Figure 4.4**.

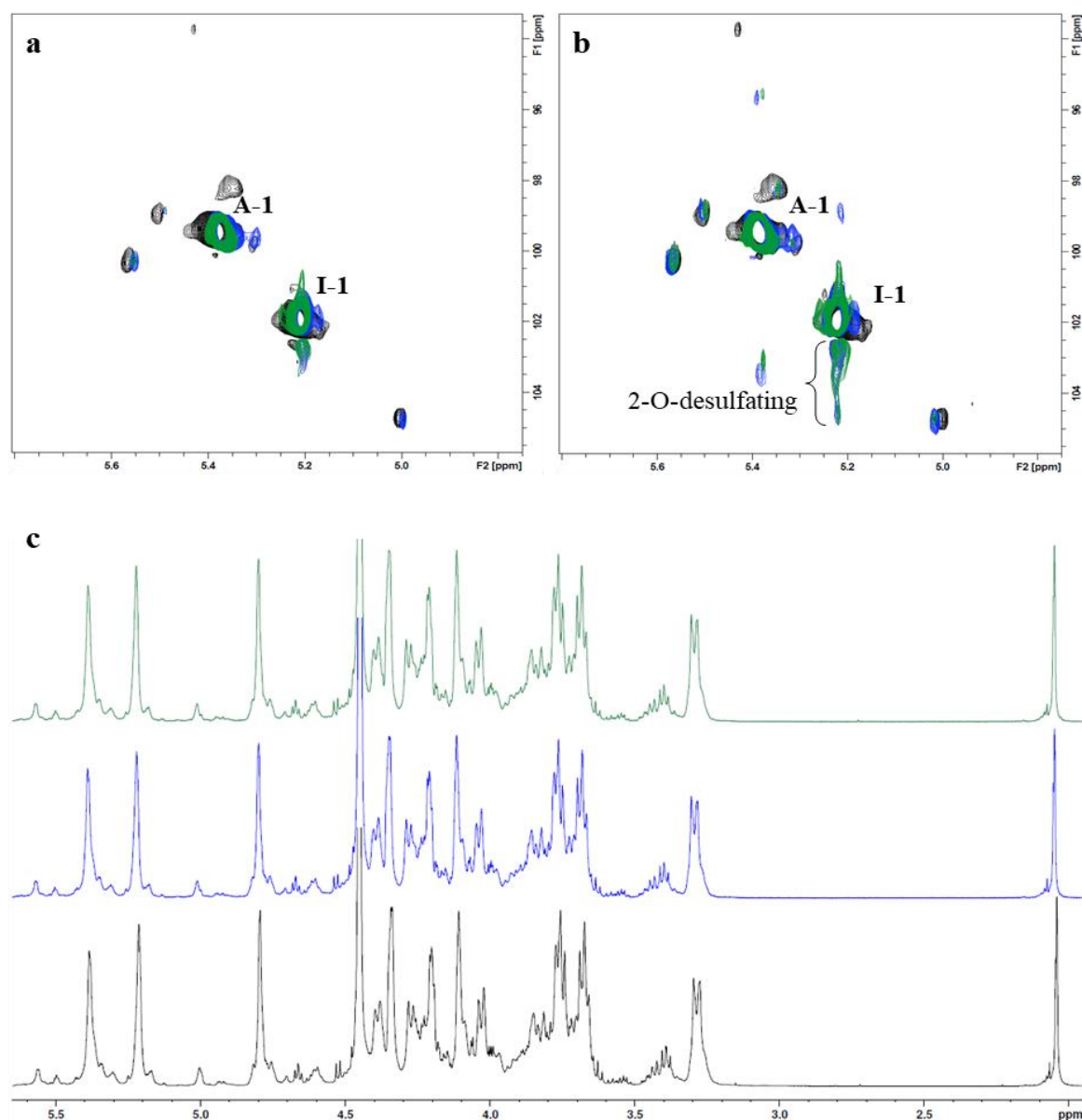


**Figure 4.17** The anomeric regions of **a)** ● pH 10/ 60 °C; ● pH 11/ 60 °C hydrolysates and **b)** ● pH 10/ 80 °C; ● pH 11/ 80 °C hydrolysates over the heparin standard in HSQC NMR spectra. **c)** The complete NMR spectra of ● pH 10/ 60 °C, ● pH 11/ 60 °C hydrolysates and heparin standard in proton multi-display.

#### 4.3.4.5 NMR analysis of alkali hydrolysed samples - concluding remarks

The NMR spectroscopy was used to fingerprint the modifications at the molecular level of heparin, catalysed by hydrolytic alkali treatment. Monitoring of chemical shifts of  $^1\text{H}$  and  $^{13}\text{C}$  signals of hydrolysates, in comparison to polysaccharide standard spectra, showed the lability of 2-O-sulfate of iduronate at pH 10 and pH 11/ 80 °C and pH 12/ 40 and 60 °C. The prolonged processing at pH 12/ 80 °C led to more prominent 2-O-desulfation with a

following stereochemical modifications of  $\alpha$ -L-iduronate to  $\alpha$ -L-galacturonate, according to reaction scheme given in **Figure 4.18**. The acquired spectra did not contain signals characteristic for 2,3-anhydro intermediate. The exclusive formation of above two uronic acid stereoisomers was hypothesised to be a result of a mechanism omitting anhydrite-associated intramolecular displacement, unique for the applied conditions. However, it could be that the buffer environment catalysed the 2,3-anhydro rearrangement so rapidly that it was impossible to capture *via* the applied NMR methodology. The presented reasoning is of course only hypothetical, but it certainly opens a new door to future discussion around heparin stability in alkaline conditions, especially that the alteration associated with (N- or 6O-) desulfation of glucosamine residues or glycosidic scission were not observed in any of discussed spectra, which excludes the affinity of both processes to applied alkaline conditions.

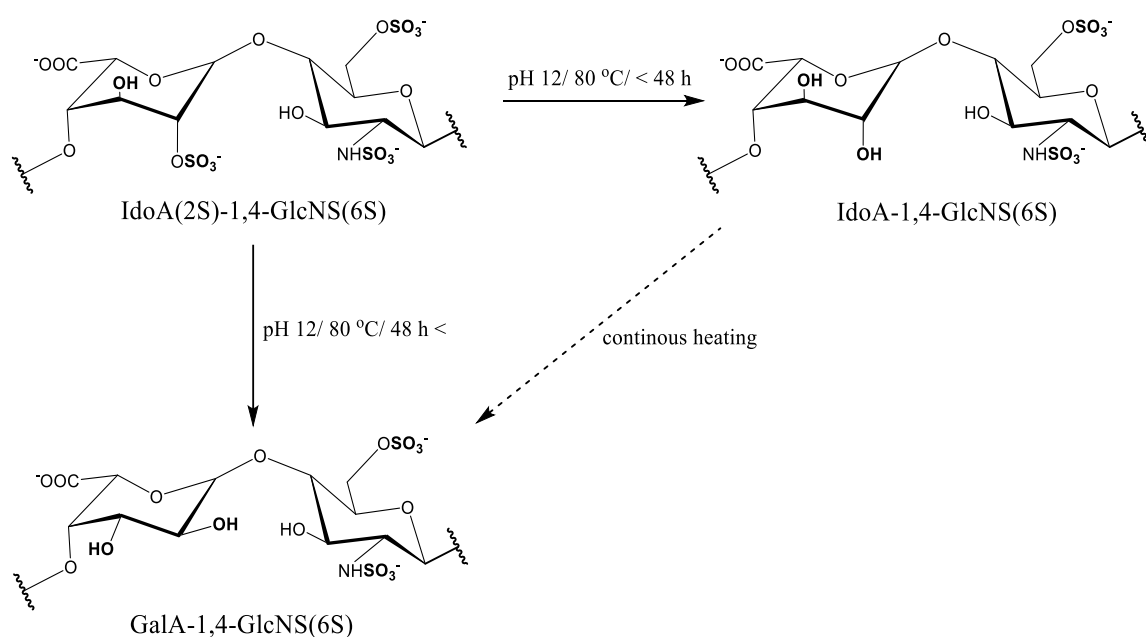


**Figure 4.18** Reaction scheme showing the intramolecular changes of major disaccharide unit of heparin, observed in this study, after hydrolysis in pH 12 at 80 °C.

#### 4.4 THE KINETICS APPROXIMATION OF HYDROLYTIC DEGRADATION OF HEPARIN IN ALKALINE ENVIRONMENTS

##### 4.4.1 Introduction

Following the kinetics approximation for the hydrolytic degradation in acidic environments, a similar procedure was applied for heparin treated with alkali solutions. The reasoning was based on reaction scheme, summarising the major findings of **section 4.3**, with the same assumptions (as in **3.4**) regarding the pseudo- order and specific catalysis.

##### 4.4.2 Proposed kinetic model of hydrolytic degradation of heparin in alkaline environments

On the basis of results collected *via* the multi-analytical protocol, mainly- the NMR screening (summarised in **4.3.4**), the major findings of **section 4.3** included pH 12 catalysed 2-O-desulfation of IdoA of heparin, with following stereochemical rearrangements (IdoA → GalA). At the same time, the remaining sulfate groups (NS-, 6OS-), as well as glycosidic bonds between heparin units were not affected, ergo, characterised by great stability (under the applied alkaline conditions). Also, the desulfation and modification of iduronate bypassed the anhydrous intermediate (as discussed in **4.3.4.3**). Therefore, the alteration of heparin observed in alkaline conditions could be summarised *via* straight-forward scheme:



where  $k_{-2S}$  is a pseudo- 2-O-desulfation rate constant,  $k_G$  is a pseudo-rate constant associated with stereochemical rearrangements of iduronate (IdoA → GalA).

Scheme 4.1 assumes the consecutive order of alkali-catalysed, degradative reactions of heparin. Indeed, considering the nature of summarised rearrangements (see **4.3.4**), one could expect that the concentration of 2-O-desulfated heparin (*Heparin* -2*S*) would reach maximum over time and concentration of heparin with galacturonate unit (*Heparin* *G*) would depend on the reaction step (Loftsson, 2013; Sinko, 2011; Wyman & Yang, 2017; Yablonsky et al., 2010). Consequently, the series of reactions summarised in Scheme 4.1 can be kinetically expressed as:

$$\frac{d[Hep]}{dt} = -k_{-2s} \cdot [Hep] \quad 4.1$$

$$\frac{d[Hep_{-2s}]}{dt} = (k_{-2s} \cdot [Hep]) - (k_G \cdot [Hep_{-2s}]) \quad 4.2$$

$$\frac{d[Hep_G]}{dt} = k_G \cdot [Hep_{-2s}] \quad 4.3$$

Equation 4.1 solves by integration and differential calculus, as **equations 1.10 - 1.12**, which gives:

$$[Hep] = [Hep]_0 \exp(-k_{-2s}t) \Rightarrow \frac{[Hep]}{[Hep]_0} = \exp(-k_{-2s}t) \quad 4.4$$

Following the rearrangement presented in **equation 3.6**, the fractional form of equation 4.4 can be re-written to include the influence of temperature upon the examined reaction:

$$\frac{[Hep]}{[Hep]_0} = \exp\left(A \cdot \exp\left(\frac{E_a}{RT}\right) t\right) \quad 4.5$$

To solve the equation 4.2, the substitution of 4.4, integration and differential calculus is applied, which gives (Loftsson, 2013; Wyman & Yang, 2017; Yablonsky et al., 2010):

$$\begin{aligned} \frac{d[Hep_{-2s}]}{dt} &= (k_{-2s} \cdot [Hep]) - (k_G \cdot [Hep_{-2s}]) \\ [Hep_{-2s}] &= [Hep]_0 \cdot \frac{k_{-2s}}{(k_G - k_{2s})} \cdot \{\exp(-k_{-2s}t) - (\exp(-k_G t))\} \end{aligned} \quad 4.6$$

And finally, recalling the relationship between the concentrations of reagents of constitutive reaction, presented in **equation 3.17**, the  $[Hep G]$  of equation 4.3 can be simply calculated by subtraction, using equations 4.4 and 4.6, which gives:

$$[\text{Hep}]_0 = [\text{Hep}] + [\text{Hep}_{-2S}] + [\text{Hep}_G] \Rightarrow [\text{Hep}_G] = [\text{Hep}]_0 - [\text{Hep}] - [\text{Hep}_{-2S}]$$

$$[\text{Hep}_G] = [\text{Hep}_0] \cdot \left( 1 - \frac{k_G \exp(-k_{-2S}t) - k_{-2S} \exp(-k_G t)}{k_G - k_{-2S}} \right) \quad 4.7$$

Both equations can be further re-written, as equation 4.5, to include the influence of temperature upon the considered processes.

#### 4.4.3 The choice of kinetic plots in a proof-of-concept verification of presented kinetics approximation

As in **section 3.4.3**, the molecular weights of heparin hydrolysed at pH 12/ 80 °C/ over 168 h were plotted as functions of time, following the simple pseudo-first order (according to **equation 3.19**) and pseudo-second order (as in **equation 3.20**) rate equations.

As presented in **Figure 4.19** and **Figure 4.20**, the fits of both pseudo-first order and pseudo-second-rate order equations, respectively, are not linear. Ergo, the description of alkali catalysed degradation of heparin *via* single rate equations would be inadequate. The observed rearrangements would require more complex kinetic models. As mentioned earlier in **section 3.4.3**, until the adequate examination of equations 4.4 - 4.7 against the numerical data, the demonstrated plots can serve as proof-of-concept of assumed kinetic models of heparin degradation in alkaline environments.

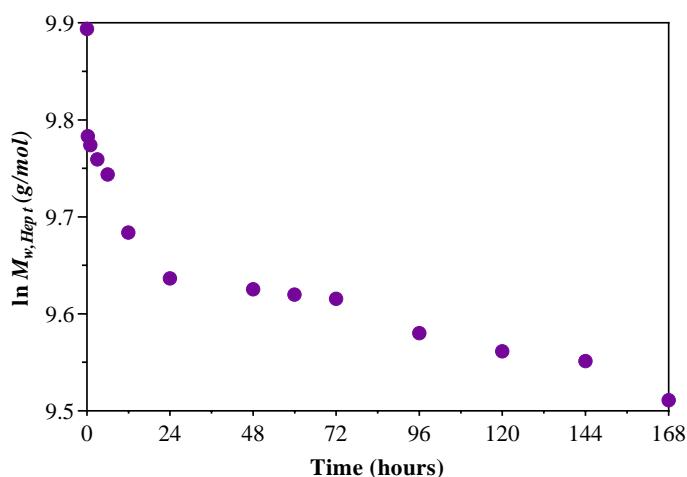


**Figure 4.19** The natural logarithm of molecular weight of heparin, measured after hydrolysis at pH 12/ 80 °C/ 168 h, plotted as a function of time according to first-order kinetics equation.

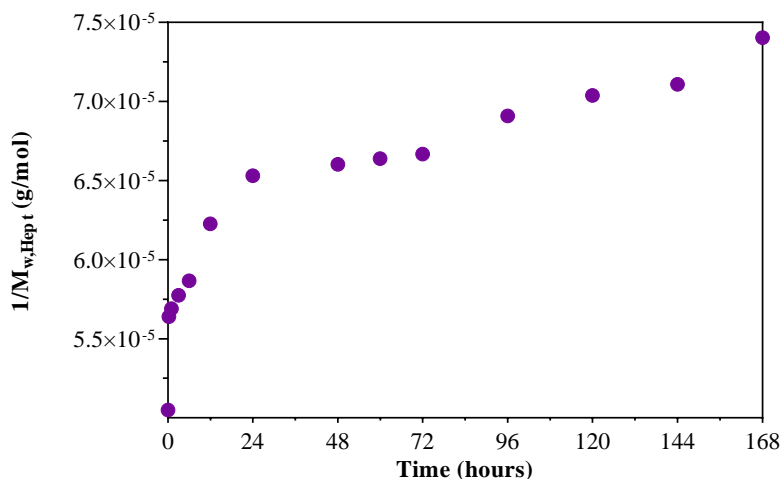


**Figure 4.20** The fraction of molecular weight of heparin, measured after hydrolysis at pH 12/ 80 °C/ 168 h, plotted as a function of time according to second-order kinetic-equation.

#### 4.4.4 Concluding remarks

The kinetics approximation concerning the hydrolytic desulfation (2OS-) and following rearrangements of iduronate to galacturonate stereoisomer, catalysed by alkali treatment of heparin, was designed according to parallel reaction scheme. The presented approximation was based on experimental results; however, it was not tested against the numerical data. Yet, the non-fitting of first-order and second-order kinetic plots for the molecular weight loss of heparin measured at pH 12/ 80 °C over 168 h served as a proof of presented concept. Considering the complexity of estimated equations, matrix or graphical modelling (*via*

analytical software like Mathcad, Maple or MATLAB) against experimental data would be necessary (Korobov & Ochkov, 2011) that could be considered an excellent task for future work.

#### 4.5 CHAPTER CONCLUSIONS

This chapter has focused on the physicochemical changes of heparin in aqueous medium, catalysed by alkaline environments (pH 7 - 12) and temperature (40, 60 and 80 °C) that were followed overtime (up to 168 h) through a variety of analytical techniques.

It has been demonstrated that main processes affecting the heparin molecule at alkaline conditions are 2-O-desulfation and stereochemical rearrangements of iduronate. Among these two, 2-O-desulfation was major result of processing at milder conditions, *i.e.*: pH 10 – 11/ 80 °C and pH 12/ 40 & 60 °C, while the stereochemical rearrangements followed more prominent 2-O-desulfation at the harshest of studied conditions, *i.e.*, pH 12/ 80 °C. As these conditions compromised the heparin stability, the question regarding the pharmacological functionality of the molecule was raised. Taking the opportunity kindly created by LEO Pharma A/S (Ballerup, Denmark), chosen hydrolysates of heparin were subjected to anticoagulant activity test. The test results discussed in **APPENDIX B** have demonstrated reduction in anticoagulant activity of pH 12/ 80 °C/ 48 h alkali hydrolysed heparin to  $\frac{1}{3}$  with respect to heparin standard. Bearing in mind complete anticoagulant activity loss caused by acid-catalysed N-desulfation of heparin (discussed in **section 3.3.3.3**), it may be assumed that changes upon the iduronate unit of heparin have less impact on anticoagulant activity of the molecule. From the practical point of view the presented findings may be of great interest for those seeking heparin derivatives of decreased anticoagulant functionality. As neither depolymerisation of polysaccharide chain, nor hydrolytic scission of glucosamine sulfates (NS-, 6OS-) were observed during the alkaline treatment, there perhaps would be an opportunity to design new heparin pharmaceuticals *via* iduronate-concentrated alkali modifications.

On the other hand, the following conditions: pH 7 – 12/ 40 °C; pH 7 – 11/ 60 °C; pH 7 – 9/ 80 °C did not induce any critical intramolecular changes of heparin. Thus, when applied in

industrial or research applications these environments can be considered as safe with regard to stability or functionality of the molecule.

Furthermore, two uronic acid stereoisomers, *i.e.*,  $\alpha$ -L-iduronate and  $\alpha$ -L-galacturonate were exclusively formed during the prolonged alkaline hydrolysis of heparin in pH 12 phosphate buffer at 80 °C without the production of 2,3-anhydro intermediate (usually observed in pH-similar treatment as discussed in chapter introduction in **4.1**). Considering that until now this exclusive rearrangement was observed only under reflux conditions, the straight- forward hydrolytic reaction could present a potential to simplify the process aiming similar modifications of the heparin molecule. It could, for example, be used to design galacturonate-enriched product, especially that some early studies suggested enhanced antithrombotic activity, lowered the risk of hemorrhage and reduced anti-coagulating activity of such heparins (Piani et al., 1993, 1995).

Finally, based on the results of comprehensive study of heparin degradation in aqueous alkaline solutions a theoretical kinetics approximation was presented. Such a detailed kinetic model could be useful to characterise the thermochemical degradation of heparin in hydrolytic conditions, to produce new pharmacological derivatives or effectively avoid unwanted rearrangements.

# 5

## CONCLUSIONS

---

### 5.1 CONCLUDING REMARKS

This work has focused on the degradative reactions of pharmacologically active heparin in acidic (pH 1 – 6) and alkaline (pH 7 – 12) hydrolytic systems at elevated temperatures (40, 60 and 80 °C). The changes induced by applied conditions were studied over time (up to 168 h), with the aim of sketching a comprehensive picture of the stability of the molecule that could further serve as platform for pharmaceutical scientists and heparin manufacturers. Considering the complexity of heparin polysaccharide, a great deal of work and detailed analytical studies were required to reach the set target.

Acidic environments appeared to be an effective medium for hydrolytic desulfation of heparin, the order of which was established as 6OS $\leq$ 2OS $\ll$ NS. The conclusions regarding desulfation order of heparin were mostly based on NMR spectroscopy. This approach highlighted the great potential of NMR in the analysis of the stability of complex, heterogeneous macromolecules that could be of particular importance in pharmacological research.

The hydrolytic sulfate loss has been linked with molecular weight reduction of heparin to the point of statistical significance. Furthermore, the extent of acid desulfation of heparin, N-desulfation in particular, has been reflected by the loss of anticoagulant activity of the molecule. The hydrolytic desulfation of heparin (although not prominent) was noted as early as at pH 3/ 60 °C. Considering that different stages of industrial purification (*e.g.*, bleaching) requires more aggressive environments, the presented findings should

particularly interest heparin manufacturers as the quality of finished product could be affected by an unoptimized process.

The hydrolytic scission of glycosidic bonds connecting the elemental units of heparin have been a parallel process to 2/6-O-desulfation. Both reactions have been observed at the later stage of processing and at the harshest of studied conditions (*i.e.*, pH 1/ 80 °C/ 24 h  $\leq$ ). The rate of 2/6-O-desulfation and glycosidic scission increased with time. Whereas the selectivity of first one was fairly difficult (but not impossible) to establish, the order of second one was certainly random. Nevertheless, the presented results opened the doors for further studies that should be of particular interest to those seeking heparin-derived products of altered anticoagulant functionality.

Alkaline solutions created a relatively stable environments for heparin as neither depolymerisation of polysaccharide chain nor hydrolytic scission of glucosamine sulfates (NS-, 6OS-) were observed during the applied treatment. The recognised modifications were iduronate-concentrated and susceptible to harsh conditions. In contrast to acid-catalysed N-desulfation, none of discussed alkaline modifications altered the anticoagulant activity of heparin to a significant extent. From a practical perspective, the alkaline conditions could be perceived as 'safer' in industrial and pharmacological processing. Furthermore, during the undertaken studies the exclusive rearrangements of iduronate to galacturonate were observed. The studied conditions create a potential for controlled stereochemical rearrangements of heparin that could be taken as an advantage by those interested in heparin products with activities other than anticoagulant activity.

Connecting all the pieces from this complex analytical puzzle, a more complete understanding of the mechanism and kinetics of heparin degradation in acidic and alkaline aqueous environments was elucidated. Overall, the discussed study demonstrates the influence of applied conditions upon the stability of heparin, but also the strength of carefully selected analytical techniques to create a (more) complete and certain picture of heterogeneous, sulfated macromolecules.

## 5.2 FUTURE WORK

Considering the wide range of heparin applications, conditional upon the structure of the molecule in aqueous conditions, results in almost infinite possibilities for future work.

Following the findings of this study, it could be of commercial interest to extract consecutively desulfated heparin compounds and test their pharmacological functionality. The galacturonate-enriched products also require a more extensive analysis, especially considering that a thorough search of relevant literature revealed that many have focused on conditions catalysing the iduronate modifications, while few have investigated their impact towards heparin functionality. Furthermore, the preliminary kinetic model opens the door for more detailed study of thermochemical degradation of heparin in hydrolytic conditions that could be useful in designing new pharmacological derivatives. At first, however, it would be crucial to test presented model against numerical data. This could be approached by matrix modelling in analytical software like Mathcad, Maple or MATLAB. As the presented molecular weight results were affected by relatively high measurement error (following from application of SEC-MALS-RI method), it would be beneficial to collect new data, *via* more accurate method, like ultracentrifugation or quantitative NMR.

Recalling the literature review in the introduction to this work, both sulfation degree and iduronate dynamics have a powerful impact towards the confirmation and shape of heparin. As both of these features, next to the sulfate distribution, are essential to sustain heparin interactions with proteins, it is nearly certain that desulfation, as well as iduronate rearrangements, would influence the macromolecular interactions. As already presented, the reduction in anticoagulant activity was a consequence of these changes. To investigate deeper the scope of both alterations the analysis focusing on hydrodynamic properties of heparin in acidic and alkaline environments would be desirable.

Finally, the hydrolytic stability research was partially inspired by industrial purification process of heparin, for the most part carried in water, but also by the character of pharmacological drug (water suspension). Considering variety of stressing conditions applied during the industrial treatment, *e.g.*, oxidation, precipitation, bleaching, speed-drying, *etc.*, each component of this system would create a potential study environment.

## APPENDICES

### APPENDIX A SEC-MALS-RI OUTPUT OF PROLONGED ACID HYDROLYSIS OF HEPARIN

The average weight molecular weight of hydrolysed samples of heparin was studied using SEC-MALS-RI. However, due to the chain polymerisation proceeding with time, the measurements of samples subjected to hydrolysis at pH 1/ 80 °C from 120 h onwards was impossible, as the sample peak was partially covered by the buffer peak, as illustrated **Figure A- 1**. The molecular weight for these samples was mathematically estimated.

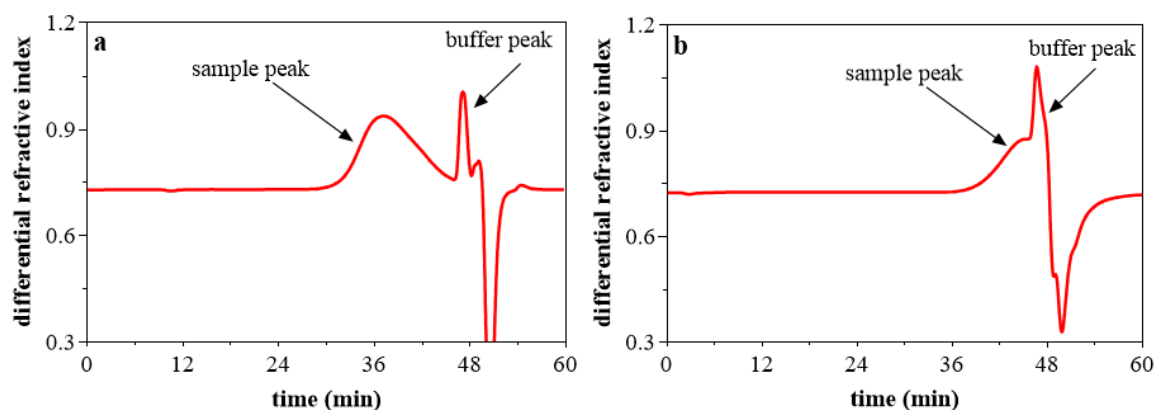


**Figure A- 1** Elution SEC-MALS-RI chromatograms of samples hydrolysed at pH 1/ 80 °C for **a)** 12 h, showing good separation of sample and buffer peaks and **b)** 120 h, where the separation of peak and buffer was impossible. Both profiles show normalised data collected by the refractive index detector.

## APPENDIX B      ACTIVITY TEST OF HYDROLYSED SAMPLES OF HEPARIN

Taking the opportunity kindly created by LEO Pharma A/S (Ballerup, Denmark), chosen hydrolysed samples of heparin discussed in this study were subjected to anticoagulant activity test. Although the industrial requirements prevent disclosing test details, the collected results were shared and are presented in **Figure B- 1**. As noted, the activity results of acid hydrolysed samples performed in LEO Pharma match the results of aPTT and PTT studies discussed in **section 3.3.3.3**, confirming that N-desulfation of heparin significantly affect the anticoagulant functionality of the compound. The analysis of bio-synthesised N-desulfated standard of heparin (**Figure B- 1**), was also deprived of anticoagulant activity upon the sulfate loss, which doubly confirms the presented findings. On the other hand, the activity of pH 12/ 80 °C/ 48 h alkali hydrolysed sample, which was characterised ‘by’ ongoing 2-O-desulfation and initial IdoA rearrangements to GalA in NMR studies (**section 4.3.4.3**), decreased to  $\frac{1}{3}$  of this of heparin standard (**Figure B- 1**), but did not completely disappear. This suggests that changes upon the iduronate unit of heparin have less impact on anticoagulant activity of the molecule, but also create an opportunity for those interested in heparin derivatives of decreased anticoagulant functionality.



## REQUISITION FOR ANALYSIS

<b>Item Description</b>	Liquid samples of heparin
<b>Item no.</b>	1 heparin sodium pH 1/48h/ 80°C
	2 heparin sodium pH 3/48h/ 60°C
	3 heparin sodium pH 6/48h/ 40°C
	4 heparin sodium pH 10/48h/ 40°C
	5 heparin sodium pH 11/48h/ 60°C
	6 heparin sodium pH 12/48h/ 80°C
	7 heparin sodium de N-sulfated
	8 heparin sodium de N/O-sulfated
	9 heparin sodium standard
<b>Lot no.</b>	

<b>Testing Method</b> eg. Validation protocol / specification	Biological activity PENTRA	
<b>Analysis</b>	IU/mL	
<b>Limits</b>		Storage RT
<b>Remarks</b>	9 different samples prepared by Aleksandra Kozlowski at the University of Huddersfield. NMR has been run to confirm heparin. Estimation heparin is 130-250 IU/mL	

<b>Sampled by</b>	Signed init. OUHDK	Date 2020-05-12
-------------------	-----------------------	--------------------

<b>Reply eMail for</b>	LEO ID (in Capitals)/Department OUHDK@leo-pharma.com Global MSAT	Phone no. 31526948
------------------------	--	-----------------------

QC Laboratories		Method: TM_001049 version 21.0				
Tests	Determination		Limits	Result	Analysed by	Controlled by
	1.	2.				
1.	< 1 IU/ml	< 1 IU/ml	Kombination	< 1 IU/ml	MKR	LEG
2.	262 IU/ml	270 IU/ml	Kombination	266 IU/ml	MKR	LEG
3.	510 IU/ml	503 IU/ml	Kombination	509 IU/ml	MKR	LEG
4.	722 IU/ml	734 IU/ml	Kombination	723 IU/ml	MKR	LEG
5.	682 IU/ml	680 IU/ml	Kombination	682 IU/ml	MKR	LEG
6.	322 IU/ml	322 IU/ml	Kombination	322 IU/ml	MKR	LEG
7.	1,07 IU/ml	1,06 IU/ml	Kombination	1,1 IU/ml	MKR	LEG
8.	< 1 IU/ml	< 1 IU/ml	Kombination	< 1 IU/ml	MKR	LEG
9.	906 IU/ml	920 IU/ml	Kombination	911 IU/ml	MKR	LEG

Ref. to raw data: WS\_000292-5-0051 Audience: Hep. Pptver Johannes P. Roubroeks 2020-10-21  
WS\_000292-5-0052 Audience: Hep. Pptver Johannes P. Roubroeks 2020-10-23

Data transfer by (date/sign): 2020-10-30/MKR	Verified by (date/sign): 03 NOV. 2020 <i>LEG</i>	Filing code: MS
Conclusion (date/sign): 03 NOV. 2020 <i>Amhr</i>		

**Figure B- 1** Results of activity test of chosen heparin hydrolysates, kindly performed by analytical scientist of LEO Pharma A/S (Ballerup, Denmark).

## REFERENCES

- A Practical Guide to Ion Chromatography. (2007). In *A practical guide to ion chromatography* (2nd ed.). SeQuant AB. <https://doi.org/10.1002/9783527613243>
- Alyassin, M., Campbell, G. M., Masey O'Neill, H., & Bedford, M. R. (2020). Simultaneous determination of cereal monosaccharides, xylo- and arabinoxylo-oligosaccharides and uronic acids using HPAEC-PAD. *Food Chemistry*, 315, 126221. <https://doi.org/10.1016/j.foodchem.2020.126221>
- Anderson, K., Li, S. C., & Li, Y. T. (2000). Diphenylamine-aniline-phosphoric acid reagent, a versatile spray reagent for revealing glycoconjugates on thin-layer chromatography plates. *Analytical Biochemistry*, 287(2), 337–339. <https://doi.org/10.1006/abio.2000.4829>
- Bahadir, O. (2013). Ion-Exchange Chromatography and Its Applications. In *Column Chromatography* (pp. 31–58). InTech. <https://doi.org/10.5772/55744>
- Banks, W., & Greenwood, C. T. (1963). Physical Properties of Solutions of Polysaccharides. *Advances in Carbohydrate Chemistry*, 18(C), 357–398. [https://doi.org/10.1016/S0096-5332\(08\)60247-7](https://doi.org/10.1016/S0096-5332(08)60247-7)
- Bauer, K. H., Frömming, K.-H., & Führe, C. (2012). Szybkości zmian właściwości układu. In *Technologia postaci leku z elementami biofarmacji* (8th ed., p. 542). MedPharm Poland.
- Baumann, H., Scheen, H., Huppertz, B., & Keller, R. (1998). Novel regio- and stereoselective O-6-desulfation of the glucosamine moiety of heparin with N-methylpyrrolidinone-water or N,N-dimethylformamide-water mixtures. *Carbohydrate Research*, 308(3–4), 381–388. [https://doi.org/10.1016/S0008-6215\(98\)00097-4](https://doi.org/10.1016/S0008-6215(98)00097-4)
- Bedini, E., Laezza, A., Parrilli, M., & Iadonisi, A. (2017). A review of chemical methods for the selective sulfation and desulfation of polysaccharides. *Carbohydrate Polymers*, 174(5), 1224–1239. <https://doi.org/10.1016/j.carbpol.2017.07.017>
- Bertini, S., Risi, G., Guerrini, M., Carrick, K., Szajek, A., & Mulloy, B. (2017). Molecular Weights of Bovine and Porcine Heparin Samples: Comparison of Chromatographic Methods and Results of a Collaborative Survey. *Molecules*, 22(7), 1214. <https://doi.org/10.3390/molecules22071214>

- Bhaskar, U., Sterner, E., Hickey, A. M., Onishi, A., Zhang, F., Dordick, J. S., & Linhardt, R. J. (2012). Engineering of routes to heparin and related polysaccharides. *Applied Microbiology and Biotechnology*, *93*(1), 1–16. <https://doi.org/10.1007/s00253-011-3641-4>
- Bienkowski, M. J., & Conrad, H. E. (1985). Structural characterization of the oligosaccharides formed by depolymerization of heparin with nitrous acid. *Journal of Biological Chemistry*, *260*(1), 356–365.
- Bradley, T. D., & Mitchell, J. R. (1988). The determination of the kinetics of polysaccharide thermal degradation using high temperature viscosity measurements. *Carbohydrate Polymers*, *9*(4), 257–267. [https://doi.org/10.1016/0144-8617\(88\)90044-6](https://doi.org/10.1016/0144-8617(88)90044-6)
- Brady, J., Drig, T., Lee, P. I., & Li, J. X. (2016). Polymer properties and characterization. In *Developing Solid Oral Dosage Forms: Pharmaceutical Theory and Practice: Second Edition*. <https://doi.org/10.1016/B978-0-12-802447-8.00007-8>
- Casu, B. (1985). Structure and Biological Activity of Heparin. In *Advances in Carbohydrate Chemistry and Biochemistry* (Vol. 43, Issue C, pp. 51–134). [https://doi.org/10.1016/S0065-2318\(08\)60067-0](https://doi.org/10.1016/S0065-2318(08)60067-0)
- Casu, B. (1989). Structure of Heparin and Heparin Fragments. *Annals of the New York Academy of Sciences*, *556*(1 Heparin and R), 1–17. <https://doi.org/10.1111/j.1749-6632.1989.tb22485.x>
- Casu, B., & Lindahl, U. (2001). Structure and biological interactions of heparin and heparan sulfate. *Advances in Carbohydrate Chemistry and Biochemistry*, *57*, 159–206. [https://doi.org/10.1016/S0065-2318\(01\)57017-1](https://doi.org/10.1016/S0065-2318(01)57017-1)
- Casu, B., Naggi, A., & Torri, G. (2015). Re-visiting the structure of heparin. *Carbohydrate Research*, *403*, 60–68. <https://doi.org/10.1016/j.carres.2014.06.023>
- Center for Macromolecular Interactions- University of Harvard. (n.d.). *SEC-MALS Getting Started Guidelines*. University Harvard. Retrieved April 5, 2020, from <https://cmi.hms.harvard.edu/light-scattering>
- Center for Macromolecular Interactions. (n.d.). *SEC-MALS Getting Started Guidelines Getting* (Vol. 5, pp. 1–6).
- Cesaretti, M., Luppi, E., Maccari, F., & Volpi, N. (2004). Isolation and characterization of a heparin with high anticoagulant activity from the clam *Tapes philippinarum*: Evidence for the presence of a high content of antithrombin III binding site. *Glycobiology*, *14*(12), 1275–1284. <https://doi.org/10.1093/glycob/cwh128>
- Conrad, H. E. (1980). The acid lability of the glycosidic bonds of L-iduronic acid residues in glycosaminoglycans. *The Biochemical Journal*, *191*(2), 355–363. <https://doi.org/10.1042/bj1910355>
- Cui, S. W. (2005). FOOD CARBOHYDRATES: Chemistry, Physical Properties, and Applications. In *Food Carbohydrates* (1st ed.). Taylor & Francis Group, LLC.

- Danishefsky, I., Eiber, H. B., & Carr, J. J. (1960). Investigations on the chemistry of heparin. I. Desulfation and acetylation. *Archives of Biochemistry and Biophysics*, 90(1), 114–121. [https://doi.org/10.1016/0003-9861\(60\)90621-4](https://doi.org/10.1016/0003-9861(60)90621-4)
- Deakin, J. A., & Lyon, M. (2008). A simplified and sensitive fluorescent method for disaccharide analysis of both heparan sulfate and chondroitin/dermatan sulfates from biological samples. *Glycobiology*, 18(6), 483–491. <https://doi.org/10.1093/glycob/cwn028>
- Desai, U. R., Wang, H. ming, Kelly, T. R., & Linhardt, R. J. (1993). Structure elucidation of a novel acidic tetrasaccharide and hexasaccharide derived from a chemically modified heparin. *Carbohydrate Research*, 241(C), 249–259. [https://doi.org/10.1016/0008-6215\(93\)80112-R](https://doi.org/10.1016/0008-6215(93)80112-R)
- Devlin, A., Mycroft-West, C., Procter, P., Cooper, L., Guimond, S., Lima, M., Yates, E., & Skidmore, M. (2019). Tools for the quality control of pharmaceutical heparin. *Medicina (Lithuania)*, 55(10), 1–19. <https://doi.org/10.3390/medicina55100636>
- Dietrich, C. P., Paiva, J. F., Castro, R. A. B., Chavante, S. F., Jeske, W., Fareed, J., Gorin, P. A. J., Mendes, A., & Nader, H. B. (1999). Structural features and anticoagulant activities of a novel natural low molecular weight heparin from the shrimp *Penaeus brasiliensis*. *Biochimica et Biophysica Acta - General Subjects*, 1428(2–3), 273–283. [https://doi.org/10.1016/S0304-4165\(99\)00087-2](https://doi.org/10.1016/S0304-4165(99)00087-2)
- Dionex Corporation. (2008). *Determination of Galactosamine Containing Organic Impurities in Heparin by HPAE-PAD Using the CarboPac PA20 Column* (Application Note 233; LPN 2286).
- Drummond, K. J., Yates, E. A., & Turnbull, J. E. (2001). Electrophoretic sequencing of heparin/heparan sulfate oligosaccharides using a highly sensitive fluorescent end label. *Proteomics*, 1(2), 304–310. [https://doi.org/10.1002/1615-9861\(200102\)1:2<304::AID-PROT304>3.0.CO;2-B](https://doi.org/10.1002/1615-9861(200102)1:2<304::AID-PROT304>3.0.CO;2-B)
- Ehrlich, J., & Stivala, S. S. (1973). Chemistry and Pharmacology of Heparin. *Journal of Pharmaceutical Sciences*, 62(4), 517–544. <https://doi.org/10.1002/jps.2600620402>
- Einbu, A., & Vårum, K. M. (2008). Characterization of chitin and its hydrolysis to GlcNAc and GlcN. *Biomacromolecules*, 9(7), 1870–1875. <https://doi.org/10.1021/bm8001123>
- Fareed, J., Hoppensteadt, D., Schultz, C., Ma, Q., Kujawski, M., & Messmore, H. (2005). Biochemical and Pharmacologic Heterogeneity in Low Molecular Weight Heparins. Impact on the Therapeutic Profile. *Current Pharmaceutical Design*, 10(9), 983–999. <https://doi.org/10.2174/1381612043452811>
- Finch, P. (1999). *Carbohydrates Structures, Syntheses and Dynamics* (1st ed.). Springer Science+Business Media Dordrecht.
- Flengsrud, R., Larsen, M. L., & Odegaard, O. R. (2010). Purification, characterization and in vivo studies of salmon heparin. *Thrombosis Research*, 126(6), e409–e417. <https://doi.org/10.1016/j.thromres.2010.07.004>

- Fraidenraich y Waisman, D., & Cirelli, A. F. (1992). Selective O-desulphation of heparin in triethylamine. *Carbohydrate Polymers*, 17(2), 111–114. [https://doi.org/10.1016/0144-8617\(92\)90103-W](https://doi.org/10.1016/0144-8617(92)90103-W)
- Fu, L., Li, G., Yang, B., Onishi, A., Li, L., Sun, P., Zhang, F., & Linhardt, R. J. (2013). Structural Characterization of Pharmaceutical Heparins Prepared from Different Animal Tissues. *Journal of Pharmaceutical Sciences*, 102(5), 1447–1457. <https://doi.org/10.1002/jps.23501>
- Fu, L., Suflita, M., & Linhardt, R. J. (2016). Bioengineered heparins and heparan sulfates. *Advanced Drug Delivery Reviews*, 97(2), 237–249. <https://doi.org/10.1016/j.addr.2015.11.002>
- Galanos, C., Luderitz, O., & Himmelspach, K. (1969). The Partial Acid Hydrolysis of Polysaccharides: A New Method for Obtaining Oligosaccharides in High Yield. *European Journal of Biochemistry*, 8(3), 332–336. <https://doi.org/10.1111/j.1432-1033.1969.tb00532.x>
- Gray, E., Mulloy, B., & Barrowcliffe, T. W. (2008). Heparin and low-molecular-weight heparin. *Thrombosis and Haemostasis*, 99(5), 807–818. <https://doi.org/10.1160/TH08-01-0032>
- Groisman, J. F., & de Lederkremer, R. M. (1987). d-Galactofuranose in the N-linked sugar chain of a glycopeptide from *Ascobolus furfuraceus*. *European Journal of Biochemistry*, 165(2), 327–332. <https://doi.org/10.1111/j.1432-1033.1987.tb11445.x>
- Guerrini, M., Zhang, Z., Shriver, Z., Naggi, A., Masuko, S., Langer, R., Casu, B., Linhardt, R. J., Torri, G., & Sasisekharan, R. (2009). Orthogonal analytical approaches to detect potential contaminants in heparin. *Proceedings of the National Academy of Sciences*, 106(40), 16956–16961. <https://doi.org/10.1073/pnas.0906861106>
- Guerrini, Marco, Bisio, A., & Torri, G. (2001). Combined Quantitative <sup>1</sup>H and <sup>13</sup>C Nuclear Magnetic Resonance Spectroscopy for Characterization of Heparin Preparations. *Seminars in Thrombosis and Hemostasis*, 27(5), 473–482. <https://doi.org/10.1055/s-2001-17958>
- Guerrini, Marco, Naggi, A., Guglieri, S., Santarsiero, R., & Torri, G. (2005). Complex glycosaminoglycans: Profiling substitution patterns by two-dimensional nuclear magnetic resonance spectroscopy. *Analytical Biochemistry*, 337(1), 35–47. <https://doi.org/10.1016/j.ab.2004.10.012>
- Harding, S. E. (2005). Analysis of polysaccharides by ultracentrifugation. Size, conformation and interactions in solution. *Advances in Polymer Science*, 186(September), 211–254. <https://doi.org/10.1007/b136821>
- Harding, S. E., Tombs, M. P., Adams, G. G., Paulsen, B. S., Inngjerdingen, K. T., & Barsett, H. (2017). An Introduction to Polysaccharide Biotechnology. In *Biochimie* (Vol. 80, Issue 4). CRC Press. <https://doi.org/10.1201/9781315372730>

- Harding, S. E., Varum, K. M., Stokke, B. T., & Smidsrød, O. (1991). Molecular Weight Determination of Polysaccharides. In C. A. White (Ed.), *Advances in Carbohydrate Analysis* (Vol. 1, pp. 63–144). Elsevier Science & Technology.
- Hardy, M. R., & Reid Townsend, R. (1994). High-pH anion-exchange chromatography of glycoprotein-derived carbohydrates. In *Methods* (Vol. 230, Issue 1989, pp. 208–225). [https://doi.org/10.1016/0076-6879\(94\)30014-3](https://doi.org/10.1016/0076-6879(94)30014-3)
- Hofmann, A. (2010). Spectroscopic techniques: I Spectrophotometric techniques. In K. Wilson & J. Walker (Eds.), *Principles and Techniques of Biochemistry and Molecular Biology* (7th ed., pp. 477–522). Cambridge University Press.
- Holme, K. R., Liang, W., Yang, Z., Lapierre, F., Shaklee, P. N., & Lam, L. (1996). A Detailed Evaluation of the Structural and Biological Effects of Alkaline O-Desulfation Reactions of Heparin. In J. Harenberg & B. Casu (Eds.), *Nonanticoagulant Actions of Glycosaminoglycans* (1st ed., pp. 139–162). Plenum Press. <https://doi.org/10.1007/978-1-4613-0371-8>
- Hook, M. (1974). Distribution of Sulphate and Iduronic Acid Residues in Heparin and Heparan Sulphate. *Biochem. J*, *137*, 33–43. <https://doi.org/10.1042/bj1370033>
- Hricovíni, M. (2015). Solution Structure of Heparin Pentasaccharide: NMR and DFT Analysis. *Journal of Physical Chemistry B*, *119*(38), 12397–12409. <https://doi.org/10.1021/acs.jpcc.5b07046>
- Hsieh, P. H., Thieker, D. F., Guerrini, M., Woods, R. J., & Liu, J. (2016). Uncovering the Relationship between Sulphation Patterns and Conformation of Iduronic Acid in Heparan Sulphate. *Scientific Reports*, *6*(June), 1–8. <https://doi.org/10.1038/srep29602>
- Human Metabolome Database*. (n.d.-a). Retrieved February 10, 2021, from <https://hmdb.ca/metabolites/HMDB0001659#spectra>
- Human Metabolome Database*. (n.d.-b). Retrieved October 23, 2020, from [https://hmdb.ca/spectra/nmr\\_one\\_d/1080](https://hmdb.ca/spectra/nmr_one_d/1080)
- Inoue, Y., & Nagasawa, K. (1976). Selective N-desulfation of heparin with dimethyl sulfoxide containing water or methanol. *Carbohydrate Research*, *46*(1), 87–95. [https://doi.org/10.1016/S0008-6215\(00\)83533-8](https://doi.org/10.1016/S0008-6215(00)83533-8)
- Jaffer, I. H., & Weitz, J. I. (2014). Antithrombotic Therapy. In J. L. Cronenwett & K. Wayne Johnston (Eds.), *Rutherford's vascular surgery*. (8th ed., pp. 549–566). Saunders Elsevier.
- Jandik, K. A., Kruep, D., Cartier, M., & Linhardt, R. J. (1996). Accelerated Stability Studies of Heparin. *Journal of Pharmaceutical Sciences*, *85*(1), 45–51. <https://doi.org/10.1021/js9502736>

- Jaseja, M., Rej, R. N., Sauriol, F., & Perlin, A. S. (1989). Novel regio- and stereoselective modifications of heparin in alkaline solution. Nuclear magnetic resonance spectroscopic evidence. *Canadian Journal of Chemistry*, 67(9), 1449–1456. <https://doi.org/10.1139/v89-221>
- Jorpes, E., & Bergström, S. (1939). On the relationship between the sulphur content and the anticoagulant activity of heparin preparations. *The Biochemical Journal*, 33(1), 47–52. <http://www.pubmedcentral.nih.gov/articlerender.fcgi?artid=1264337&tool=pmcentrez&rendertype=abstract>
- Kariya, Y., Kyogashima, M., Suzuki, K., Isomura, T., Sakamoto, T., Horie, K., Ishihara, M., Takano, R., Kamei, K., & Hara, S. (2000). Preparation of completely 6-O-desulfated heparin and its ability to enhance activity of basic fibroblast growth factor. *Journal of Biological Chemistry*, 275(34), 25949–25958. <https://doi.org/10.1074/jbc.M004140200>
- Karlsson, A., & Singh, S. K. (1999). Acid hydrolysis of sulphated polysaccharides. Desulphation and the effect on molecular mass. *Carbohydrate Polymers*, 38(1), 7–15. [https://doi.org/10.1016/S0144-8617\(98\)00085-X](https://doi.org/10.1016/S0144-8617(98)00085-X)
- Keire, D. A., Buhse, L. F., & Al-Hakim, A. (2013). Characterization of currently marketed heparin products: composition analysis by 2D-NMR. *Analytical Methods*, 5(12), 2984. <https://doi.org/10.1039/c3ay40226f>
- Khan, S., Fung, K. W., Rodriguez, E., Patel, R., Gor, J., Mulloy, B., & Perkins, S. J. (2013). The solution structure of heparan sulfate differs from that of heparin: Implications for function. *Journal of Biological Chemistry*, 288(39), 27737–27751. <https://doi.org/10.1074/jbc.M113.492223>
- Kocourek, J., Tichá, M., & Košťír, J. (1966). The use of diphenylamine-aniline-phosphoric acid reagent in the detection and differentiation of monosaccharides and their derivatives on paper chromatograms. *Journal of Chromatography A*, 24(C), 117–124. [https://doi.org/10.1016/s0021-9673\(01\)98109-9](https://doi.org/10.1016/s0021-9673(01)98109-9)
- Korobov, V. I., & Ochkov, V. F. (2011a). Multi-Step Reactions: The Methods for Analytical Solving the Direct Problem. In *Chemical Kinetics with Mathcad and Maple* (pp. 35–72). Springer Vienna. [https://doi.org/10.1007/978-3-7091-0531-3\\_2](https://doi.org/10.1007/978-3-7091-0531-3_2)
- Korobov, V. I., & Ochkov, V. F. (2011b). Numerical Solution of the Direct Problem in Chemical Kinetics. In *Chemical Kinetics with Mathcad and Maple* (pp. 73–114). Springer Vienna. [https://doi.org/10.1007/978-3-7091-0531-3\\_3](https://doi.org/10.1007/978-3-7091-0531-3_3)
- Kuizenga, M. H., Nelson, J. W., & Cartland, G. F. (1943). THE BIOASSAY OF HEPARIN PREPARATIONS. *American Journal of Physiology-Legacy Content*, 139(4), 612–616. <https://doi.org/10.1152/ajplegacy.1943.139.4.612>
- LEO Pharma A/S. (2016). *Heparin (Mucous) Injection BP*.

- LEO Pharma Inc, & LEO Pharma A/S. (2016). *Innohep- Summary of Product Characteristics*.  
<http://www.medicines.ie/medicine/14668/SPC/Innohep+20,000+IU+ml+Solution+for+Injection/#linkToThisPage>
- Lima, De Farias, E. H. C., Rudd, T. R., Ebner, L. F., Gesteira, T. F., Mendes, A., Bouas, R. I., Martins, J. R. M., Hoppensteadt, D., Fareed, J., Yates, E. A., Sasaki, G. L., Tersariol, I. L. S., & Nader, H. B. (2011). Low molecular weight heparins: Structural differentiation by spectroscopic and multivariate approaches. *Carbohydrate Polymers*, 85(4), 903–909. <https://doi.org/10.1016/j.carbpol.2011.04.021>
- Lima, M., Rudd, T., & Yates, E. (2017). New applications of heparin and other glycosaminoglycans. *Molecules*, 22(5), 1–11. <https://doi.org/10.3390/molecules22050749>
- Limtiaco, J. F. K., Beni, S., Jones, C. J., Langeslay, D. J., & Larive, C. K. (2011). NMR methods to monitor the enzymatic depolymerization of heparin. *Analytical and Bioanalytical Chemistry*, 399(2), 593–603. <https://doi.org/10.1007/s00216-010-4132-7>
- Linhardt. (2003). 2003 Claude S. Hudson award address in carbohydrate chemistry. Heparin: Structure and activity. *Journal of Medicinal Chemistry*, 46(13), 2551–2564. <https://doi.org/10.1021/jm030176m>
- Linhardt, R. (1992). Chemical and Enzymatic Methods for the Depolymerization and Modification of Heparin. In T. Suami, H. Ogura, & A. Hasegava (Eds.), *Carbohydrates- Synthetic Methods and Applications in Medicinal Chemistry* (1st ed., pp. 385–401). VCH Publishers.
- Linhardt, R. J., Loganathan, D., Al-Hakim, A., Wang, H. M., Walenga, J. M., Hoppensteadt, D., & Fareed, J. (1990). Oligosaccharide Mapping of Low Molecular Weight Heparins: Structure and Activity Differences. *Journal of Medicinal Chemistry*, 33(6), 1639–1645. <https://doi.org/10.1021/jm00168a017>
- Linhardt, R. J., & Sibel Gunay, N. U. R. (1999). Production and chemical processing of low molecular weight heparins. In *Seminars in Thrombosis and Hemostasis* (Vol. 25, Issue SUPPL. 3, pp. 5–16).
- Liu, H., Zhang, Z., & Linhardt, R. J. (2009). Lessons learned from the contamination of heparin. *Natural Product Reports*, 26(3), 313. <https://doi.org/10.1039/b819896a>
- Liu, L., Linhardt, R. J., & Zhang, Z. (2014). Quantitative analysis of anions in glycosaminoglycans and application in heparin stability studies. *Carbohydrate Polymers*, 106(1), 343–350. <https://doi.org/10.1016/j.carbpol.2014.02.076>
- Loftsson, T. (2013). Drug Stability for Pharmaceutical Scientists. In *Drug Stability for Pharmaceutical Scientists* (1st ed.). Academic Press. <https://doi.org/10.1016/C2012-0-07703-4>

- Lundin, L., Larsson, H., Kreuger, J., Kanda, S., Lindahl, U., Salmivirta, M., & Claesson-Welsh, L. (2000). Selectively desulfated heparin inhibits fibroblast growth factor-induced mitogenicity and angiogenesis. *Journal of Biological Chemistry*, 275(32), 24653–24660. <https://doi.org/10.1074/jbc.M908930199>
- Makkar, H. P. S., Siddhuraju, P., & Becker, K. (2010). *Plant Secondary Metabolites* (1st ed.). Humana Press Inc.
- Mascellani, G., Guerrini, M., Torri, G., Liverani, L., Spelta, F., & Bianchini, P. (2007). Characterization of di- and monosulfated, unsaturated heparin disaccharides with terminal N-sulfated 1,6-anhydro- $\beta$ -d-glucosamine or N-sulfated 1,6-anhydro- $\beta$ -d-mannosamine residues. *Carbohydrate Research*, 342(6), 835–842. <https://doi.org/10.1016/j.carres.2006.12.010>
- Mauri, L., Boccardi, G., Torri, G., Karfunkle, M., Macchi, E., Muzi, L., Keire, D., & Guerrini, M. (2017). Qualification of HSQC methods for quantitative composition of heparin and low molecular weight heparins. *Journal of Pharmaceutical and Biomedical Analysis*, 136, 92–105. <https://doi.org/10.1016/j.jpba.2016.12.031>
- Mauri, L., Marinozzi, M., Mazzini, G., Kolinski, R. E., Karfunkle, M., Keire, D. A., & Guerrini, M. (2017). Combining NMR Spectroscopy and Chemometrics to Monitor Structural Features of Crude Hep-ar-in. *Molecules (Basel, Switzerland)*, 22(7). <https://doi.org/10.3390/molecules22071146>
- McLean, J. (1959). The Discovery of Heparin. *Circulation Research*, 19, 75–79.
- Mehn, D., Caputo, F., & Roesslein, M. (2016). *FFF-MALS method development and measurements of size and molecular weight Measurement of particle size distribution of protein binding, of mean molecular weight of polymeric NP components, study of batch to batch reproducibility, and study of release of f* (EUNCL-PCC-22). <http://www.euncl.eu/about-us/assay-cascade/PDFs/PCC/EUNCL-PCC-022.pdf?m=1468937868&>
- Melander, C., & Tømmeraas, K. (2010). Heterogeneous hydrolysis of hyaluronic acid in ethanolic HCl slurry. *Carbohydrate Polymers*, 82(3), 874–879. <https://doi.org/10.1016/j.carbpol.2010.06.010>
- Meneghetti, M. C. Z., Hughes, A. J., Rudd, T. R., Nader, H. B., Powell, A. K., Yates, E. A., & Lima, M. A. (2015). Heparan sulfate and heparin interactions with proteins. *Journal of the Royal Society Interface*, 12(110). <https://doi.org/10.1098/rsif.2015.0589>
- Michael B. Smith. (2020). *March's Advanced Organic Chemistry: Reactions, Mechanisms, and Structure* (8th ed.). John Wiley & Sons, Inc.
- Mohan, C. (2003). A guide for the preparation and use of buffers in biological systems. In *Calbiochem* (p. 32). EMD.

- Monakhova, Y. B., & Diehl, B. W. K. (2018). Nuclear magnetic resonance spectroscopy as a tool for the quantitative analysis of water and ions in pharmaceuticals: Example of heparin. *Journal of Pharmaceutical and Biomedical Analysis*, *154*, 332–338. <https://doi.org/10.1016/j.jpba.2018.03.028>
- Monakhova, Y. B., Diehl, B. W. K., & Fareed, J. (2018). Authentication of animal origin of heparin and low molecular weight heparin including ovine, porcine and bovine species using 1D NMR spectroscopy and chemometric tools. *Journal of Pharmaceutical and Biomedical Analysis*, *149*, 114–119. <https://doi.org/10.1016/j.jpba.2017.10.020>
- Monakhova, Y. B., Fareed, J., Yao, Y., & Diehl, B. W. K. (2018). Improving reliability of chemometric models for authentication of species origin of heparin by switching from 1D to 2D NMR experiments. *Journal of Pharmaceutical and Biomedical Analysis*, *153*, 168–174. <https://doi.org/10.1016/j.jpba.2018.02.041>
- Morris, G. A., Adams, G. G., & Harding, S. E. (2014). On hydrodynamic methods for the analysis of the sizes and shapes of polysaccharides in dilute solution: A short review. *Food Hydrocolloids*, *42*(P3), 318–334. <https://doi.org/10.1016/j.foodhyd.2014.04.014>
- Morris, G. A., Castile, J., Smith, A., Adams, G. G., & Harding, S. E. (2009). The kinetics of chitosan depolymerisation at different temperatures. *Polymer Degradation and Stability*, *94*(9), 1344–1348. <https://doi.org/10.1016/j.polymdegradstab.2009.06.001>
- Morrison, I. M. (1988). Hydrolysis of plant cell walls with trifluoroacetic acid. *Phytochemistry*, *27*(4), 1097–1100. [https://doi.org/10.1016/0031-9422\(88\)80281-4](https://doi.org/10.1016/0031-9422(88)80281-4)
- Mourier, P., Anger, P., Martinez, C., Herman, F., & Viskov, C. (2015). Quantitative compositional analysis of heparin using exhaustive heparinase digestion and strong anion exchange chromatography. *Analytical Chemistry Research*, *3*, 46–53. <https://doi.org/10.1016/j.ancr.2014.12.001>
- Mulloy, B. (2012). Heparin - A Century of Progress. In R. Lever, B. Mulloy, & C. P. Page (Eds.), *The American Journal of The Medical Sciences* (Vol. 207, Issue 5). Springer Berlin Heidelberg. <https://doi.org/10.1007/978-3-642-23056-1>
- Mulloy, B., & Forster, M. J. (2000). Conformation and dynamics of heparin and heparan sulfate. *Glycobiology*, *10*(11), 1147–1156. <https://doi.org/10.1093/glycob/10.11.1147>
- Mulloy, B., Forster, M. J., Jones, C., & Davies, D. B. (1993). N.m.r. and molecular-modelling studies of the solution conformation of heparin. *Biochemical Journal*, *293*(3), 849–858. <https://doi.org/10.1042/bj2930849>
- Mulloy, B., Heath, A., Shriver, Z., Jameison, F., Al Hakim, A., Morris, T. S., & Szajek, A. Y. (2014). USP compendial methods for analysis of heparin: chromatographic determination of molecular weight distributions for heparin sodium. *Analytical and Bioanalytical Chemistry*, *406*(20), 4815–4823. <https://doi.org/10.1007/s00216-014-7940-3>

- Mulloy, B., Hogwood, J., Gray, E., Lever, R., & Page, C. P. (2015). Pharmacology of Heparin and Related Drugs. *Pharmacological Reviews*, 68(1), 76–141. <https://doi.org/10.1124/pr.115.011247>
- Mulloy, B., Khan, S., & Perkins, S. J. (2012). Molecular architecture of heparin and heparan sulfate: Recent developments in solution structural studies. *Pure and Applied Chemistry*, 84(1), 65–76. <https://doi.org/10.1351/Pac-Con-11-10-27>
- Mulloy, B., Lever, R., & Page, C. P. (2017). Mast cell glycosaminoglycans. *Glycoconjugate Journal*, 34(3), 351–361. <https://doi.org/10.1007/s10719-016-9749-0>
- Murray, R. K., Granner, D. K., Mayes, P. A., & Rodwell, V. W. (1994). Biochemia Harpera. In *Biochemical Education* (Vol. 24, Issue 4). [https://doi.org/10.1016/S0307-4412\(97\)80776-5](https://doi.org/10.1016/S0307-4412(97)80776-5)
- Mycroft-West, Su, D., Elli, S., Guimond, S. E., Miller, G. J., Turnbull, J. E., Yates, E. A., Guerrini, M., Fernig, D. G., Lima, M. A. de, & Skidmore, M. A. (2020). The 2019 coronavirus (SARS-CoV-2) surface protein (Spike) S1 Receptor Binding Domain undergoes conformational change upon heparin binding. *BioRxiv*, April, 2020.02.29.971093. <https://doi.org/10.1101/2020.02.29.971093>
- Mycroft-West, Su, D., Pagani, I., Rudd, T., Elli, S., Guimond, S., Miller, G., Meneghetti, M., Nader, H., Li, Y., Nunes, Q., Procter, P., Mancini, N., Clementi, M., Bisio, A., Forsyth, N., Turnbull, J., Guerrini, M., Fernig, D., ... Skidmore, M. A. (2020). Heparin inhibits cellular invasion by SARS-CoV-2: structural dependence of the interaction of the surface protein (spike) S1 receptor binding domain with heparin. *BioRxiv*, May, 2020.04.28.066761. <https://doi.org/10.1101/2020.04.28.066761>
- Nagasawa, K., Inoue, Y., & Kamata, T. (1977). Solvolytic desulfation of glycosaminoglycuronan sulfates with dimethyl sulfoxide containing water or methanol. *Carbohydrate Research*, 58(1), 47–55. [https://doi.org/10.1016/S0008-6215\(00\)83402-3](https://doi.org/10.1016/S0008-6215(00)83402-3)
- Nidhi, K., Indrajeet, S., Khushboo, M., Gauri, K., & Sen, D. J. (2011). Structural Characterization of Pharmaceutical Heparins Prepared from Different Animal Tissues. *International Journal of Drug Development and Research*, 3(2), 26–33. <https://doi.org/10.1002/jps>
- Oduah, E. I., Linhardt, R. J., & Sharfstein, S. T. (2016). Heparin: Past, present, and future. *Pharmaceuticals*, 9(3), 1–12. <https://doi.org/10.3390/ph9030038>
- Onishi, A., Ange, K. S., Dordick, J. S., & Linhardt, R. J. (2016). Heparin and anticoagulation. *Frontiers in Bioscience*, 21(7), 1372–1392. <https://doi.org/10.2741/4462>
- Ouyang, Y., Zeng, Y., Yi, L., Tang, H., Li, D., Linhardt, R. J., & Zhang, Z. (2017). Qualitative and quantitative analysis of heparin and low molecular weight heparins using size exclusion chromatography with multiple angle laser scattering/refractive index and inductively coupled plasma/mass spectrometry detectors. *Journal of Chromatography A*, 1522, 56–61. <https://doi.org/10.1016/j.chroma.2017.09.040>

- Panagos, C. G., August, D. P., Jesson, C., & Uhrin, D. (2016). Photochemical depolymerisation of dermatan sulfate and analysis of the generated oligosaccharides. *Carbohydrate Polymers*, *140*, 13–19. <https://doi.org/10.1016/j.carbpol.2015.11.078>
- Partial Thromboplastin Time (PTT) Test: MedlinePlus Medical Test*. (n.d.). Retrieved October 21, 2020, from <https://medlineplus.gov/lab-tests/partial-thromboplastin-time-ptt-test/>
- Pharmacopeial Forum. (2009). *Heparin Sodium compliance* (Vol. 35, Issue 5).
- Piani, S., Egidio, M., & Fabrizio, T. G. U. (1995). *Semi-Synthetic Glycosaminoglycans Containing C-L-Galacturonic Acid Substituted With Nucleophilic Groups In Position 3* (Patent No. 5,430,132). United States Patent.
- Piani, S., Marchi, E., Tamagnone, G., & Ungarelli, F. (1993). Semi-synthetic glycosaminoglycans containing alpha-L-galacturonic acid substituted with nucleophilic radicals in position 3 (Patent No. EP 0 565 862 B1). In *European Patent Office* (EP 0 565 862 B1). European Patent Office.
- Podzimek, S. (2009). *A Review of the Applications of Size-Exclusion Chromatography — Multiangle Light Scattering to the Characterization of Synthetic and Natural Polymers*. *iv*, 94–112. <https://doi.org/10.1021/bk-2005-0893.ch005>
- Pomin, V. H. (2012). Unravelling Glycobiology by NMR Spectroscopy. In *Glycosylation*. InTech. <https://doi.org/10.5772/48136>
- Pomin, V. H. (2014a). NMR chemical shifts in structural biology of glycosaminoglycans. *Analytical Chemistry*, *86*(1), 65–94. <https://doi.org/10.1021/ac401791h>
- Pomin, V. H. (2014b). Solution NMR conformation of glycosaminoglycans. *Progress in Biophysics and Molecular Biology*, *114*(2), 61–68. <https://doi.org/10.1016/j.pbiomolbio.2014.01.001>
- Powell, A. K., Ahmed, Y. A., Yates, E. A., & Turnbull, J. E. (2010). Generating heparan sulfate saccharide libraries for glycomics applications. *Nature Protocols*, *5*(5), 829–841. <https://doi.org/10.1038/nprot.2010.17>
- Preparation of buffer solutions*. (2018). <http://delloyd.50megs.com/moreinfo/buffers2.html>
- Puvirajasinghe, T. M., & Turnbull, J. E. (2012). Glycomics approaches for the bioassay and structural analysis of heparin/heparan sulphates. *Metabolites*, *2*(4), 1060–1089. <https://doi.org/10.3390/metabo2041060>
- Rabenstein, D. L. (2002). Heparin and heparan sulfate: structure and function. *Natural Product Reports*, *19*(3), 312–331. <https://doi.org/10.1039/b100916h>

- Racaud, A., Antoine, R., Joly, L., Mesplet, N., Dugourd, P., & Lemoine, J. (2009). Wavelength-Tunable Ultraviolet Photodissociation (UVPD) of Heparin-Derived Disaccharides in a Linear Ion Trap. *Journal of the American Society for Mass Spectrometry*, *20*(9), 1645–1651. <https://doi.org/10.1016/j.jasms.2009.04.022>
- Racine, E. (2001). Differentiation of the Low-Molecular-Weight Heparins. *Pharmacotherapy*, *21*(6 Part 2), 62S-70S. <https://doi.org/10.1592/phco.21.8.62S.34594>
- Raman, K., Mencio, C., Desai, U. R., & Kuberan, B. (2013). Sulfation patterns determine cellular internalization of heparin-like polysaccharides. *Molecular Pharmaceutics*, *10*(4), 1442–1449. <https://doi.org/10.1021/mp300679a>
- Rej, R. N., & Perlin, A. S. (1990). Base-catalyzed conversion of the a-l-iduronic acid 2-sulfate unit of heparin into a unit of a-l-galacturonic acid, and related reactions. *Carbohydrate Research*, *200*(C), 437–447. [https://doi.org/10.1016/0008-6215\(90\)84209-D](https://doi.org/10.1016/0008-6215(90)84209-D)
- Riesenfeld, J., & Roden, L. (1990). Quantitative analysis of N-sulfated, N-acetylated, and unsubstituted glucosamine amino groups in heparin and related polysaccharides. *Analytical Biochemistry*, *188*(2), 383–389. [https://doi.org/10.1016/0003-2697\(90\)90624-I](https://doi.org/10.1016/0003-2697(90)90624-I)
- Robyt, J. F. (1998). *Essentials of Carbohydrate Chemistry*. Springer New York. <https://doi.org/10.1007/978-1-4612-1622-3>
- Rountree, K. M., Yaker, Z., & Lopez, P. P. (2020). *Partial Thromboplastin Time*. <https://www.ncbi.nlm.nih.gov/books/NBK507772/>
- Rubinson, K. A., Chen, Y., Cress, B. F., Zhang, F., & Linhardt, R. J. (2016). Heparin's solution structure determined by small-angle neutron scattering. *Biopolymers*, *105*(12), 905–913. <https://doi.org/10.1002/bip.22936>
- Rudd, T. R., Skidmore, M. A., Guerrini, M., Hricovini, M., Powell, A. K., Siligardi, G., & Yates, E. A. (2010). The conformation and structure of GAGs: recent progress and perspectives. *Current Opinion in Structural Biology*, *20*(5), 567–574. <https://doi.org/10.1016/j.sbi.2010.08.004>
- Rudd, Timothy R., Mauri, L., Marinozzi, M., Stancanelli, E., Yates, E. A., Naggi, A., & Guerrini, M. (2019). Multivariate analysis applied to complex biological medicines. *Faraday Discussions*, *218*, 303–316. <https://doi.org/10.1039/C9FD00009G>
- Santini, F., Bisio, A., Guerrini, M., & Yates, E. A. (1997). *Modifications under basic conditions of the minor sequences of heparin containing 2,3 or 2,3,6 sulfated D-glucosamine residues*. *302*, 103–108.
- Screening Tests in Haemostasis: The APTT*. (n.d.). Retrieved October 20, 2020, from [https://practical-haemostasis.com/Screening Tests/aptt.html](https://practical-haemostasis.com/Screening%20Tests/aptt.html)

- Shi, C. S., Sang, Y. X., Sun, G. Q., Li, T. Y., Gong, Z. S., & Wang, X. H. (2017). Characterization and bioactivities of a novel polysaccharide obtained from *Gracilariopsis lemaneiformis*. *Anais Da Academia Brasileira de Ciencias*, 89(1), 175–189. <https://doi.org/10.1590/0001-3765201720160488>
- Shrivastava, A., & Gupta, V. (2011). Methods for the determination of limit of detection and limit of quantitation of the analytical methods. *Chronicles of Young Scientists*, 2(1), 21. <https://doi.org/10.4103/2229-5186.79345>
- Sinko, P. J. (2011). Chemical Kinetics and Stability. In *Chemical kinetics and stability. Martin's Physical Pharmacy and Pharmaceutical Sciences: Physical Chemical and Biopharmaceutical Principles in the Pharmaceutical Sciences* (6th ed., pp. 318–354). Wolters Kluwer Health Adis (ESP).
- Skidmore, M., Guimond, S., Rudd, T., Fernig, D., Turnbull, J., & Yates, E. (2008). The activities of heparan sulfate and its analogue heparin are dictated by biosynthesis, sequence, and conformation. *Connective Tissue Research*, 49(3–4), 140–144. <https://doi.org/10.1080/03008200802148595>
- Smidsrød, O., Haug, A., Larsen, B., von Hofsten, B., Williams, D. H., Bunnenberg, E., Djerassi, C., & Records, R. (1966). The Influence of pH on the Rate of Hydrolysis of Acidic Polysaccharides. *Acta Chemica Scandinavica*, 20, 1026–1034. <https://doi.org/10.3891/acta.chem.scand.20-1026>
- St Ange, K., Onishi, A., Fu, L., Sun, X., Lin, L., Mori, D., Zhang, F., Dordick, J. S., Fareed, J., Hoppensteadt, D., Jeske, W., & Linhardt, R. J. (2016). Analysis of Heparins Derived From Bovine Tissues and Comparison to Porcine Intestinal Heparins. *Clinical and Applied Trombosis/Homeostasis*, 22(6), 520–527. <https://doi.org/10.1177/1076029616643822>
- Stringer, S. E., Mayer-Proschel, M., Kalyani, A., Rao, M., & Gallagher, J. T. (1999). Heparin is a unique marker of progenitors in the glial cell lineage. *Journal of Biological Chemistry*, 274(36), 25455–25460. <https://doi.org/10.1074/jbc.274.36.25455>
- Suflita, M., Fu, L., He, W., Koffas, M., & Linhardt, R. J. (2015). Heparin and related polysaccharides: synthesis using recombinant enzymes and metabolic engineering. *Applied Microbiology and Biotechnology*, 99(18), 7465–7479. <https://doi.org/10.1007/s00253-015-6821-9>
- Sugaya, N., Habuchi, H., Nagai, N., Ashikari-Hada, S., & Kimata, K. (2008). 6-O-sulfation of heparan sulfate differentially regulates various fibroblast growth factor-dependent signalings in culture. *Journal of Biological Chemistry*, 283(16), 10366–10376. <https://doi.org/10.1074/jbc.M705948200>
- Sun, S. F. (2004). *Physical Chemistry of Macromolecules. Basic Principles and Issues* (2nd ed.). John Wiley & Sons, Inc.

- Surapaneni, L., Huang, G., Bodine, A. B., Brooks, J., Podila, R., & Haley-Zitlin, V. (2014). *Correlations between Chondroitin Sulfate Physicochemical Properties and its in-vitro Absorption and Anti-inflammatory Activity*. 2030. <http://arxiv.org/abs/1412.5562>
- Szajek, A. Y., Chess, E., Johansen, K., Gratzl, G., Gray, E., Keire, D., Linhardt, R. J., Liu, J., Morris, T., Mulloy, B., Nasr, M., Shriver, Z., Torralba, P., Viskov, C., Williams, R., Woodcock, J., Workman, W., & Al-Hakim, A. (2016). The US regulatory and pharmacopeia response to the global heparin contamination crisis. *Nature Biotechnology*, 34(6), 625–630. <https://doi.org/10.1038/nbt.3606>
- Tanford, C. (1961). *Physical Chemistry of Macromolecules* (N. G. Gaylord & J. H. Gibbs (Eds.)). John Wiley & Sons, Inc.
- Taylor, S. L., Hogwood, J., Guo, W., Yates, E. A., & Turnbull, J. E. (2019). By-Products of Heparin Production Provide a Diverse Source of Heparin-like and Heparan Sulfate Glycosaminoglycans. *Scientific Reports*, 9(1), 2679. <https://doi.org/10.1038/s41598-019-39093-6>
- Theisen, A., Deacon, M. P., Johann, C., & Harding, S. (2000). *Refractive Increment Data-book: for Polymer and Biomolecular Scientists* (1st ed.). Nottingham University Press.
- Toida, T., Vlahov, I. R., Smith, A. E., Hileman, R. E., & Linhardt, R. J. (1996). C-2 epimerization of N-acetylglucosamine in an oligosaccharide derived from heparan sulfate. *Journal of Carbohydrate Chemistry*, 15(3), 351–360. <https://doi.org/10.1080/07328309608005658>
- Tømmeraas, K., & Melander, C. (2008). Kinetics of hyaluronan hydrolysis in acidic solution at various pH values. *Biomacromolecules*, 9(6), 1535–1540. <https://doi.org/10.1021/bm701341y>
- Tømmeraas, K., Varum, K. M., Christensen, B. E., & Smidsrød, O. (2001). Preparation and characterization of oligosaccharides produced by nitrous acid depolymerization of chitosan. *Carbohydrate Research*, 333, 137–144.
- Turnbull, J. E. (2009). Sequencing Heparan Sulfate Saccharides. In *The Protein Protocols Handbook* (Issue 10, pp. 1321–1334). [https://doi.org/10.1007/978-1-59745-198-7\\_145](https://doi.org/10.1007/978-1-59745-198-7_145)
- Turnbull, J. E. (2011). Getting the farm out of pharma for heparin production. *Science*, 334(6055), 462–463. <https://doi.org/10.1126/science.1211605>
- Ucakturk, E., Cai, C., Li, L., Li, G., Zhang, F., & Linhardt, R. J. (2014). Capillary electrophoresis for total glycosaminoglycan analysis. *Analytical and Bioanalytical Chemistry*, 406(19), 4617–4626. <https://doi.org/10.1007/s00216-014-7859-8>
- Uçar, G., & Balaban, M. (2003). Hydrolysis of polysaccharides with 77% sulfuric acid for quantitative saccharification. *Turkish Journal of Agriculture and Forestry*, 27(6), 361–365. <https://doi.org/10.3906/tar-0307-8>

- Van Der Meer, J. Y., Kellenbach, E., & Van Den Bos, L. J. (2017). From farm to pharma: An overview of industrial heparin manufacturing methods. *Molecules*, 22(6), 1–13. <https://doi.org/10.3390/molecules22061025>
- Vázquez-Martínez, J., & G. López, M. (2019). Chemometrics-Based TLC and GC-MS for Small Molecule Analysis: A Practical Guide. In *Chemometrics and Data Analysis in Chromatography: Vol. I* (Issue tourism, p. 13). IntechOpen. <https://doi.org/10.5772/intechopen.77160>
- Volpi, N., Maccari, F., Suwan, J., & Linhardt, R. J. (2012). Electrophoresis for the analysis of heparin purity and quality. *Electrophoresis*, 33(11), 1531–1537. <https://doi.org/10.1002/elps.201100479>
- Vuong, T. V., Liu, B., Sandgren, M., & Master, E. R. (2017). Microplate-Based Detection of Lytic Polysaccharide Monooxygenase Activity by Fluorescence-Labeling of Insoluble Oxidized Products. *Biomacromolecules*, 18(2), 610–616. <https://doi.org/10.1021/acs.biomac.6b01790>
- Warda, M., Gouda, E. M., Toida, T., Chi, L., & Linhardt, R. J. (2003). Isolation and characterization of raw heparin from dromedary intestine: Evaluation of a new source of pharmaceutical heparin. *Comparative Biochemistry and Physiology - C Toxicology and Pharmacology*, 136(4), 357–365. <https://doi.org/10.1016/j.cca.2003.10.009>
- Warttinger, U., Giese, C., & Krämer, R. (2017). Comparison of Heparin Red, Azure A and Toluidine Blue assays for direct quantification of heparins in human plasma. *ArXiv*.
- Whistler, R. L. (1973). Solubility of Polysaccharides and Their Behavior in Solution. In *Carbohydrates in Solution* (pp. 242–255). <https://doi.org/10.1021/ba-1971-0117.ch014>
- WHO | WHO Model Lists of Essential Medicines. (n.d.). Retrieved June 9, 2020, from <https://www.who.int/medicines/publications/essentialmedicines/en/>
- Wyatt Technology. (n.d.). *Next steps in biophysical characterization by MALS: ion-exchange and reversed-phase chromatography* | Wyatt Technology. Retrieved April 5, 2020, from <https://www.wyatt.com/blogs/next-steps-in-biophysical-characterization-by-mals.html>
- Wyman, C. E., & Yang, B. (2017). Combined Severity Factor for Predicting Sugar Recovery in Acid-Catalyzed Pretreatment Followed by Enzymatic Hydrolysis. In *Hydrothermal Processing in Biorefinerie* (pp. 161–180). <https://doi.org/10.1007/978-3-319-56457-9>
- Xie, S., Guan, Y., Zhu, P., Li, F., Yu, M., Linhardt, R. J., Chi, L., & Jin, L. (2018). Preparation of low molecular weight heparins from bovine and ovine heparins using nitrous acid degradation. *Carbohydrate Polymers*, 197(January), 83–91. <https://doi.org/10.1016/j.carbpol.2018.05.070>

- Yablonsky, G. S., Constales, D., & Marin, G. B. (2010). Coincidences in chemical kinetics: Surprising news about simple reactions. *Chemical Engineering Science*, 65(23), 6065–6076. <https://doi.org/10.1016/j.ces.2010.04.007>
- Yamada, S., Watanabe, M., & Sugahara, K. (1998). Conversion of N-sulfated glucosamine to N-sulfated mannosamine in an unsaturated heparin disaccharide by non-enzymatic, base-catalyzed C-2 epimerization during enzymatic oligosaccharide preparation. *Carbohydrate Research*, 309(3), 261–268. [https://doi.org/10.1016/S0008-6215\(98\)00144-X](https://doi.org/10.1016/S0008-6215(98)00144-X)
- Yan, H., Yalagala, R. S., & Yan, F. (2015). Fluorescently labelled glycans and their applications. *Glycoconjugate Journal*, 32(8), 559–574. <https://doi.org/10.1007/s10719-015-9611-9>
- Yates, E A, Santini, F., De Cristofano, B., Payre, N., Cosentino, C., Guerrini, M., Naggi, A., Torri, G., & Hricovini, M. (2000). Effect of substitution pattern on <sup>1</sup>H, <sup>13</sup>C NMR chemical shifts and <sup>1</sup>J(CH) coupling constants in heparin derivatives. *Carbohydr Res*, 329(1), 239–247. [https://doi.org/S0008-6215\(00\)00144-0](https://doi.org/S0008-6215(00)00144-0) [pii]
- Yates, Edwin A., Santini, F., Guerrini, M., Naggi, A., Torri, G., & Casu, B. (1996). <sup>1</sup>H and <sup>13</sup>C NMR spectral assignments of the major sequences of twelve systematically modified heparin derivatives. *Carbohydrate Research*, 294, 15–27. [https://doi.org/10.1016/S0008-6215\(96\)90611-4](https://doi.org/10.1016/S0008-6215(96)90611-4)
- Yates, Edwin A, Gallagher, J. T., & Guerrini, M. (2019). Introduction to the Molecules Special Edition Entitled ‘Heparan Sulfate and Heparin: Challenges and Controversies’: Some Outstanding Questions in Heparan Sulfate and Heparin Research. *Molecules*, 24(7), 1399. <https://doi.org/10.3390/molecules24071399>
- Ye, H., Toby, T. K., Sommers, C. D., Ghasriani, H., Trehy, M. L., Ye, W., Kolinski, R. E., Buhse, L. F., Al-Hakim, A., & Keire, D. A. (2013). Characterization of currently marketed heparin products: Key tests for LMWH quality assurance. *Journal of Pharmaceutical and Biomedical Analysis*, 85(July 2014), 99–107. <https://doi.org/10.1016/j.jpba.2013.06.033>
- Zhang, F., Yang, B., Ly, M., Solakyildirim, K., Xiao, Z., Wang, Z., Beaudet, J. M., Torelli, A. Y., Dordick, J. S., & Linhardt, R. J. (2011). Structural characterization of heparins from different commercial sources. *Analytical and Bioanalytical Chemistry*, 401(9), 2793–2803. <https://doi.org/10.1007/s00216-011-5367-7>
- Zhang, H., Lu, Y., Wang, Y., Zhang, X., & Wang, T. (2018). D-Glucosamine production from chitosan hydrolyzation over a glucose-derived solid acid catalyst. *RSC Advances*, 8(10), 5608–5613. <https://doi.org/10.1039/c7ra12490b>
- Zhang, P., & Sutheerawattananonda, M. (2020). Kinetic Models for Glucosamine Production by Acid Hydrolysis of Chitin in Five Mushrooms. *International Journal of Chemical Engineering*, 2020, 13–15. <https://doi.org/10.1155/2020/5084036>

- Zhang, Z., Khan, N. M., Nunez, K. M., Chess, E. K., & Szabo, C. M. (2012). Complete monosaccharide analysis by high-performance anion-exchange chromatography with pulsed amperometric detection. *Analytical Chemistry*, 84(9), 4104–4110. <https://doi.org/10.1021/ac300176z>
- Zhang, Z., Xie, J., Zhang, F., & Linhardt, R. J. (2007). Thin-layer chromatography for the analysis of glycosaminoglycan oligosaccharides. *Analytical Biochemistry*, 371(1), 118–120. <https://doi.org/10.1016/j.ab.2007.07.003>
- Zhang, Z., Yu, G., Zhao, X., Liu, H., Guan, H., Lawson, A. M., & Chai, W. (2006). Sequence analysis of alginate-derived oligosaccharides by negative-ion electrospray tandem mass spectrometry. *Journal of the American Society for Mass Spectrometry*, 17(4), 621–630. <https://doi.org/10.1016/j.jasms.2006.01.002>
- Zhou, D., Porter, W. R., & Zhang, G. G. Z. (2016). Drug Stability and Degradation Studies. In Y. Qiu, Y. Chen, G. Zhang, L. Yu, & R. V. Mantri (Eds.), *Developing Solid Oral Dosage Forms: Pharmaceutical Theory and Practice*. (2nd ed., pp. 113–149). Academic Press. <https://doi.org/10.1016/B978-0-12-802447-8.00005-4>